

**METAL-CATALYZED COUPLING REACTIONS
OF CONJUGATED ENYNE ALCOHOL
DERIVATIVES WITH ORGANOMETALLICS: AN
EFFECTIVE METHOD IN SYNTHESIS OF
FUNCTIONALIZED VINYLALLENES**

**A Thesis Submitted to
the Graduate School of Engineering and Sciences of
İzmir Institute of Technology
in Partial Fulfillment of the Requirements for the Degree of**

DOCTOR OF PHILOSOPHY

in Chemistry

**by
Doğan TAÇ**

November 2016

İZMİR

We approve the thesis of **Dođan TAÇ**

Examining Committee Members:

Prof. Dr. Levent ARTOK

Department of Chemistry, İzmir Institute of Technology

Prof. Dr. Stephen ASTLEY

Department of Chemistry, İzmir Institute of Technology

Assoc. Prof. Dr. Mustafa EMRULLAHOĐLU

Department of Chemistry, İzmir Institute of Technology

Prof. Dr. Canan VARLIKLI

Department of Photonics, İzmir Institute of Technology

Prof. Dr. Hayati TÜRKMEN

Department of Chemistry, Ege University

10 November 2016

Prof. Dr. Levent ARTOK

Supervisor, Department of Chemistry
İzmir Institute of Technology

Prof. Dr. Ahmet Emin EROĐLU

Head of Department of Chemistry

Prof. Dr. R. Bilge KARAÇALI

Dean of the Graduate School of
Engineering and Sciences

ACKNOWLEDGEMENT

During my PhD study, I have come across so many people who contributed to finish my thesis. First of all, I would like express my deepest appreciation to my supervisor Prof. Dr Levent ARTOK who always lead me to the right path.

I have my special thanks to Prof. Dr. Stephen ASTLEY and Assoc. Prof. Dr. Mustafa EMRULLAHOĞLU for their valuable suggestions, support and participating as a committee member through my thesis progress seminars and PhD defense seminar. I would like to offer my gratitude to Prof. Dr. Hayati TÜRKMEN and Prof. Dr. Canan VARLIKLI for participating as committee members and for reviewing my work.

During my doctoral studies I have collaborated with many good friends like Fırat ZİYANAK, Erman KIBRIS and İsmet Arınç AYTAÇ. I would like to specially thank Fırat and Erman for their support in all matters during my thesis studies. I wish them all a very successful and happy life. Also, I would like to thank Prof. Dr. Durmuş ÖZDEMİR for having permission to use FT-IR instrument in his research laboratory.

I am deeply and forever indebted to my parents for their support and encouragement throughout my entire life. I would like to specially thank Güzde DUMAN for her support and everything she provided throughout my PhD studies. Without her help this dissertation would not have been possible.

The financial support of TUBITAK with contact numbers of 210T092 and 113Z155 is greatly acknowledged.

ABSTRACT

METAL-CATALYZED COUPLING REACTIONS OF CONJUGATED ENYNE ALCOHOL DERIVATIVES WITH ORGANOMETALLICS: AN EFFECTIVE METHOD IN SYNTHESIS OF FUNCTIONALIZED VINYLALLENES

Transformations of organic compounds using transition metals are common methods in the toolbox of a synthetic chemist. Metal catalyzed C-C couplings are one of the most useful technique in this toolbox. Conjugate addition of soft/hard carbon nucleophiles to form allenes which are synthetically and pharmaceutically key precursors has been of great interest.

Within the scope of this thesis functionalized vinylallene derivatives were prepared in two different types of new methods. The first method is Pd/Cu-catalyzed conjugate addition of terminal alkynes on enyne carbonates. The other method is iron-catalyzed conjugate addition of Grignard reagents on enyne acetates.

In the case of the former method, alkynyl-substituted vinylallenes (1,3,4-trien-6-yne) were prepared with optimized conditions up to 91% yield in relatively short reaction periods. The optimized conditions of the cross coupling were successfully applied with various types of terminal alkynes and enyne substrates.

The latter method involves the synthesis of alkylated vinylallenes with up to 90% yield with proper conditions.

ÖZET

KONJUGE ENİN ALKOL TÜREVLERİNİN ORGANOMETALİKLER İLE METAL KATALİZLİ KENETLENME TEPKİMELERİ: FONKSİYONLANMIŞ VINİLALLENLERİN SENTEZİNDE VERİMLİ BİR YÖNTEM

Organik bileşiklerin geçiş metalleri kullanılarak dönüşümleri sentetik kimyagerlerin sık olarak kullandığı metodlardandır. Yumuşak veya sert nükleofiller ile sentetik ve potent ilaç etken madde olarak vinilallen türevlerinin oluşturulması en sık kullanılan yöntemlerden biridir ve günümüzde bu yöntemler yüksek ilgi görmektedir.

Bu tez çalışmasında fonksiyonlandırılmış vinilallen türevleri iki tip yeni eşleşme tepkimesi ile hazırlanmıştır. İlk metod paladyum/bakır-katalizi ile terminal alkinlerin konjuge katılma ile enin karbonatlara katılma tepkimesidir. İkinci metod ise bakır-katalizli Grignard reaktiflerinin enin asetatlar ile 1,5-(SN²) süstitüsyon tepkimeleridir.

İlk metod ile alkinil gruplu vinilallen (1,3,4-trien-6-in) bileşiklerin sentezi optimize koşullar altında %91 verime kadar sentezlenebilmiştir. Eşleşme tepkimelerinin optimize koşulları çeşitli terminal alkinenin substratlara başarılı olarak uygulanabilmiştir.

İkinci metod ile vinilallen türevleri alkil ve aril Grignard reaktifleri eşliğinde %90 veime kadar sentezlenebilmiştir.

TABLE OF CONTENTS

| | |
|---|----|
| LIST OF FIGURES | iv |
| LIST OF TABLES | ix |
| ABBREVIATIONS | x |
| CHAPTER 1. INTRODUCTION | 1 |
| CHAPTER 2. LITERATURE SURVEY | 4 |
| 2.1. Transition-Metal-Catalyzed Reactions of Propargyl Compounds | 4 |
| 2.1.1. Palladium-Catalyzed Reactions of Propargyl Compounds..... | 4 |
| 2.1.2. Palladium-Catalyzed Type 2 Reactions of Propargyl Compounds | 7 |
| 2.1.3. Iron-Catalyzed Reactions of Propargyl Compounds | 9 |
| 2.1.4. Reactions of Propargyl Compounds in the Presence of Various Transition Metals | 11 |
| 2.2. Transition-Metal-Catalyzed Reactions of Allyl Compounds..... | 13 |
| 2.2.1. Palladium Catalyzed Reactions of Allylic Compounds..... | 13 |
| 2.2.2. Transmetallation of π -Allylpalladium Complexes..... | 14 |
| 2.2.3. Iron-Catalyzed Reactions of Allyl Compounds..... | 16 |
| 2.3. Transition-Metal-Catalyzed Synthesis of Vinylallenes..... | 18 |
| CHAPTER 3. EXPERIMENTAL STUDY | 20 |
| 3.1. General Methods | 20 |
| 3.2. Preparation of Substrates..... | 21 |
| 3.2.1. Preparation of E-Enyne Derivatives | 21 |
| 3.2.1.1. Step A | 21 |
| 3.2.1.2. Step B..... | 22 |
| 3.2.1.3. Step C..... | 23 |
| 3.2.1.4. Step D | 24 |
| 3.2.1.5. Preparation of E-Enyne Carbonates and Acetates | 25 |

| | |
|--|-----|
| 3.2.2. Preparation of Z-Enyne Acetate Z-2a, Z-1b and Carbonate Z-1a..... | 27 |
| 3.2.3. Synthesis of (R, E)-4-methyldec-3-en-5-yn-2-ol..... | 28 |
| 3.2.4. Preparation of Enyne Epoxides E-ox and Z-ox | 29 |
| 3.3 General Procedure for Catalytic Reactions | 30 |
| 3.3.1. Palladium/Copper-Catalyzed Coupling Reactions | 31 |
| 3.3.2. Iron-Catalyzed Coupling Reactions | 31 |
| 3.3.3. Cycloaddition Reaction of Vinyl Allene E-1bb..... | 32 |
| 3.4. Spectral Data for Prepared Compounds | 33 |
| 3.4.1. Spectral Data for Enyne Carbonates | 33 |
| 3.4.2. Spectral Data for Enyne Acetates | 40 |
| 3.4.3. Spectral Data for Enyne Oxiranes..... | 47 |
| 3.4.4. Spectral Data for Products | 48 |
| CHAPTER 4. RESULTS AND DISCUSSION..... | 66 |
| 4.1. Palladium/Copper-Catalyzed Alkynylation of E-Enyne Carbonates..... | 66 |
| 4.2. Iron-Catalyzed Alkylation of E-Enyne Acetates with Grignard Reagents | 82 |
| CHAPTER 5. CONCLUSION..... | 84 |
| REFERENCES | 85 |
| APPENDICES | |
| APPENDIX A. ¹ H NMR AND ¹³ C NMR SPECTRUM OF PRODUCTS | 91 |
| APPENDIX B. MASS SPECTRA of PRODUCTS | 162 |

LIST OF FIGURES

| <u>Figure</u> | <u>Page</u> |
|---|-------------|
| Figure 1.1. Standard and improved synthesis of ibuprofen. | 1 |
| Figure 2.1. Reaction of propargyl chlorides 6 and 7 with a Pd complex..... | 4 |
| Figure 2.2. Type 1, 2, and 3 of allenylpalladium complexes and type 4 as β - hydrate elimination. (Source: Tsuji, 2000) | 6 |
| Figure 2.3. Palladium-catalyzed coupling of Grignard reagents with propargyl chlorides. | 7 |
| Figure 2.4. Palladium-catalyzed addition of organozinc compounds to propargyl acetates. | 7 |
| Figure 2.5. Palladium/copper-catalyzed coupling reaction of terminal alkynes with propargyl carbonates..... | 8 |
| Figure 2.6. Palladium/copper-catalyzed coupling reaction of terminal alkynes with cyclic propargyl carbonates. | 8 |
| Figure 2.7. Palladium/copper-catalyzed coupling of terminal alkynes with propargyl oxiranes 33 | 9 |
| Figure 2.8. Synthesis of allenes from propargyl chlorides via S_N2' type substitution with Grignard reagents over the catalytic amount of $FeCl_2$ | 9 |
| Figure 2.9. Synthesis of allenes from propargyl bromides via S_N2' syn- selective substitution over an iron catalyst. | 10 |
| Figure 2.10. Synthesis of allenes from propargyl carboxylates via S_N2' pathway. | 10 |
| Figure 2.11. A temperature dependent synthesis of optically active allenes from 42 | 10 |
| Figure 2.12. Synthesis of allenes from propargyl acetates via S_N2' substitution with dialkylcuprates. | 11 |
| Figure 2.13. Synthesis of allenes from propargyl bromides via anti-selective S_N2' substitution with organocuprates. | 11 |
| Figure 2.14. Synthesis of allenes from propargyl bromides via S_N2' anti- selective substitution over samarium diiodide. | 12 |

| | |
|--|----|
| Figure 2.15. A copper-based catalyzed direct coupling of polyfluoroarenes with propargyl phosphates. | 12 |
| Figure 2.16. SN ₂ -type reductive substitution of propargyl alcohols by Cp ₂ Zr(H)Cl to yield allenes. | 12 |
| Figure 2.17. Schematic illustration of synthetic methods involving π -allyl- palladium complexes. | 13 |
| Figure 2.18. Mechanism of transmetalation of main group metals with π - allylpalladium. | 14 |
| Figure 2.19 Alkoxyacylation of allyl phosphates. | 14 |
| Figure 2.20. Palladium-catalyzed synthesis of trans polyene homobenzene derivatives with Grignard reagents. | 15 |
| Figure 2.21. Synthesis of allene derivatives via homoallyl zinc intermediate. | 15 |
| Figure 2.22. Reactions of allylic phosphates with Grignard reagent catalyzed by iron salts. | 16 |
| Figure 2.23. Reactions of allyl carbonates with nucleophiles over TBAFe catalyst. | 16 |
| Figure 2.24. Fe(acac) ₃ -catalyzed allylic arylation of allyl acetates. | 17 |
| Figure 2.25. Reaction between Grignard reagents with unsaturated esters in the catalytic presence of FeCl ₂ | 17 |
| Figure 2.26. Fe(acac) ₃ catalyzed allylic alkylation of vinylcyclopropanes. | 17 |
| Figure 2.27. Synthesis vinylallenes with Grignard reagents. | 18 |
| Figure 2.28. Synthesis of vinylallenes via organoaluminum reagents. | 18 |
| Figure 2.29. Palladium-catalyzed synthesis of vinylallenes via alkenylation of propargyl carbonates. | 18 |
| Figure 2.30. Palladium-catalyzed synthesis of a vinylallenes (92) via the reaction of enyne acetate (93) with lithium dialmethylcuprate. | 19 |
| Figure 2.31. Synthesis of vinylallenes via the rhodium-catalyzed arylation of enyne acetates. | 19 |
| Figure 2.32. Palladium-catalyzed enantioselective synthesis of the vinylallene 92 via an alkoxyacylation method. | 19 |
| Figure 3.1. Schematic pathway for the preparation of E-Enyne Carbonates and Acetates. | 26 |
| Figure 3.2. Synthetic pathway to obtain enyne acetate Z-2, Z-1a and Z-1b. | 27 |
| Figure 3.3. (<i>R, E</i>)-4-methyldec-3-en-5-yn-2-ol (<i>R, E</i>)-1b. | 28 |

| | |
|--|----|
| Figure 3.4. Synthesis of <i>E</i> and <i>Z</i> enyne epoxides. | 30 |
| Figure 3.5. Methyl (<i>E</i>)-4-methylhept-3-en-5-yn-2-yl carbonate. | 33 |
| Figure 3.6. Methyl (<i>E</i>)-4-methyldec-3-en-5-yn-2-yl carbonate..... | 33 |
| Figure 3.7. Methyl (<i>E</i>)-3-en-5-yn-2-yl carbonate. | 34 |
| Figure 3.8. Methyl (<i>E</i>)-4,7,7-trimethyloct-3-en-5-yn-2-yl carbonate..... | 34 |
| Figure 3.9. (<i>E</i>)-6-cyclohexyl-4-methylhex-3-en-5-yn-2-yl methyl carbonate..... | 35 |
| Figure 3.10. Methyl (<i>E</i>)-4-methyl-6-phenylhex-3-en-5-yn-2-yl carbonate..... | 35 |
| Figure 3.11. (<i>E</i>)-dec-3-en-5-yn-2-yl methyl carbonate. | 36 |
| Figure 3.12. Methyl (<i>E</i>)-4-phenyldec-3-en-5-yn-2-yl carbonate..... | 36 |
| Figure 3.13. (<i>E</i>)-4-butyldec-3-en-5-yn-2-yl methyl carbonate..... | 37 |
| Figure 3.14. Methyl (<i>E</i>)-2,5-dimethyloct-4-en-6-yn-3-yl carbonate. | 37 |
| Figure 3.15. Methyl (<i>E</i>)-3-methylnon-2-en-4-yn-1-yl carbonate. | 38 |
| Figure 3.16. Methyl (<i>E</i>)-3-methylnon-2-en-4-yn-1-yl carbonate. | 38 |
| Figure 3.17. Methyl (<i>E</i>)-3-methyl-1-phenylnon-2-en-4-ynyl carbonate. | 39 |
| Figure 3.18. Methyl-(<i>Z</i>)- 4-methyldec-3-en-5-yn-2-yl carbonate. | 39 |
| Figure 3.19. (<i>E</i>)-7-methyltridec-6-en-8-yn-5-yl acetate. | 40 |
| Figure 3.20. (<i>E</i>)-7,10,10-trimethylundec-6-en-8-yn-5-yl acetate. | 40 |
| Figure 3.21. (<i>E</i>)-1-cyclohexyl-3-methylnon-3-en-1-yn-5-yl acetate..... | 41 |
| Figure 3.22. (<i>E</i>)-3-methyl-1-phenylnon-3-en-1-yn-5-yl acetate..... | 41 |
| Figure 3.23. (<i>E</i>)-4-methylhex-3-en-5-yn-2-yl acetate. | 42 |
| Figure 3.24. (<i>E</i>)-7-phenyltridec-6-en-8-yn-5-yl acetate. | 42 |
| Figure 3.25. (<i>E</i>)-2,5-dimethylundec-4-en-6-yn-3-yl acetate. | 43 |
| Figure 3.26. (<i>E</i>)-7-butyltridec-6-en-8-yn-5-yl acetate..... | 43 |
| Figure 3.27. (<i>E</i>)-2,5-dimethylundec-4-en-6-yn-3-yl acetate. | 44 |
| Figure 3.28. (<i>E</i>)-4-methyldec-3-en-5-yn-2-yl acetate..... | 44 |
| Figure 3.29. (<i>E</i>)-3-methylnon-2-en-4-yn-1-yl acetate. | 45 |
| Figure 3.30. (<i>E</i>)-3-methyl-1-phenylnon-2-en-4-yn-1-yl acetate..... | 45 |
| Figure 3.31. (<i>Z</i>)-7-methyltridec-6-en-8-yn-5-yl acetate. | 46 |
| Figure 3.32. (<i>Z</i>)- 4-methyldec-3-en-5-yn-2-yl acetate..... | 46 |
| Figure 3.33. (<i>E</i>)-2-(methoxymethyl)-3-(2-methyloct-1-en-3-yn-1-yl)oxirane..... | 47 |
| Figure 3.34. (<i>Z</i>)-2-(methoxymethyl)-3-(2-methyloct-1-en-3-yn-1-yl)oxirane..... | 47 |
| Figure 3.35. (<i>E</i>)-5,7-dimethyldeca-5,6,8-trien-3-yn-1-ol. | 48 |
| Figure 3.36. (<i>E</i>)-5-butyl-7-methyldeca-5,6,8-trien-3-yn-1-ol. | 48 |
| Figure 3.37. (<i>E</i>)-5-(tert-butyl)-7-methyldeca-5,6,8-trien-3-yn-1-ol. | 49 |

| | |
|---|----|
| Figure 3.38. (<i>E</i>)-5-cyclohexyl-7-methyldeca-5,6,8-trien-3-yn-1-ol. | 49 |
| Figure 3.39. (<i>E</i>)-7-methyl-5-phenyldeca-5,6,8-trien-3-yn-1-ol..... | 50 |
| Figure 3.40. (<i>E</i>)-5-butyldeca-5,6,8-trien-3-yn-1-ol. | 50 |
| Figure 3.41. (<i>E</i>)-5-butyl-7-phenyldeca-5,6,8-trien-3-yn-1-ol..... | 51 |
| Figure 3.42. (<i>E</i>)-5-butyl-7-(prop-1-en-1-yl)undeca-5,6-dien-3-yn-1-ol..... | 51 |
| Figure 3.43. (<i>E</i>)-5-butyl-7,10-dimethylundeca-5,6,8-trien-3-yn-1-ol. | 52 |
| Figure 3.44. 5-butyl-7-methylnona-5,6,8-trien-3-yn-1-ol. | 52 |
| Figure 3.45. (<i>E</i>)-5-butyl-7-methyltrideca-5,6,8-trien-3-yn-1-ol..... | 53 |
| Figure 3.46. (<i>E</i>)-5-butyl-7-methyl-9-phenylnona-5,6,8-trien-3-yn-1-ol. | 53 |
| Figure 3.47. (<i>E</i>)-6-butyl-4-methyldodeca-2,4,5-trien-7-yne. | 54 |
| Figure 3.48. (<i>E</i>)-(3-butyl-5-methylocta-3,4,6-trien-1-yn-1-yl)benzene | 54 |
| Figure 3.49. (<i>E</i>)-1-(3-butyl-5-methylocta-3,4,6-trien-1-yn-1-yl)-4- methoxybenzene. | 55 |
| Figure 3.50 (<i>E</i>)-3-butyl-5-methylocta-3,4,6-trien-1-yn-1-yl)cyclohexane..... | 55 |
| Figure 3.51 (<i>E</i>)-6-butyl-4,9,9-trimethyldeca-2,4,5-trien-7-yne..... | 56 |
| Figure 3.52. (<i>E</i>)-(3-butyl-5-methylocta-3,4,6-trien-1-yn-1- yl)triisopropylsilane. | 56 |
| Figure 3.53. (<i>E</i>)-1-(3-butyl-5-methylocta-3,4,6-trien-1-yn-1-yl)-4- (trifluoromethyl)benzene. | 57 |
| Figure 3.54. (<i>E</i>)-5,7-dimethyl-2-phenyl-4-(undec-6-yn-5-ylidene)-3a,4,7,7a- tetrahydro-1H-isoindole-1,3(2H)-dione..... | 58 |
| Figure 3.55. (<i>E</i>)-5-butyl-7-methyltrideca-5,6,8-triene..... | 58 |
| Figure 3.56. (<i>E</i>)-(7-methyltrideca-5,6,8-trien-5-yl) cyclohexane..... | 59 |
| Figure 3.57. (<i>E</i>)-(7-methyltrideca-5,6,8-trien-5-yl) benzene..... | 59 |
| Figure 3.58. (<i>E</i>)-5-butyltrideca-5,6,8-triene. | 60 |
| Figure 3.59. (<i>E</i>)-5,7-dibutyltrideca-5,6,8-triene. | 60 |
| Figure 3.60. (<i>E</i>)-7-butyl-2,5-dimethylundeca-3,5,6-triene. | 61 |
| Figure 3.61. (<i>E</i>)-6-butyl-4-methyldeca-2,4,5-triene. | 61 |
| Figure 3.62. (<i>E</i>) 5-butyl-3-methylnona-1,3,4-triene. | 62 |
| Figure 3.63. (<i>E</i>)-(5-butyl-3-methylnona-1,3,4-trien-1-yl) benzene..... | 62 |
| Figure 3.64. (<i>E</i>)-9-butyl-7-methyltetradeca-5,7,8-triene. | 63 |
| Figure 3.65. (<i>E</i>)-9-butyl-7-methylheptadeca-5,7,8-triene. | 63 |
| Figure 3.66. (<i>E</i>)-(7-methyltrideca-5,6,8-trien-5-yl)benzene..... | 64 |
| Figure 3.67. (<i>E</i>)-5,7-dimethyltrideca-5,6,8-triene. | 64 |

| | |
|--|----|
| Figure 3.68. (<i>E</i>)-(2-butyl-4-methyldeca-2,3,5-trien-1-yl)benzene. | 65 |
| Figure 4.1. Pd-catalyzed alkynylation of enyne carbonates and iron- catalyzed reaction of enyne acetates with Grignard reagents. | 66 |
| Figure 4.2. Copper-mediated Glacier or self-coupling of terminal alkynes in the presence of catalytic oxygen. | 67 |
| Figure 4.3. Coupling reaction of 3-butyne-1-ol with Z1-a | 79 |
| Figure 4.4. Reaction of an enantio-enriched enyne carbonate with terminal alkynes. | 79 |
| Figure 4.5. Reaction of enyne epoxides with 1-hexyne. | 80 |
| Figure 4.6. [4+2] Cyclization of <i>E</i> -1bb and exact structure of <i>E</i>-1bb-DA | 80 |
| Figure 4.7. Proposed reaction mechanism of alkynylation of (<i>E</i>)-enyne carbonates. | 81 |
| Figure 4.8. ¹ H NMR spectrum of the mixture of a reduction product and alkylated vinylallene product. | 84 |
| Figure 4.9. The reaction of benzophenone with MeMgBr | 85 |
| Figure 4.10. Reaction of propargyl chloride with unactivated Mg. | 85 |
| Figure 4.11. Magnesium-THF complex and butanol formation. | 85 |
| Figure 4.12. Proposed reaction mechanism of alkylation of (<i>E</i>)-enyne carbonates with Grignard reagents. | 92 |

LIST OF TABLES

| <u>Table</u> | <u>Page</u> |
|--|-------------|
| Table 4.1. Effect of additives on Pd/Cu-Catalyzed alkyne reactions of the <i>E</i> -Enyne Carbonate <i>E-1b</i> | 68 |
| Table 4.2. Effect of Pd/ligand ratio on alkyne reaction of <i>E</i> -Enyne Carbonate <i>E-1b</i> | 69 |
| Table 4.3. Screening of amine bases on alkyne reaction of <i>E</i> -Enyne Carbonate <i>E-1b</i> | 70 |
| Table 4.4. Effect of amount of HNEt ₂ and KBr on the reactivity..... | 71 |
| Table 4.5. Effect of various ligands at room temperature on reactivity was shown | 73 |
| Table 4.6. Attempts to stabilize reaction conditions..... | 74 |
| Table 4.7. Optimization of the reaction conditions for phenyl acetylene. | 75 |
| Table 4.8. Visualizing different coupling partners. | 76 |
| Table 4.9. Screening various enyne carbonates for the coupling reaction. | 78 |
| Table 4.10. Optimization studies on the alkylation of enyne acetates..... | 83 |
| Table 4.11. Screening of various inorganic additives for the alkylation reaction..... | 86 |
| Table 4.12. Screening of various inorganic salts for the alkylation reaction..... | 87 |
| Table 4.13. The reaction of <i>E-2a</i> with various Grignard reagents. | 89 |
| Table 4.14. The reaction of various enyne acetate structures with BuMgCl..... | 91 |

ABBREVIATIONS

| | | | |
|--------------|------------------------------------|--------------|--|
| Ac | Acetate | min. | minutes |
| acac | acetylacetone | mm | millimeter |
| aq. | Aqueous | mL | milliliters |
| Ar | Aryl | Ph | phenyl |
| ATR | Attenuated total reflectance | ppm | parts per million |
| Bu | Butyl | RT | room temperature |
| Bn | Benzyl | <i>t</i> -Bu | tertiary butyl |
| Cy | Cyclohexyl | TEA | triethylamine |
| DABCO | 1,4 diazabicyclo [2.2.2] octane | TDMPP | tris(2,6-dimethoxyphenyl) phosphine |
| dba | dibenzylideneacetone | THF | tetrahydrofuran |
| DBA | dibutylamine | TLC | thin layer chromatography |
| DCM | dichloromethane | Xantphos | 4,5-Bis (diphenyl-phosphino) - 9,9-dimethylxanthene |
| DIBALH | diisobutylaluminium hydride | | |
| DIPA | diisopropylamine | | |
| DMAP | 4-dimethylamino pyridine | | |
| Et | Ethyl | | |
| etc. | expected to complete | | |
| eq. | equivalent | | |
| g | gram | | |
| GC | gas chromatography | | |
| h | hour | | |
| <i>i</i> -Pr | isopropyl | | |
| M | molar | | |
| Me | methyl | | |
| m | meter | | |
| mg | milligram | | |

CHAPTER 1

INTRODUCTION

For last two decades use of transition-metal-catalysis on the organic synthesis has gained huge importance as can be perceived from the frequency of published articles in major chemistry journals. Furthermore, Nobel Prizes of chemistry were awarded to Noyori and Knowles (2001), Schrock, Grubbs, and Chauvin (2005), and Heck, Suzuki, and Negishi (2010) for their contributions to the area of transition-metal-catalysis. It is generally accepted that transition metals have the advantage of a wide area of application on synthesis and sometimes metal-mediated processes would be superior on large scale production compared to the standard methods as in the example of ibuprofen (Figure 1.1, an active ingredient of some medicines) production in industrial scale, which comparatively is a more atom economic and time saving method (Magano and Dunetz, 2013).

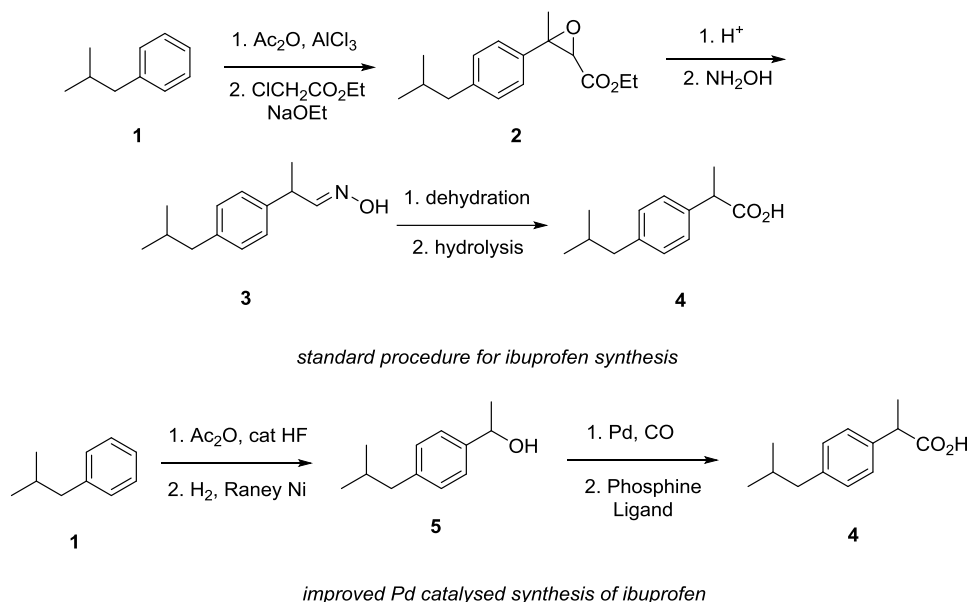


Figure 1.1. Standard and improved synthesis of ibuprofen.
(Source: Magano and Dunetz, 2013)

In the field of transition-metal-catalysis, sustainability, accessibility and non-toxicity are the key words that should be taken into account. The iron is a most suitable transition metal from the point of availability, cost and sustainability. The usage of iron salts in catalytic systems well date back to the 1960s with the invention of a ferrocene compound (Kealy and Pauson, 1951). The first iron-catalyzed alkylation reaction with Grignard reagents were to happen in this decade by the Kochi group (Tamura and Kochi, 1971). Up to this period the late transition metals like palladium and rhodium were in their early stages in catalytic synthetic chemistry. Milestones in the development of organo-palladium chemistry were the publication of Heck and Nolley which reported the C-C coupling between aryl halides or vinyl halides and activated alkenes (Heck and Nolley, 1972) and the reaction of allyl acetates and allyl bromides with nucleophiles (Trost and Fullerton, 1973). Up to date palladium catalysts demonstrated their worth on synthetic chemistry.

The use of transition metals in the synthesis of neutral product mimics or structures that are valuable reagents to medications is an attractive topic to chemists. Vinylallene structures are one of the important intermediate en-route to the synthesis of such structures. The gifted reactivity of allenes towards catalytic or non-catalytic systems to result in propargylation, addition, cycloaddition, cycloisomerization and cyclization makes vinylallene structures significant (Yu and Ma, 2012). There are various methods to synthesize vinylallene derivatives. However, in the 1990s multistep reactions or impractical methods were used for synthesis vinylallene derivatives (Ruitenberg et al., 1981, Tolstikov et al., 1985). However, the use of efficient synthesis for vinylallenes via palladium catalyst with olefins and propargyl compounds (Mandai et al., 1991) led the facile synthesis of vinylallene derivatives in a simple procedure. In recent two decades, alkylation (Purpura and Krause, 1999), arylation (Üçüncü et al., 2011), and alkoxyacylation (Karagöz et al., 2014) of the enyne derivatives bearing a leaving group on the allylic position have become effective methods in the synthesis of functionalized vinylallenes.

In the light of such information, the synthesis of functionalized vinylallene derivatives has been an essential class of this studies and attracted our attention. At first; further functionalization of vinylallenes with an alkynyl group via 1,5-substitution type reaction of terminal alkynes with 1, 3-enyne compounds was investigated in this study. The alkylation of enyne compounds with organocuprates was already reported in the literature. For sure iron catalysts, would offer practical advantages; which are inexpensive compared to other class of transition metals, non-toxic to user and environmentally friendly. The alkylation of enyne acetates via iron catalyst in the presence of Grignard reagents would be a valuable class of study.

CHAPTER 2

LITERATURE SURVEY

2.1. Transition-Metal-Catalyzed Reactions of Propargyl Compounds

2.1.1. Palladium-Catalyzed Reactions of Propargyl Compounds

Propargyl compounds are valuable intermediates that are used in various synthetic applications, especially to synthesize allenic intermediates with the catalytic usage of transition metals. There are several reports in the literature on the synthesis of allenic structures from propargyl compounds over various transition metals. Up to date palladium complexes were widely used for the reaction of propargyl compounds leading to allenes.

In 1983, Vermeer group has studied the structures of allenylpalladium(II) (**8**) species in a stoichiometric S_N2' reaction of propargyl chlorides (**6** and **7**) and $Pd[PPh_3]_4$. A direct oxidative addition of palladium complex was also observed to form with the substrate substituted with a bulky group (**9**). This finding led to understand the mechanism of palladium-catalyzed reactions of propargyl compounds (Elsevier et al., 1983).

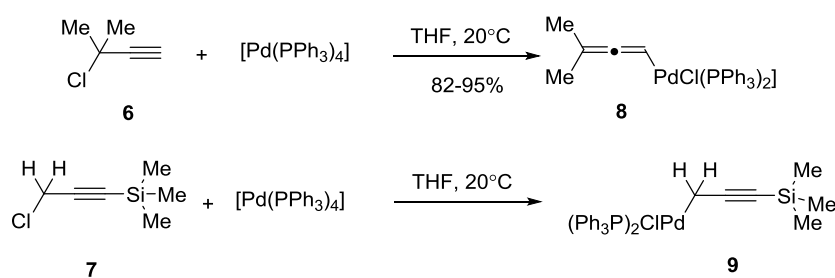


Figure 2.1. Reaction of propargyl chlorides **6** and **7** with a Pd complex.

The palladium-catalyzed reactions, with the knowledge up to this date can be divided into four distinct mechanistic pathways. Allenyl palladium intermediate **10** yields various products depending on the substrates reacted with the active complex of allenylpalladium (Figure 2.2).

Type 1 reaction involves the insertion of alkynes, alkenes (Figure 2.2, Type **1a**) and carbon monoxide (Figure 2.2, Type **1b**) palladium. By the insertion of alkenes trienes are formed (**11**) via β -hydrate elimination. Alkynes react with allenylpalladium complex to yield active alkenylpalladium complexes which further involve with various transformations (**12**). Using carbon monoxide as a substrate with the allenylpalladium complex leads to an acylpalladium complex. Further alkoxy carbonylation with alcohols produces allenolate derivatives (**13**).

With main group metal carbon nucleophiles (Hard nucleophiles), such as; Grignard reagents, organocopper and organozinc *etc.* nucleophiles, allenylpalladium complexes undergo transmetallation to yield allenylpalladium complex **14** which leads to an allene derivative **15** via reductive elimination step which composes type **2** reactions.

Since the central sp carbon atom of allenyl palladium intermediate **10** highly electron deficient, it readily reacts with soft nucleophiles which leads to type **3** reactions. The reaction with a nucleophile from central sp atom generates a carbene palladium complex intermediate **16**. Protonation of the intermediate **16**, hence, generates a π -allyl palladium complex **17**. π -Allyl palladium complex further reacts with a nucleophile and the alkene **18** is observed.

The reaction of propargylpalladium complex **19** is known as type **4** reactions. Propargylpalladium complexes undergo direct hydride addition or elimination reactions to form alkyne species **20** and **21**.

Because of its relevance to the subject of this study, in the following section the literature survey will be focused on palladium catalyzed type **2** reactions of propargyl compounds. Besides, in the section about the transition-metal-catalyzed synthesis of vinylallenes other reaction types will also be discussed.

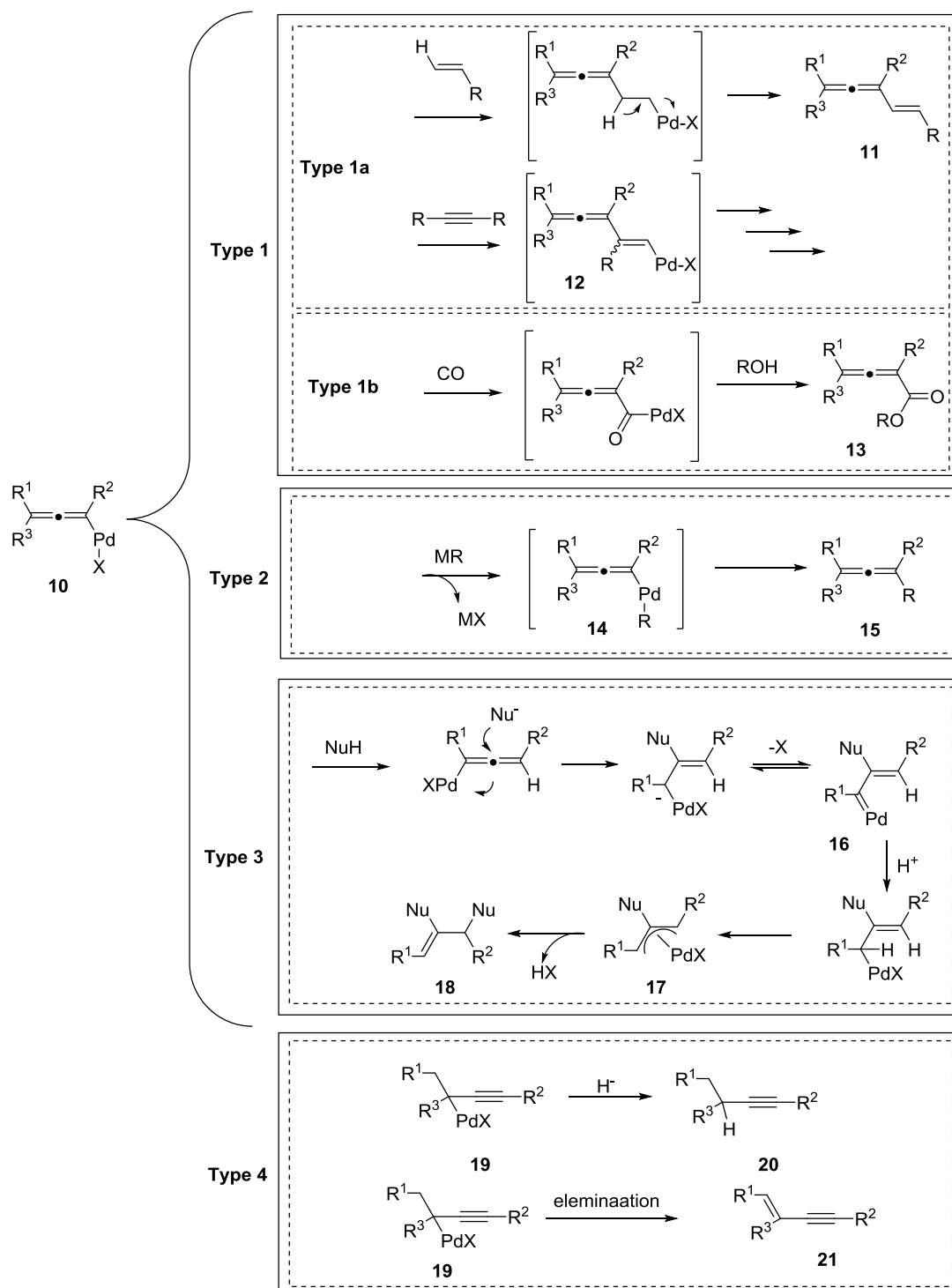


Figure 2.2. Type 1, 2, and 3 of allenylpalladium complexes and type 4 as β -hydride elimination. (Source: Tsuji, 2000)

2.1.2. Palladium-Catalyzed Type 2 Reactions of Propargyl Compounds

An early approach by Luong group reports the palladium catalyzed coupling of propargyl chloride **22** with Grignard reagents in fair to good yields. (Figure 2.3) (Jeffery-Luong and Linstrumelle, 1980).

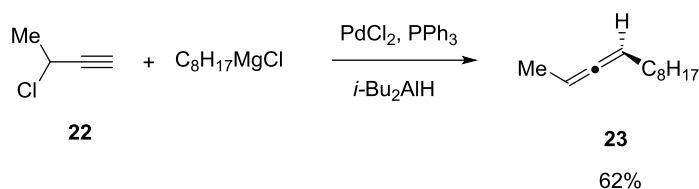


Figure 2.3. Palladium-catalyzed coupling of Grignard reagents with propargyl chlorides.

Vermeer *et al.* reported that *R*-(-)-1-trifluoroacetoxy-1-phenyl-2-propyne (**23**) when reacted, in proper conditions, with $PhZnCl$ formed allenes in excellent yields. The stereo- and region-selectivities of the reaction were also superior. The insertion of the palladium at first takes place, and then follows by transmetalation with $PhZnCl$ to form allenyl(phenyl)chloride. The reductive elimination then produces aryl-substituted allenes (Figure 2.4) (Elsevier *et al.*, 1983).

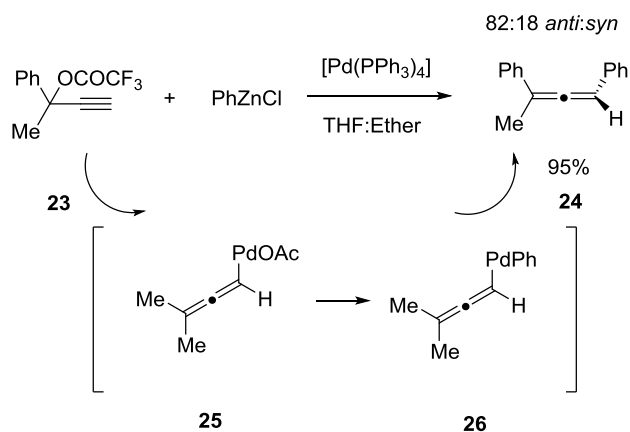


Figure 2.4. Palladium-catalyzed addition of organozinc compounds to propargyl acetates.

The reaction of propargyl carbonates and terminal alkynes in the presence of copper or palladium were studied by the Tsuji group in 1990 (Mandai et al., 1990). The copper activation of terminal alkynes produced active organocuprates. Organocuprates react with σ -allenyl palladium complex, inducing transmetalation. Following the reductive elimination of the palladium yield alkynyl allenes (Figure 2.5).

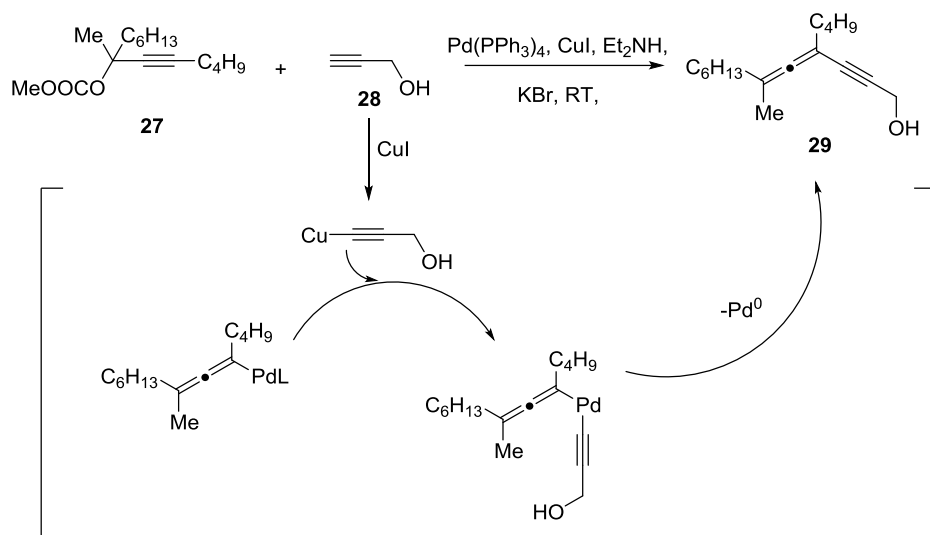


Figure 2.5. Palladium/copper-catalyzed coupling reaction of terminal alkynes with propargyl carbonates.

Darcel *et al.* used alkynyl cyclic carbonates (**30**) with phenyl acetylene (**31**) to achieve allenylmethyl alcohols (**32**) via $\text{Pd}(0)$ catalyzed reaction (Darcel et al., 1994). The mechanistic pathway proposed is the same as that of propargyl carbonates as mentioned above (Figure 2.6).

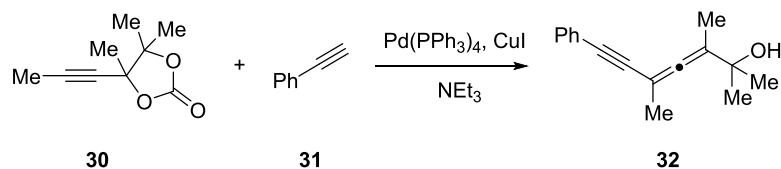


Figure 2.6. Palladium/copper-catalyzed coupling reaction of terminal alkynes with cyclic propargyl carbonates.

Yoshida *et al.* (Yoshida et al., 2007) reported the palladium-catalyzed coupling of propargylic oxiranes with terminal alkynes (**33**). An optically active anti-substituted allene (**34**) was synthesized from the reaction of an enantiomerically enriched propargylic oxirane (**35**) without loss of chirality (Figure 2.7).

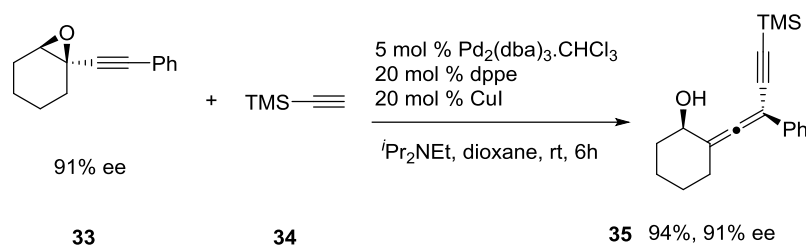


Figure 2.7. Palladium/copper-catalyzed coupling of terminal alkynes with propargylic oxiranes **33**.

2.1.3. Iron-Catalyzed Reactions of Propargyl Compounds

Patso and coworkers (Pasto et al., 1976) developed a method for the $\text{S}_{\text{N}}2'$ addition of Grignard reagents on propargyl chlorides (**36**) in the presence of catalytic FeCl_3 , which produced allenes (**37**) in fair to good yields. The reaction was also suitable for terminal propargyl chlorides (Figure 2.8).

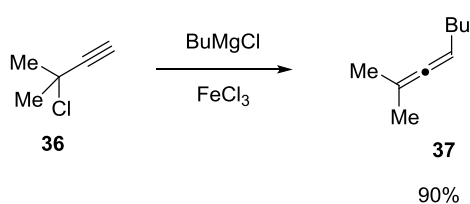


Figure 2.8. Synthesis of allenes from propargyl chlorides via $\text{S}_{\text{N}}2'$ type substitution with Grignard reagents over the catalytic amount of FeCl_2 .

Fürstner's group (Fürstner and Méndez, 2003) inspired from the study of Patso *et al*, synthesized allenol derivatives from propargyl oxiranes through an iron-catalyzed procedure using Grignard reagents. The product allene (**39**) could be obtained in high yields and *syn* selectivity (Figure 2.9).

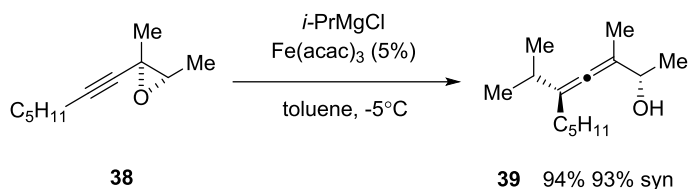


Figure 2.9. Synthesis of allenes from propargyl bromides via $\text{S}_{\text{N}}2'$ *syn*-selective substitution over an iron catalyst.

Kessler and Bäckvall (Kessler and Bäckvall, 2016) reported a mild, facile, and efficient iron-catalyzed synthesis of substituted allenes from propargyl carboxylates (**40**) and Grignard reagents. Only 1–5 mol% of the iron catalyst was enough to yield a wide range of substituted allenes (**41**) (Figure 2.10). Also, they observed a temperature dependent chirality transfer from an enantiomerically enriched substrate, (*S*)-3-phenylpropynyl pivalate (**42**) with Grignard reagents to form **43** and **44** (Figure 2.11).

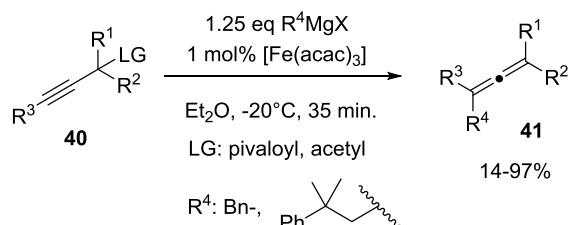


Figure 2.10. Synthesis of allenes from propargyl carboxylates via $\text{S}_{\text{N}}2'$ pathway.

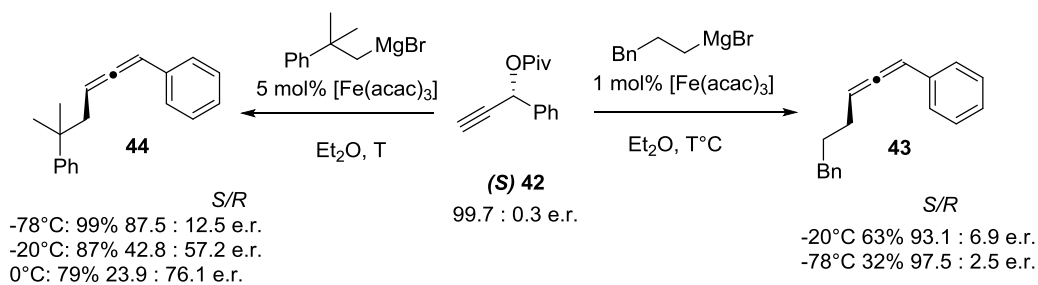


Figure 2.11. A temperature dependent synthesis of optically active allenes from **42**

2.1.4. Reactions of Propargyl Compounds in the Presence of Various Transition Metals

The first known synthesis of alkylated allene **46** from propargyl acetate **45** via S_N2' mechanism with dialkylcuprate reagents was reported by Rona and Crabbe (Rona and Crabbe, 1968). This innovation brings the popularity for the synthesis of allenes by organocoppers (Figure 2.12).

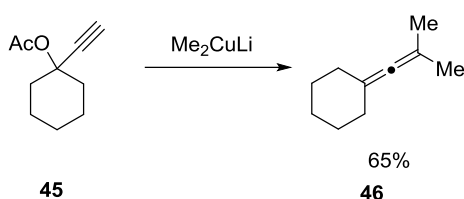


Figure 2.12. Synthesis of allenes from propargyl acetates via S_N2' substitution with dialkylcuprates.

Gooding and coworkers (Gooding et al., 1991) reported the synthesis of the allenic structure (**49**) by an *anti*-selective S_N2' reaction of an organocopper with a propargyl bromide in gram scales which has an antifungal activity (Figure 2.13).

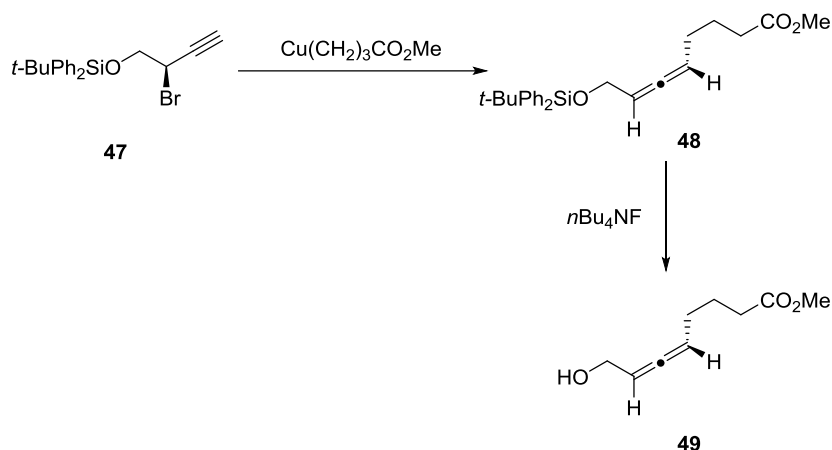


Figure 2.13. Synthesis of allenes from propargyl bromides via *anti*-selective S_N2' substitution with organocuprates.

Aurrecoechea *et al* (Aurrecoechea *et al.*, 1998) concluded that samarium diiodide catalyzes the reaction of propargyl oxiranes (**50**) and ketones (**51**) to produce dihydroxy allenes (**52**) in anti-selective S_N2' type substitution without the need of a palladium catalyst (Figure 2.14).

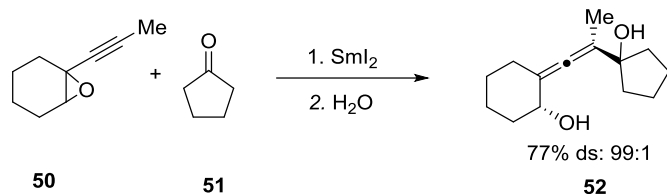


Figure 2.14. Synthesis of allenes from propargyl bromides via S_N2' *anti*-selective substitution over samarium diiodide.

Copper-catalyzed coupling of polyfluoroarenes (**53**) with propargyl phosphates (**54**) has been reported by Nakatani and co-workers (Nakatani *et al.*, 2012). The synthesis biologically important building blocks (polyfluoroaryl)allenes (**55**) obtained in a simple and fast way (Figure 2.15).

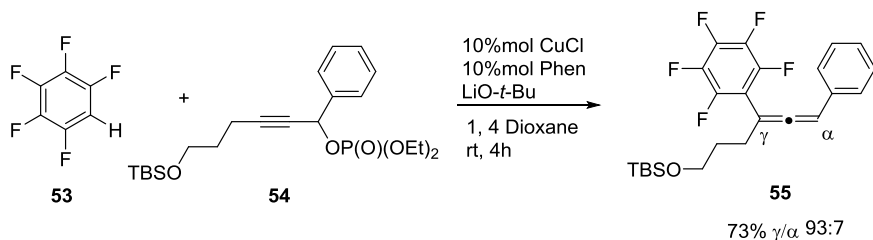


Figure 2.15. A copper-based catalyzed direct coupling of polyfluoroarenes with propargyl phosphates.

Ready group applied $\text{Cp}_2\text{Zr}(\text{H})\text{Cl}$ to the anti- S_N2 -type reductive substitution of the propargylic alcohols (**56**) produced allenes (**57**) in good yields and in high optical purities (Figure 2.16). This approach provides direct and stereospecific access to allenes directly from propargylic (Pu and Ready, 2008).

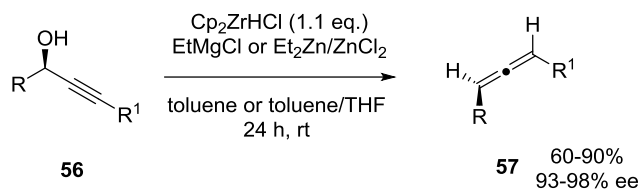


Figure 2.16. S_N2 -type reductive substitution of propargylic alcohols by $\text{Cp}_2\text{Zr}(\text{H})\text{Cl}$ to yield allenes.

2.2. Transition-Metal-Catalyzed Reactions of Allyl Compounds

2.2.1. Palladium Catalyzed Reactions of Allylic Compounds

Allylic compounds undergo palladium-catalyzed reactions via the intermediate of π -allylpalladium complexes. In a synthetic manner π -allylpalladium complexes (**58**) offer many valuable methods for the synthetic chemistry. In the report of Tsuji and co-workers, they exhibited that the π -allylpalladium complexes are naturally electrophilic to react with malonate and acetoacetate nucleophiles (Tsuji et al., 1965). Electrophilic π -allylpalladium complexes react with various kinds of nucleophiles of carbon, oxygen, and nitrogen. A summary of reactions of π -allylpalladium complexes shown in figure 2.17.

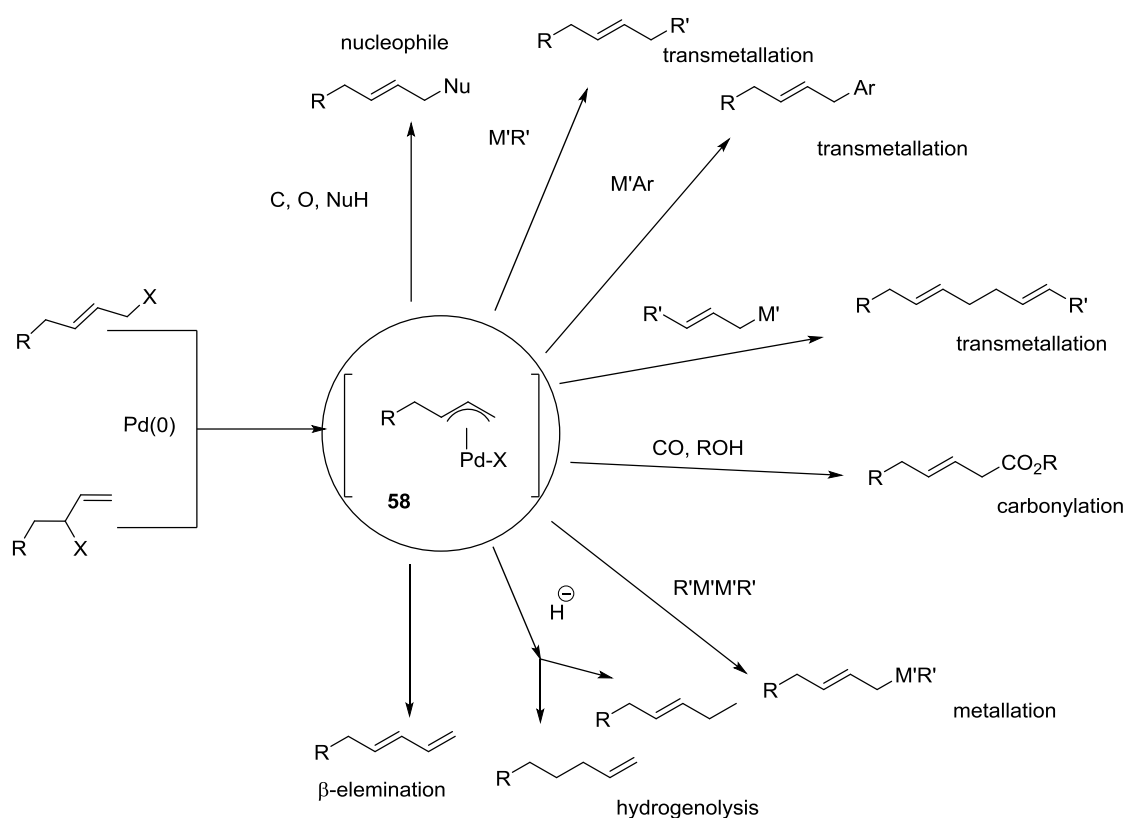


Figure 2.17. Schematic illustration of synthetic methods involving π -allyl-palladium complexes.

2.2.2. Transmetalation of π -Allylpalladium Complexes

Allylic compounds (**59**) react with palladium to undergo cross-coupling with main group organometallic compounds. Substitution occurs mainly at less hindered position of allylic terminal (Tsuji, 2000).

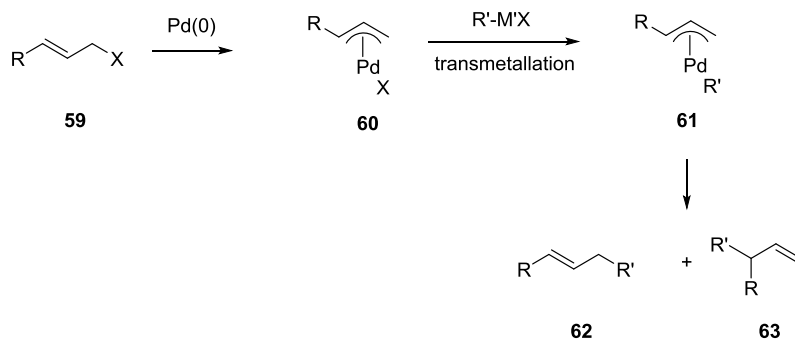


Figure 2.18. Mechanism of transmetalation of main group metals with π -allylpalladium.

Murahashi and co-workers (Murahashi et al., 1993) demonstrated that the allyl phosphates react with carbon monoxide in the presence of palladium/triphenylphosphine catalytic system to undergo alkoxy carbonylation reactions. β , γ -Unsaturated esters formed in high yields with excellent stereoselectivities (Figure 2.19).

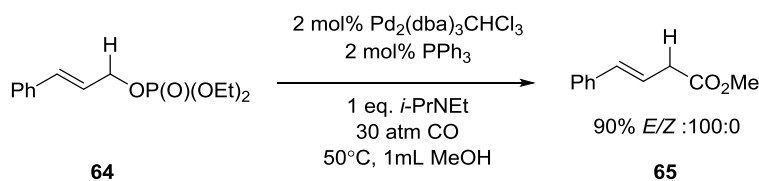


Figure 2.19 Alkoxy carbonylation of allyl phosphates.

In 2002 Rosales and co-workers reported a highly regio-selective palladium-catalyzed benzylation reaction of allylic bromides with Grignard reagents. The *trans* polyene homobenzene derivatives were obtained in excellent yields and with superior regio-selectivities. (Rosales et al., 2002).

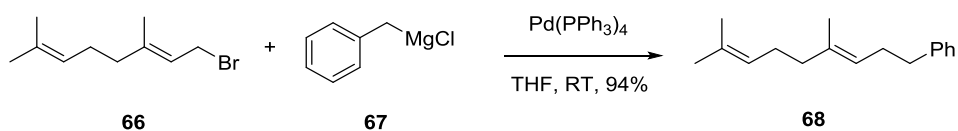


Figure 2.20. Palladium-catalyzed synthesis of *trans* polyene homobenzene derivatives with Grignard reagents.

In 2000, Matsubara and co-workers performed a coupling reaction of cinnamyl acetate (**69**) and 1,1-bis(iodozinc) ethane (**70**) in the presence of a palladium-chiral phosphine catalyst afforded an optically active homoallyl zinc compound. Although yields of allene **71** obtained were high enantiomeric excess found were low (22%) (Matsubara et al., 2000).

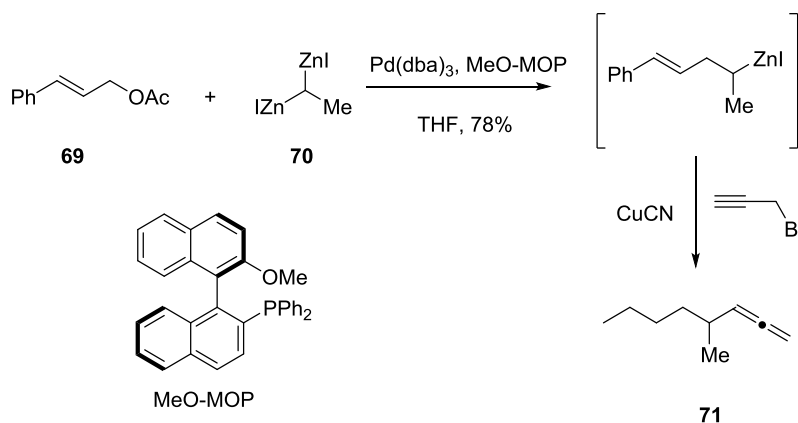


Figure 2.21. Synthesis of allene derivatives via homoallyl zinc intermediate.

2.2.3. Iron-Catalyzed Reactions of Allyl Compounds

Yamamoto and co-workers summarized the results obtained in the reaction of primary allylic phosphates (**72**) using a combination of a Grignard reagent and catalytic amounts of Fe(acac)₃ (Figure 2.22). The reaction proceeded at low temperatures with high selectivity in favor of the S_N substitution product (**73**) independent of the double bond geometry (Yanagisawa et al., 1991).

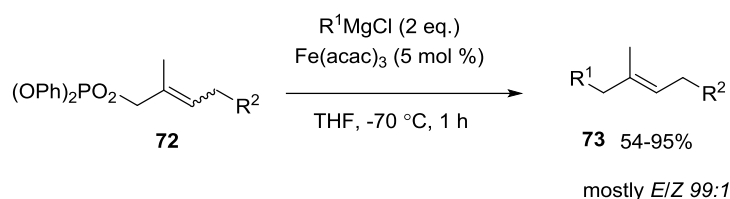


Figure 2.22. Reactions of allylic phosphates with Grignard reagent catalyzed by iron salts.

Plietker's group performed iron-catalyzed (TBAFe) allylation reactions (Plietker, 2006). Various allyl carbonates (**74**) and nucleophiles reacted under the established conditions to yield the products **75** with excellent regioselectivities (Figure 2.23).

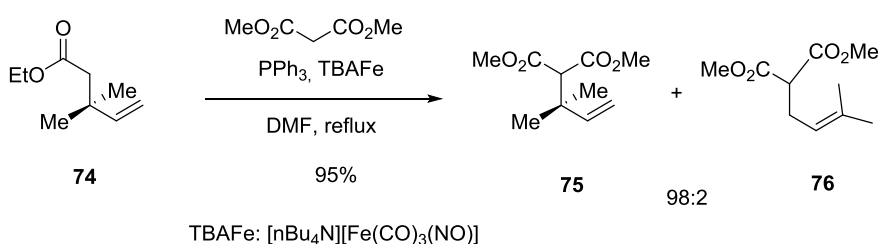
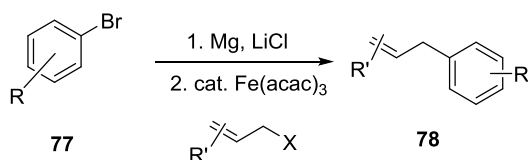


Figure 2.23. Reactions of allyl carbonates with nucleophiles over TBAFe catalyst.

Wangelin group (Mayer et al., 2010) accomplished iron-catalyzed arylation of allylic reagents with variety of leaving groups such as acetates, tosylates, diethyl phosphates, methyl carbonates, trimethylsilanolates, methanethiolates, chlorides, and bromides. In all cases the formation of *E*-alkenes was observed (Figure 2.24).



X: Br, Cl, OAc, OTs, OTMS, OP(O)(OEt)₂, OCO₂Me, SME

Figure 2.24. Fe(acac)₃-catalyzed allylic arylation of allyl acetates.

Hata and co-workers investigated the reaction between γ , δ -Epoxy- α , β -unsaturated esters (**79**) and Grignard reagents were reacted to give homoallyl alcohols (**80**) in good yields as single diastereoisomers (Figure 2.25). The nucleophile attacks regioselectively at the allylic epoxide carbon with inversion of the configuration at this center. This observation was explained by the formation of an intermediate η^3 -allyliron complex which stereoselectively transfers an alkyl ligand (Hata et al., 2010).

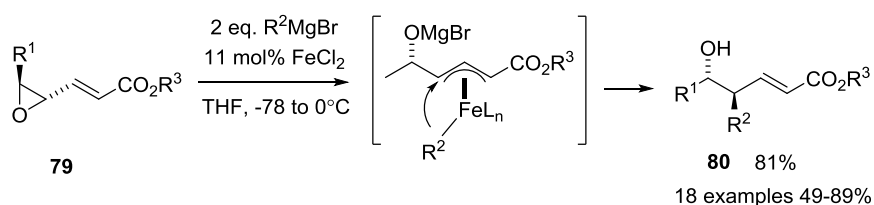


Figure 2.25. Reaction between Grignard reagents with unsaturated esters in the catalytic presence of FeCl₂.

Sherry and Fürstner reported the reaction of vinylcyclopanes (**81**) and the alkyl Grignard species catalyzed by Fe(acac)₃. Reaction enables of regioselective attack of the nucleophile at the double bond in an S_N2 fashion. Good diastereoselectivity in favor of the *E*-olefin **82** was achieved. Nucleophilic addition mechanism is preferred over radical or η^3 -allyliron based pathways (Sherry and Fürstner, 2009).

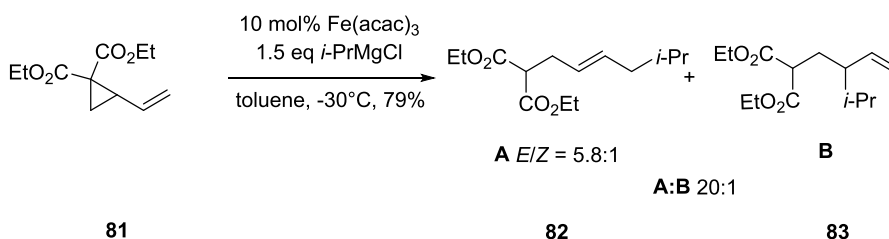


Figure 2.26. Fe(acac)₃ catalyzed allylic alkylation of vinylcyclopanes.

2.3. Transition-Metal-Catalyzed Synthesis of Vinylallenes

An early approach by Gore and Dulcere (Gore and Dulcere, 1972) provided the synthesis of vinylallenes (**85** and **86**) in moderate yields via the reaction of chloro enyne (**84**) with MeMgI or trimethylsilylmagnesium chloride without using any catalyst (Figure 2.27).

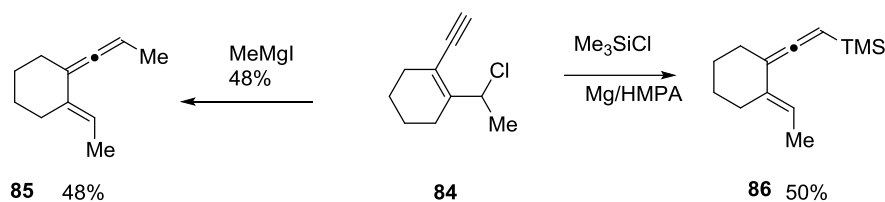


Figure 2.27. Synthesis vinylallenes with Grignard reagents.

Tolstikov and co-workers (Tolstikov et al., 1985) acknowledged that with iron catalysis, propargyl acetates (**87**) undergo alkylation reactions by organoaluminums, leading to vinylallenes (**88**) in good yields (Figure 2.28).

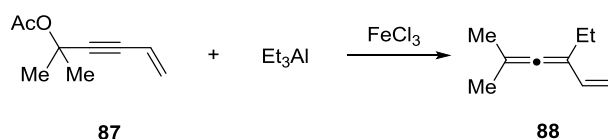


Figure 2.28. Synthesis of vinylallenes via organoaluminum reagents.

A simple Pd-catalyzed alkenylative reaction of propargyl carbonate was applied by Tsuji group (Mandai et al., 1991), to synthesize vinylallenes (**91**) in good yield (Figure 2.29).

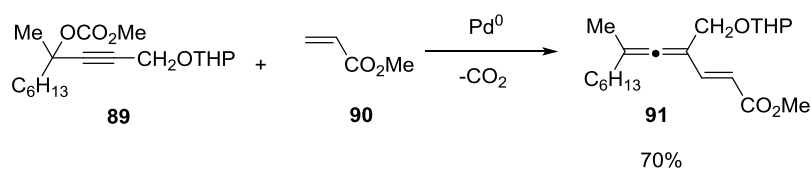


Figure 2.29. Palladium-catalyzed synthesis of vinylallenes via alkenylation of propargyl carbonates.

Krause and Purpura (Purpura and Krause, 1999) obtained vinylallene derivatives by the reaction of enyne acetates with lithium dialkylcuprates. Not all the substrate reacts with in in good diastereoselectivity but enyne derivative substituted with *t*-Bu in R² and Bu in R¹ position produced vinylallene with MeCuLi mostly in *E* configuration (Figure 2.30).

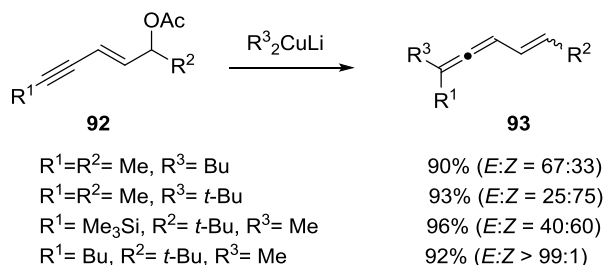


Figure 2.30. Palladium-catalyzed synthesis of a vinylallenes (**92**) via the reaction of enyne acetate (**93**) with lithium dialkylcuprate.

The synthesis of vinylallenes via rhodium-catalyzed arylation of enyne derivatives was reported by the Artok's group (Üçüncü et al., 2011). With the optimized reaction conditions, the reaction was tolerable for both electron withdrawing and donating arylboronic acids.

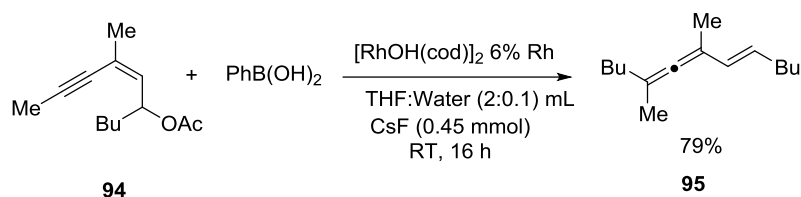


Figure 2.31. Synthesis of vinylallenes via the rhodium-catalyzed arylation of enyne acetates.

Artok group reported (Karagöz et al., 2014) the alkoxy carbonylation of enantio-enriched enyne carbonate **96** under a balloon pressure of carbon monoxide in the catalytic presence of palladium/DPEphos combination, which proceeded with excellent center-to-axial chirality transfer to produce the corresponding vinylallenoate structure **97** vinylallene with a high ee.

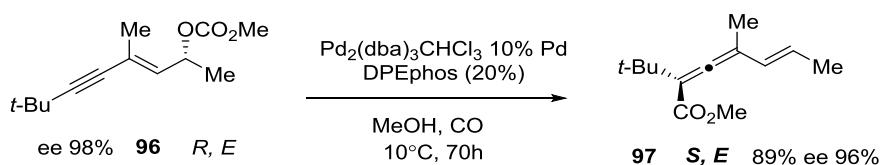


Figure 2.32. Palladium-catalyzed enantioselective synthesis of the vinylallene **92** via an alkoxy carbonylation method.

CHAPTER 3

EXPERIMENTAL STUDY

3.1. General Methods

Prepared substrates and products were purified over silica gel by column or flash chromatography (Teledyne Isco Combiflash Companion Personal Flash Chromatography System) with hexane or hexane/ethyl acetate as eluent system. Yields of crude mixtures and purity of prepared substrates were determined by quantitative $^1\text{H-NMR}$ technique, using *p*-anisaldehyde as the internal standard (Hays and Thompson, 2009). Pure samples were analyzed via: GC-MS (Thermo/ISQ) equipped with Thermo TR-5MS (30 m, 0.25 mm ID) column; nuclear magnetic resonance (NMR) spectra were acquired on Varian VnmrJ 400 spectrometer, CDCl_3 was used as the NMR solvent and chemical shifts reported in δ (ppm); a Perkin-Elmer Spectrum 100 used to achieve infra-red spectra by ATR method with dry samples; high-resolution mass spectral analyses were performed at the Dortmund University of Technology Mass Spectrometry Laboratory on a Thermo Electron system.

Aryl- or alkylmagnesium halides were purchased from Sigma-Aldrich and used as received. Molarity of Grignard reagents were determined according to study of Watson and Eastham (Watson and Eastham, 1967). Palladium catalysts were used as $\text{Pd}_2(\text{dba})_3 \cdot \text{CHCl}_3$ (Zaleskiy and Ananikov, 2012) or $\text{Pd}[\text{P}(\text{C}_6\text{H}_5)_3]_4$ (Brandsma, Verkrujisse, and Vasilevsky, 1999) and synthesized in our laboratory.

For substrate synthesis: Diethyl ether was dried under argon gas with a mixture of sodium metal and benzophenone. Tetrahydrofuran (THF) and dichloromethane (DCM) was dried via simple storage of the solvent over activated 3\AA molecular sieves (include (Deperox[®] for THF) for 2 days (Williams and Lawton, 2010).

For catalytic experiments: THF was dried under argon with a mixture of sodium metal and benzophenone for the Pd/Cu-catalyzed alkynylation reactions. For the iron catalyzed alkylation reactions, THF was dried with LiAlH_4 . KBr, KI, LiCl, LiBr and NaI was dried under vacuum at $130\text{ }^\circ\text{C}$. Amine bases refluxed over KOH and stored under

CaO in order to obtain better purity for catalytic experiments (Armarego and Chai, 2014). *Iso*-Propyl alcohol was dried over activated 3Å molecular sieves (Jain and Gupta, 1994).

3.2. Preparation of Substrates

3.2.1. Preparation of E-Enyne Derivatives

The preparation of *E*-enyne acetates and carbonates were synthesized as reported in the following sections. Summary of all reaction steps were depicted in a schematic pathway, in Figure 3.1.

3.2.1.1. Step A

Into the neat mixture of enyne alcohol (**S1a** R²: Me) and 3,4-dihydropyran (1.1 eq), *p*-toluenesulphonic acid (0.005 eq) was added at room temperature and stirred for 2 hours to yield quantitatively **S2a**. Following the protection of **S1a**, nucleophilic substitution of enyne alcohol derivative **S2a** was performed without purification (Step a was skipped for the synthesis of R¹: H, R²: Me, and gone straight to oxidation step d).

The crude residue of **S2a** was dissolved in 200 mL of dry THF and the mixture was cooled down to -78 °C, under an Ar atmosphere. 2.5 M solution of BuLi in hexane (1.2 eq) was added drop wise via a syringe. Mixture continued stirring about 2 hours at room temperature. Solution was then cooled down to -78 °C. Following the addition of 6 eq of bromobutane in small proportions, reaction media was refluxed for 4 days (overnight at room temperature when the alkyl halide used as MeI). Proved by TLC analyses, reaction mixture cooled down to RT then quenched with saturated solution of NH₄Cl. Mixture was extracted with diethyl ether and then organic layer was dried over MgSO₄. After filtration of MgSO₄, solution concentrated under vacuum to obtain **S2a** (Betzer et al., 1997).

Without further purification compound **S2a** was diluted with 150 mL of technical grade methanol. While stirring the solution of substrate **S2a**, 0.3 equivalent of *p*-toluenesulphonic acid was added in one proportion at room temperature. After completion

of the reaction, proved by TLC analyses, 0.6 eq of triethylamine was added to quench the media. Crude mixture was concentrated under vacuum, and then organic phase was extracted with DCM. Organic layer was dried with MgSO₄ then filtered. Filtrate was concentrated under vacuum and then purified with column chromatography (10:1 hexane/ethyl acetate as the solvent system) to yield **S3a** (R¹: Me, R²: Me 88%; R¹: Bu, R²: Me 78%) (Purpura and Krause, 1999).

3.2.1.2. Step B

In an oven dried Schlenk flask under a stream of Ar gas was charged corresponding propargyl ester (1 M), 2 mol % of Pd(OAc)₂ and 2% mol of TDMPP in dry degassed THF. Mixture was stirred for 5 minutes until color change appears from black to red. Following the change of color, corresponding solution of alkyne (1 M, 1.5 eq) in THF was added via syringe dropwise. Reaction was surveyed until the substrates consumed proved by TLC analyses. Final solution was filtered over a layer of Celite, then concentrated under reduced pressure. Crude product was purified by column **S3b** (R¹: *t*-Bu, R²: Me 78%; R¹: Cy, R²: Me 81%; R¹: Ph, R²: Me 88%; R¹: Bu, R²: Ph 86%; R¹: Bu, R²: Cy 68%; R¹: Bu, R²: Bu 82%) (Troost et al., 1997).

Enyne ester **S3b** was then reduced into enyne alcohol **S1d** with a solution of DIBAL-H (1 M in DCM) in a flask under inert Ar atmosphere. A solution of enyne alcohol **S3b** (1 M in DCM) at -78 °C was added 1.4 eq of DIBAL-H dropwise via syringe. Solution was then stirred at -78 °C for 1 hour and for 5 hours at RT. After completion of the reaction was monitored by TLC, 1 M solution of HCl was used to quench the reaction in an ice bath. Aqueous phase was extracted with dichloromethane, and the organic phase was then dried over NaSO₄, filtered and concentrated in under reduced pressure. Crude product was purified by column chromatography on silica using ethyl acetate in hexane as eluent system to give the enyne alcohol **S1d** (R¹: *t*-Bu, R²: Me 81%; R¹: Chex, R²: Me 88%; R¹: Ph, R²: Me 85%; R¹: Bu, R²: Ph 81%; R¹: Bu, R²: Cy 88%; R¹: Bu, R²: Bu 90% from pathway *c* R¹: Bu, R²: H 68%) (Garrais et al., 2009).

3.2.1.3. Step C

An acetic acid (6 eq) suspension of NaI (1.5 eq) was heated up to 70°C. Methylpropiolate was added in one proportion into suspension. The mixture stirred for 24 hours under reflux conditions in an inert atmosphere. Solution was cooled down to room temperature, diluted with water and diethyl ether. In an ice bath mixture neutralized with 2 M aqueous solution of KOH. Then aqueous phase was separated, extracted with DCM. Combined organic phases were dried over MgSO₄, filtered through a filter paper and concentrated under reduced pressure to yield **S2c** in 99% yield (Garrais et al., 2009).

57% v/v, solution of hydriodic acid in water (0.15 eq) was added to a solution of benzene and vinyl iodide (**S2c**) (2 M) was stirred at 80°C for 3 days. Reaction flask was cooled to room temperature, and then diluted with diethyl ether. Excess iodine was neutralized with a saturated aqueous solution of sodium thiosulfate and the separated aqueous phase was extracted with diethyl ether. Organic layers were then dried over MgSO₄, filtered and concentrated in vacuum to yield vinyl iodide **S3c** in 99% (Garrais et al., 2009).

A 1 M solution of vinyl iodide **S3c** was prepared in degassed Et₃N under inert atmosphere. PdCl₂(PPh₃)₂ (10% mol) and CuI (10% mol) were added into solution and stirred for 5 minutes. Continuing stirring 1.2 eq of 1-hexyne was added dropwise into reaction. The mixture was stirred at 55 °C for at least 24 h. The reaction was diluted with Et₂O, washed with aqua, and the aqueous layer was further extracted with Et₂O. The organic phases were dried over MgSO₄, and concentrated under reduced pressure. Purification of the crude product by column chromatography on silica gel with hexane as an eluent system yield corresponding enyne-ester **S3b** (R₁: Bu, R₂: H) in 89% yield (Burns et al., 2015).

3.2.1.4. Step D

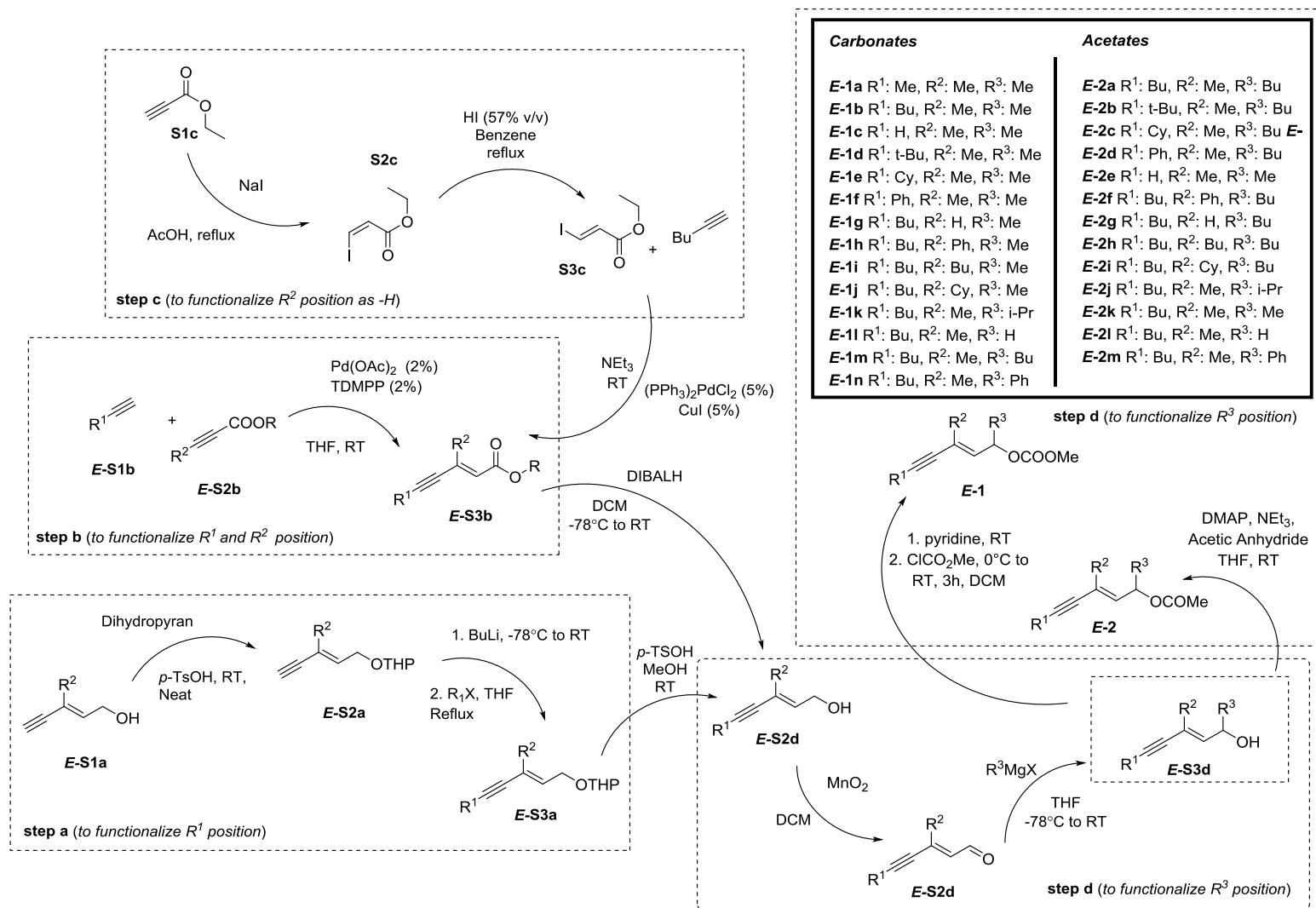
Oxidation of enyne alcohol derivative **S1d** (Step d was passed for the preparation of R¹: Bu, R²: Me, R³: H) was performed with 20 eq of MnO₂ in dry DCM (0.5 M) under an inert Ar atmosphere. While vigorously stirring the solution of enyne alcohol **S1d**, slowly addition of MnO₂ into mixture yield enyne aldehyde over 3 hours. The mixture was then filtered over a pad of silica gel/celite plug with a filtration apparatus. Solvent residue was concentrated under reduced pressure to yield enyne aldehyde **S2d** quantitatively and need no further purification (Tsuboi et al., 1990).

The crude aldehyde (**S2d**) was dissolved in anhydrous THF (1 M) and cooled down to -78°C. The mixture charged with a solution of 1.4 eq RMgCl (2-3.0 M ethereal or THF solution) by dropwise addition under Ar gas. At the end of the addition of the Grignard reagent, the mixture was warmed with stirring to RT at nearly 2 h and then, hydrolyzed by a saturated NH₄Cl solution. After extraction with diethyl ether, the combined organic layers were washed with water, dried over MgSO₄, and filtered. The solvent was removed in vacuum, and the crude residue was purified by column chromatography on silica gel (hexane/ethyl acetate, **S2d**: R¹: Me, R²: Me, R³: Me 74%; R¹: Bu, R²: Me, R³: Me 72%, Bu 67%; R¹: H, R²: Me, R³: Me 62%; R¹: t-Bu, R²: Me, R³: Me 72%, Bu 65%; R¹: Cy, R²: Me, R³: Me 77%, Bu 62%; R¹: Ph, R²: Me, R³: Me 78%, Bu 66%; R¹: Bu, R²: H, R³: Me 52%, Bu 42%; R¹: Bu, R²: Ph, R³: Me 75%, Bu 55%; R¹: Bu, R²: Cy 88%: R³: Me 50%, Bu 43%; R¹: Bu, R²: Bu 90%: R³: Me 65%, Bu 68%; R¹: Bu, R²: Me, R³: *i*-Pr 51%; R¹: Bu, R²: Me, R³: Bu 66%; R¹: Bu, R²: Me, R³: Ph 52%)

3.2.1.5. Preparation of *E*-Enyne Carbonates and Acetates

To a mixture of enyne alcohol (**S3d**) and pyridine (8 eq) in methylene chloride was added methyl chloroformate (3 eq) at 0 °C. The reaction mixture was stirred at 0 °C for 2.5 h and then quenched by addition of saturated aqueous ammonium chloride. Aqueous phase extracted with diethyl ether, dried over MgSO₄ following filtration yield crude enyne carbonate **E-1**. Solvent was removed under reduced pressure. The concentrate was purified by flash column 10:1 hexane/ethyl acetate as eluent system to obtain the desired enyne carbonates in: **E-1a** R¹: Me, R²: Me, R³: Me 85%; **E-1b** R¹: Bu, R²: Me, R³: Me 82%; **E-1c** R¹: H, R²: Me, R³: Me 76%; **E-1d** R¹: t-Bu, R²: Me, R³: Me 88%; **E-1e** R¹: Cy, R²: Me, R³: Me 83%; **E-1f** R¹: Ph, R²: Me, R³: Me 88%; **E-1g** R¹: Bu, R²: H, R³: Me 62%; **E-1h** R¹: Bu, R²: Ph, R³: Me 85%; **E-1i** R¹: Bu, R²: Bu, R³: Me 88%; **E-1j** R¹: Bu, R²: Cy, R³: Me 88%; **E-1k** R¹: Bu, R²: Me, R³: *i*-Pr 88%; **E-1l** R¹: Bu, R²: Me, R³: H 85%; **E-1m** R¹: Bu, R²: Me, R³: Bu 89%; **E-1n** R¹: Bu, R²: Me, R³: Ph 87%; **Z-1a** R¹: Me, R²: Me, R³: Me 83% (Zhao et al., 2012).

Enyne acetate substrates were prepared from corresponding enyne alcohol derivatives (**S3d**) in presence of NEt₃ (1.8 eq), acetic anhydride (1.2 eq) and catalytic amount of DMAP (5% mol) in a solution of THF. Proved by TLC to follow the disappearance of the enyne alcohol derivatives and the appearance of the enyne acetates, mixture diluted with diethyl ether, filtered over a pad of silica gel and residue concentrated under reduced pressure. Crude product isolated by column chromatography using hexane/ethyl acetate as mobile phase to yield enyne acetates in: **E-2a** R¹: Bu, R²: Me, R³: Bu 89%; **E-2b** R¹: t-Bu, R²: Me, R³: Bu 82%; **E-2c** R¹: Cy, R²: Me, R³: Bu 84%; **E-2d** R¹: Ph, R²: Me, R³: Bu 80%; **E-2e** R¹: H, R²: Me, R³: Me 75%; **E-2f** R¹: Bu, R²: Ph, R³: Bu 90%; **E-2g** R¹: Bu, R²: H, R³: Bu 88%; **E-2h** R¹: Bu, R²: Bu, R³: Bu 88% **E-2i** R¹: Bu, R²: Cy, R³: Bu 85%; **E-2j** R¹: Bu, R²: Me, R³: *i*-Pr 94%; **E-2k** R¹: Bu, R²: Me, R³: Me 85%; **E-2l** R¹: Bu, R²: Me, R³: H 88%; **Z-2m** R¹: Bu, R²: Me, R³: Ph 78% (Garrais et al., 2009).

Figure 3.1. Schematic pathway for the preparation of *E*-Enyne Carbonates and Acetates.

3.2.2. Preparation of Z-Enyne Acetate Z-2a, Z-1b and Carbonate Z-1a

The preparation of **Z-2**, **Z-1a** and **Z-1b** follows the synthetic pathway as demonstrated in earlier sections (step **a** and **d**). A summary of synthetic route to obtain **Z-2**, **Z-1a** and **Z-1b** substrates shown on Figure 3.2.

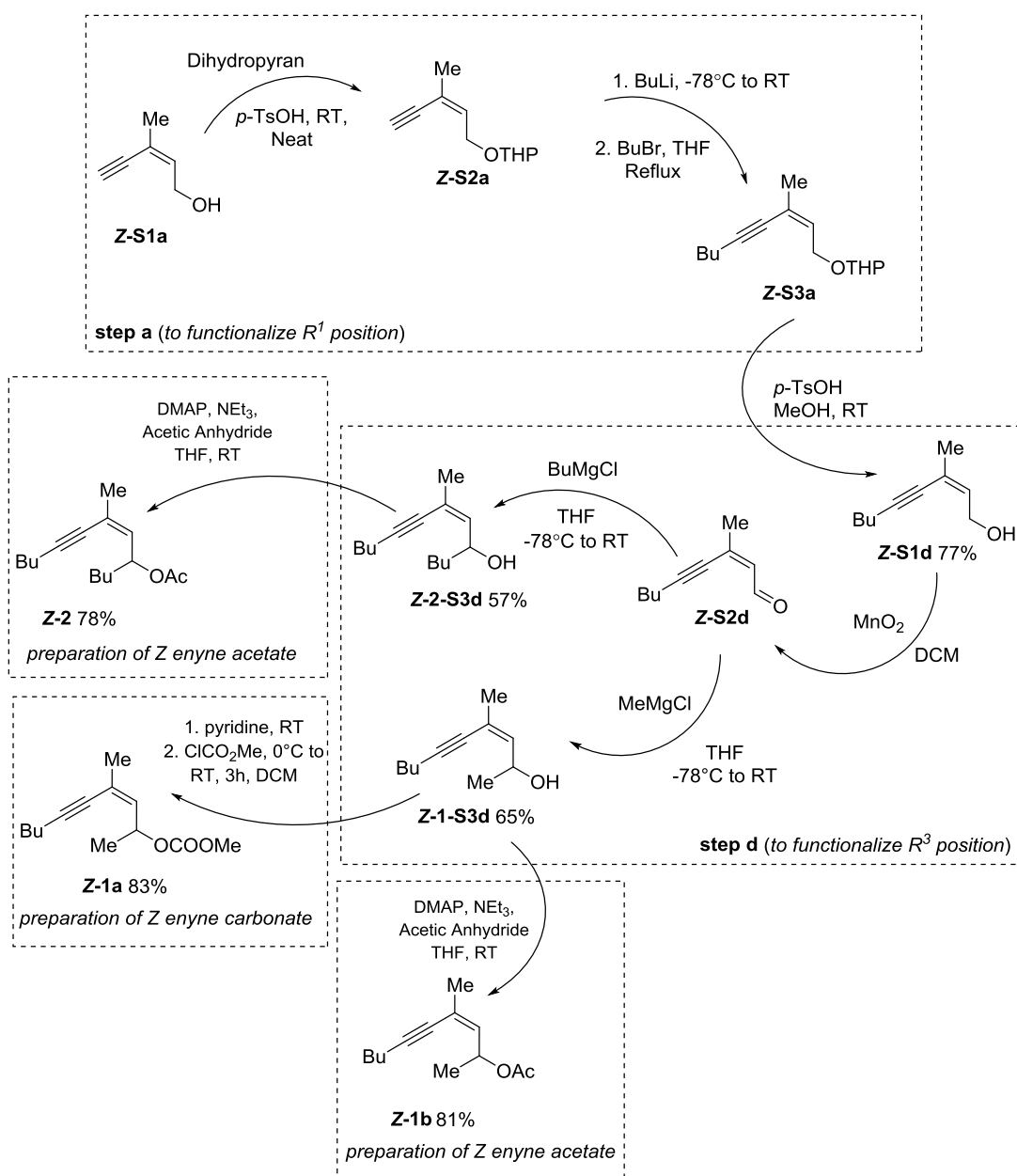


Figure 3.2. Synthetic pathway to obtain enyne acetate **Z-2**, **Z-1a** and **Z-1b**.

3.2.3. Synthesis of (*R, E*)-4-methyldec-3-en-5-yn-2-ol

%70 TBHP in water (50 mL), and then toluene (60 mL) were added to a separator funnel (No shaking preferred). The aqueous layer was separated and the organic layer was transferred to a two-necked flask equipped with a Dean-Stark trap, a reflux condenser, and a thermometer. After addition of several boiling chips, the solution was refluxed at 90 °C under Ar until all water was collected. The solution of TBHP in toluene was stored over activated 4 Å molecular sieves (Hill et al., 1983).

Sharpless's kinetic resolution (Katsuki and Sharpless, 1980) method was employed for the preparation of (*R, E*)-4-methyldec-3-en-5-yn-2-ol. Accordingly, 6.4 mmol of Ti(OiPr)₄, and 7.7 mmol of L-(+)-diisopropyl tartrate, were dissolved in 200 mL of dry DCM and cooled to -20 °C. To this mixture, dry DCM solution of 6.4 mmol of racemic mixture of (*E*)-4-methyldec-3-en-5-yn-2-ol was added and then stirred for 30 min at -30 °C. Then, 12.8 mmol of dry *t*-butyl hydroperoxide (4.3 M in toluene) was added and left in a freezer (-20 °C) for 18.5 h. After completion, a pre-cooled (0 °C) 10.3 mL aqueous solution of 11.9 mmol FeSO₄ and 19.2 mmol tartaric acid mixture was added to the reaction mixture with small portions while stirring at -20 °C. The mixture was slowly warmed to room temperature over 1 h, and then extracted with DCM. The DCM solution was concentrated by evaporation and 30 mL of Et₂O was added. The ethereal solution was cooled to 0 °C, and 30 mL of aqueous NaOH was added and stirred at this temperature for 1.5 h. Extraction with ether, drying with MgSO₄, and following column chromatography on silica gel using hexane/ethyl acetate eluent yielded the isolated product at 36%. Enantiomeric purity was determined as 98.9% ee by GC method using a Hydodex-beta-3P column (25 m, 0.25 mm ID).

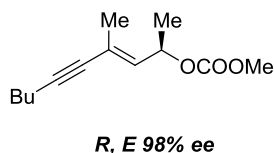


Figure 3.3. (*R, E*)-4-methyldec-3-en-5-yn-2-ol (*R, E*)-1b.

3.2.4. Preparation of Enyne Epoxides *E*-ox and *Z*-ox

To a solution of NaH (525 g, 22 mmol) in THF (50 mL) was added triethyl phosphonoacetate (4.8 mL, 24 mmol) at 0 °C, and the mixture stirred 1 h, at RT. Subsequently, to the reaction mixture was added **Z-S2d** (3 g, 20 mmol) dropwise at -78 °C and stirred for 1 h, at RT. The reaction was terminated by the addition of aqueous NH₄Cl(aq) solution and extracted with Et₂O. The organic layer was dried over MgSO₄, filtered and concentrated under reduced pressure. The crude mixture was purified on silica gel column to obtain **Z-S1-ox** in pure isomeric form (hexane-EtOAc, yield: 3.17 g, 72%), (Urabe, *et al.* 1997).

A DIBALH (44 mL, 44 mmol, 1.0 M in cyclohexane) solution was added dropwise to the solution of **Z-S1-ox** (3.85 g, 17.5 mmol) in DCM (120 mL) at -78 °C. After the reaction mixture was stirred for 4 h at the same temperature, 1 M HCl(aq) solution was added before extracting with DCM. The organic layers were combined, washed with brine, dried over MgSO₄, filtered, and concentrated under reduced pressure. The crude mixture was subjected to silica gel column chromatography to purify the corresponding **Z-S2ox** compound (hexane-EtOAc, yield: 2.65 g, 85%), (Kajikawa, *et al.* 2009).

To a solution of **Z-S2ox** (352 mg, 2 mmol) in DCM (30 mL) was added 12 mL solution of Na₂CO₃(aq) (25%) followed by 3.4 mmol (587 mg) *m*-chloroperbenzoic acid in portions at 0 °C. The mixture was stirred at the same temperature and monitored with TLC until the reactant was consumed completely. At the end of the epoxidation process, the mixture was extracted with DCM, dried over anhydrous MgSO₄, filtered, and concentrated under reduced pressure. The crude mixture was chromatographed on NEt₃-pretreated short silica gel column which afforded the enyne oxirane **Z-S3ox** as a colorless oil (hexane-EtOAc, yield: 269 mg, 70%).

A suspension of sodium hydride (1.1 eq) in DMF (1 mL) was added to a solution of **Z-S3ox** (1 mmol) in DMF (1 mL/mmol) at -20 °C. The mixture was stirred for further 30 min before the addition of methyl iodide (1.2 eq). The mixture was stirred for 4 h at the same temperature and then the reaction was terminated by the addition of MeOH (5 mL) and brine (5 mL), and extracted with DCM. The combined extracts were dried over MgSO₄, filtered, and concentrated under reduced pressure. The crude mixture was subjected to column chromatography over NEt₃-pretreated short silica gel column to

afford the corresponding alkoxy-substituted enyne oxirane products as colorless oil **Z-ox** (hexane-EtOAc, yield: 87%), (Caldentey, *et al.* 2011).

Synthesis of **E-ox** was performed starting from (*E*)-configured **E-S2d** following the same method employed for the synthesis of **Z-S2d**. Yield: ($R^1 = \text{Bu}$, $R^2 = \text{Me}$): **E-ox**, 1.12 g, 79%.

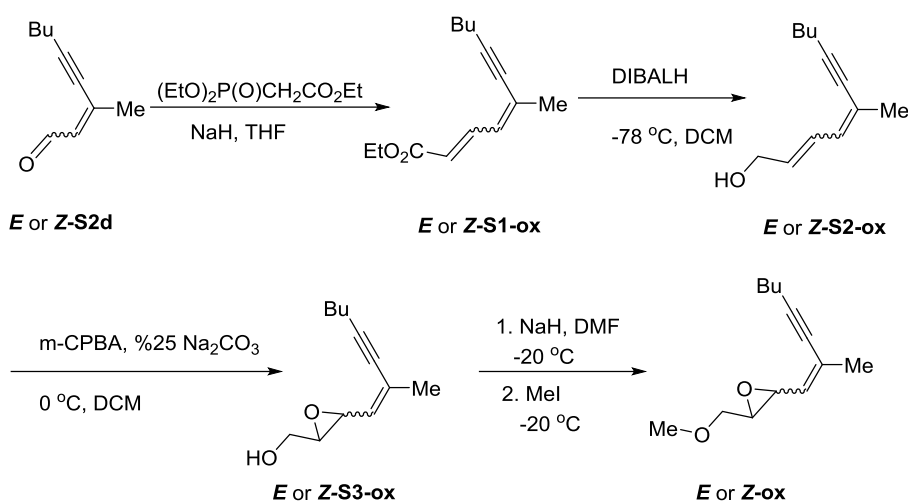


Figure 3.4. Synthesis of *E* and *Z* enyne oxiranes.

3.3 General Procedure for Catalytic Reactions

All glassware was oven-dried at $120\text{ }^\circ\text{C}$ and cooled down under positive atmosphere of argon or nitrogen, prior to use for catalytic experiments. All reactions were conducted under argon atmosphere. KI, KBr and Iron catalysts were weighted in a glow box under an inert N_2 atmosphere. CuI (99.9%) was commercial from Alfa-Easer and used as received. Before the Schlenk line, a KOH/ P_2O_5 /KOH moisture trap was also employed.

3.3.1. Palladium/Copper-Catalyzed Coupling Reactions

Method A: Coupling reaction is as follows: In a Schlenk flask; KBr (3 eq), terminal alkyne (1.5 eq), 0.2 mmol of enyne derivative and 1 mL of dry degassed THF were added. With continually stirring at room temperature, CuI (5%) and 40 eq of HNEt₂ were added and mixture stirred for 5 minutes. A preconditioned 1 mL THF solution of Pd₂(dba)₃.CHCl₃ (2% of mole) and phosphine PPh₃ (4% of mole) was drawn into a syringe and added into solution dropwise at 55°C. When the reaction was over, confirmed by TLC or the precipitation of green CuBr, mixture was filtered over a pad of silica gel and residue concentrated under vacuum. The residue was chromatographed on silica gel with hexane-ethyl acetate (10:1 v/v) as eluent to yield product (for *method b* Pd content was 4%, ligand was PPh₃ and used 16%; for *method c* Pd content was 4%, ligand was Tris(2-furyl)phosphine and used 16%).

3.3.2. Iron-Catalyzed Coupling Reactions

Into a Schlenk tube were added FeCl₂, KI and 2 mL of THF at -40 °C to prevent immediate dissolution of iron catalyst. After a bright red color was observed, 0.1 mmol of enyne acetate in 1 mL THF was added dropwise and solution allowed to cool down for 2 minutes. Grignard reagent was then transferred during 20 minutes into reaction media by syringe and a deep red color was observed. Within several hours, deep red solution was turned into brown and reaction quenched with 0.2 mL of water. Residue filtered over a plug of celite then concentrated under reduced pressure. Crude residue chromatographed on silica gel with hexane as eluent to yield product.

3.3.3. Cycloaddition Reaction of Vinyl Allene *E-1bb*

Under Ar atmosphere in a Schlenk tube 0.15 mmol of Vinyl allene *E-1bb* and N-phenylsuccinimide were added and solved with 0.5 mL of toluene. Reaction was terminated at 48 hours when vinylallene disappearance was observed on TLC. Crude mixture directly concentrated under reduced pressure, and purified by column chromatography with hexane and ethyl acetate as eluent system. Bicyclic compound *E-1bb-DA* was obtained in 65% yield. Clear structure of *E-1bb-DA* was confirmed by ¹H NOE studies (Figure 4.6).

3.4. Spectral Data for Prepared Compounds

3.4.1. Spectral Data for Enyne Carbonates

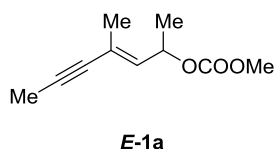


Figure 3.5. Methyl (*E*)-4-methylhept-3-en-5-yn-2-yl carbonate.

E-1a: ^1H NMR (CHLOROFORM-*d*, 400MHz) δ : 5.66 (d, $J= 9.2$ Hz, 1H), 5.43 (dq, $J= 9.2, 6.4$ Hz, 1H), 3.75 (s, 3H), 1.92 (s, 3H), 1.87 (d, $J= 1.2$ Hz, 3H), 1.33 (d, $J= 6.8$ Hz, 3H); ^{13}C NMR (CHLOROFORM-*d*, 101MHz) δ : 155.3, 134.0, 122.4, 85.0, 81.7, 71.6, 54.7, 20.5, 18.2, 4.3; FTIR ($\nu_{\text{max}}/\text{cm}^{-1}$): 2981, 2957, 2920, 2853, 2227, 1742, 1639, 1441, 1327, 1255, 1154, 1034, 938, 898, 864, 791; MS (EI, m/z): 182 (13, M^+), 167 (5), 123 (100), 107 (84), 91 (99), 79 (62). HRMS (EI, $m/z, \text{M}^+$): 182.09375 (calculated), 182.09455 (found).

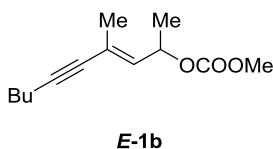
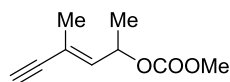


Figure 3.6. Methyl (*E*)-4-methyldec-3-en-5-yn-2-yl carbonate.

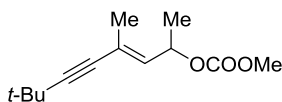
E-1b: ^1H NMR (CHLOROFORM-*d*, 400MHz) δ : 5.62 (d, $J= 9.2, ^1\text{H}$), 5.26-5.32 (m, 1H), 3.75 (s, 3H), 1.93 (s, 1H), 1.88 (d, $J= 1.2$ Hz, 3H), 1.68-1.77 (m, 1H), 1.49-1.58 (s, 1H), 1.37-1.24 (m, 4H), 0.88 (t, $J= 6.6$ Hz, 3H); ^{13}C NMR (CHLOROFORM-*d*, 101MHz) δ : 155.4, 133.1, 123.2, 85.0, 82.0, 75.2, 55.0, 34.2, 27.1, 23.0, 18.4, 14.1; FTIR ($\nu_{\text{max}}/\text{cm}^{-1}$): 2958, 2933, 2873, 2220, 1743, 1638, 1441, 1326, 1257, 1154, 1036, 939, 865, 792; MS (EI, m/z): 224 (6, M^+), 182 (9), 165 (70), 149 (50), 133 (19), 119 (41), 105 (77), 91 (100), 77 (53); HRMS: (ESI, $m/z, (\text{M}+\text{H})^+$): 225.14873 (calculated), 225.14852 (found).



E-1c

Figure 3.7. Methyl (*E*)-3-en-5-yn-2-yl carbonate.

E-1c: ^1H NMR (CHLOROFORM-*d*, 400MHz) δ = 5.83 (dd, J = 9.0, 0.8 Hz, 1H), 5.37-5.48 (m, 1 H), 3.74-3.76 (m, 3H), 2.84 (s, 1H), 1.89 (d, J = 1.6 Hz, 3H), 1.32-1.35 ppm (m, 3H); ^{13}C NMR (CHLOROFORM-*d*, 101MHz) δ = 155.0, 136.7, 120.7, 85.3, 76.0, 71.1, 54.6, 20.0, 17.6 ppm; FTIR ($\lambda_{\text{max}}/\text{cm}^{-1}$) 2957, 2931, 2860, 2244, 146 1441, 1258, 1033, 944, 791, 762, 697; MS (EI, m/z) 168 (2, M^+), 153 (4), 109 (100), 91 (77), 77 (44); HRMS (EI) calcd for $\text{C}_9\text{H}_{12}\text{O}_3$ 168.0781, found 168.0780.



E-1d

Figure 3.8. Methyl (*E*)-4,7,7-trimethyloct-3-en-5-yn-2-yl carbonate.

E-1d: ^1H NMR (CHLOROFORM-*d*, 400MHz) δ : 5.66 (dd, J = 9.2, 1.2Hz, 1H), 5.44 (dq, J = 9.2, 6.4 Hz, 1H), 3.75 (s, 3H), 1.87(s, 3H), 1.33(d, J = 6.4, Hz, 3H), 1.22 (s, 9H); ^{13}C NMR (CHLOROFORM-*d*, 101MHz) δ : 155.3, 133.7, 122.5, 97.7, 81.0, 71.7, 54.7, 31.1, 27.9, 20.5, 18.4; FTIR ($\nu_{\text{max}}/\text{cm}^{-1}$): 2969, 2929, 2902, 2868, 2205, 1744, 1442, 1327, 1255, 1150, 1038, 948, 938, 864, 791; MS (EI, m/z): 224 (6, M^+), 165 (98), 167 (23), 149 (53), 133 (74), 123 (32), 121 (41), 107 (54), 105 (100), 93(44), 91 (96), 79 (41), 77 (42), 43 (90). HRMS (EI, m/z , M^+): 224.14070 (calculated), 224.14027 (found).

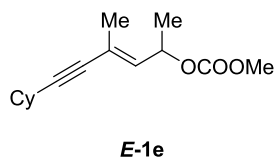


Figure 3.9. (*E*)-6-cyclohexyl-4-methylhex-3-en-5-yn-2-yl methyl carbonate.

E-1e: ^1H NMR (CHLOROFORM-*d*, 400MHz): δ : 5.97 (dd, $J= 15.2, 1.6\text{Hz}$, 1H), 5.67 (dq, $J= 15.2, 6.8\text{ Hz}$, 1H), 3.70 (s, 3H), 2.39 (tt, $J= 11.6, 3.2\text{Hz}$, 1H), 1.87(s, 3H), 1.83-1.63(m, 8H), 1.33 (qt, $J= 12.8, 3.2\text{ Hz}$, 2H), 1.15 (tt, $J= 12.4-3.2\text{Hz}$, ^1H), 1.00 dq, $J= 12.4, 3.2\text{Hz}$, 2H); ^{13}C NMR (CHLOROFORM-*d*, 101MHz) δ : 155.3, 133.7, 122.5, 93.6, 82.5, 71.7, 54.7, 32.8, 29.6, 26.0, 25.0, 20.5, 18.4; FTIR ($\nu_{\text{max}}/\text{cm}^{-1}$): 3423, 2931, 2855, 2217, 1744, 1443, 1327, 1257, 1151, 1036, 939, 864, 791; MS (EI, m/z): 250 (4, M^+), 191 (45), 175 (36), 159 (29), 145 (24), 131 (54), 117 (42), 109 (100), 105 (74), 91 (93), 81 (44), 79 (47), 77 (40), 55 (34) 43 (55). HRMS (EI, $m/z, \text{M}^+$): 250.1564 (calculated), 250.1557 (found).

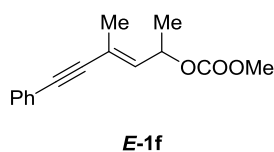


Figure 3.10. Methyl (*E*)-4-methyl-6-phenylhex-3-en-5-yn-2-yl carbonate.

E-1f: ^1H NMR (CHLOROFORM-*d*, 400MHz) δ : 7.41-7.45 (m, 2H), 7.28-7.33 (m, 3H), 5.87 (dq, $J= 8.8, 1.2\text{ Hz}$, 1H), 5.50 (dq, $J= 8.8, 6.4\text{ Hz}$, 1H), 3.77 (s, 3H), 2.00 (d, $J= 1.2\text{ Hz}$, 3H), 1.39 (d, $J= 6.4\text{ Hz}$, 3H); ^{13}C NMR (CHLOROFORM-*d*, 101MHz) δ : 155.3, 135.5, 131.7, 128.4, 123.3, 121.9, 91.3, 88.5, 71.6, 54.8, 20.4, 18.0; FTIR ($\nu_{\text{max}}/\text{cm}^{-1}$): 3059, 2982, 2956, 2923, 1741, 1489, 1441, 1328, 1255, 1142, 1036, 942, 866, 754, 690; MS (EI, m/z): 244 (6, M^+), 185 (100), 167 (90), 153 (95), 152 (88), 141 (44), 128 (38), 115 (54), 102 (22), 91 (35), 77 (36). HRMS (EI, $m/z, \text{M}^+$): 244.10940 (calculated), 244.10998 (found).

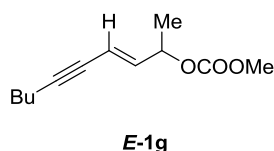


Figure 3.11. (*E*)-dec-3-en-5-yn-2-yl methyl carbonate.

E-1g: ^1H NMR (CHLOROFORM-*d*, 400MHz) δ : 5.98 (dd, $J= 16.0, 6.8\text{Hz}$, 1H), 5.72 (d, $J= 16\text{Hz}$, ^1H), 5.19 (quint, $J= 6.8\text{ Hz}$, 1H), 3.76 (s, 3H), 2.29 (t, $J= 6.8\text{Hz}$, 2H), 1.53-1.39 (m, 4H), 1.36 (d, $J= 6.4\text{Hz}$, 3H), 0.90 (t, $J= 7.2\text{Hz}$, 3H); ^{13}C NMR (CHLOROFORM-*d*, 101MHz) δ : 155.1, 139.6, 113.1, 92.6, 78.0, 74.6, 54.8, 30.8, 22.1, 20.2, 19.2, 13.7; FTIR ($\nu_{\text{max}}/\text{cm}^{-1}$): 2958, 2934, 2873, 2217, 1745, 1441, 1256, 1154, 1036, 942, 868, 791; MS (EI, m/z): 210 (2, M^+), 168 (8), 151 (66), 135 (34), 119 (11), 109 (27), 105 (22), 95 (61), 91 (100), 79 (52), 77 (38), 65 (33), 43 (67); HRMS (EI, m/z , M^+): 210.12505 (calculated), 210.12495 (found).

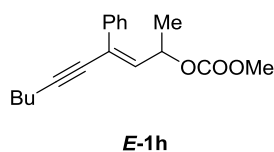


Figure 3.12. Methyl (*E*)-4-phenyldec-3-en-5-yn-2-yl carbonate.

E-1h: ^1H NMR (CHLOROFORM-*d*, 400MHz) δ : 7.37-7.29 (m, 5H), 5.99 (d, $J= 5.6\text{Hz}$, 1H), 5.33 (dq, $J= 9.6, 6.4\text{Hz}$, 1H), 3.73 (s, 3H), 2.32(t, $J= 7.2\text{Hz}$, 2H), 1.55-1.40 (m, 4H), 1.37(d, $J= 6.8\text{Hz}$, 3H), 0.91 (t, $J= 7.4\text{Hz}$, 3H); ^{13}C NMR (CHLOROFORM-*d*, 101MHz) δ : 154.9, 137.4, 135.1, 128.48, 128.43, 128.1, 127.3, 91.7, 81.5, 72.3, 54.7, 30.8, 22.1, 20.8, 19.2, 13.7; FTIR ($\nu_{\text{max}}/\text{cm}^{-1}$): 3019, 2957, 2933, 2873, 1744, 1442, 1258, 1154, 1029, 941, 866, 791, 772, 736, 699; MS (EI, m/z): 286 (2, M^+), 227 (25), 211 (20), 195 (18), 185 (14), 171 (23), 168 (51), 167 (39), 153 (35), 141 (24), 129 (22), 115 (21), 105 (8), 91 (22), 81 (21), 77 (13), 43 (100); HRMS: (ESI, m/z , $(\text{M}+\text{H})^+$): 287.16473 (calculated), 287.16417 (found).

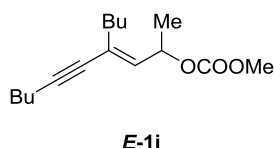


Figure 3.13. (*E*)-4-butyldec-3-en-5-yn-2-yl methyl carbonate.

E-1i: ^1H NMR (400 MHz, CDCl_3) δ 5.66 (d, $J = 9.4$, 1H), 5.46 (dq, $J = 9.2$, 6.5 Hz, 1H), 3.74 (s, 3H), 2.28 (t, $J = 6.8$ Hz, 2H), 2.24– 2.10 (m, 2H), 1.53–1.27 (m, 11H), 0.9 (t, $J = 7.6$ Hz, 6H); ^{13}C NMR (101 MHz, CDCl_3) δ 155.2, 133.5, 127.8, 90.2, 81.5, 71.4, 54.7, 31.5, 30.94, 30.75, 22.4, 22.1, 20.8, 19.1, 14.1, 13.7; FTIR ($\nu_{\text{max}}/\text{cm}^{-1}$) 2957, 2932, 2862, 2219, 1744, 1441, 1259, 1151, 1036, 941, 866, 791; MS (EI, m/z) 266 (1, M^+), 207 (24), 191 (14), 161 (9), 148 (14), 119 (29), 105 (55), 91 (83), 77 (50), 55 (52), 43 (100); HRMS (ESI) calculated for $\text{C}_{16}\text{H}_{27}\text{O}_3$ ($\text{M}+\text{H}$) 267.1956, found 267.1955.

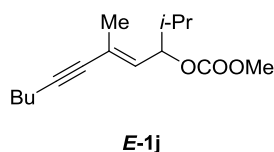


Figure 3.14. Methyl (*E*)-2,5-dimethyloct-4-en-6-yn-3-yl carbonate.

E-1k: ^1H NMR (CHLOROFORM- d , 400MHz) δ = 5.63 (dd, J = 9.6, 1.4 Hz, 1H), 5.07 (dd, J = 9.8, 7.0 Hz, 1H), 3.75 (s, 3H), 2.29 (t, J = 7.0 Hz, 2H), 1.84-1.95 (m, 4H), 1.35-1.55 (m, 4 H), 0.89-0.97 ppm (m, 9H); ^{13}C NMR (CHLOROFORM- d , 101MHz) δ = 155.4, 131.2, 123.9, 89.4, 82.6, 79.5, 54.6, 32.4, 30.8, 22.0, 18.9, 18.5, 18.1, 17.8, 13.6 ppm; MS (EI, m/z): 252 (1 > M^+), 193 (48), 165 (80), 119 (46), 105 (100), 93 (47), 91 (88), 79 (51), 55 (44), 43 (44), 41 (50).

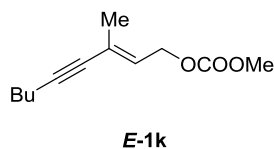


Figure 3.15. Methyl (*E*)-3-methylnon-2-en-4-yn-1-yl carbonate.

E-1l: ^1H NMR (CHLOROFORM-*d*, 400MHz): δ : 5.83 (t, $J= 7.2\text{Hz}$, 1H), 4.67 (d, $J= 7.2\text{Hz}$, 2H), 3.77 (s, 3H), 2.29 (t, $J= 6.8$, Hz, 2H), 1.85 (s, 3H), 1.53 (quint, $J= 7.2\text{Hz}$, 2H), 1.41 (sext, $J= 7.2\text{Hz}$, 2H), 0.91 (t, $J= 7.2\text{Hz}$, 3H); ^{13}C NMR (CHLOROFORM-*d*, 101MHz) δ : 155.8, 127.9, 124.9, 90.1, 82.5, 64.0, 55.0, 30.9, 22.1, 19.1, 18.2, 13.7; FTIR ($\nu_{\text{max}}/\text{cm}^{-1}$): 2958, 2933, 2873, 2219, 1748, 1442, 1378, 1329, 1254, 943, 791; MS (EI, m/z): 210 (2, M^+), 168 (16), 151 (22), 135 (30), 119 (8), 109 (16), 105 (20), 95 (71), 92 (100), 91 (71), 81(30), 79 (53), 77 (42); HRMS (EI, m/z , M^+): 210.12505 (calculated), 210.12565 (found)

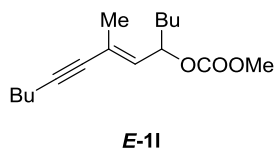


Figure 3.16. Methyl (*E*)-3-methylnon-2-en-4-yn-1-yl carbonate.

E-1m: ^1H NMR (CHLOROFORM-*d*, 400MHz): δ = 5.62 (dd, $J= 9.4, 1.2$ Hz, 1H), 5.29 (dt, $J= 9.4, 6.8$ Hz, 1H), 3.74 (s, 3H), 2.28 (t, $J= 7.0$ Hz, 2H), 1.88 (d, $J= 1.6$ Hz, 3H), 1.72 (d, $J= 7.8$ Hz, 1H), 1.23-1.57 (m, 8H), 0.85-0.93 ppm (m, 6H); ^{13}C NMR (CHLOROFORM-*d*, 101MHz) δ = 155.3, 132.8, 123.1, 89.4, 82.5, 75.1, 54.5, 34.1, 30.8, 27.0, 22.4, 21.9, 18.9, 18.3, 13.9, 13.6 ppm; MS (EI, m/z): 266 (1 > M^+), 207 (73), 165 (36), 119 (58), 106 (51), 105 (100), 93 (45), 91 (83), 79 (46), 77 (37), 41 (43).

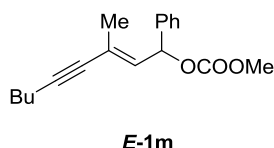


Figure 3.17. Methyl (*E*)-3-methyl-1-phenylnon-2-en-4-ynyl carbonate.

E-1n: ^1H NMR (CHLOROFORM- d , 400MHz): δ : 7.36 (d, J = 4.4Hz, 4H), 7.43-7.29(m, 1H), 6.34 (d, J = 9.2Hz, 1H), 5.93 (d, J = 9.2Hz, 1H), 3.77 (s, 3H), 2.28 (t, J = 7.2, Hz, 2H), 1.85 (s, 3H), 1.97 (d, J = 1.2Hz, 3H), 1.53-1.44 (m, 2H), 1.43-1.35(m, 2H), 0.91 (t, J = 7.2Hz, 3H); ^{13}C NMR (CHLOROFORM- d 101MHz) δ : 155.2, 138.8, 132.2, 128.7, 128.3, 126.6, 123.1, 90.2, 82.4, 76.1, 54.8, 30.8, 22.0, 19.0, 18.5, 13.6; FTIR ($\nu_{\text{max}}/\text{cm}^{-1}$): 3085, 3059, 3028, 2957, 2931, 2872, 2215, 1746, 1440, 1311, 1255, 1217, 942, 907, 878, 789, 763, 696; MS (EI, m/z): 242 (16), 227 (31), 199 (38), 185 (34), 165 (37), 153 (36), 152 (42), 141 (36), 128 (30), 115 (36), 105 (100), 91 (86), 77 (97), 41 (51).

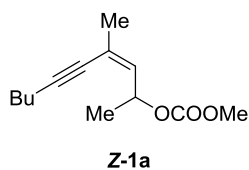


Figure 3.18. Methyl-(*Z*)- 4-methyldec-3-en-5-yn-2-yl carbonate.

Z-1a: ^1H NMR (CHLOROFORM- d , 400MHz): 6.05 (dq, J = 8.4, 2.4, Hz 1H), 5.55 (dq, J = 8.4, 1.2 Hz, 1H), 3.34 (s, 3H), 2.12 (t, J = 6.8 Hz, 2H), 1.71 (d, J = 1.2 Hz, 3H), 1.41-1.26 (m, 4H), 1.34 (d, J = 6.0 Hz, 3H), 0.80 (t, J = 7.2 Hz, 3H); ^{13}C NMR: (101 MHz, C_6D_6): δ : 155.7, 135.0, 122.3, 96.7, 79.1, 74.1, 54.0, 31.0, 23.5, 22.2, 20.5, 19.4, 13.7; FTIR ($\nu_{\text{max}}/\text{cm}^{-1}$): 2980, 2932, 1744, 1441, 1257, 1152, 1100, 1040, 941, 865, 791; MS (EI, m/z): 224 (7, M^+), 209 (2), 182 (7), 165 (100), 149 (55), 133 (21), 123 (25), 115 (5), 105 (58), 91 (88), 77 (42); HRMS: (EI, m/z , M^+): 224.1407 (calculated), 224.1403 (found)

3.4.2. Spectral Data for Enyne Acetates

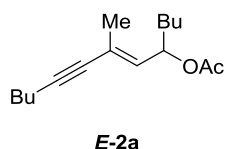


Figure 3.19. (*E*)-7-methyltridec-6-en-8-yn-5-yl acetate.

E-2a: ^1H NMR (CHLOROFORM-*d*, 400MHz): δ : 5.58 (dd, J = 9.2, 1.6 Hz 1H), 5.48-5.42 (m, 1H), 2.27 (t, J = 7.6 Hz, 2H), 2.00 (s, 3H), 1.86 (d, J = 1.6 Hz, 3H), 1.69-1.53 (m, 2H), 1.54-1.21 (m, 8H), 0.90 (t, J = 7.2 Hz, 3H), 0.88 (t, J = 7.2 Hz, 3H); ^{13}C NMR (CHLOROFORM-*d*, 101MHz) δ : 170.3, 133.5, 122.5, 89.0, 82.6, 70.8, 34.2, 30.8, 27.1, 22.5, 21.9, 21.2, 18.9, 18.3, 13.9, 13.6; MS (EI, m/z) 250 (2, M^+), 207 (52), 151 (74), 105 (38), 95 (100), 91 (38), 85 (28), 91 (30), 85 (28), 79 (28), 57 (32), 43 (55), 41 (30).

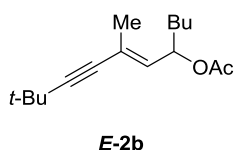


Figure 3.20. (*E*)-7,10,10-trimethylundec-6-en-8-yn-5-yl acetate.

E-2b: ^1H NMR (CHLOROFORM-*d*, 400MHz): δ = 5.59 (d, J = 9.4 Hz, 1 H), 5.47 (dd, J = 16.0, 6.7 Hz, 1H), 2.01 (s, 3H), 1.85 (s, 3H), 1.44-1.72 (m, 3H), 1.26-1.35 (m, 3H), 1.23 (d, J = 0.8 Hz, 9H), 0.89 ppm (t, J = 6.7 Hz, 3H); ^{13}C NMR (CHLOROFORM-*d*, 101MHz) δ = 170.3, 133.3, 122.4, 97.1, 81.1, 70.9, 34.2, 31.0, 27.1, 22.5, 21.2, 18.5, 13.9; MS (EI, m/z) 250 (2, M^+), 207 (34), 193 (27), 151 (100), 133 (31), 123 (32), 105 (31), 91 (28), 81 (32), 57 (36), 43 (41).

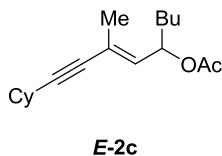


Figure 3.21. (*E*)-1-cyclohexyl-3-methylnon-3-en-1-yn-5-yl acetate.

E-2c: ^1H NMR (CHLOROFORM-*d*, 400MHz): δ = 5.57-5.63 (m, 1H), 5.47 (dt, J = 9.2, 6.9 Hz, 1H), 2.39-2.52 (m, 1H), 2.01 (s, 3H), 1.87 (d, J = 1.6 Hz, 3 H), 1.75-1.84 (m, 2H), 1.37-1.74 (m, 8H), 1.19-1.37 (m, 6H), 0.89 ppm (t, J = 7.0 Hz, 3H); ^{13}C NMR (CHLOROFORM-*d*, 101MHz) δ = 170.3, 133.4, 122.5, 93.1, 82.6, 70.8, 34.2, 32.7, 29.5, 27.1, 25.9, 24.9, 22.5, 21.2, 18.5, 13.9; MS (EI, m/z) 276 (2, M^+), 233 (46), 177 (38), 151 (83), 105 (51), 93 (100), 93 (34), 91 (47), 81 (48), 79 (32), 43 (45).

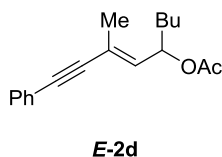


Figure 3.22. (*E*)-3-methyl-1-phenylnon-3-en-1-yn-5-yl acetate.

E-2d: ^1H NMR (CHLOROFORM-*d*, 400MHz): δ = 7.40-7.45 (m, 2 H), 7.28-7.32 (m, 3 H), 5.80 (dq, J =9.3, 1.5 Hz, 1 H), 5.52 (dt, J =9.3, 6.8 Hz, 1 H), 2.04 (s, 3 H), 1.99 (d, J =1.5 Hz, 3 H), 1.50-1.77 (m, 2 H), 1.32 (tdd, J =8.7, 4.7, 1.6 Hz, 4 H), 0.91 ppm (t, J =7.0 Hz, 3 H); ^{13}C NMR (cdcl_3 , 101MHz): δ = 170.3, 135.2, 131.5, 128.3, 128.1, 123.2, 121.9, 91.4, 87.9, 70.8, 34.1, 27.1, 22.5, 21.2, 18.0, 14.0 ppm; MS (EI, m/z) 270 (2, M^+), 228 (33), 227 (100), 185 (48), 171 (56), 128 (74), 115 (42), 91 (30), 85 (42), 57 (45), 43 (70).

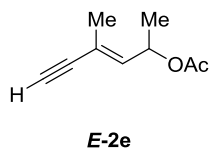


Figure 3.23. (*E*)-4-methylhex-3-en-5-yn-2-yl acetate.

E-2e: ^1H NMR (CHLOROFORM-*d*, 400MHz): δ = 5.82 (dq, $J=8.9, 1.5$ Hz, 1 H), 5.57 (dq, $J=8.9, 6.5$ Hz, 1 H), 2.83 (s, 1 H), 2.02 (s, 3 H), 1.88 (d, $J=1.5$ Hz, 3 H), 1.28 ppm (d, $J=6.5$ Hz, 3 H); ^{13}C NMR (CHLOROFORM-*d*, 101MHz) δ = 170.2, 137.5, 120.0, 85.5, 75.7, 67.0, 21.2, 20.1, 17.6 ppm.

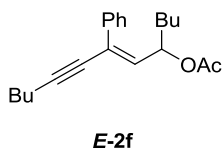


Figure 3.24. (*E*)-7-phenyltridec-6-en-8-yn-5-yl acetate.

E-2f: ^1H NMR (CHLOROFORM-*d*, 400MHz): δ = 7.28 - 7.40 (m, 5 H), 6.00 (d, $J=9.4$ Hz, 1 H), 5.34 (dd, $J=9.4, 6.3$ Hz, 1 H), 3.73 (s, 3 H), 2.32 (t, $J=7.0$ Hz, 2 H), 1.39 - 1.55 (m, 4 H), 1.37 (d, $J=6.7$ Hz, 3 H), 0.91 ppm (t, $J=7.2$ Hz, 3 H); ^{13}C NMR (cdcl₃, 101MHz): δ = 154.8, 137.3, 134.9, 128.3, 128.3, 127.9, 127.2, 110.0, 91.5, 81.4, 77.3, 77.0, 76.7, 72.2, 54.6, 30.7, 22.0, 20.7, 19.1, 13.6 ppm; MS (EI, m/z) 227 (60), 211 (46), 168 (100), 167 (95), 165 (74), 153 (85), 152 (64), 141 (44), 115 (45), 43 (66).

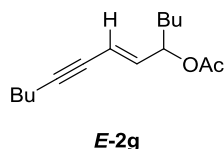


Figure 3.25. (*E*)-2,5-dimethylundec-4-en-6-yn-3-yl acetate.

E-2g: ^1H NMR (CHLOROFORM- d , 400MHz): δ = 5.92 (dd, $J=15.9, 7.0$ Hz, 1 H), 5.63 - 5.70 (m, 1 H), 5.22 (q, $J=6.4$ Hz, 1 H), 2.25 - 2.32 (m, 2 H), 2.00 - 2.05 (m, 3 H), 1.34 - 1.67 (m, 8 H), 1.21 - 1.33 (m, 4 H), 0.85 - 0.94 ppm (m, 6 H); ^{13}C NMR (cdcl_3 , 101MHz): δ = 170.2, 139.3, 112.8, 92.0, 78.0, 74.0, 33.9, 30.7, 27.1, 22.4, 21.9, 21.2, 19.0, 13.9, 13.6, 13.6 ppm; MS (EI, m/z) 236 (1, M^+), 193 (37), 137 (70), 105 (38), 95 (39), 91 (61), 85 (44), 81 (96), 57 (47), 43 (100), 41 (38).

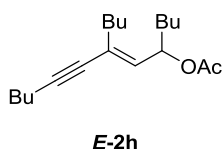


Figure 3.26. (*E*)-7-butyltridec-6-en-8-yn-5-yl acetate.

E-2h: ^1H NMR (CHLOROFORM- d , 400MHz): δ = 5.56 - 5.62 (m, 1 H), 5.50 (dt, $J=9.4, 6.6$ Hz, 1 H), 2.29 (t, $J=6.9$ Hz, 2 H), 2.19 (td, $J=8.9, 6.6$ Hz, 2 H), 2.00 (s, 3 H), 1.57 - 1.71 (m, 2 H), 1.20 - 1.56 (m, 12 H), 0.83 - 0.95 ppm (m, 9 H); ^{13}C NMR (cdcl_3 , 101MHz): δ = 170.3, 133.2, 127.9, 89.7, 81.5, 77.3, 77.0, 76.7, 70.4, 34.4, 31.4, 30.8, 30.6, 27.2, 22.5, 22.3, 21.9, 21.3, 19.0, 14.0, 13.9, 13.6 ppm MS (EI, m/z) 292 (1, M^+), 249 (60), 193 (88), 137 (45), 105 (47), 95 (100), 91 (55), 85 (53), 57 (54), 43 (61), 41 (40).

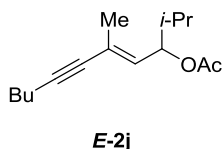


Figure 3.27. (*E*)-2,5-dimethylundec-4-en-6-yn-3-yl acetate.

E-2j: ^1H NMR (CHLOROFORM-*d*, 400MHz): δ = 5.68-5.75 (m, 1H), 4.09 (dd, J = 9.0, 6.7 Hz, 1H), 2.29 (t, J = 7.0 Hz, 2H), 1.83 (d, J = 1.5 Hz, 12 H), 1.67-1.76 (m, 4H), 1.37-1.55 (m, 4H), 0.86-0.98 ppm (m, 9H); ^{13}C NMR (CHLOROFORM-*d*, 101MHz) δ = 170.7, 136.3, 121.5, 88.6, 82.9, 73.3, 34.2, 30.9, 22.0, 18.9, 18.3, 18.1, 18.0, 13.6 ppm; MS (EI, m/z) 236 (3, M^+), 193 (30), 152 (14), 151 (94), 137 (14), 95 (100), 91 (12), 79 (11), 43 (30), 41 (12);

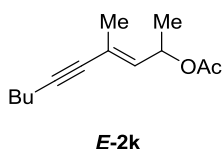


Figure 3.28. (*E*)-4-methyldec-3-en-5-yn-2-yl acetate.

E-2k: ^1H NMR (CHLOROFORM-*d*, 400MHz) δ = 5.62 (d, J = 9.2, 1H), 5.26-5.32 (m, 1H), 3.75 (s, 3H), 1.93 (s, ^1H), 1.88 (d, J = 1.2 Hz, 3H), 1.68-1.77 (m, 1H), 1.49-1.58 (s, 1H), 1.37-1.24 (m, 4H), 0.88 (t, J = 6.6 Hz, 3H); ^{13}C NMR (CHLOROFORM-*d*, 101MHz) δ = 155.4, 133.1, 123.2, 85.0, 82.0, 75.2, 55.0, 34.2, 27.1, 23.0, 18.4, 14.1, 4.3; FTIR ($\nu_{\text{max}}/\text{cm}^{-1}$) 2957, 2930, 2862, 2222, 1743, 1638, 1441, 1380, 1321, 1259, 1152, 1091, 1036, 933, 879, 866, 791; MS (EI, m/z) 224 (4, M^+), 167 (31), 148 (26), 133 (19), 123 (38), 119 (51), 105 (47), 91 (94), 77 (56).

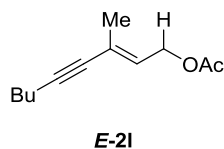


Figure 3.29. (*E*)-3-methylnon-2-en-4-yn-1-yl acetate.

E-2l: ^1H NMR (CHLOROFORM-*d*, 400MHz): δ = 5.82 (td, $J=7.1, 1.4$ Hz, 1 H), 4.61 (d, $J=7.4$ Hz, 2 H), 2.29 (t, $J=7.0$ Hz, 2 H), 2.04 (s, 3 H), 1.83 - 1.84 (m, 3 H), 1.35 - 1.54 (m, 4 H), 0.91 ppm (7.1 Hz, 3 H); ^{13}C NMR (CHLOROFORM-*d*, 101MHz) δ = 170.9, 128.5, 123.9, 89.5, 82.4, 60.6, 30.8, 21.9, 20.9, 18.9, 18.0, 13.6 ppm; MS (EI, m/z) 224 (4, M^+), 167 (31), 148 (26), 133 (19), 123 (38), 119 (51), 105 (47), 91 (94), 77 (56).

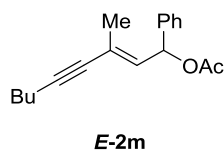


Figure 3.30. (*E*)-3-methyl-1-phenylnon-2-en-4-yn-1-yl acetate.

E-2k: ^1H NMR (CHLOROFORM-*d*, 400MHz): δ = 7.33-7.35 (m, 4 H), 7.30 (dd, $J=5.0, 3.6$ Hz, 3 H), 6.51 (d, $J=9.2$ Hz, 1 H), 5.90 (dd, $J=9.3, 1.5$ Hz, 1 H), 2.28 (t, $J=7.0$ Hz, 2 H), 2.08 (s, 4 H), 1.95 (d, $J=1.5$ Hz, 3 H), 1.35-1.54 (m, 4 H), 0.88-0.93 ppm (m, 6 H); ^{13}C NMR (cdcl_3 , 101MHz): δ = 170.0, 139.4, 132.8, 128.6, 128.0, 126.6, 122.5, 89.8, 82.5, 72.1, 30.7, 21.9, 21.2, 18.9, 18.4, 13.6 ppm; MS (EI, m/z) 270 (1, M^+), 227 (13), 210 (54), 181 (26), 167 (100), 153 (58), 141 (30), 77 (14), 43 (14).

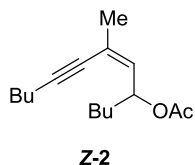


Figure 3.31. (Z)-7-methyltridec-6-en-8-yn-5-yl acetate.

Z-2: ^1H NMR (CHLOROFORM-d, 400MHz) δ 5.66 (dt, $J= 8.6, 6.8$ Hz, 1H), 5.50 (dd, $J= 8.6, 1.6$ Hz, 1H), 2.34 (t, $J= 6.8$ Hz, 2H), 2.02 (s, 3H), 1.84 (d, $J= 1.6$ Hz, 3H) 1.73-1.62 (m, 2H), 1.59-1.22 (m, 8H), 0.9 (dt, $J= 7.2, 11.6$ Hz, 6H); ^{13}C NMR (CHLOROFORM-d, 101MHz) δ : 170.2, 133.8, 122.11, 95.92, 78.67, 73.56, 34.17, 30.75, 27.09, 23.52, 22.50, 21.93, 21.29, 19.15, 13.97, 13.57.

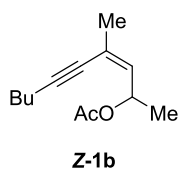


Figure 3.32. (Z)- 4-methyldec-3-en-5-yn-2-yl acetate.

Z-1b: ^1H NMR (CHLOROFORM-d, 400MHz) δ : 5.73 (dq, $J= 8.4, 6.4$ Hz, 1H), 5.56 (dq, $J= 8.4, 1.4$ Hz, 1H), 2.34 (t, $J= 7.0$ Hz, 2H), 2.02 (s, 3H), 1.83 (d, $J= 1.6$ Hz, 3H), 1.38-1.58 (m, 4H), 1.29 (d, $J= 6.4$ Hz, 3H), 0.92 (t, $J= 7.2$ Hz, 3H); ^{13}C NMR (CHLOROFORM-d, 101MHz) δ : 170.3, 134.9, 121.6, 96.4, 78.6, 70.4, 30.9, 23.6, 22.1, 21.5, 20.4, 19.3, 13.7; IR ($\nu_{\text{max}}/\text{cm}^{-1}$): 2941, 2870, 2223, 1736, 1636, 1371, 1232, 1036; MS (EI, m/z): 208 (8, M^+), 193 (8), 179 (4), 165 (100), 151 (24), 137 (14), 123 (49), 109 (88), 91 (82), 79 (47); HRMS (EI, m/z , M^+), 208.1458 (calculated); 208.1455 (measured).

3.4.3. Spectral Data for Enyne Oxiranes

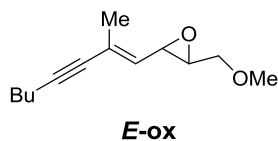


Figure 3.33. (*E*)-2-(methoxymethyl)-3-(2-methyloct-1-en-3-yn-1-yl)oxirane.

E-ox: ^1H NMR (CHLOROFORM- d , 400MHz): δ : 5.35 (dd, $J= 9.0, 1.0$ Hz, 1H), 3.67 (dd, $J= 11.3, 3.0$ Hz, 1H), 3.48 (dd, $J= 9.0, 2.2$ Hz, 1H), 3.44 (dd, $J= 11.3, 5.1$ Hz, 1H), 3.38 (s, 3H), 3.06 (ddd, $J= 5.1, 3.0, 2.2$ Hz, 1H), 2.28 (t, $J= 6.8$ Hz, 2H), 1.93 (d, $J= 1.0$ Hz, 3H), 1.54-1.37 (m, 4H), 0.90 (t, $J= 7.6$ Hz, 3H); ^{13}C NMR (100 MHz, CDCl_3) δ : 131.3, 125.2, 90.3, 82.4, 80.0, 59.2, 58.6, 51.9, 30.7, 21.9, 18.9, 18.2, 13.6.

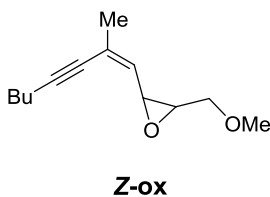


Figure 3.34. (*Z*)-2-(methoxymethyl)-3-(2-methyloct-1-en-3-yn-1-yl)oxirane.

Z-ox: ^1H NMR (CHLOROFORM- d , 400MHz): δ : 5.23 (dd, $J= 8.9, 1.2$ Hz, 1H), 3.74 (dd, $J= 8.9, 2.4$ Hz, 1H), 3.71 (dd, $J= 11.6, 3.2$ Hz, 1H), 3.40 (dd, $J= 11.6, 5.7$ Hz, 1H), 3.40 (s, 3H), 3.08 (ddd, $J= 5.7, 3.2, 2.4$ Hz, 1H), 2.35 (t, $J= 7.2$ Hz, 2H), 1.87 (d, $J= 1.2$ Hz, 3H), 1.55-1.40 (m, 4H), 0.92 (t, $J= 7.2$ Hz, 3H); ^{13}C NMR (100 MHz, CDCl_3) δ : 131.5, 125.7, 95.9, 78.7, 72.5, 59.2, 58.3, 54.2, 30.7, 23.8, 21.9, 19.1, 13.6.

3.4.4. Spectral Data for Products

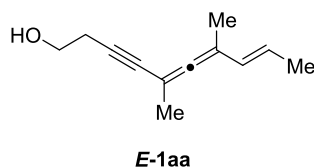


Figure 3.35. (*E*)-5,7-dimethyldeca-5,6,8-trien-3-yn-1-ol.

E-1aa: ^1H NMR (CHLOROFORM- d , 400MHz): δ = 5.93-5.99 (m, 1 H), 5.61 (dq, J =15.7, 6.7 Hz, 1 H), 3.72 (t, J =5.7 Hz, 2 H), 2.58 (t, J =6.3 Hz, 2 H), 1.83 (s, 3 H), 1.80 (s, 3 H), 1.77 (dd, J =6.7, 1.6 Hz, 3 H), 1.58-1.65 ppm (m, 1 H); ^{13}C NMR (cdcl_3 , 101MHz): δ = ^{13}C NMR (cdcl_3 , 101MHz): δ = 211.6, 128.4, 125.4, 100.8, 85.9, 84.1, 79.2, 61.1, 24.0, 20.9, 18.3, 15.4 ppm; IR ($\nu_{\text{max}}/\text{cm}^{-1}$): 3370, 2959, 2924, 2874, 2855, 2727, 2360, 2341, 2324, 2275, 2242, 2214, 2202, 2167, 2116, 2098, 2070, 2026, 2012, 1995, 1963, 1931, 1887, 1696, 1438, 1375, 1330, 1285, 1212, 1181, 1120, 1045, 964, 919, 848, 795, 747, 723, 696, 663; MS (EI, m/z): 176 (100, M^+), 145 (56), 130 (52), 115 (63), 105 (69), 91 (79), 65 (40), 41 (34).

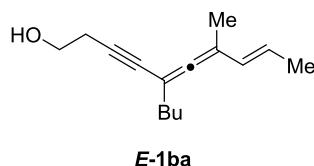


Figure 3.36. (*E*)-5-butyl-7-methyldeca-5,6,8-trien-3-yn-1-ol.

E-1ba: ^1H NMR (CHLOROFORM- d , 400MHz): δ : ppm 5.96 (dq, J = 15.60, 1.58 Hz, 1H), 5.60 (dq, J = 15.65, 6.65 Hz, 1H), 3.72 (t, J = 6.06 Hz, 2H), 2.58 (t, J = 6.26 Hz, 2H), 2.06-2.12 (m, 2H), 1.80 (s, 3H), 1.78 (dd, J = 6.65, 1.57 Hz, 3H), 1.28-1.49 (m, 4H), 0.89 (t, J = 7.24 Hz, 3H); ^{13}C NMR (CHLOROFORM- d , 101MHz) δ : ppm 211.17, 128.44, 125.27, 101.50, 88.99, 86.25, 78.49, 61.14, 34.18, 29.79, 24.00, 21.94, 18.31, 15.51, 14.00; 3350, 2956, 2925, 2857, 1458, 1438, 1377, 1330, 1044, 962, 745, 729, 692; MS (EI, m/z): 218 (13, M^+), 143 (11), 128 (15), 91 (17), 77 (18), 63 (16), 55 (27), 41 (100). HRMS (EI, m/z , M^+): $[\text{M}+\text{H}]^+$, 219.17446 (calculated); 219.17434 (measured).

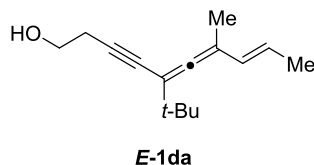


Figure 3.37. (*E*)-5-(tert-butyl)-7-methyldeca-5,6,8-trien-3-yn-1-ol.

E-1da: ^1H NMR (CHLOROFORM-*d*, 400MHz): δ = 5.95 (dd, J =15.7, 1.6 Hz, 1H), 5.60 (dd, J =15.7, 6.7 Hz, 1H), 3.73 (t, J =6.5 Hz, 2H), 2.61 (t, J =6.3 Hz, 2H), 1.85 (br. s, 1H), 1.81 (s, 4H), 1.77 (dd, J =6.7, 1.6 Hz, 4H), 1.09 ppm (s, 12H); ^{13}C NMR (CHLOROFORM-*d*, 101MHz): δ = 209.5, 128.6, 125.1, 102.7, 99.7, 88.0, 76.9, 61.2, 35.1, 24.0, 18.3, 15.6 ppm; IR ($\nu_{\text{max}}/\text{cm}^{-1}$): 3360, 2956, 2925, 2857, 1737, 1640, 1458, 1438, 1377, 1330, 1270, 1232, 1186, 1121, 1098, 1044, 962, 903, 847, 820, 745, 729, 692; MS (EI, m/z): 218 (53, M^+), 161 (50), 131 (28) 128 (60), 91 (59), 57 (100), 41 (58).

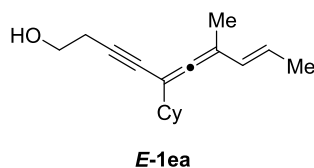


Figure 3.38. (*E*)-5-cyclohexyl-7-methyldeca-5,6,8-trien-3-yn-1-ol.

E-1ea: ^1H NMR (CHLOROFORM-*d*, 400MHz): δ = 5.96 (dq, J =15.6, 1.7Hz, 1H), 5.60 (dq, J =15.5, 6.6 Hz, 1H), 3.73 (q, J =6.3 Hz, 2H), 2.60 (t, J =6.2 Hz, 2H), 1.97 (tt, J =11.3, 3.5 Hz, 1H), 1.69-1.89 (m, 10H), 1.02-1.33 ppm (m, 6H); ^{13}C NMR (CHLOROFORM-*d*, 101MHz): δ = 210.5, 128.6, 125.2, 102.5, 94.8, 87.0, 77.7, 61.2, 42.1, 32.0, 32.0, 26.1, 26.1, 24.1, 18.3, 15.6 ppm; IR ($\nu_{\text{max}}/\text{cm}^{-1}$): 3038, 2924, 2852, 1738, 1647, 1607, 1508, 1448, 1373, 1330, 1290, 1264, 1229, 1194, 1136, 1121, 1040, 998, 961, 891, 849, 818, 793, 755, 728, 691, 666, 621, 602; MS (EI, m/z): 244 (63, M^+), 199 (92), 157 (98), 143 (88), 131 (85), 91 (91), 55 (93), 41 (100); HRMS (EI, m/z , M^+): 245,18999 (calculated), 245,19009 (found).

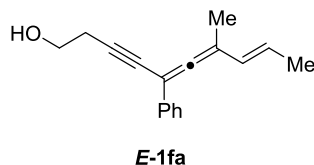


Figure 3.39. (*E*)-7-methyl-5-phenyldeca-5,6,8-trien-3-yn-1-ol.

E-1fa: ^1H NMR (CHLOROFORM-*d*, 400MHz): δ = 7.48-7.52 (m, 2H), 7.29-7.35 (m, 2H), 7.20-7.25 (m, 1H), 6.06 (dq, J =15.6, 1.7 Hz, 1H), 5.77 (dq, J =15.5, 6.7 Hz, 1H), 3.82 (q, J =6.3 Hz, 2H), 2.72 (t, J =6.3 Hz, 2H), 1.96 (s, 3H), 1.88 (t, J =6.4 Hz, 1H), 1.82 ppm (dd, J =6.7, 1.7 Hz, 3 H); ^{13}C NMR (CHLOROFORM-*d*, 101MHz): δ = 213.4, 134.7, 128.4, 127.2, 127.1, 127.0, 126.1, 105.2, 92.3, 89.3, 76.0, 61.2, 24.1, 18.4, 15.2 ppm; IR ($\nu_{\text{max}}/\text{cm}^{-1}$): 3081, 3057, 2967, 2926, 2872, 2856, 2158, 2023, 1597, 1491, 1444, 1377, 1291, 1263, 1143, 1049, 964, 797, 757, 695; MS (EI, m/z): 220 (27), 205 (100), 189 (5), 177 (11), 161 (4), 145 (15), 131 (6), 105 (8), 91 (8), 57 (18).

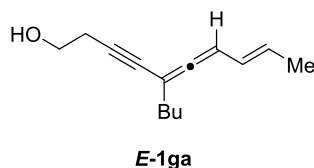


Figure 3.40. (*E*)-5-butyldeca-5,6,8-trien-3-yn-1-ol.

E-1ga: ^1H NMR (CHLOROFORM-*d*, 400MHz): δ = 5.91 - 5.98 (m, 1 H), 5.79 - 5.88 (m, 1 H), 5.63 - 5.74 (m, 1 H), 3.72 (t, J =6.3 Hz, 2 H), 2.59 (td, J =6.3, 1.1 Hz, 2 H), 2.11 (td, J =7.4, 2.6 Hz, 2 H), 1.76 (dd, J =6.5, 1.4 Hz, 3 H), 1.60 (br. s., 1 H), 1.42 - 1.51 (m, 2 H), 1.28 - 1.40 (m, 2 H), 0.87 - 0.93 ppm (m, 3 H); ^{13}C NMR (CHLOROFORM-*d*, 101MHz): δ = 211.6, 129.0, 125.6, 95.4, 91.2, 87.4, 61.1, 33.9, 29.8, 24.0, 22.0, 18.2, 13.8 ppm; IR ($\nu_{\text{max}}/\text{cm}^{-1}$): 3551, 2957, 2929, 2872, 1454, 1437, 1377, 1332, 1299, 1172, 1143, 1104, 1044, 964, 927, 844, 727; MS (EI, m/z): 204 (33, M^+), 141 (22), 131 (72), 115 (40), 105 (40), 91 (100), 76 (33), 41 (46).

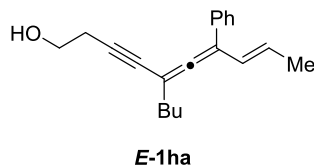


Figure 3.41. (*E*)-5-butyl-7-phenyldeca-5,6,8-trien-3-yn-1-ol.

E-1ha: ^1H NMR (CHLOROFORM-*d*, 400MHz): δ = 7.32 - 7.36 (m, 3 H), 7.26 - 7.28 (m, 2 H), 6.02 - 6.13 (m, 1 H), 5.75 - 5.88 (m, $J=15.3$, 6.7 Hz, 1 H), 3.73 (br. s., 2 H), 2.56 - 2.65 (m, 2 H), 2.15 - 2.29 (m, 2 H), 1.80 - 1.87 (m, 3 H), 1.75 (br. s., 1 H), 1.29 - 1.55 (m, 4 H), 0.85 - 0.93 ppm (m, 3 H); ^{13}C NMR (CHLOROFORM-*d*, 101MHz): δ = 211.5, 135.9, 129.7, 128.3, 127.8, 127.2, 125.7, 108.7, 92.4, 87.3, 77.7, 77.2, 61.1, 34.3, 30.0, 24.1, 22.1, 18.5, 13.9 ppm; IR ($\nu_{\text{max}}/\text{cm}^{-1}$): 3376, 2957, 2928, 2872, 2858, 1493, 1446, 1377, 1328, 1261, 1184, 1103, 1045, 966, 802, 758, 699 MS (EI, m/z): 280 (16, M^+), 207 (61), 193 (57), 179 (74), 178 (100), 165 (72), 115 (67), 91 (90), 77 (73), 69 (67), 41 (77).

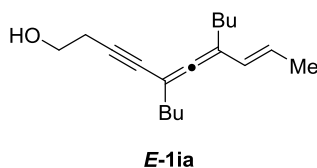


Figure 3.42. (*E*)-5-butyl-7-(prop-1-en-1-yl)undeca-5,6-dien-3-yn-1-ol

E-1ia: ^1H NMR (CHLOROFORM-*d*, 400MHz): δ = 5.88 (dd, $J=15.7$, 1.6 Hz, 1 H), 5.65 (dq, $J=15.7$, 6.7 Hz, 1 H), 3.71 (t, $J=6.1$ Hz, 2 H), 2.58 (t, $J=6.1$ Hz, 2 H), 2.06 - 2.17 (m, 4 H), 1.76 (dd, $J=6.5$, 1.4 Hz, 3 H), 1.30 - 1.51 (m, 8 H), 0.90 ppm (td, $J=7.2$, 3.1 Hz, 6 H); ^{13}C NMR (cdcl_3 , 101MHz): δ = 210.8, 127.8, 124.9, 106.4, 90.6, 86.2, 78.6, 61.2, 34.2, 30.1, 29.7, 28.7, 24.0, 22.5, 22.1, 18.4, 14.0, 13.9 ppm; IR ($\nu_{\text{max}}/\text{cm}^{-1}$): 3350, 2957, 2929, 2873, 2859, 1466, 1377, 1331, 1261, 1188, 1105, 1044, 962, 800, 730; MS (EI, m/z): 260 (7, M^+), 131(45), 129 (36, M^+), 117 (34), 105 (52), 91 (66), 77 (36), 69 (42), 55 (49), 41 (100).

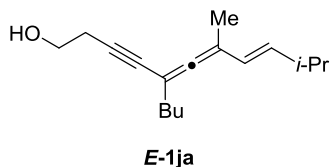


Figure 3.43. (E)-5-butyl-7,10-dimethylundeca-5,6,8-trien-3-yn-1-ol.

E-1ka: ^1H NMR (CHLOROFORM- d , 400MHz): δ = 5.90 (dd, J =15.7, 1.2 Hz, 1H), 5.55 (dd, J =15.8, 6.8 Hz, 1 H), 3.73 (t, J =6.3 Hz, 2 H), 2.59 (t, J =6.3 Hz, 2 H), 2.36 (ddd, J =13.5, 6.7, 1.2 Hz, 1 H), 2.10 (t, J =7.3 Hz, 2 H), 1.81 (s, 3 H), 1.68 (br. s, 1 H), 1.29-1.50 (m, 6 H), 1.02 (d, J =6.7 Hz, 6 H), 0.86-0.93 ppm (m, 3 H); ^{13}C NMR (CHLOROFORM- d , 101MHz): δ = 211.5, 137.6, 124.4, 110.0, 101.5, 88.9, 86.3, 61.1, 34.2, 31.4, 29.9, 24.0, 22.5, 22.5, 21.9, 15.5, 13.8 ppm; IR ($\nu_{\text{max}}/\text{cm}^{-1}$): 3358, 2957, 2924, 2856, 1527, 1464, 1378, 1332, 1296, 1262, 1231, 1184, 1100, 1044, 965, 888, 848, 803, 776, 746, 728, 700; MS (EI, m/z): 246 (28, M^+), 161 (79), 145 (29), 143 (53), 131 (55), 119 (52), 105 (68), 91 (86), 65 (33), 41 (100);

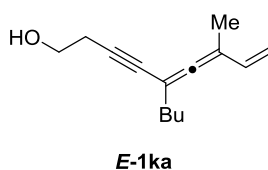


Figure 3.44. 5-butyl-7-methylnona-5,6,8-trien-3-yn-1-ol.

E-1la: ^1H NMR (CHLOROFORM- d , 400MHz): δ = 6.29 (dd, J =17.2, 10.6 Hz, 1 H), 5.01 - 5.21 (m, 2 H), 3.66 - 3.79 (m, 2 H), 2.59 (t, J =6.3 Hz, 2 H), 2.11 (t, J =7.2 Hz, 2 H), 1.83 (s, 3 H), 1.78 (br. s., 1 H), 1.28 - 1.50 (m, 4 H), 0.90 ppm (t, J =7.2 Hz, 3 H); ^{13}C NMR (CHLOROFORM- d , 101MHz): δ = 212.2, 134.8, 113.5, 101.8, 89.4, 86.9, 78.0, 61.1, 34.0, 29.8, 24.0, 21.9, 14.7, 13.8 ppm; IR ($\nu_{\text{max}}/\text{cm}^{-1}$): 3551, 2958, 2927, 2858, 1615, 1458, 1406, 1377, 1322, 1167, 1128, 1105, 1066, 1017, 962, 841 MS (EI, m/z): 204 (1^+ , M^+), 119 (12), 105 (24), 95 (19), 91 (25), 81 (30), 75 (100), 73 (60), 55 (12).

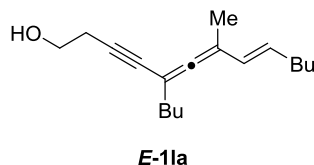


Figure 3.45. (*E*)-5-butyl-7-methyltrideca-5,6,8-trien-3-yn-1-ol.

E-1a: ^1H NMR (CHLOROFORM-*d*, 400MHz): δ = 5.93 (dt, J =15.6, 1.4 Hz, 1 H), 5.58 (dt, J =15.6, 6.9 Hz, 1 H), 3.72 (t, J =6.3 Hz, 2 H), 2.58 (t, J =6.3 Hz, 2 H), 2.06-2.15 (m, 4 H), 1.87 (br. s, 1 H), 1.81 (s, 3 H), 1.26-1.50 (m, 8 H), 0.82-0.94 ppm (m, 6 H); ^{13}C NMR (CHLOROFORM-*d*, 101MHz): δ = 211.4, 130.8, 127.1, 101.5, 88.9, 86.3, 78.5, 61.1, 34.2, 32.6, 31.6, 29.9, 24.0, 22.3, 21.9, 15.5, 13.9, 13.9 ppm; IR ($\nu_{\text{max}}/\text{cm}^{-1}$): 3353, 2956, 2925, 2857, 1737, 1640, 1458, 1438, 1377, 1330, 1270, 1232, 1186, 1121, 1098, 1044, 962, 903, 847, 820, 745, 729, 692; MS (EI, m/z): 260 (46, M^+), 173 (38), 161 (88), 143 (76), 131 (90), 128 (90), 105 (72), 91 (58), 69 (58), 41 (100); HRMS (EI, m/z , M^+): 261,22129 (calculated), 261,22118 (found).

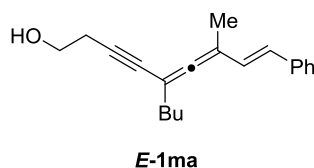


Figure 3.46. (*E*)-5-butyl-7-methyl-9-phenylnona-5,6,8-trien-3-yn-1-ol.

E-1ma: ^1H NMR (CHLOROFORM-*d*, 400MHz): δ = 7.38-7.43 (m, 2 H), 7.27-7.34 (m, 2 H), 7.19-7.25 (m, 1 H), 6.70 (d, J =16.0 Hz, 1 H), 6.46 (d, J =16.0 Hz, 1 H), 3.74 (t, J =6.3 Hz, 2 H), 2.61 (t, J =6.3 Hz, 2 H), 2.12-2.20 (m, 2 H), 1.96 (s, 3 H), 1.32-1.52 (m, 5 H), 0.87-0.94 ppm (m, 3 H); ^{13}C NMR (CHLOROFORM-*d*, 101MHz): δ = 213.4, 137.3, 128.6, 128.3, 127.4, 126.7, 126.3, 102.1, 89.6, 87.1, 78.0, 61.1, 34.2, 29.9, 24.0, 22.0, 15.5, 13.9 ppm; IR ($\nu_{\text{max}}/\text{cm}^{-1}$): 3362, 3082, 3059, 3026, 2955, 2927, 2871, 2858, 1943, 1663, 1624, 1599, 1494, 1452, 1376, 1328, 1299, 1262, 1182, 1156, 1102, 1044, 959, 910, 891, 846, 748, 693, 648, 618; MS (EI, m/z): 280 (20, M^+), 237 (30), 205 (24), 188 (38), 178 (63), 128 (28), 105 (91), 91 (77), 79 (41), 59 (28), 41 (100);

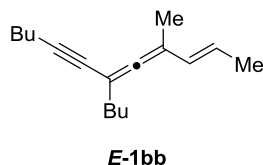


Figure 3.47. (*E*)-6-butyl-4-methyldodeca-2,4,5-trien-7-yne.

E-1bb: ^1H NMR (CHLOROFORM-*d*, 400MHz) δ = 5.97 (dq, J =15.54, 1.60 Hz, 1 H), 5.58 (dq, J =15.56, 6.65 Hz, 1 H), 2.30 (t, J =7.09 Hz, 2 H), 2.06-2.12 (m, 2 H) 1.80 (s, 3 H), 1.77 (dd, J =6.60, 1.61 Hz, 3 H), 1.30-1.54 (m, 6 H), 0.90 (td, J =7.26, 5.23 Hz, 6 H); ^{13}C NMR (CHLOROFORM-*d*, 101MHz) δ : ppm 210.90, 128.82, 124.78, 101.09, 90.65, 89.48, 76.11, 34.38, 30.93, 29.88, 21.99, 21.92, 19.27, 18.25, 15.55, 13.86, 13.60; IR ($\nu_{\text{max}}/\text{cm}^{-1}$): 2958, 2931, 2873, 2861, 1458, 1377, 1326, 1142, 1106, 962; MS (EI, m/z): 230 (42, M^+), 172 (27), 145 (54), 130 (69), 90 (55), 65 (49), 43 (100), 41 (31); HRMS (EI, m/z , M^+): 231.21073 (calculated); 231.21049 (measured).

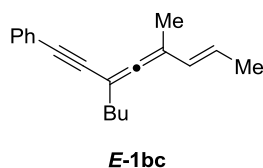


Figure 3.48. (*E*)-(3-butyl-5-methylocta-3,4,6-trien-1-yn-1-yl)benzene

E-1bc: ^1H NMR (CHLOROFORM-*d*, 400MHz) δ = 7.40-7.46 (m, 2 H), 7.26-7.31 (m, 3 H), 6.02 (dq, J =15.6, 1.7 Hz, 1 H), 5.64 (dq, J =15.5, 6.7 Hz, 1 H), 2.18-2.25 (m, 2 H), 1.86 (s, 3 H), 1.80 (dd, J =6.7, 1.8 Hz, 3 H), 1.48-1.57 (m, 2 H), 1.34-1.45 (m, 2 H), 0.93 ppm (t, J =7.3 Hz, 3 H); ^{13}C NMR (CHLOROFORM-*d*, 101MHz) δ = 211.6, 131.4, 128.4, 128.1, 127.8, 125.4, 123.7, 101.6, 89.5, 89.4, 85.6, 34.1, 30.0, 22.0, 18.3, 15.5, 13.9 ppm; IR ($\nu_{\text{max}}/\text{cm}^{-1}$): 3080, 3019, 2956, 2926, 2857, 1743, 1667, 1597, 1572, 1490, 1442, 1376, 1315, 1293, 1248, 1231, 1176, 1157, 1120, 1101, 1069, 1027, 1012, 962, 930, 911, 861, 840, 793, 754, 690, 624, 602; MS (EI, m/z): 251 (9, $\text{M}^+ + 1$) 250 (38, M^+), 235 (9), 207 (16), 193 (100), 179 (27), 152 (12), 129 (10), 115 (36), 91 (37), 41 (14).

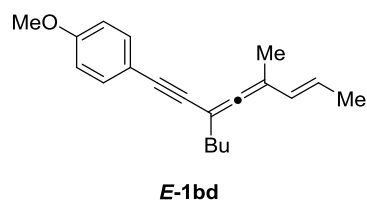


Figure 3.49. (*E*)-1-(3-butyl-5-methylocta-3,4,6-trien-1-yn-1-yl)-4-methoxybenzene.

E-1bd: ^1H NMR (CHLOROFORM-*d*, 400MHz) δ = 7.32-7.40 (m, 7 H), 6.78-6.87 (m, 8 H), 5.96-6.07 (m, 1 H), 5.63 (dq, J =15.5, 6.6 Hz, 1 H), 3.80 (s, 3 H), 2.20 (t, J =7.3 Hz, 3 H), 1.85 (s, 5 H), 1.80 (dd, J =6.7, 1.6 Hz, 5 H), 1.48-1.55 (m, 2 H), 1.40 (dt, J =15.0, 7.3 Hz, 2 H), 0.92 ppm (t, J =7.3 Hz, 3 H); ^{13}C NMR (CHLOROFORM-*d*, 101MHz) δ = 211.4, 159.2, 132.8, 128.5, 125.2, 115.9, 113.8, 101.5, 89.6, 89.4, 84.0, 55.2, 34.2, 30.0, 22.0, 18.3, 15.6, 13.9 ppm; IR ($\nu_{\text{max}}/\text{cm}^{-1}$): 2958, 2928, 2871, 2857, 1714, 1661, 1601, 1573, 1509, 1460, 1422, 1378, 1288, 1250, 1169, 1106, 1030, 883, 832, 807, 771, 734, 696, 676, 635, 611; MS (EI, m/z): 281 (20, $\text{M}^{+}+1$) 280 (51, M^{+}), 265 (12), 251 (5), 237 (21), 223 (100), 207 (27), 191 (13), 178 (25), 121 (25), 105 (9), 77 (8), 44 (75).

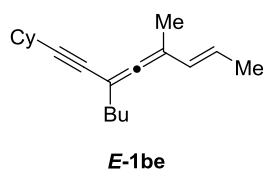


Figure 3.50 (*E*)-3-butyl-5-methylocta-3,4,6-trien-1-yn-1-yl)cyclohexane.

E-1be: ^1H NMR (CHLOROFORM-*d*, 400MHz) δ = 5.98 (dq, J =15.5, 1.6 Hz, 1 H), 5.48-5.67 (m, 1 H), 2.41-2.51 (m, 1 H), 2.09 (t, J =7.2 Hz, 2 H), 1.74-1.83 (m, 8 H), 1.65-1.73 (m, 2 H), 1.41-1.54 (m, 6 H), 1.25-1.38 (m, 6 H), 0.90 (t, J =7.2 Hz, 3 H), 0.85-0.93 ppm (m, 3 H); ^{13}C NMR (CHLOROFORM-*d*, 101MHz) δ = 210.8, 128.9, 124.7, 101.0, 94.8, 89.5, 81.9, 76.0, 34.5, 32.8, 32.3, 29.9, 25.9, 24.9, 21.9, 18.3, 15.5, 13.9 ppm; MS (EI, m/z): 256 (4, M^{+}), 214 (80), 199 (8), 185 (15), 171 (32), 157 (27), 143 (40), 129 (70), 117 (85), 105 (37), 91 (100), 79 (45), 44 (41).

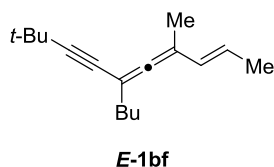


Figure 3.51 (*E*)-6-butyl-4,9,9-trimethyldeca-2,4,5-trien-7-yne.

E-1bf: ^1H NMR (CHLOROFORM-*d*, 400MHz): δ = 5.98 (dq, J =15.7, 1.6 Hz, 1 H), 5.58 (dq, J =15.3, 6.7 Hz, 1 H), 2.08 (t, J =7.4 Hz, 2 H), 1.80 (s, 3 H), 1.78 (dd, J =6.7, 1.6 Hz, 3 H), 1.29-1.49 (m, 4 H), 1.23 (s, 9 H), 0.90 ppm (t, J =7.2 Hz, 3 H); ^{13}C NMR (CHLOROFORM-*d*) δ ppm 210.74, 128.98, 124.56, 100.86, 98.85, 89.42, 74.56, 34.57, 31.11, 29.84, 28.00, 21.92, 18.26, 15.50, 13.89; IR ($\nu_{\text{max}}/\text{cm}^{-1}$): 2961, 2930, 2872, 2213, 2199, 2176, 2159, 2144, 1956, 1931, 1717, 1690, 1458, 1363, 1261, 1203, 1096, 1052, 1023, 976, 938, 864, 803; MS (EI, m/z): 230 (1, M^+), 215 (5), 188 (16), 173 (100), 158 (17), 145 (20), 131 (56), 105 (18), 91 (18), 77 (15), 57 (13), 41 (14); HRMS (EI, m/z , M^+): 231,21073 (calculated), 231,21077 (found).

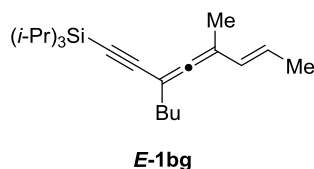


Figure 3.52. (*E*)-(3-butyl-5-methylocta-3,4,6-trien-1-yn-1-yl)triisopropylsilane.

E-1bg: ^1H NMR (CHLOROFORM-*d*, 400MHz) δ = 5.98 (dd, J = 15.7, 1.6 Hz, 1 H), 5.60 (dq, J = 15.7, 6.7 Hz, 1 H), 2.12 (t, J = 7.2 Hz, 2 H), 1.81 (s, 3 H), 1.79 (dd, J = 6.7, 1.6 Hz, 3 H), 1.29-1.53 (m, 4 H), 1.06-1.08 (m, 18 H), 0.89 ppm (t, J = 7.2 Hz, 3 H); ^{13}C NMR (CHLOROFORM-*d*, 101MHz) δ = 211.8, 128.5, 125.0, 103.0, 101.1, 90.6, 89.4, 34.3, 29.8, 21.8, 18.6, 18.5, 18.3, 15.4, 13.9, 11.3, 11.3 ppm; IR ($\nu_{\text{max}}/\text{cm}^{-1}$): 2957, 2941, 2926, 2893, 2865, 2726, 2139, 2063, 1743, 1463, 1380, 1290, 1242, 1161, 1101, 1073, 1015, 996, 961, 919, 882, 827, 795, 757, 731, 675; MS (EI, m/z): 330 (25, M^+) 287 (80), 245 (35), 203 (20), 173 (15), 159 (16), 145 (18), 94 (28), 87 (35), 73 (50), 59 (100).

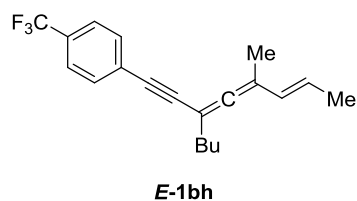
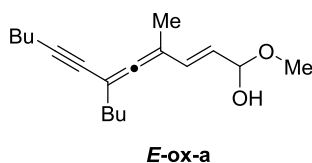


Figure 3.53. (*E*)-1-(3-butyl-5-methylocta-3,4,6-trien-1-yn-1-yl)-4-(trifluoromethyl)benzene.

E-1bh: ^1H NMR (CHLOROFORM- d , 400MHz): δ = 7.48 - 7.57 (m, 4 H), 6.01 (dq, $J=15.7$, 1.6 Hz, 1 H), 5.66 (dq, $J=15.7$, 6.7 Hz, 1 H), 2.19 - 2.25 (m, 2 H), 1.86 (s, 3 H), 1.81 (dd, $J=6.7$, 1.6 Hz, 3 H), 1.47 - 1.57 (m, 2 H), 1.33 - 1.46 (m, 2 H), 0.93 ppm (t, $J=7.2$ Hz, 3 H); ^{13}C NMR (CHLOROFORM- d , 101MHz) δ : 212.0, 131.6, 128.0, 127.6 (q, $J_{\text{F-C}} = 1.36$ Hz), 125.8, 125.1 (q, $J_{\text{F-C}} = 3.86$ Hz), 102.0, 89.1, 88.3, 88.1, 33.9, 30.0, 21.9, 18.3, 15.4, 13.9 ppm; IR ($\nu_{\text{max}}/\text{cm}^{-1}$): 2958, 2927, 2858, 1615, 1458, 1406, 1377, 1322, 1167, 1128, 1105, 1066, 1017, 962, 841; MS (EI, m/z): 318 (1>, M^+) 162 (12), 105 (20), 91 (33), 77 (33), 67 (53), 65 (88), 63 (92), 55 (71), 51 (100), 41 (78).



E-ox-a: ^1H NMR (BENZENE- d_6 , 400MHz): δ = 6.38 (dd, $J=15.8$, 1.4 Hz, 1 H, Major), 6.40 (dd, $J=15.7$, 1.6 Hz, 1 H, Minor), 5.45 - 5.53 (m, 1 H), 4.15 - 4.23 (m, 1 H), 2.96 - 3.10 (m, 3 H), 2.93 - 2.96 (m, 3 H), 2.19 - 2.28 (m, 2 H), 2.08 - 2.16 (m, 2 H), 1.67 - 1.72 (m, 3 H), 1.48 - 1.63 (m, 2 H), 1.18 - 1.36 (m, 8 H), 0.78 - 0.86 (m, 3 H), 0.682 - 0.717 (t, $J=7.04$, 3 H, Major), 0.685-0.722 (t, $J=7.04$, 3H, Minor) 0.43 ppm (br. s., 1 H); ^{13}C NMR (CHLOROFORM- d , 101MHz): δ = 212.4, 130.7, 130.4, 126.9, 126.9, 110.0, 100.5, 91.5, 90.0, 76.5, 75.6, 71.3, 71.1, 70.5, 59.0, 34.2, 34.2, 30.9, 30.8, 29.8, 29.7, 22.0, 21.9, 19.3, 15.4, 13.8, 13.6 ppm; IR ($\nu_{\text{max}}/\text{cm}^{-1}$): 3435, 2957, 2927, 2872, 2857, 1719, 1458, 1378, 1326, 1260, 1194, 1098, 1027, 968, 868, 800; MS (EI, m/z): 290 (10, M^+), 281 (4), 245 (8), 229 (9), 173 (16), 131 (21), 105 (18), 91 (20), 77 (11), 55 (7), 44 (100).

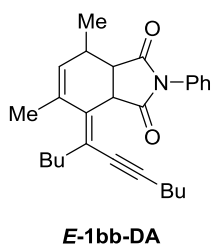


Figure 3.54. (*E*)-5,7-dimethyl-2-phenyl-4-(undec-6-yn-5-ylidene)-3a,4,7,7a-tetrahydro-1H-isoindole-1,3(2H)-dione.

E-1bb-DA: ^1H NMR (CHLOROFORM-*d*, 400MHz): δ = 7.38 - 7.46 (m, 2 H), 7.31 - 7.37 (m, 1 H), 7.16 - 7.22 (m, 2 H), 5.50 (dd, $J=3.1, 1.6$ Hz, 1 H), 4.70 (d, $J=8.2$ Hz, 1 H), 3.22 (dd, $J=8.2, 6.7$ Hz, 1 H), 2.33 - 2.42 (m, 3 H), 2.14 - 2.31 (m, 2 H), 1.93 (dd, $J=2.3, 1.6$ Hz, 3 H), 1.51 - 1.64 (m, 4 H), 1.26 - 1.50 (m, 7 H), 0.85 - 0.97 ppm (m, 6 H, Major), 0.88 - 0.94 ppm (m, 6 H, Minor); ^{13}C NMR (cdcl_3 , 101MHz): δ = 176.9, 176.1, 136.6, 136.0, 132.1, 128.9, 128.3, 126.4, 125.0, 95.0, 80.2, 77.3, 77.0, 76.7, 49.3, 45.3, 33.7, 31.9, 30.9, 30.7, 22.3, 22.0, 21.6, 19.3, 16.7, 13.9, 13.6 ppm; IR ($\nu_{\text{max}}/\text{cm}^{-1}$): 2989, 2957, 2932, 2871, 1715, 1500, 1457, 1380, 1180, 1143, 1074; MS (EI, m/z): 403 (100, M^+), 374 (16), 346 (27), 304 (10), 241 (18), 199 (35), 157 (44), 119 (39), 91 (40), 65 (16), 41 (28).

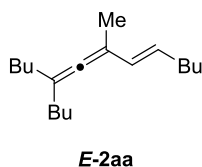


Figure 3.55. (*E*)-5-butyl-7-methyltrideca-5,6,8-triene.

E-2aa: ^1H NMR (CHLOROFORM-*d*, 400MHz) δ = 5.95 (dt, $J=15.6, 1.4$ Hz, 1 H), 5.46 (dt, $J=15.6, 6.9$ Hz, 1 H), 2.10 (qd, $J=7.2, 1.3$ Hz, 2 H), 1.89 - 1.97 (m, 4 H), 1.76 (s, 3 H), 1.28 - 1.41 (m, 12 H), 0.89 ppm (m, $J=7.2$ Hz, 9 H); ^{13}C NMR (CHLOROFORM-*d*, 101MHz) δ : 203.2, 129.7, 128.0, 103.2, 100.3, 32.6, 32.5, 31.9, 29.9, 22.4, 22.3, 16.0, 14.0, 13.9; IR ($\nu_{\text{max}}/\text{cm}^{-1}$): 2956, 2924, 2857, 1742, 1465, 1377, 1333, 1299, 1236, 1155, 1129, 1106, 1017, 961, 929, 895, 838, 818, 779; MS (EI, m/z): 248 (6, M^+), 233 (6), 206 (20), 163 (19), 149 (100), 135 (14), 121 (12), 107 (40), 93 (89), 79 (21), 57 (55), 41 (25);

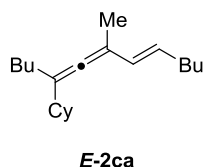


Figure 3.56. (*E*)-(7-methyltrideca-5,6,8-trien-5-yl) cyclohexane.

E-2ca: $^1\text{H NMR}$ (CHLOROFORM-*d*, 400MHz) δ = 5.88-6.03 (m, 1 H), 5.48-5.67 (m, 1 H), 2.38-2.53 (m, 1 H), 2.09 (t, J =7.2 Hz, 2 H), 1.74-1.83 (m, 9 H), 1.65-1.73 (m, 3 H), 1.41-1.54 (m, 5 H), 1.25-1.38 (m, 5 H), 0.90 (t, J =7.2 Hz, 3 H), 0.85-0.93 ppm (m, 3 H); $^{13}\text{C NMR}$ (CHLOROFORM-*d*, 101MHz) δ = 203.0, 129.8, 127.8, 109.0, 101.4, 41.4, 32.62, 32.59, 32.5, 31.9, 30.9, 30.1, 26.6, 26.4, 22.4, 22.3, 16.06, 14.02, 13.97 ppm; IR ($\nu_{\text{max}}/\text{cm}^{-1}$): 2956, 2924, 2853, 1741, 1449, 1377, 1299, 1261, 1235, 1027, 991, 961, 889; MS (EI, m/z): 275 (4, M^++1), 274 (20, M^+), 259 (14), 232 (25), 217 (32), 205 (22), 191 (15), 175 (42), 161 (100), 149 (45), 133 (19), 119 (52), 105 (58), 93 (64), 83 (35), 55 (41), 41 (37).

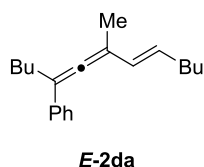


Figure 3.57. (*E*)-(7-methyltrideca-5,6,8-trien-5-yl) benzene.

E-2da: $^1\text{H NMR}$ (CHLOROFORM-*d*, 400MHz) δ = 7.34-7.38 (m, 2 H), 7.27-7.32 (m, 2 H), 7.15-7.21 (m, 1 H), 6.04 (dt, J =15.7, 1.6 Hz, 1 H), 5.62 (dt, J =15.5, 6.9 Hz, 1 H), 2.40-2.47 (m, 2 H), 2.13 (qd, J =7.2, 1.6 Hz, 2 H), 1.90 (s, 3 H), 1.30-1.53 (m, 8 H), 0.86-0.98 ppm (m, 6 H); $^{13}\text{C NMR}$ (CHLOROFORM-*d*, 101MHz) δ = 207.0, 137.6, 129.8, 128.2, 128.0, 126.3, 126.1, 104.8, 103.0, 32.6, 31.7, 30.1, 30.0, 29.7, 22.4, 22.3, 15.5, 14.0, 14.0 ppm; IR ($\nu_{\text{max}}/\text{cm}^{-1}$): 3082, 3060, 3026, 2956, 2924, 2855, 1930, 1740, 1598, 1493, 1458, 1378, 1340, 1304, 1232, 1184, 1156, 1105, 1076, 1030, 1001, 962, 906, 889, 837, 819, 798, 757, 692, 643, 605; MS (EI, m/z): 268 (2, M^+), 226 (9), 169 (100), 141 (22), 128 (13), 115 (19), 91 (31), 41 (42); HRMS (EI, m/z , M^+): 269,22638 (calculated), 269,22656 (found).

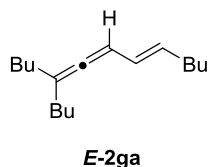


Figure 3.58. (*E*)-5-butyltrideca-5,6,8-triene.

E-2ga: ^1H NMR (CHLOROFORM-*d*, 400MHz): δ = 5.70 - 5.88 (m, 2 H), 5.51 - 5.63 (m, 1 H), 1.90 - 2.17 (m, 6 H), 1.55 (s, 3 H), 1.23 - 1.43 (m, 12 H), 0.86 - 0.92 ppm (m, 9 H); ^{13}C NMR (cdcl₃, 101MHz): δ = 203.3, 131.4, 126.9, 94.7, 77.2, 32.5, 32.4, 31.6, 29.8, 22.4, 22.3, 14.0, 14.0 ppm; IR ($\nu_{\text{max}}/\text{cm}^{-1}$): 2958, 2927, 2859, 1466, 1378, 1261, 1097, 1019, 964, 864, 803, 730; MS (EI, *m/z*): 192 (23, M^+), 150 (34), 135 (32), 107 (38), 94 (37), 93 (100), 91 (36), 81 (21), 79 (62), 77 (23).

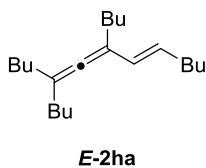


Figure 3.59. (*E*)-5,7-dibutyltrideca-5,6,8-triene.

E-2ha: ^1H NMR (CHLOROFORM-*d*, 400MHz): δ = 5.88 (dd, $J=15.7, 1.0$ Hz, 1 H), 5.52 (dt, $J=15.7, 6.9$ Hz, 2 H), 2.01 - 2.27 (m, 12 H), 1.78 - 2.01 (m, 10 H), 1.20 - 1.46 (m, 41 H), 0.82 - 0.97 ppm (m, 29 H); ^{13}C NMR (CHLOROFORM-*d*, 101MHz): δ = 202.5, 129.2, 127.5, 105.3, 104.8, 32.7, 31.9, 30.3, 30.2, 30.0, 29.7, 29.0, 22.7, 22.5, 22.3, 14.1, 14.0, 14.0 ppm; IR ($\nu_{\text{max}}/\text{cm}^{-1}$): 2957, 2926, 2873, 2859, 1466, 1378, 1143, 962; MS (EI, *m/z*): 290 ($1 > \text{M}^+$), 105 (17), 93 (37), 91 (47), 79 (50), 57 (100), 55 (41).

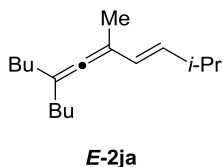


Figure 3.60. (*E*)-7-butyl-2,5-dimethylundeca-3,5,6-triene.

E-2ha: ^1H NMR (CHLOROFORM-*d*, 400MHz) δ = 5.91 (dd, J =15.7, 1.4 Hz, 1 H), 5.43 (dd, J =15.7, 6.7 Hz, 1 H), 2.28-2.41 (m, J =13.5, 6.8, 1.3 Hz, 1 H), 1.92-1.97 (m, 4 H), 1.76 (s, 3 H), 1.27-1.41 (m, 8 H), 1.02 (s, 3 H), 1.01 (s, 3 H), 0.85-0.92 ppm (m, 6 H); ^{13}C NMR (CHLOROFORM-*d*, 101MHz) δ = 203.3, 134.9, 126.9, 103.1, 100.2, 32.6, 31.3, 29.9, 22.7, 22.4, 14.0 ppm; IR ($\nu_{\text{max}}/\text{cm}^{-1}$): 2957, 2926, 2872, 2859, 1946, 1465, 1377, 1331, 1298, 1261, 1234, 1199, 1156, 1105, 1014, 961, 899, 860, 830, 791, 745, 728, 683, 656, 632; MS (EI, m/z): 234 (2, M^+), 192 (3), 149 (28), 121 (14), 107 (35), 93 (100), 57 (55), 41 (52).

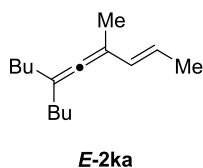


Figure 3.61. (*E*)-6-butyl-4-methyldeca-2,4,5-triene.

E-2ka: ^1H NMR (CHLOROFORM-*d*, 400MHz) δ : 5.98 (dq, J =14.8, 1.6 Hz, 1H), 5.53-5.44 (m, 1H), 1.94 (t, J = 8.0 Hz, 4H), 1.77 (dd, J = 6.8, 1.6 Hz, 3H), 1.76 (s, 3H), 1.38-1.26 (m, 8H), 0.89 (t, J =7.2 Hz, 3H); ^{13}C NMR (CHLOROFORM-*d*, 101MHz) δ : 202.9, 131.1, 122.3, 103.3, 100.3, 32.6, 29.9, 22.4, 18.3, 15.9, 14.0; IR ($\nu_{\text{max}}/\text{cm}^{-1}$): 2957, 2924, 2854, 1740, 1459, 1376, 962; MS (EI, m/z): 206 (19, M^+), 205 (100), 177 (12), 105 (9), 74 (15), 59 (23), 57 (23), 45 (16), 41 (23).

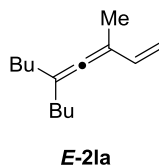


Figure 3.62. (*E*) 5-butyl-3-methylnona-1,3,4-triene.

E-2la: ^1H NMR (CHLOROFORM-*d*, 400MHz): δ = 6.31 (dd, J =17.6, 10.6 Hz, 1 H), 4.98 - 5.05 (m, 1 H), 4.93 (dd, J =10.6, 1.2 Hz, 1 H), 1.89 - 1.98 (m, 4 H), 1.78 (s, 3 H), 1.55 (s, 3 H), 1.28 - 1.39 (m, 8 H), 0.85 - 0.91 ppm (m, 6 H) ^{13}C NMR (CHLOROFORM-*d*, 101MHz): δ = 204.3, 137.5, 110.7, 103.6, 100.8, 32.4, 29.8, 22.3, 15.1, 14.0 ppm; IR ($\nu_{\text{max}}/\text{cm}^{-1}$): 2958, 2928, 2859, 1458, 1378, 1323, 1261, 1168, 1132, 1105, 1067, 1017, 842, 803; MS (EI, m/z): 192 (1>, M^+), 108 (20), 93 (88), 81 (23), 77 (100), 65 (47), 53 (28), 43 (20).

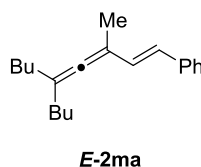


Figure 3.63. (*E*)-(5-butyl-3-methylnona-1,3,4-trien-1-yl) benzene.

E-2ka: ^1H NMR (CHLOROFORM-*d*, 400MHz): δ = 7.37-7.43 (m, 2 H), 7.28-7.36 (m, 3 H), 7.16-7.21 (m, 1 H), 6.73 (d, J =16.0 Hz, 1 H), 6.37 (d, J =16.0 Hz, 1 H), 1.97-2.03 (m, 4 H), 1.91 (s, 3 H), 1.29-1.43 (m, 8 H), 0.87-0.93 ppm (m, 6 H); ^{13}C NMR (cdcl_3 , 101MHz): δ = 205.4, 138.0, 129.7, 128.5, 126.7, 126.0, 125.8, 103.8, 101.1, 32.6, 29.9, 22.4, 15.9, 14.0 ppm; IR ($\nu_{\text{max}}/\text{cm}^{-1}$): 3080, 3059, 3025, 2956, 2926, 2857, 1940, 1793, 1739, 1622, 1599, 1493, 1465, 1447, 1377, 1331, 1299, 1260, 1199, 1180, 1155, 1108, 1072, 1020, 957, 907, 890, 842, 747, 691, 638; MS (EI, m/z): 268 (8, M^+), 226 (18), 211 (12), 184 (17), 169 (100), 155 (34), 141 (30), 91 (91), 77 (16), 57 (22), 43 (18), 41 (60).

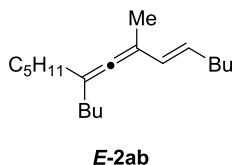


Figure 3.64. (*E*)-9-butyl-7-methyltetradeca-5,7,8-triene.

E-2ab: ^1H NMR (CHLOROFORM-*d*, 400MHz): δ = 5.95 (dt, J =15.6, 1.4 Hz, 1 H), 5.46 (dt, J =15.6, 6.9 Hz, 1 H), 2.09 (qd, J =7.2, 1.4 Hz, 2 H), 1.90-1.96 (m, 4 H), 1.76 (s, 3 H), 1.26-1.43 (m, 14 H), 0.85-0.93 ppm (m, 9 H); ^{13}C NMR (CHLOROFORM-*d*, 101MHz) δ = 203.2, 129.7, 127.9, 103.2, 100.3, 32.8, 32.6, 32.6, 31.9, 31.5, 29.9, 27.4, 22.5, 22.4, 22.3, 16.0, 14.1, 14.0, 14.0 ppm; IR ($\nu_{\text{max}}/\text{cm}^{-1}$): 2956, 2925, 2857, 1704, 1465, 1378, 1339, 1236, 1154, 1129, 1108, 1057, 1016, 962, 934, 876, 729; MS (EI, m/z): 262 (5, M^+), 247 (3), 206 (11), 164 (15), 150 (14), 149 (58), 107 (45), 93 (100), 71 (32), 57 (67), 43 (64), 41 (64).

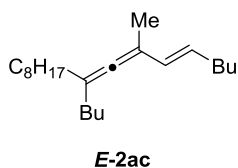


Figure 3.65. (*E*)-9-butyl-7-methylheptadeca-5,7,8-triene.

E-2ac: ^1H NMR (CHLOROFORM-*d*, 400MHz) δ = 5.95 (d, J =15.7 Hz, 1 H), 5.46 (dt, J =15.5, 6.9 Hz, 1 H), 2.09 (q, J =6.8 Hz, 2 H), 1.93 (t, J =7.0 Hz, 4 H), 1.76 (s, 3 H), 1.22-1.42 (m, 26 H), 0.83-0.95 ppm (m, 9 H); ^{13}C NMR (CHLOROFORM-*d*, 101MHz) δ = 203.18, 129.73, 127.91, 103.18, 100.31; 2956, 2923, 2854, 1465, 1378, 1340, 1301, 1236, 1018, 962, 722; IR ($\nu_{\text{max}}/\text{cm}^{-1}$): 2956, 2923, 2854, 1465, 1378, 962 MS (EI, m/z): 304 (4, M^+) 247 (6), 206 (14), 191 (8), 164 (16), 150 (22), 149 (88), 107 (47), 93 (98), 57 (100), 43 (49); HRMS (EI, m/z , M^+): 305,32028 (calculated), 305,32046 (found).

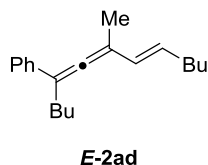


Figure 3.66. (*E*)-(7-methyltrideca-5,6,8-trien-5-yl)benzene

E-2ad: ^1H NMR (CHLOROFORM-*d*, 400MHz): δ = 7.33-7.39 (m, 2 H), 7.27-7.33 (m, 2 H), 7.15-7.21 (m, 1 H), 6.04 (dt, $J=15.7$, 1.6 Hz, 1 H), 5.62 (dt, $J=15.6$, 6.9 Hz, 1 H), 2.40-2.47 (m, 2 H), 2.09-2.17 (m, 2 H), 1.90 (s, 3 H), 1.31-1.53 (m, 8 H), 0.88-0.96 ppm (m, 6 H); ^{13}C NMR CHLOROFORM-*d*, 101MHz): δ = 207.0, 137.6, 129.8, 128.2, 128.0, 126.3, 126.1, 104.8, 103.0, 32.6, 31.7, 30.1, 30.0, 29.7, 22.4, 22.3, 15.5, 14.0, 14.0 ppm; IR ($\nu_{\text{max}}/\text{cm}^{-1}$): 3082, 3060, 3026, 2956, 2924, 2855, 1930, 1740, 1598, 1493, 1458, 1378, 1340, 1304, 1232, 1184, 1156, 1105, 1076, 1030, 1001, 962, 906, 889, 837, 819, 798, 757, 692, 643, 605; MS (EI, m/z): 268 (2, M^+), 226 (9), 169 (100), 141 (22), 128 (13), 115 (19), 91 (31), 41 (42); HRMS (EI, m/z , M^+): 269,22638 (calculated), 269,22656 (found).

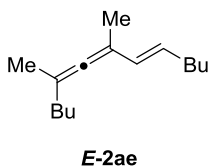


Figure 3.67. (*E*)-5,7-dimethyltrideca-5,6,8-triene.

E-2ae: ^1H NMR (CHLOROFORM-*d*, 400MHz): δ = 5.96 (dt, $J=15.7$, 1.4 Hz, 1 H), 5.47 (dt, $J=15.7$, 7.0 Hz, 1 H), 2.09 (qd, $J=7.2$, 1.6 Hz, 2 H), 1.91-1.98 (m, 2 H), 1.75 (s, 3 H), 1.67 (s, 3 H), 1.28-1.43 (m, 8 H), 0.89 ppm (td, $J=7.2$, 4.7 Hz, 6 H); ^{13}C NMR (cdcl_3 , 101MHz): δ = 203.4, 129.6, 128.2, 98.9, 98.3, 34.0, 32.6, 31.9, 29.7, 22.3, 22.3, 19.1, 15.9, 14.0 ppm; IR ($\nu_{\text{max}}/\text{cm}^{-1}$): 2957, 2924, 2857, 1465, 1441, 1367, 1236, 1023, 961, 729, 608; MS (EI, m/z): 206 (2, M^+), 191 (2), 121 (11), 107 (100), 91 (17), 41 (17).

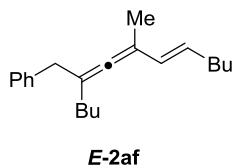


Figure 3.68. (*E*)-(2-butyl-4-methyldeca-2,3,5-trien-1-yl)benzene.

***E*-2af:** ^1H NMR (CHLOROFORM-*d*, 400MHz): δ = 7.24-7.30 (m, 2 H), 7.15-7.23 (m, 3 H), 5.96 (dt, $J=15.7$, 1.4 Hz, 1 H), 5.48 (dt, $J=15.6$, 6.9 Hz, 1 H), 3.29 (s, 2 H), 2.10 (qd, $J=7.2$, 1.2 Hz, 2 H), 1.86-1.92 (m, 2 H), 1.74-1.77 (m, 3 H), 1.24-1.42 (m, 8 H), 0.88-0.94 (m, 3 H), 0.82-0.87 ppm (m, 3 H); ^{13}C NMR (cdcl₃, 101MHz): δ = 204.3, 140.2, 129.3, 128.8, 128.6, 128.1, 125.9, 102.6, 100.2, 40.2, 32.6, 31.8, 31.5, 29.7, 22.3, 22.2, 15.9, 13.9 ppm; IR (vmax/cm⁻¹): 2956, 2924, 2854, 1494, 1454, 1378, 1073, 1016, 962, 801, 698; MS (EI, m/z): 282 (6, M⁺), 239 (3), 169 (9), 91 (100), 78 (12), 55 (13), 41 (24). HRMS (EI, m/z , M⁺): 283,24203 (calculated), 283,2425 (found).

CHAPTER 4

RESULTS AND DISCUSSION

This thesis describes two different methods of transition-metal-catalyzed 1,5-substitution of reactions of enyne derivatives: I) Palladium/copper-catalyzed reactions of enyne carbonates (Section 4.1) with terminal alkynes and iron-catalyzed reaction of enyne acetates with Grignard reagents (Section 4.2) were investigated. Both methods effectively yielded vinylallenes exclusively in (*E*)-configuration.

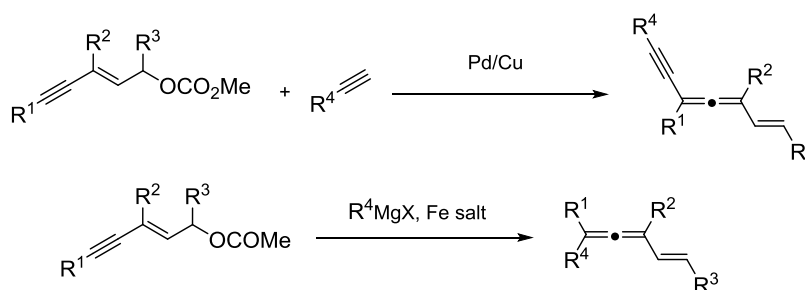


Figure 4.1. Pd-catalyzed alkylation of enyne carbonates and iron-catalyzed reaction of enyne acetates with Grignard reagents.

4.1. Palladium/Copper-Catalyzed Alkylation of *E*-Enyne Carbonates

The optimization of the reaction conditions was performed using enyne carbonate **E-1b** with 3-butyn-1-ol as the terminal alkyne. Considering easy separation of Glaser coupling by-product produced by self-coupling of the terminal alkyne 3-butyn-1-ol from the desired product, the optimization studies were performed using this alkyne in 1.5 equivalents amount (Glaser, 1869) (Figure 4.2). When palladium and CuI were used by 2% and 5% with respect to the enyne substrate, among the solvents used THF was the best option leading the alkynyl-substituted vinylallene proceeded cleaner and as a result led to higher yields (Table 4.1, entry 8-11). Palladium complex and triphenylphosphine were stirred about 15 minutes for in situ activation of palladium. As an amine base, diethyl amine was the choice of the base for the process. Screening the parameters such as: ligand,

percentage of the catalyst, the catalyst to ligand ratio, amine base and other additives are outlined below.

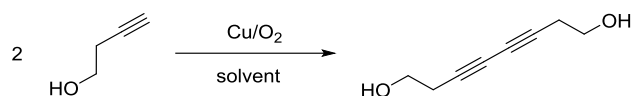
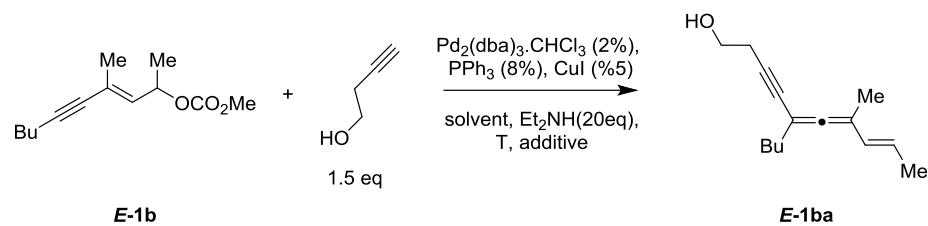


Figure 4.2. Copper-mediated Glacier or self-coupling of terminal alkynes in the presence of catalytic oxygen.

Initial results of the optimization studies for the cross coupling reaction are given in Table 4.1. With the use of high boiling point solvents as dioxane and DMF, at elevated temperatures, the reactions gave rise to unsatisfactory yields of the vinylallene (Table 4.1, Entry 1 and 2). With the use of THF as a solvent at room temperature no conversion was observed (Table 4.1, Entry 3). A promising yield of 72% could be obtained when the reaction was conducted at 55 °C vinylallene (Table 4.1, Entry 4). In order to drive further the reaction towards higher yields, some additives have been employed to influence the reactivity of the system. The use of inorganic salts in the reaction medium had positive effects on the product formation (Rao *et al.*, 2009). As an additive, the insertion of 2 equivalents of potassium bromide provided superior result compared to other inorganic salts (Table 4.1, Entry 5-8). The use of water with potassium bromide additive was apparently detrimental on the yield (Table 4.1, Entry 12-13).

Table 4.1. Effect of additives on Pd/Cu-Catalyzed alkynylation Reactions of the *E*-Enyne Carbonate **E-1b**



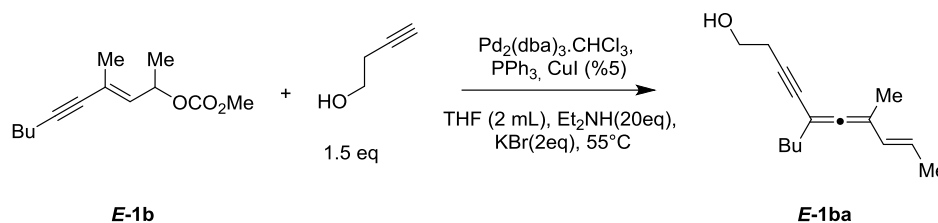
| Entry | Additive | Water | Solvent | T | Time | Yield* |
|------------|----------------------|-------------------|--------------|--------|---------|--------|
| 1** | | | Dioxane 4 mL | 100 °C | 1h | trace |
| 2 | - | - | DMF 2 mL | 80 °C | 2h | 49 % |
| 3** | | | THF 2 mL | RT | 24h | trace |
| 4 | | | THF 2 mL | 55 °C | 3.5h | 72% |
| 5 | KI 2 eq | - | THF 2 mL | 55 °C | 24h | 7% |
| 6 | LiBr 2 eq | - | THF 2 mL | 55 °C | 16h | 48% |
| 7 | AgNO_3 2 eq | - | THF 2 mL | 55 °C | 5h | No rxn |
| 8 | KBr 2 eq | - | THF 2 mL | 55 °C | 3h | 86% |
| 9 | KBr 2 eq | - | DMF 2 mL | 55 °C | 1 h | 50% |
| 10 | KBr 2 eq | - | Toluene 2 mL | 55 °C | 3.5 h | 61% |
| 11 | KBr 2 eq | - | Dioxane 2 mL | 55 °C | 30 min. | 40% |
| 12 | KBr 2 eq | 100 μL | THF 2 mL | 55 °C | 3h | 44% |
| 13 | - | 100 μL | THF 2 mL | 55 °C | 3h | 44% |

* Determined by NMR using *p*-anisaldehyde as an internal standard.

** Pd 5%, PPh_3 20%.

Palladium-to-ligand ratio has a critical role on the coupling reactions. Except for entry 4, the solution of palladium/phosphine combination was stirred about 15 minutes for in situ activation of $\text{Pd}_2(\text{dba})_3\cdot\text{CHCl}_3$ (Amatore and Jutand, 1998). A mixture of palladium complex and 2 equivalents (with respect to Pd) of phosphine ligand and 3 equivalents of phosphine ligand gave moderate yields (Table 4.2, Entry 1 and 2). Stirring Pd/phosphine mixture for 1 hour to in situ activation of palladium decreased the yield of the coupling reaction (Table 4.2, Entry 4). Longer activation times for in situ activation of palladium species with triphenylphosphine causes the poisoning of active palladium species in time. Using $\text{Pd}_2(\text{dba})_3\cdot\text{CHCl}_3$ complex alone in the cross coupling, observed yield was low (Table 4.2, Entry 3).

Table 4.2. Effect of Pd/ligand ratio on alkylation of E-Enyne Carbonate **E-1b**



| Entry | Pd% | Ligand | Time | Yield* |
|-------|-------|---------------------|------|--------|
| 1 | 2% Pd | 4% PPh ₃ | 3h | 65% |
| 2 | 2% Pd | 6% PPh ₃ | 3.5h | 68% |
| 3 | 2% Pd | - | 16h | 14% |
| 4** | 2% Pd | 8% PPh ₃ | 3h | 62% |

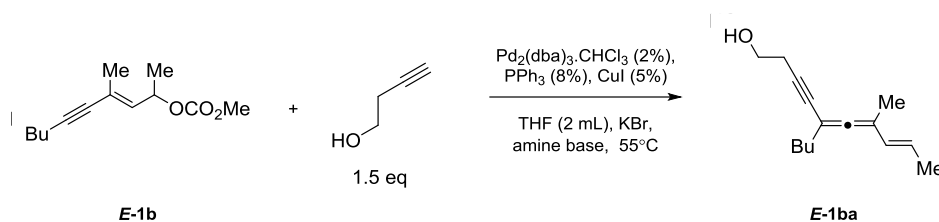
* Determined by NMR using *p*-anisaldehyde as an internal standard.

** Pd and phosphine ligand was stirred 1 hour before addition.

With the optimized conditions so far, activity of amine bases on the coupling reaction was also examined. While triethylamine, Pyrrolidine and Piperidine had a moderate effect on the coupling reaction (Table 4.3, Entry 4-7), 1,4-Diazabicyclo[2.2.2]octane (DABCO), diisoptopylamine and dibutylamine provide higher activities (Table 4.3, Entry 1-3). On the other hand, no other amine bases compared to diethyl amine were able to improve the yield of the reaction. In fact, increasing the amount

of diethyl amine from 20 equivalents to 40 equivalents improved the yield up to 92% (Table 4.3, Entry 7). With 40 equivalents of diethyl amine, an increase of KBr content to 3 equivalents significantly accelerated the reaction (Table 4.3, Entry 8) and this established condition was assigned as the *method a* in the rest of the study.

Table 4.3. Screening of amine bases on alkynylation of *E*-Enyne Carbonate **E-1b**

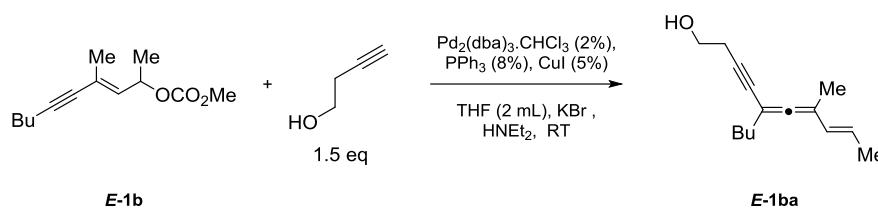


| Entry | Amine base | KBr | Time | Yield* |
|-------|-------------------------|------|-------|--------|
| 1 | DABCO 20 eq | 2 eq | 3 h | 78% |
| 2 | DIPA 20 eq | 2 eq | 3 h | 74% |
| 3 | DBA 20 eq | 2 eq | 3 h | 79% |
| 4 | TEA 20 eq | 2 eq | 3 h | 57% |
| 5 | Pyrrolidine 20 eq | 2 eq | 3 h | 47% |
| 6 | Piperidine 20 eq | 2 eq | 3 h | 31% |
| 7 | HNEt ₂ 40 eq | 2 eq | 2.5 h | 92% |
| 8 | HNEt ₂ 40 eq | 3 eq | 1.5 h | 91% |

* Determined by NMR using *p*-anisaldehyde as an internal standard.

We also surveyed the effect of base and additive amounts, but at RT this time because the employment of highly active conditions would impede observation of changes resulting from the slight activity changes. On the basis of the results illustrated in Table 4.4., it seems that 2 equivalent of base and 3 equivalent KBr would be sufficient amount that can be used in for the catalytic reactions.

Table 4.4. Effect of amount of HNEt₂ and KBr on the reactivity



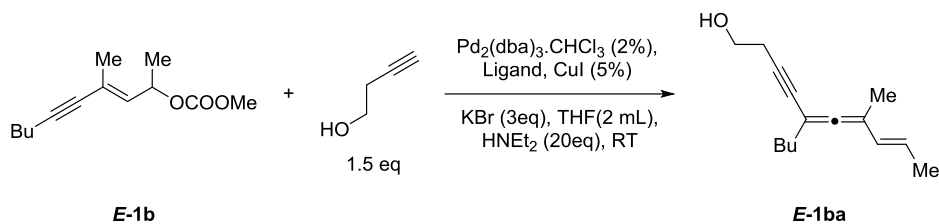
| Entry | HNEt ₂ eq | KBr | Time | Yield* |
|-------|----------------------|------|------|--------|
| 1 | 20 eq | 1 eq | 5 h | 34% |
| 2 | 20 eq | 2 eq | 8 h | 44% |
| 3 | 20 eq | 3 eq | 7 h | 58% |
| 4 | 20 eq | 4 eq | 3 h | 47% |
| 5 | 40 eq | 2eq | 3 h | 36% |
| 6 | 80 eq | 2 eq | 3 h | 13% |
| 7 | 40 eq | 3eq | 5 h | 28% |
| 8 | 80 eq | 3eq | 4 h | 22% |

* Determined by NMR using *p*-anisaldehyde as an internal standard.

Effect of various mono-dentate and bidentate phosphine, phosphite and arsine ligands were evaluated for the cross coupling reaction at room temperature (Table 4.5). Many of mono-dentate phosphine ligands, especially large cone angle ligands such as; Tris(2-methoxyphenyl)phosphine, Tris(2, 6-dimethoxyphenyl)phosphine and Tris(2, 4, 6-trimethylphenyl)phosphine resulted in low conversions (Table 4.5, Entry 1, 5 and 6). Low sigma donor tris(4-fluorophenyl)phosphine had no influence on the reaction (Table 4.5, entry 8). Bi-dentate phosphine ligands, phosphite ligands and arsine ligand were also ended in low yields of alkynylated vinylallene **E-1ba** (Table 4.5, Entry 9-15). Ligands having higher average sigma donor ability like dibenzylphenylphosphine and tris(4-methoxyphenyl)phosphine resulted in high yields but low reaction rates (Table 4.5, Entry 2 and 7). Despite its low sigma donor ability but having similar cone angle to dibenzylphenylphosphine and tris(4-methoxyphenyl)phosphine, tris(2-furyl)phosphine ligand provided a higher reaction rate and elevated yield of the desired vinylallene (Table 4.5, Entry 3) (For specific information for phosphine ligands, Andersen and Keay, 2001).

Although the vinylallene **E-1ba** could be synthesized at room temperature in satisfactory yields, however the reactions at RT were not so repeatable. The major problem was the formation of high quantity of self-coupling product of 3-butyn-1ol. To diminish self-coupling product produced by 3-butyn-1ol and favor the desired pathway, experiments were also done according to methods described in literature (Table 4.6) (Elangovan et al., 2003; Bag et al., 2011). The reducing agents such as sodium ascorbate and H₂ were used in order to reduce oxygen by specific reduction mechanisms. The trials with sodium ascorbate did not improve the yield compared to optimized conditions at room temperature (Table 4.5, Entry 3, Table 4.6, Entry 2-6). The use of one to one mixture of argon and hydrogen in a balloon in a reaction medium improved the yield up to 80% and diminished the self-coupling product successfully (Table 4.6, Entry 1). However, conditions with hydrogen argon mixtures were not again stable and gave variable results.

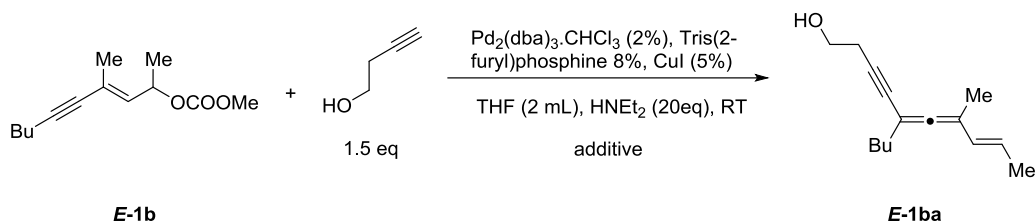
Table 4.5. Effect of various ligands at room temperature on reactivity was shown



| Entry | Ligand % | Time | Yield* |
|-------|---|------|--------|
| 1 | Tris(2-methoxyphenyl)phosphine 8% | 22h | 30% |
| 2 | Tris(4-methoxyphenyl)phosphine 8% | 13h | 84% |
| 3 | Tris(2-furyl)phosphine 8% | 5.5h | 78% |
| 5 | Tris(2, 6-dimethoxyphenyl)phosphine 8% | 5.5h | 26% |
| 6 | Tris(2, 4, 6-trimethylphenyl)phosphine 8% | 4h | 13% |
| 7 | Dibenzylphenylphosphine 8% | 9h | 73% |
| 8 | Tris(4-fluorophenyl)phosphine 8% | 4h | 7% |
| 9 | Triethylphosphite %8 | 7h | 11% |
| 10 | Triphenylphosphite %8 | 3h | No rxn |
| 11 | Triphenylarsine %8 | 4h | 12% |
| 12 | Xantphos 4% | 2.5h | 16% |
| 13 | 1,2-Bis(diphenylphosphino)ethane 4% | 24h | 2% |
| 14 | 1,3-Bis(diphenylphosphino)propane 4% | 24h | 8% |
| 15 | 1,4-Bis(diphenylphosphino)butane 4% | 24h | 26% |

* Determined by NMR using *p*-anisaldehyde as an internal standard.

Table 4.6. Attempts to stabilize reaction conditions

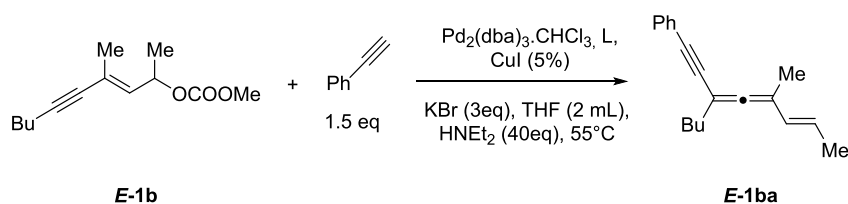


| Entry | Additive | KBr | Time | Yield* |
|-------|--------------------------|------|------|--------|
| 1 | $\text{H}_2 + \text{Ar}$ | 3 eq | 7h | 80% |
| 2 | 10% mol Na-Ascorbate | 3 eq | 8h | 56% |
| 3 | 10% mol Na-Ascorbate | - | 3h | 28% |
| 4 | 3 eq Na-Ascorbate | - | 5.5h | 60% |
| 5 | 10 eq Na-Ascorbate | - | 4h | 55% |
| 6 | 3 eq Na-Ascorbate | 3 eq | 7h | 62% |

* Determined by NMR using *p*-anisaldehyde as an internal standard.

Screening different types of alkyne coupling partners is an important issue for the synthesis of alkynylated vinylallene products. However, phenyl acetylene with the optimized condition (*method a*) gave poor yield (Table 4.7, Entry 1). Increasing Pd content in the coupling reaction up to two folds gave moderate yield of cross coupling product and this modification to *method a* named as *method b* (Table 4.7, Entry 2). Applying tris(2-furyl)phosphine instead of PPh_3 with the conditions of *method a*, gave average yield of cross coupling product (Table 4.7, Entry 3). Increasing catalyst equivalency by 2 folds into the reaction mixture increased the yield up to 71% and this condition was a modified version of *method a* and named as *method c* (Table 4.7, Entry 4). However, loading extra palladium up to 10% favored homo-coupling product and decreased the desired yield of cross coupling (Table 4.7, Entry 5). Increasing the molarity of alkyne in reaction mixture from 1.5 to and 2 equivalent also favored homo-coupling and reduced cross-coupling (Table 4.7, Entry 6).

Table 4.7. Optimization of the reaction conditions for phenyl acetylene.



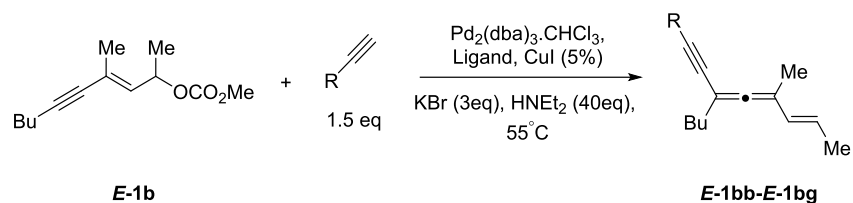
| Entry | Pd% | Ligand (% to Pd) | Alkyne eq. | Time | Yield* |
|-------|-----|-----------------------|------------|---------|--------|
| 1 | 2 | PPh ₃ (8) | 1.5 h | 4 h | 28% |
| 2 | 4 | PPh ₃ (16) | 1 h | | 69% |
| 3 | 2 | TFP (8) | 1.5 h | 7 h | 58% |
| 4 | 4 | TFP (16) | 1.5 h | 1 h | 71% |
| 5 | 10 | TFP (40) | 1.5 h | 30 min. | 48% |
| 6 | 4 | TFP (16) | 2 h | 30 min. | 46% |

* Determined by NMR using *p*-anisaldehyde as an internal standard.

** (Tris(2-furyl)phosphine).

With various terminal alkynes in hand, *method a*, *method b* and *method c* were screened for the cross coupling reaction between terminal alkynes and (*E*)-enone carbonate *E*-1b (Table 4.8). Terminal alkynes substituted with alkyl groups except *tert*-butyl substituted terminal alkyne, gave smoother reactions compared to aryl substituted alkynes in moderate to high yields with *method a* (Table 4.8, Entry 1, 6 and 7). The use of *method b* with *tert*-butyl substituted terminal alkyne gave good yield (Table 4.8, Entry 7). With the case of aryl substituted terminal acetylenes, phenyl acetylene gave better result with the use of *method c* (Table 4.8, Entry 2). However, ethynyl-4-methoxybenzene resulted in an inverse manner compared to phenyl acetylene gave better result with *method a* (Table 4.8, Entry 3). Electron-withdrawing substituent on the aromatic ring such as nitro group (Table 4.8, Entry 4) interfere the outcome of the coupling reaction and result in a complex mixture. However trifluoromethyl substitution on para position of terminal alkyne gave moderate yield with *method b* (Table 4.8, Entry 8). Coupling of silyl substituted terminal acetylene (tri-isopropylsilyl acetylene) gave also moderate yields with both *methods a, b* and *c*. (Table 4.8, Entry 7).

Table 4.8. Visualizing different coupling partners.



| Entry | R | Pd% | Ligand (%) | Method | Time | Product | Yield* |
|----------|---|-----|------------------------|----------|---------|--------------|---------|
| 1 | | 2% | PPh ₃ 8% | <i>a</i> | 1.5 h | E1-bb | 88% |
| | | 2% | PPh ₃ 8% | <i>a</i> | 4 h | | 28% |
| 2 | | 4% | PPh ₃ 16% | <i>b</i> | 1 h | E1-bc | 69% |
| | | 4% | TFP** 16% | <i>c</i> | 1 h | | 71% |
| | | 2% | PPh ₃ (8%) | <i>a</i> | 3 h | | 74% |
| 3 | | 4% | PPh ₃ (16%) | <i>b</i> | 1 h | E1-bd | 55% |
| | | 4% | TFP** (16%) | <i>c</i> | 2 h | | 50% |
| | | 2% | PPh ₃ (8%) | <i>a</i> | 2 h | E1-be | mixture |
| 4 | | 2% | PPh ₃ (8%) | <i>a</i> | 2 h | | 28% |
| | | 4% | PPh ₃ (16%) | <i>b</i> | 2 h | | 68% |
| | | 4% | TFP** (16%) | <i>c</i> | 10 min. | | 20% |
| 5 | | 2% | PPh ₃ (8%) | <i>a</i> | 2 h | E1-bf | 82% |
| | | 2% | PPh ₃ (8%) | <i>a</i> | 2 h | | 64% |
| 6 | | 4% | PPh ₃ (16%) | <i>b</i> | 2.5 h | E1-bg | 75% |
| | | 4% | TFP** (16%) | <i>b</i> | 2 h | | 65% |
| | | 2% | PPh ₃ (8%) | <i>a</i> | 2 h | | 65% |
| 7 | | 4% | PPh ₃ (16%) | <i>b</i> | 1.5 h | E1-bh | 66% |
| | | 4% | TFP** (16%) | <i>c</i> | 2 h | | 56% |
| | | 2% | PPh ₃ (8%) | <i>a</i> | 2 h | | |

* Isolated yields

**Tris(2-furyl)phosphine.

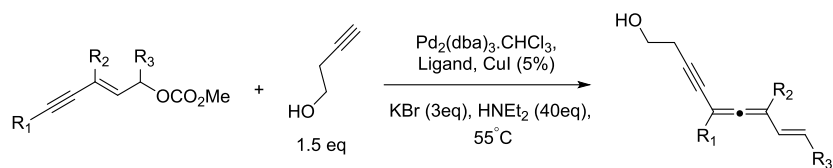
With a set of substituted (*E*)-enynes prepared, the scope of different substrates was screened on catalytic alkynylation (Table 4.9). **Method b** and **c** was also applied to substrates when the **method a** resulted in unsatisfactory yields. Having alkyl groups on the alkynyl carbon (R^1), such as butyl or cyclohexyl groups resulted in high yields of alkynyl vinylallenes (Table 4.9, Entry 2 and 5). Bulky tertiary butyl substitution and less sterically hindered methyl group on R^1 position yielded desired alkynyl vinylallenes in average yields (Table 4.9, Entry 1 and 4). The use of **method b** with bulky tertiary butyl substitution on R^1 position yielded desired vinyl allene in high yield (Table 4.9, Entry 1 and 4).

The substitution of R^1 position with phenyl group gave a moderate yield of 61% via **method a**. When substrate **E-1f** subjected to **method b** and **c**, reaction yielded the desired product with relatively low yield compared to **method a**. This could be caused by deterioration of vinyl allene product in the reaction medium due to increased amount of Palladium content (Table 4.9, Entry 6). When R^1 position of (*E*)-enynes was terminal, no desired product was observed and the coupling reaction resulted in an inseparable mixture (Table 4.9, Entry 3).

The (*E*)-enynes bearing with disubstituted alkenyl moiety reacted in relatively higher rate by both **methods a** and **c** though the yield obtained for the **method a** was low and it was moderate for **method c**. The use of **method b** with substrate **E-1g** achieved a high yield of desired product (Table 4.9, Entry 7). The substitution of R^2 position with butyl group gave a smooth reaction and a high yield of desired product (Table 4.9, Entry 9). Phenyl substitution on R^2 position maintained a moderate yield of desired vinyl allene **E-1ha** with both **methods a** and **b** (Table 4.9, Entry 8).

Allylic position of the (*E*)-enynes substituted with phenyl, butyl and *i*-propyl groups. Butyl group on the allylic position of the enynes gave moderate yield of the product with both **methods a, b** and **c** (Table 4.9, Entry 11). However, a steric functional group on the R^3 position (*i*-propyl) had a remarkable negative effect on the activity, thus resulted in a low yield of the desired product **E-1ja** with **methods a** and **c**. On the other hand, a moderate yield was observed with the use of **method b** (Table 4.9, Entry 10). Phenyl substitution on R^3 position yielded in the desired product **E-1la** in a smooth manner with a fast rate of the reaction (Table 4.9, Entry 12). When allylic position of (*E*)-enynes was primary reaction yielded the desired product with moderate yield with **methods a**. Increasing the palladium content in the reaction (**method b**) did not improved the yield but caused a low yield of **E-1na** (Table 4.9, Entry 13).

Table 4.9. Screening various enyne carbonates for the coupling reaction.



| Entry | React. | R ¹ | R ² | R ³ | Pd% | Ligand (%) | Meth. | Product | Time | Yield ^a |
|-------|--------------|-----------------|----------------|----------------|-----|-----------------------|----------|---------------|---------|--------------------|
| 1 | <i>E</i> -1a | Me | Me | Me | 2% | PPh ₃ (8) | <i>a</i> | <i>E</i> -1aa | 2 h | 47% |
| | | | | | 4% | PPh ₃ (16) | <i>b</i> | | 1 h | 35% |
| | | | | | 4% | TFP**(16) | <i>c</i> | | 4 h | 61% |
| 2 | <i>E</i> -1b | Bu | Me | Me | 2% | PPh ₃ (8) | <i>a</i> | <i>E</i> -1ba | 1.5 h | 91% |
| 3 | <i>E</i> -1c | H | Me | Me | 2% | PPh ₃ (8) | <i>a</i> | <i>E</i> -1ca | 1 h | mixture |
| 4 | <i>E</i> -1d | ^t Bu | Me | Me | 2% | PPh ₃ (8) | <i>a</i> | <i>E</i> -1da | 2 h | 65% |
| | | | | | 4% | PPh ₃ (16) | <i>b</i> | | 3 h | 90% |
| | | | | | 4% | TFP (16) | <i>c</i> | | 2 h | 51% |
| 5 | <i>E</i> -1e | Cy | Me | Me | 2% | PPh ₃ (8) | <i>a</i> | <i>E</i> -1ea | 3 h | 71% |
| | | | | | 4% | PPh ₃ (16) | <i>b</i> | | 5 h | 85% |
| | | | | | 4% | TFP ** (16) | <i>c</i> | | 5 h | 85% |
| 6 | <i>E</i> -1f | Ph | Me | Me | 2% | PPh ₃ (8) | <i>a</i> | <i>E</i> -1fa | 1 h | 61% |
| | | | | | 4% | PPh ₃ (16) | <i>b</i> | | 1 h | 42% |
| | | | | | 4% | TFP**(16) | <i>c</i> | | 1 h | 25% |
| 7 | <i>E</i> -1g | Bu | H | Me | 2% | PPh ₃ (8) | <i>a</i> | <i>E</i> -1ga | 30 min. | 68% ^b |
| | | | | | 4% | PPh ₃ (16) | <i>b</i> | | 1 h | 86% ^c |
| | | | | | 4% | TFP**(16) | <i>c</i> | | 30 min. | 37% |
| 8 | <i>E</i> -1h | Bu | Ph | Me | 2% | PPh ₃ (8) | <i>a</i> | <i>E</i> -1ha | 1h. | 44% |
| | | | | | 4% | PPh ₃ (16) | <i>b</i> | | 1.5 h | 56% |
| 9 | <i>E</i> -1i | Bu | Bu | Me | 2% | PPh ₃ (8) | <i>a</i> | <i>E</i> -1ia | 2 h | 84% |
| 10 | <i>E</i> -1j | Bu | Me | <i>i</i> Pr | 2% | PPh ₃ (8) | <i>a</i> | <i>E</i> -1ia | 1.5 h | 35% |
| | | | | | 4% | PPh ₃ (16) | <i>b</i> | | 4 h | 55% |
| | | | | | 4% | TFP**(16) | <i>c</i> | | 2 h | 22% |
| 11 | <i>E</i> -1k | Bu | Me | Bu | 2% | PPh ₃ (8) | <i>a</i> | <i>E</i> -1ka | 2 h | 65% |
| | | | | | 4% | PPh ₃ (16) | <i>b</i> | | 3 h | 64% |
| | | | | | 4% | TFP** (16) | <i>c</i> | | 2 h | 51% |
| 12 | <i>E</i> -1l | Bu | Me | Ph | 2% | PPh ₃ (8) | <i>a</i> | <i>E</i> -1la | 30 min. | 90% |
| 13 | <i>E</i> -1m | Bu | Me | H | 2% | PPh ₃ (8) | <i>a</i> | <i>E</i> -1na | 1h. | 47% |
| | | | | | 4% | PPh ₃ (16) | <i>b</i> | | 1 h | 24% |

^a Isolated yields.^b purity of the sample was 88% detected by ¹H NMR analyses.^c purity of the sample was 82% detected by ¹H NMR analyses.

A cross coupling reaction was also applied for the other isomer of enyne carbonate **Z1-a**. Yet, the reaction of 3-butyn-1-ol with (*Z*)-enyne carbonate gave lower yield of (*E*) configured alkynylvinylallene compared to its (*E*) isomer (Figure 4.3).

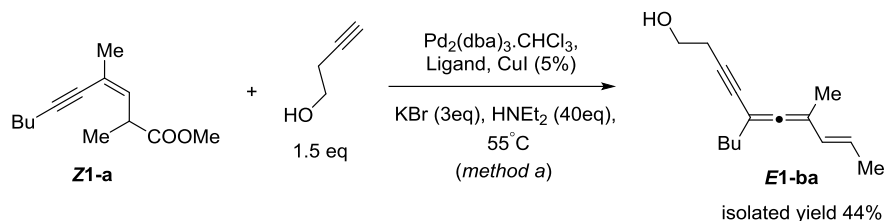


Figure 4.3. Coupling reaction of 3-butyn-1-ol with **Z1-a**.

A possible chirality transfer for the cross-coupling reaction with 3-butyn-1-ol and **R, E-1b** under the optimized conditions was investigated. Unfortunately, the reaction of enantio-enriched enyne carbonate with 3-butyn-1-ol gave a racemic mixture of **E-1ba** as determined by HPLC analyses (Figure 4.4).

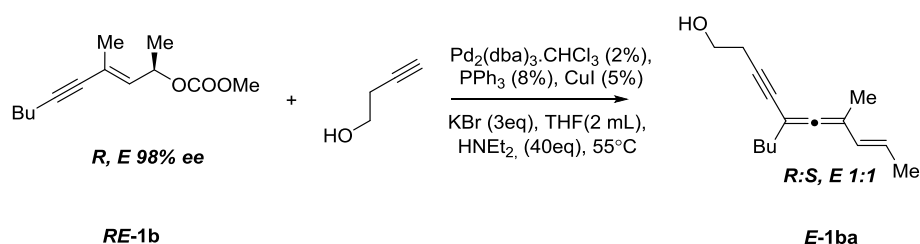


Figure 4.4. Reaction of an enantio-enriched enyne carbonate with terminal alkynes.

The outcome of the cross-coupling reaction was also applied with enyne epoxides **E-ox** and **Z-ox**. Both reaction with *E* and *Z* isomer of enyne epoxides yield vinyl allenol **E-ox-a** as a single isomeric form. Unfortunately, cross coupling reaction of enyne epoxides with 1-hexyne did not give satisfactory yields of desired product **E-ox-a** (Figure 4.5).

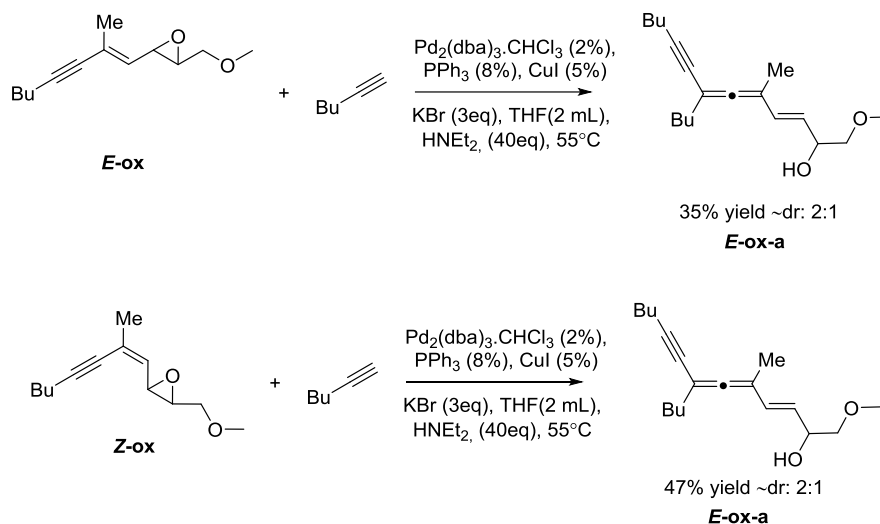


Figure 4.5. Reaction of enyne epoxides with 1-hexyne.

Prepared vinyl allene derivatives can further be used in Diels-Alder reactions. As an application of vinyl allene **E-1bb** was conducted to a Diels-Alder reaction in the presence of N-phenylsuccinimide. Reaction yielded expected [4+2] cyclization product **E-1bb-DA** in 65% yield in 48 hours. Exact structure of **E-1bb-DA** was determined with ^1H NOE studies and shown in figure 4.6.

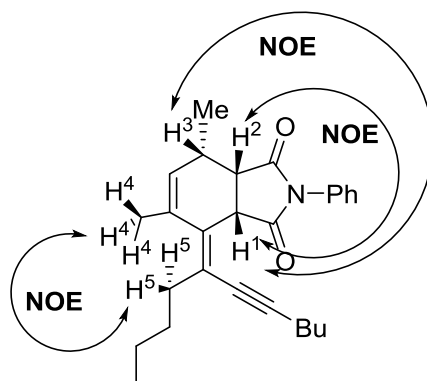
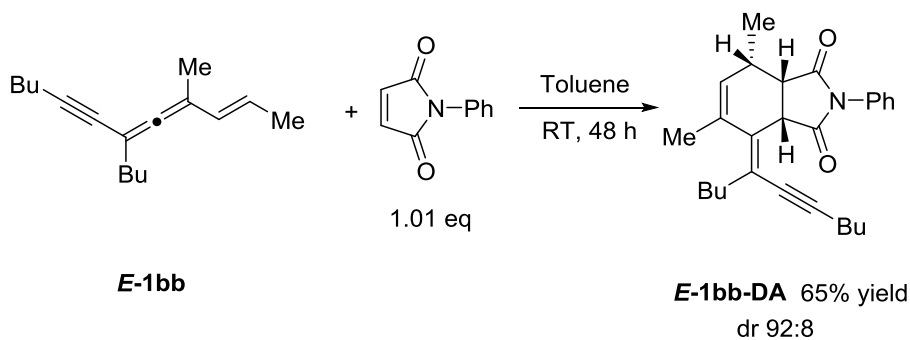


Figure 4.6. [4+2] Cyclization of **E-1bb** and exact structure of **E-1bb-DA**.

Pd/Cu-catalyzed alkynylation reaction mechanism initiates with *in-situ* formation of active Pd(0) species (**A**). Possible mechanistic route begins with oxidative addition of Pd(0) (**B**) to form allyl palladium intermediate (**C**). 1, 5- S_N2'' type substitution of Pd to alkynyl carbon yields σ -allenylpalladium intermediate (**D**). Following the formation of σ -allenylpalladium intermediate, catalytic cycle advances with the transmetalation step (**E**). Finally, reductive elimination (**F**) takes place to yields vinylallenes and Pd(0) species are reformed (Figure 4.7).

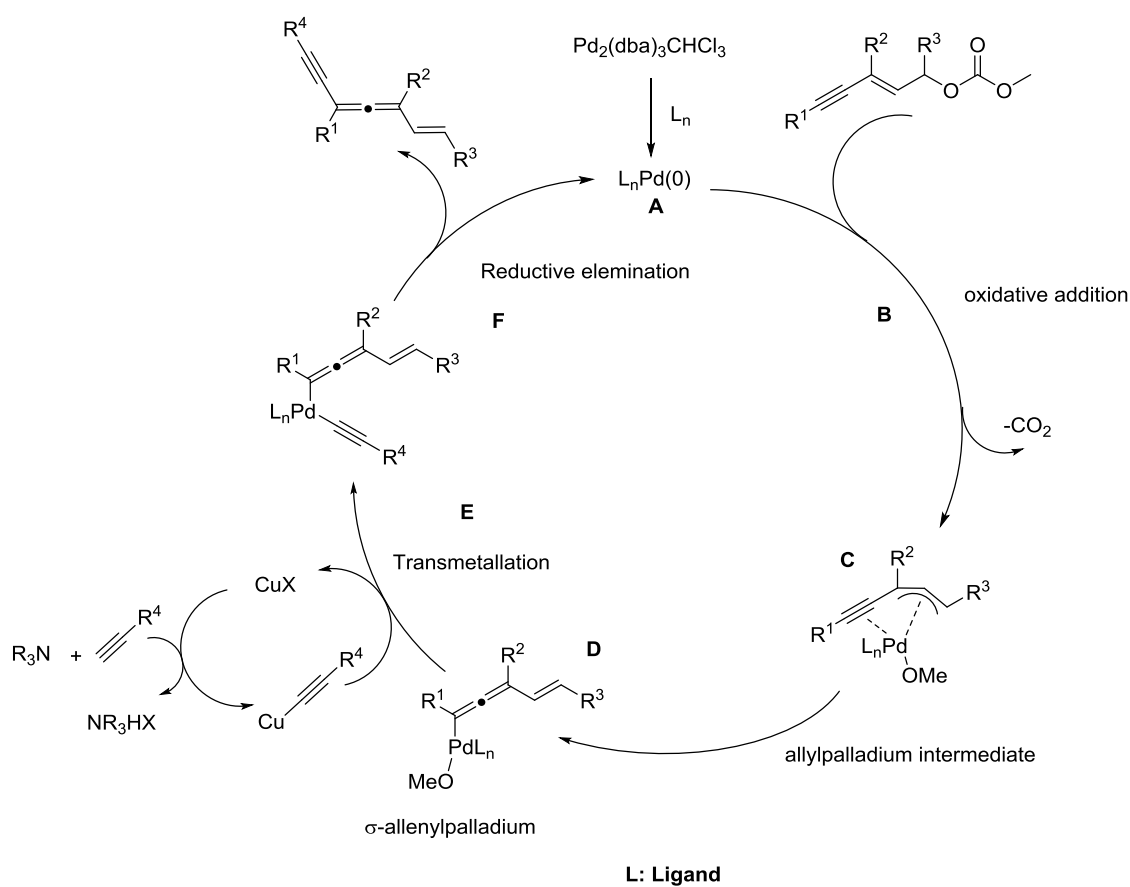


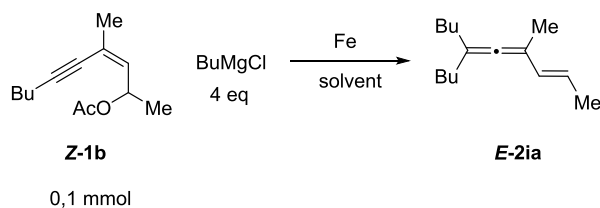
Figure 4.7. Proposed reaction mechanism of alkynylation of (*E*)-enyne carbonates.

4.2. Iron-Catalyzed Alkylation of *E*-Enyne Acetates with Grignard Reagents

Alkylation reaction of enyne acetates was performed initially with *Z*-isomer of the enyne acetate, **Z-1b** and BuMgCl was used as alkylation reagent. Optimization of catalyst, solvent, additives and temperature were screened to obtain maximum yield, minimum side products and complete regio-selectivity

The alkylation of **Z-1b** was performed with 4 equivalent of BuMgCl and in the presence of 1 equivalent of Fe(acac)₃ in 5 mL of dry Et₂O at both -50 and -80 °C reaction temperatures. Both reactions afforded comparably good yields of the expected vinylallene product (Table 4.10, Entry 1 and 2). Increasing the reaction temperature up to -20 and 0 °C was detrimental on the S_N2'' reaction and resulted in complete mixture of side products (Table 10, Entry 3 and 4). Replacement of the catalyst to stoichiometric amounts of FeCl₂ and solvent system to THF (solubility of FeCl₂ better in THF compared to diethyl ether) high yields further improved the yield formation (Table 4.10, Entry 5 and 6). The reactions were also carried out at lower catalyst loadings, such as at 0.5, 0.4, and 0.3 equivalents of FeCl₂. However, this gradual decrease of the catalyst within the reaction medium always accompanied by a parallel decrease in the yield. Unfortunately, decreasing the catalyst loading to 0.1 eq brought about the desired product formation to a poor yield (Table 4.10, Entry 10).

Table 4.10. Optimization studies on the alkylation of enyne acetates.



| Entry | Catalyst (eq) | Solvent (mL) | Temperature (°C) | Time | Yield* (%) |
|-------|-----------------------------|-----------------------|------------------|---------|------------|
| 1 | Fe(acac) ₃ (1,0) | Et ₂ O (5) | -50 | 2 h | 74 |
| 2 | Fe(acac) ₃ (1,0) | Et ₂ O (5) | -80 | 2 h | 77 |
| 3 | Fe(acac) ₃ (1,0) | Et ₂ O (5) | -20 | 30 min. | mixture |
| 4 | Fe(acac) ₃ (1,0) | Et ₂ O (5) | 0 | 30 min. | mixture |
| 5 | FeCl ₂ (1,0) | THF (5) | -50 | 2 h | 87** |
| 6 | FeCl ₂ (1.0) | THF (2) | -50 | 2 h | 90 |
| 7 | FeCl ₂ (0.5) | THF (2) | -50 | 2.5 h | 85 |
| 8 | FeCl ₂ (0.4) | THF (2) | -50 | 2.5 h | 79 |
| 9 | FeCl ₂ (0.3) | THF (2) | -50 | 2.5 h | 71 |
| 10 | FeCl ₂ (0.1) | THF (2) | -50 | 2.5 h | 27 |

* determined by ¹H NMR using *p*-anisaldehyde as an internal standard.

** isolated yield.

In some cases, depending on the conditions such as moisture, addition rate of Grignard reagent, purity of reactant and the condition of catalyst, a side product formed in the reaction as determined by ^1H NMR studies. This by-product, tentatively recognized as a reduction product as is shown in ^1H NMR spectra (Figure 4.8) and could not be isolated from alkylated vinylallene by chromatographic methods. To understand in which mechanism this reduction product formed, an extensive literature survey was performed and results obtained presented below. In light of these findings some precautions were taken to inhibit the formation of reduction product.

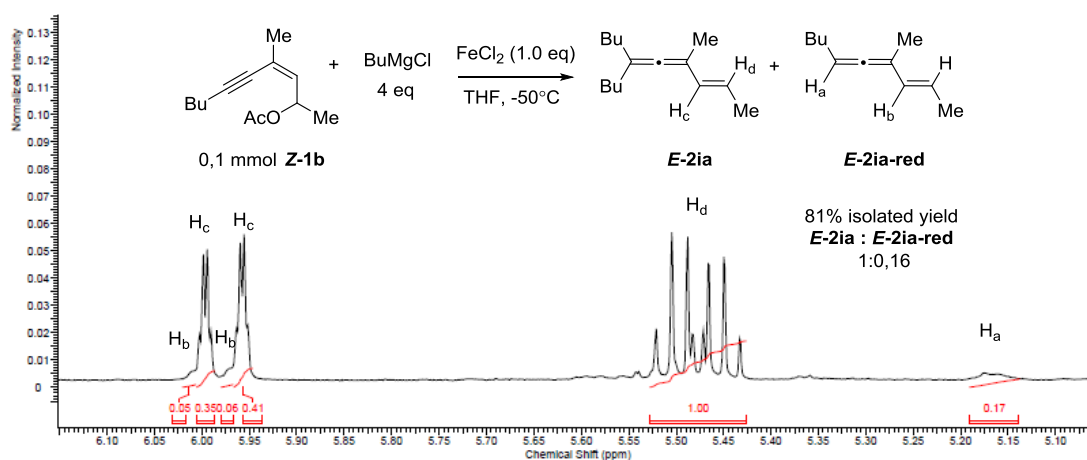


Figure 4.8. ^1H NMR spectrum of the mixture of a reduction product and alkylated vinylallene product.

In the study of Ashby (Ashby *et al.*, 1976), the addition of excess MeMgBr on benzophenone produced beside the expected 1,2-addition product (**a**), aromatic pinacols (**b**), and aromatic hydrols (**c**) (Figure 4.9). The occurrence of pinacols should be possibly due to the role of trace metal species especially iron present in Mg metal which is used to prepare the solutions of Grignard reagents. Since MeMgBr has no β -hydrogen, the reduction of aromatic ketones via hydrogen abstraction from β -carbon of MeMgBr is not possible. In the report, they clearly pointed out that MgX_2 species formed in the preparation of Grignard species extract hydrogen from solvent to produce MgH_2 as the reducing agent.

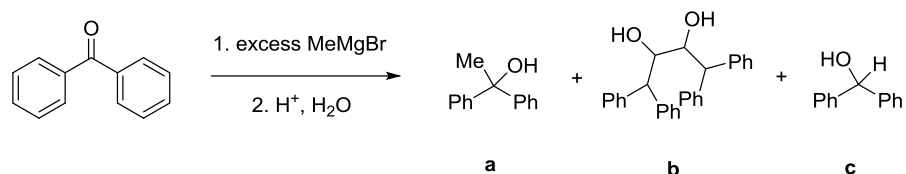


Figure 4.9. The reaction of benzophenone with MeMgBr

Another approach made by Baker group (Baker et al., 1991) addresses the reduction of propargyl halides to lead to allene structures while reacting with unactivated Mg turnings. Baker group stated that the creation of propargyl radical initially was capable of H atom abstraction from the solvent.

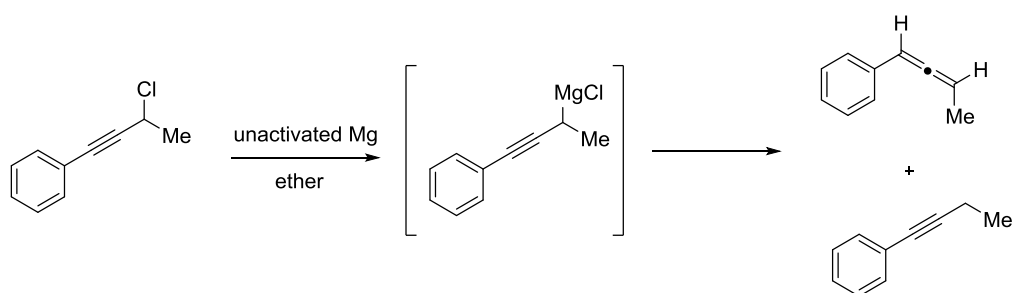


Figure 4.10. Reaction of propargyl chloride with unactivated Mg.

Observations of Ashby and Baker was also supported by the report of Bartmann (Bartmann, 1985). Bartmann concluded the formation of Mg-THF complexes. After quenching the Mg-THF complex, n-BuOH was detected (Figure 4.11).

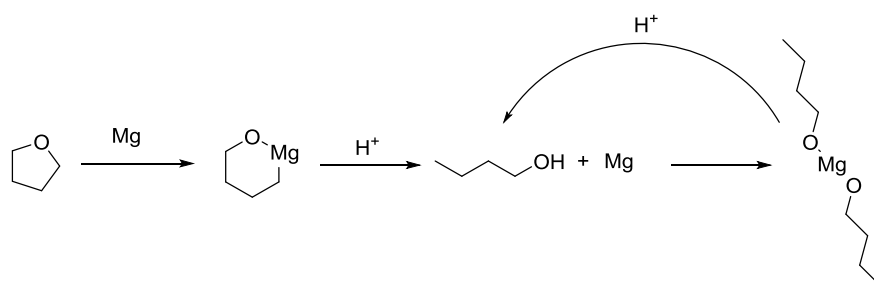
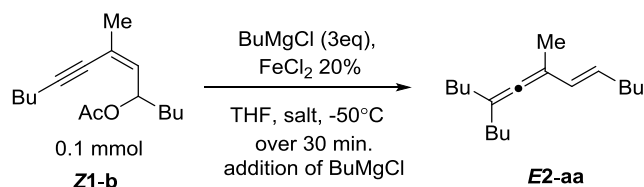


Figure 4.11. Magnesium-THF complex and butanol formation.

In the study of Rieke and Bales (Rieke and Bales, 1974), the presence of inorganic salts prevents the reduction of MgX_2 salts during Grignard solutions and thus has a positive effect on the synthesis of Grignard reagents. Using inorganic salts in the alkylation of enyne acetates with Grignard reagents may also reduce MgX_2 salts and prevent formation of MgH_2 .

In light of these findings, it was decided to decrease $RMgX$ content from 4 equivalents to 3 equivalents. As well as slow addition of $RMgX$ in the reaction media had a positive effect on the heat control. The Grignard reagents were added to the reaction medium slowly over 30 minutes. Furthermore, some of the inorganic salts were also screened for their activity in the alkylation reaction (Table 4.11). The solubility of iron complexes in THF with inorganic salts were superior, because of this, THF content was decreased to 3 mL in order to prevent negative effects of excess solvent. As the vinylallene product of **Z-2b** is remarkably volatile and to avoid the product losses with work up, the further optimization of enyne acetates were performed by using the enyne acetate **Z-2a** possessing a Bu group in R^3 . butyl substitution instead of methyl on allylic position.

Table 4.11. Screening of various inorganic additives for the alkylation reaction.



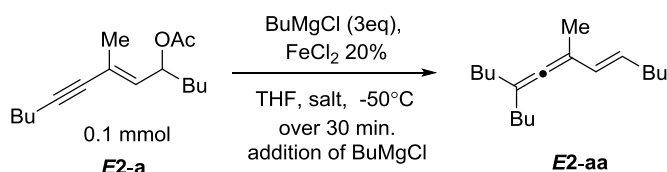
| Entry | Salt | Time | Yield* (%) |
|-------|-----------|-------|------------|
| 1 | - | 3.5 h | 74% |
| 2 | LiCl 2 eq | 1 h | 87% |
| 3 | KI 2 eq | 1 h | 82% |
| 4 | LiBr 2 eq | 1 h | 80% |
| 5 | NaI 2 eq | 1 h | 81% |
| 6 | KI 0.5 eq | 1 h | 80% |

* determined by 1H NMR using *p*-anisaldehyde as an internal standard.

The alkylation reaction with *E*-enyne acetate **E2-a** was also performed under the optimized conditions (Table 4.12). The use of inorganic salt was again apparent and provided a clear process. The yield obtained from the reaction of *E*-enyne acetate **E2-a** and BuMgCl was higher than that obtained from the *Z* isomer of enyne acetate (Table 4.12, Entry 1 and 2). of the scope of the process was surveyed for various Grignard reagents and scope *E*-enyne acetates substrate.

However, with the reaction of **E2-a** and BuMgCl, reduced vinylallene was occasionally produced in the reaction media. It was suspected that; the longer reaction times increase the formation of radicals and these radicals trigger the production of MgH₂. As is explained above, MgH₂ species could be the cause of the formation of the reduced vinylallene product. To handle this first, the temperature was increased to -40 °C. The result was satisfactory. The reaction rate increased and no reduction product was observed (Table 4.12, Entry 3)

Table 4.12. Screening of various inorganic salts for the alkylation reaction.



| Entry | Salt | Time | Yield* (%) |
|-------|---------|-------|------------|
| 1 | - | 4.5 h | 77% |
| 2 | KI 2 eq | 3.5 h | 88% |
| 3** | KI 2 eq | 1 h | 90% |

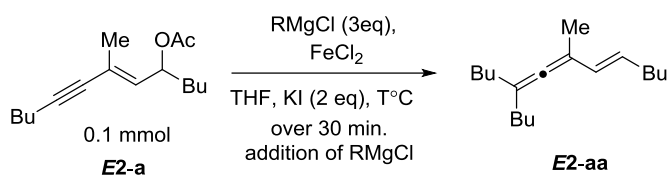
* determined by ¹H NMR using *p*-anisaldehyde as an internal standard.

** Temperature was -40°C instead of -50°C

The scope of Grignard reagents was inspected for their reactions with **E2-a**. With primary alkyl magnesium chlorides, the reactions proceeded smoothly and obtained yields were high (Table 4.13, Entry 1-4). The formation of homo-coupling products from the Grignard reagents was also observed in some extents during reactions and the coupling product of octyl magnesium chloride could not be separated from the corresponding vinylallene product of the reaction performed with this reagent.

Phenyl magnesium chloride afforded only average yields. In this reaction, medium, a large portion of the Grignard reagent was converted to biphenyl self-coupling product (Table 4.14, Entry 5). As a matter of course, increasing the catalyst ratio up to 100% doubled the yield of vinylallene obtained (Table 4.14, Entry 6). The reaction of benzyl magnesium chloride with **E2-a** resulted in a trace formation of the alkylated vinylallene product at -40 °C (Table 4.13, Entry 7). However, increasing temperature up to -20 or -10 °C some extent promoted the benzylation. (Table 4.13, Entry 8 and 9) and when the catalyst loading was 100% with respect to the substrate, benzylated vinylallene product could be obtained in a moderate yield (Table 4.13, Entry 10). The method is remarkably sensitive to the size of Grignard reagents. *i*-PrMgCl Grignard reagent appears to be reluctant toward the SN₂' reaction; low yields of the expected product along with a reductive vinylallene product was recovered in all cases regardless of the reaction temperature and catalyst level applied. The vinylallene produced by the reaction of **E2-a** with *i*-PrMgCl could not be isolated by chromatographic methods due to excess impurities and reduction product formed in the reaction (Table 4.13, Entry 11-14).

Table 4.13. The reaction of *E-2a* with various Grignard reagents.



| Entry | RMgCl | Catalyst % | Temp. °C | Time | Yield ^a (%) |
|-----------------|------------------|------------|----------|---------|------------------------|
| 1 | BuMgCl | 20 | -40 | 1 h | 90 (86) |
| 2 | PenMgCl | 20 | -40 | 1 h | 85 (78) |
| 3 | OctylMgCl | 20 | -40 | 1 h | 84 ^e |
| 4 | MeMgCl | 20 | -40 | 1 h | 80 (74) |
| 5 | PhMgCl | 20 | -40 | 1 h | (44) |
| 6 | PhMgCl | 100 | -40 | 2 h | (80) |
| 7 | BnMgCl | 20 | -40 | 30 min. | trace |
| 8 | BnMgCl | 20 | -20 | 30 min. | (18) |
| 9 | BnMgCl | 20 | -10 | 30 min. | 17 |
| 10 | BnMgCl | 100 | -20 | 30 min. | 48 (34) |
| 11 ^b | <i>i</i> -PrMgCl | 20 | -40 | 30 min. | 15 |
| 12 ^c | <i>i</i> -PrMgCl | 20 | -20 | 30 min. | (30) ^d |
| 13 ^c | <i>i</i> -PrMgCl | 20 | -10 | 30 min. | 30 |
| 14 ^d | <i>i</i> -PrMgCl | 100 | -20 | 30 min. | 34 |

^a Determined by ¹H NMR using *p*-anisaldehyde as an internal standard. isolated yields are in parenthesis.

^b Alkylated-vinylallene/reduced-vinylallene= 1:1.7

^c Alkylated-vinylallene/reduced-vinylallene= 5:1

^d Alkylated-vinylallene/reduced-vinylallene = 2:1 vinylallene

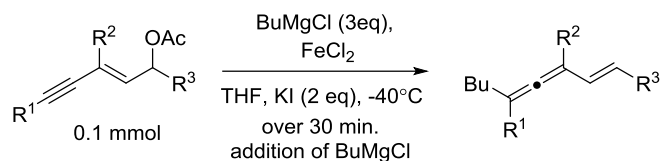
^e Vinylallene : Hexadecane was 100:5 in crude mixture.

The substitution reactions of enyne acetates with different structures and BuMgCl allowed the synthesis of a range of synthetically valuable alkylated-vinylallenes in moderate to high yields. Unfortunately, the alkylation reaction was not practical for bulky *t*-Bu group and hydrogen on the alkynyl carbon (R¹) (Table 4.14, Entries 2 and 6). On the other hand, with primary or secondary alkyl and aryl substituents in R¹, the vinylallene products are obtained in high yields. The rate of the reaction was superior when R¹ is phenyl (**E-2d**) (Table 4.14, Entry 1 and 5). Even cyclohexyl substituted enyne acetate, the desired product could be obtained in a high yield in the presence of stoichiometric amounts of FeCl₂ (Table 4.14, Entry 3 and 4).

Enyne acetates which were substituted with cyclohexyl and phenyl group on R² position did not yield vinyl allene products and result in inseparable mixtures even in the presence of stoichiometric amounts of iron salt in reaction (Table 4.14, Entry 7, 8 and 10, 11). The reaction of (*E*)-enyne acetate with disubstituted alkenyl moiety with 20% of iron salt result as an mixture of side products. However, use of stoichiometric amount of iron salt gave satisfactory yield of desired vinyl allene **E-2ia** (Table 4.14, Entry 12 and 13). Alkyl group substitution (-Bu) on R² position (*E*)-enyne acetate yield vinyl allene derivative **E-2ga** in 80% yield (Table 4.14, Entry 9)

The reaction of enyne acetates substituted with phenyl or alkyl group on allylic position (R³) with BuMgCl afforded the vinylallene structures in high yields. *Iso*-Propyl substitution on allylic position also tolerated the coupling reaction and a good yield was obtained, albeit the rate of the reaction was relatively slower in this case (Table 4.14, Entry 14). The reaction with the substrate having a methyl group on the R³ position also proceeded smoothly to produce the corresponding vinylallene product in a high yield (Table 4.14, Entry 15). Phenyl substitution on allylic position gave the desired vinylallene in a high yield with a fast reaction rate (Table 4.14, Entry 16). Primary enyne acetate on allylic position yielded vinyl allene product **E-2na** in high yield (Table 4.14, Entry 17).

Table 4.14. The reaction of various enyne acetate structures with BuMgCl.



| Entry | Code Reactant | R ¹ | R ² | R ³ | Catalyst % | Product | Time | Yield ^a |
|-------|---------------|----------------|----------------|----------------|------------|---------------|---------|----------------------|
| 1 | <i>E</i> -2a | Bu | Me | Bu | 20 | <i>E</i> -2aa | 1 h | 90 (86) |
| 2 | <i>E</i> -2b | <i>t</i> -Bu | Me | Bu | 20 or 100 | <i>E</i> -2ba | 1 h | mixture |
| 3 | <i>E</i> -2c | Cy | Me | Bu | 20 | <i>E</i> -2ca | 2 h | 35 ^c |
| 4 | <i>E</i> -2c | Cy | Me | Bu | 100 | <i>E</i> -2ca | 2 h | 83 (73) ^b |
| 5 | <i>E</i> -2d | Ph | Me | Bu | 20 | <i>E</i> -2da | 15 min. | (91) |
| 6 | <i>E</i> -2e | H | Me | Me | 20 | <i>E</i> -2ea | 4 h | mixture |
| 7 | <i>E</i> -2f | Bu | Cy | Bu | 20 | <i>E</i> -2fa | 5 h | mixture |
| 8 | <i>E</i> -2f | Bu | Cy | Bu | 100 | <i>E</i> -2fa | 3 h | mixture |
| 9 | <i>E</i> -2g | Bu | Bu | Bu | 20 | <i>E</i> -2ga | 1 h | (80) |
| 10 | <i>E</i> -2h | Bu | Ph | Bu | 20 | <i>E</i> -2ha | 30 min | mixture |
| 11 | <i>E</i> -2h | Bu | Ph | Bu | 100 | <i>E</i> -2ha | 1 h | mixture |
| 12 | <i>E</i> -2i | Bu | H | Bu | 20 | <i>E</i> -2ia | 1 h | mixture |
| 13 | <i>E</i> -2i | Bu | H | Bu | 100 | <i>E</i> -2ia | 2 h | (82) |
| 14 | <i>E</i> -2j | Bu | Me | <i>i</i> -Pr | 20 | <i>E</i> -2ja | 2 h | (78) |
| 15 | <i>E</i> -2k | Bu | Me | Me | 20 | <i>E</i> -2ka | 1 h | (91) |
| 16 | <i>E</i> -2m | Bu | Me | Ph | 20 | <i>E</i> -2ma | 30 min. | (88) ^d |
| 17 | <i>E</i> -2n | Bu | Me | H | 20 | <i>E</i> -2na | 2 h | (89) |

^a determined by ¹H NMR using *p*-anisaldehyde as an internal standard. Isolated yields are in parenthesis.

^b purity of the sample was 87% detected by ¹H NMR analyses. Alkylated-vinylallene/reduced-vinylallene= 11:1

^c Alkylated-vinylallene/reduced-vinylallene= 5:1

^d purity of the sample was 85% detected by ¹H NMR analyses

A possible pathway for the iron mediated alkylation reaction as follows: Catalytic cycle should begin with the formation of active alkyl- or aryl- iron intermediates (**A**). There are two possible pathways which should trigger the formation of oxidative addition product **D**. The first pathway follows the formation of π -allyl iron intermediate (**B**) which then follows the migration of alkyl- or aryl- group from π -allyl iron resulting in 1,5 S_N2'' σ -complex **D**. The second route should begin with the oxidative addition of alkyl- or aryl- iron intermediate to form π -allyl iron intermediate **C**. Following the shift of alkyl- or aryl- iron complex to far *sp* hybridized carbon atom produces the σ -complex **D**. Upon reductive elimination, initial alkyl- or aryl- iron complex reformed. Hydrogenation of σ -complex **D** produces the vinylallenes (**E**).

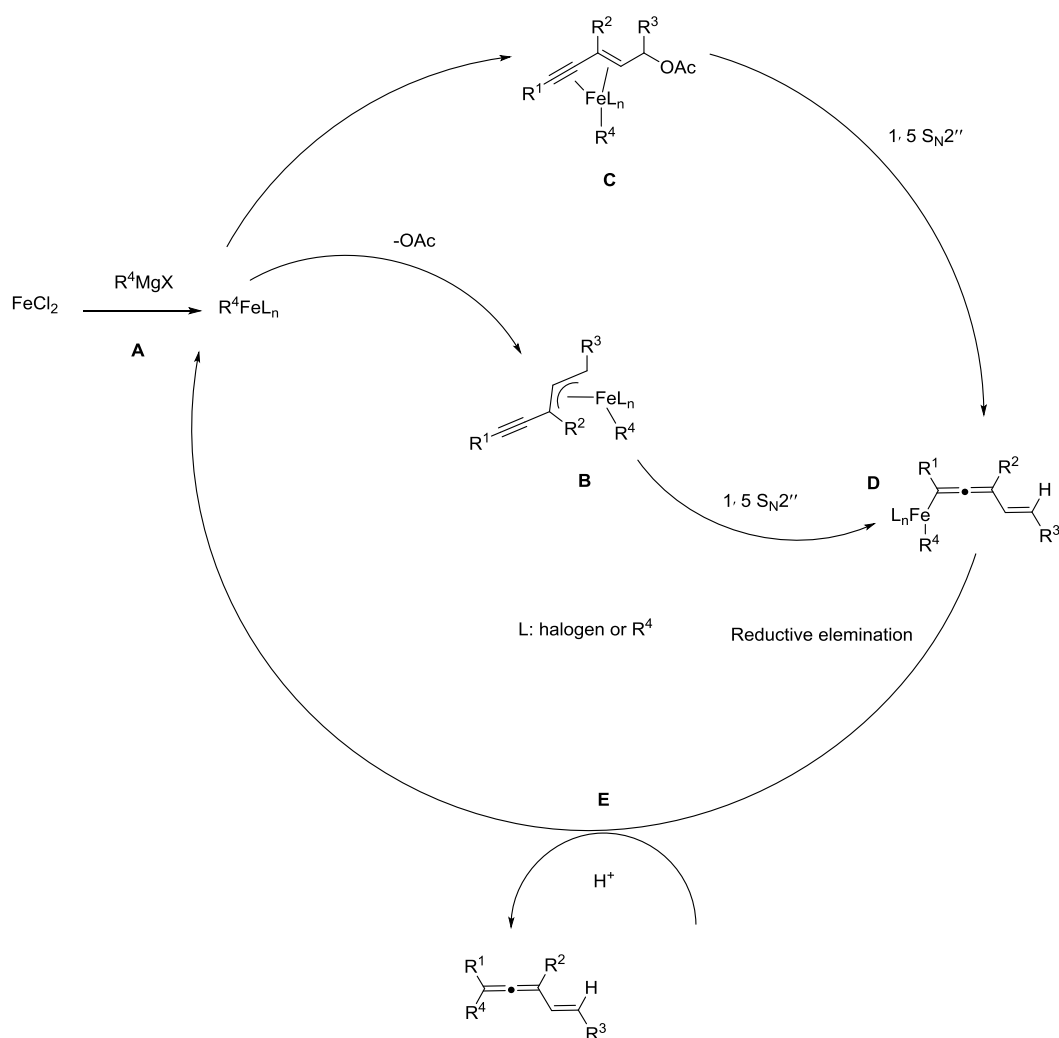


Figure 4.12. Proposed reaction mechanism of alkylation of (*E*)-enyne carbonates with Grignard reagents.

CHAPTER 5

CONCLUSION

Within the context of this thesis vinyl allene derivatives were successfully prepared by two methods. The first method is palladium-catalyzed cross coupling reaction between enyne carbonate derivatives and terminal alkynes to yield alkynyl vinyl allenes. The second method is iron catalyzed alkylation reactions of enyne acetate derivatives to produce alkylated vinyl allenes were performed.

Palladium/copper-catalyzed reaction of (*E*)-2-en-4-yne carbonates with various terminal alkynes generated vinylallenyl acetylenes as the sole product. The conditions performed were compatible with various types of terminal alkynes and with a range of substrates. Though the self-coupling production activated by the presence of catalytic oxygen and the copper catalyst could not be inhibited, the yields were obtained in moderate to high levels. Moreover, cross coupling reaction was also applicable for enyne oxiranes, yet the yields were not satisfactory. The synthetic utility of produced vinyl allenes synthesized via cross coupling reaction were applied by a Diels-Alder [4+2] cycloaddition. A bicyclic compound ***E*-1bb-DA** was synthesized in moderate yield.

The iron-catalyzed alkylation reactions of (*E*)-2-en-4-yne acetates with different organomagnesium halide reagents were performed under various conditions to obtain alkylated-vinylallenes in moderate to high yields. The outcome of the reaction is highly dependent on the substitution of R¹ and R² position of (*E*)-2-en-4-yne acetates.

REFERENCES

- "All Nobel Prizes in Chemistry". *Nobelprize.org*. Nobel Media AB 2014. Web. 25 Jun 2016. <http://www.nobelprize.org/nobel_prizes/chemistry/laureates/>
- Amatore, C.; Jutand, A. Role of Dba in the Reactivity of palladium(0) Complexes Generated in Situ from Mixtures of Pd(dba)₂ and Phosphines. *Coord. Chem. Rev.* **1998**, *178–180*, 511–528.
- Andersen, N. G.; Keay, B. A. 2-Furyl Phosphines As Ligands for Transition-Metal-Mediated Organic Synthesis. *Chem. Rev.* **2001**, *101* (4), 997–1030.
- Ashby, E. C.; Wiesemann, T. L.; Bowers, J. S.; Laemmle, J. T. Concerning the Formation of Magnesium Hydride in the Preparation of Grignard Reagents. The Origin of 2-Methylbenzhydrol in the Reaction of Methylmagnesium Bromide with 2-Methylbenzophenone. *Tetrahedron Lett.* **1976**, *17* (1), 21–24.
- Aurrecoechea, J.; Alonso, E.; Solay, M. Synthesis of Allenic Diols by Samarium Diiodide-Promoted Coupling between Alkynyloxiranes and Ketones. *Tetrahedron* **1998**, *54* (15), 3833–3850.
- Bag, S. S.; Kundu, R.; Das, M. Click-Reagent Version of Sonogashira Coupling Protocol to Conjugated Fluorescent Alkynes with No or Reduced Homocoupling. *J. Org. Chem.* **2011**, *76* (7), 2332–2337.
- Baker, K. V.; Brown, J. M.; Hughes, N.; Skarnulis, A. J.; Sexton, A. Mechanical Activation of Magnesium Turnings for the Preparation of Reactive Grignard Reagents. *J. Org. Chem.* **1991**, *56* (2), 698–703.
- Bartmann, E. Ether Cleavage by Activated Metals. I. Cleavage of Tetrahydrofuran by Transition-Metal Activated Magnesium. *J. Organomet. Chem.* **1985**, *284* (2), 149–158.
- Betzer, J.-F.; Delalogue, F.; Muller, B.; Pancrazi, A.; Prunet, J. Radical Hydrostannylation, Pd(0)-Catalyzed Hydrostannylation, Stannylcupration of Propargyl Alcohols and Enynols: Regio- and Stereoselectivities. *J. Org. Chem.* **1997**, *62* (22), 7768–7780.
- Brandsma, L.; Verkruijse, H. D.; Vasilevsky, S. F. *Application of Transition Metal Catalysts in Organic Synthesis*; Springer Berlin Heidelberg: Berlin, Heidelberg, 1999.

- Burns, D. J.; Best, D.; Wiczysty, M. D.; Lam, H. W. All-Carbon [3+3] Oxidative Annulations of 1,3-Enynes by Rhodium(III)-Catalyzed C-H Functionalization and 1,4-Migration. *Angew. Chemie Int. Ed.* **2015**, *54* (34), 9958–9962.
- Caldentey, X. C.; Cambeiro, X. C.; Pericàs, M. *Tetrahedron* **2011**, *67*, 4161–4168.
- Darcel, C.; Bruneau, C.; Dixneuf, P. H. Palladium(0), Copper(I) Catalysed Synthesis of Conjugated Alkynyl α -Allenols from Alkynyl Cyclic Carbonates and Terminal Alkynes. *J. Chem. Soc., Chem. Commun.* **1994**, No. 16, 1845–1846.
- Elangovan, A.; Wang, Y. H.; Ho, T. I. Sonogashira Coupling Reaction with Diminished Homocoupling. *Org. Lett.* **2003**, *5* (11), 1841–1844.
- Elsevier, C. J.; Stehouwer, P. M.; Westmijze, H.; Vermeer, P. Anti-Stereoselectivity in the palladium(0)-Catalyzed Conversion of Propargylic Esters into Allenes by Phenylzinc Chloride. *J. Org. Chem.* **1983**, *48* (7), 1103–1105.
- Fürstner, A.; Méndez, M. Iron-Catalyzed Cross-Coupling Reactions: Efficient Synthesis of 2,3-Allenol Derivatives. *Angew. Chemie* **2003**, *115* (43), 5513–5515.
- Garraís, S.; Turkington, J.; Goldring, W. P. D. Synthesis of Isomeric Polyacetylenes Based on Natural Hydroxy Matricaria Esters. *Tetrahedron* **2009**, *65* (40), 8418–8427.
- Glaser, C. Beiträge Zur Kenntniss Des Acetenylbenzols. *Berichte der Dtsch. Chem. Gesellschaft* **1869**, *2* (1), 422–424.
- Gooding, O. W.; Beard, C. C.; Jackson, D. Y.; Wren, D. L.; Cooper, G. F. Enantioselective Formation of Functionalized 1, 3-Disubstituted Allenes: Synthesis Of. α -Allenic. ω -Carbomethoxy Alcohols of High Optical Purity. *J. Org. Chem.* **1991**, *56* (3), 1083–1088.
- Gore, J.; Dulcere, J. P. New Synthesis of Vinylallenenes. *J. Chem. Soc. Chem. Commun.* **1972**, *1* (15), 866.
- Hata, T.; Bannai, R.; Otsuki, M.; Urabe, H. Iron-Catalyzed Regio- and Stereoselective Substitution of Γ, δ -Epoxy- α, β -Unsaturated Esters and Amides with Grignard Reagents. *Org. Lett.* **2010**, *12* (5), 1012–1014.

- Hays, P. A.; Thompson, R. A. A Processing Method Enabling the Use of Peak Height for Accurate and Precise Proton NMR Quantitation. *Magn Reson Chem* **2009**, *47* (10), 819–824.
- Heck, R. F.; Nolley, J. P. Palladium-Catalyzed Vinylic Hydrogen Substitution Reactions with Aryl, Benzyl, and Styryl Halides. *J. Org. Chem.* **1972**, *37* (14), 2320–2322.
- Hill, G.; Rossiter, B. E.; Sharpless, B. Anhydrous Tert-Butyl Hydroperoxide in Toluene: The Preferred Reagent for Applications Requiring Dry TBHP. *J. Org. Chem.* **1983**, *48* (25 mL), 3607–3608.
- Jain, A. K.; Gupta, A. K. Adsorptive Drying of Isopropyl Alcohol on 4A Molecular Sieves: Equilibrium and Kinetic Studies. *Sep. Sci. Technol.* **1994**, *29* (11), 1461–1472.
- Jeffery-Luong, T.; Linstumelle, G. Palladium-Catalyzed Synthesis of Allenes. *Tetrahedron Lett.* **1980**, *21* (52), 5019–5020.
- Kajikawa, T.; Aoki, K.; Singh, R. S.; Iwashita, T.; Kusumoto, T.; Frank, H.A.; Hashimoto, H.; Katsumura, S. *Org. Biomol. Chem.* **2009**, *7*, 3723–3733.
- Karagöz, E. Ş.; Kuş, M.; Akpınar, G. E.; Artok, L. Regio- and Stereoselective Synthesis of 2,3,5-Trienoates by Palladium-Catalyzed Alkoxy carbonylation of Conjugated Enyne Carbonates. *J. Org. Chem.* **2014**, *79* (19), 9222–9230.
- Katsuki, T.; Sharpless, K. B. The First Practical Method for Asymmetric Epoxidation. *J. Am. Chem. Soc.* **1980**, *102* (18), 5974–5976.
- Kessler, S. N.; Bäckvall, J. E. Iron-Catalyzed Cross-Coupling of Propargyl Carboxylates and Grignard Reagents: Synthesis of Substituted Allenes. *Angew. Chemie - Int. Ed.* **2016**, *55* (11), 3734–3738.
- Magano, J.; Dunetz, J. R. *Transition Metal-Catalyzed Couplings in Process Chemistry*; Dunetz, J. M. and J. R., Ed.; Wiley-VCH: Weinheim, 2013.
- Mandai, T.; Nakata, T.; Murayama, H.; Yamaoki, H.; Ogawa, M.; Kawada, M.; Tsuji, J. Palladium-Catalyzed Reactions of 2-Alkynyl Carbonates with Terminal Acetylenes: A New Synthetic Method for 1,2-Dien-4-Ynes. *Tetrahedron Lett.* **1990**, *31* (49), 7179–7180.

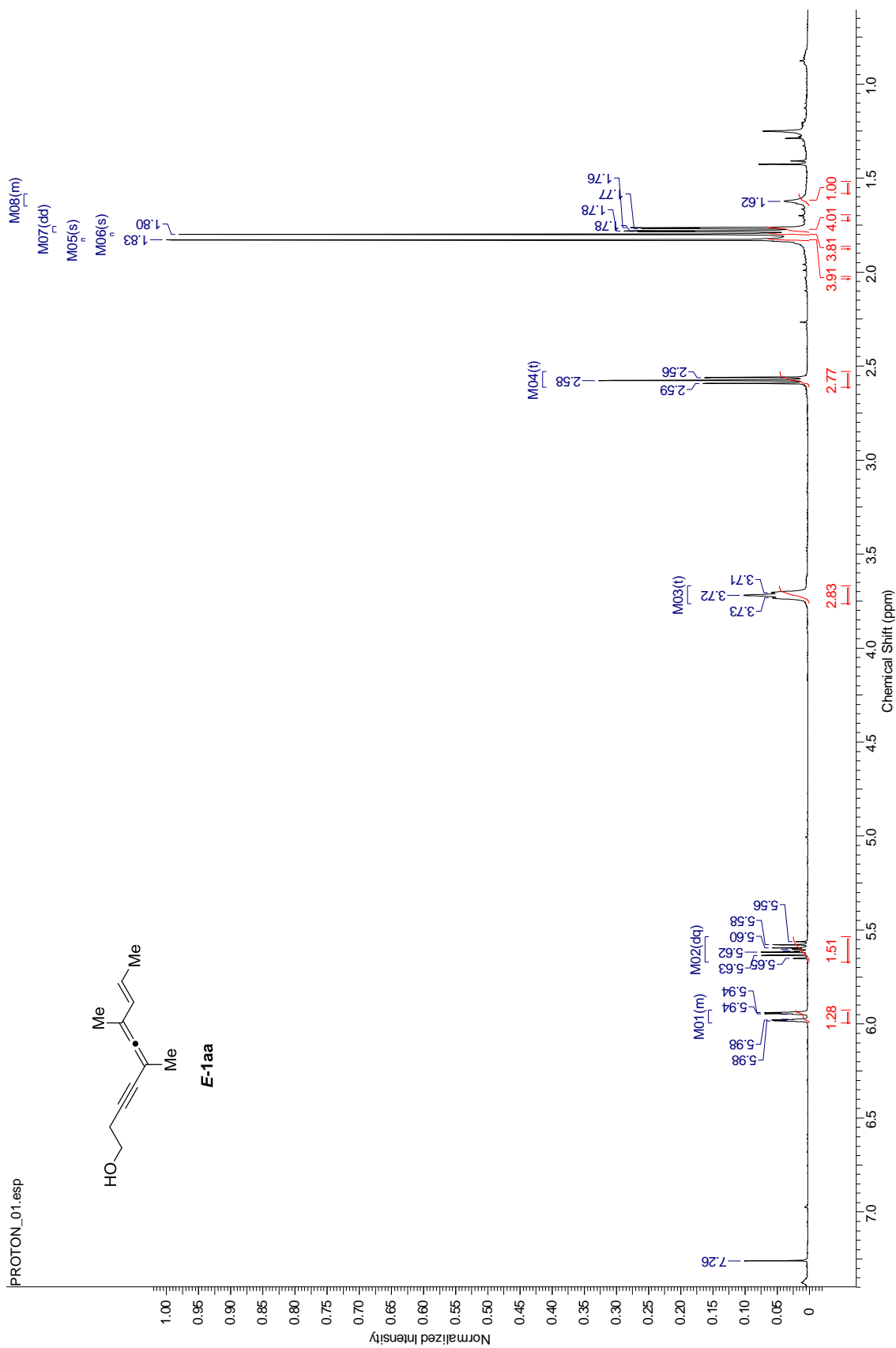
- Mandai, T.; Ogawa, M.; Yamaoki, H.; Nakata, T.; Murayama, H.; Kawada, M.; Tsuji, J. Palladium-Catalyzed Reactions of 2-Alkynyl Carbonates with Olefins. A New Synthetic Method for Vinyl Allenes. *Tetrahedron Lett.* **1991**, *32* (28), 3397–3398.
- Matsubara, S.; Toda, N.; Kobata, M.; Utimoto, K. Preparation of Chiral Organozinc Compounds via Desymmetrization of Gem-Dizincioethane. *Synlett* **2000**, *6* (7), 987–988.
- Mayer, M.; Czaplik, W. M.; Von Wangelin, A. J. Practical Iron-Catalyzed Allylations of Aryl Grignard Reagents. *Adv. Synth. Catal.* **2010**, *352* (13), 2147–2152.
- Murahashi, S.; Imada, Y.; Taniguchi, Y.; Higashiura, S. Palladium(0)-Catalyzed Alkoxy carbonylation of Allyl Phosphates and Acetates. *J. Org. Chem.* **1993**, *58* (6), 1538–1545.
- Nakatani, A.; Hirano, K.; Satoh, T.; Miura, M. A Concise Access to (Polyfluoroaryl)allenes by Cu-Catalyzed Direct Coupling with Propargyl Phosphates. *Org. Lett.* **2012**, *14* (10), 2586–2589.
- Pasto, D. J.; Hennion, G. F.; Shults, R. H.; Waterhouse, A.; Chou, S.-K. Reaction of Propargyl Halides with Grignard Reagents. Iron Trichloride Catalysis in Allene Formation. *J. Org. Chem.* **1976**, *41* (21), 3496–3496.
- Plietker, B. A Highly Regioselective Salt-Free Iron-Catalyzed Allylic Alkylation. *Angew. Chemie - Int. Ed.* **2006**, *45* (9), 1469–1473.
- Pu, X.; Ready, J. M. Direct and Stereospecific Synthesis of Allenes via Reduction of Propargylic Alcohols with Cp₂Zr(H)Cl. *J. Am. Chem. Soc.* **2008**, *130* (33), 10874–10875.
- Purpura, M.; Krause, N. Regio- and Stereoselective Synthesis of Vinylallenes by 1, 5-(S N)-Substitution of Enyne Acetates and Oxiranes with Organocuprates. **1999**, *49* (0), 267–275.
- Rao, M. L. N.; Banerjee, D.; Giri, S. Arylations of Allylic Acetates with Triaryl bismuths as Atom-Efficient Multi-Coupling Reagents under Palladium Catalysis. *Tetrahedron Lett.* **2009**, *50* (41), 5757–5761.
- Rieke, R.; Bales, S. Activated Metals. IV. Preparation and Reactions of Highly Reactive Magnesium Metal. *J. Am. Chem. Soc.* **1974**, *96* (26), 1775–1781.

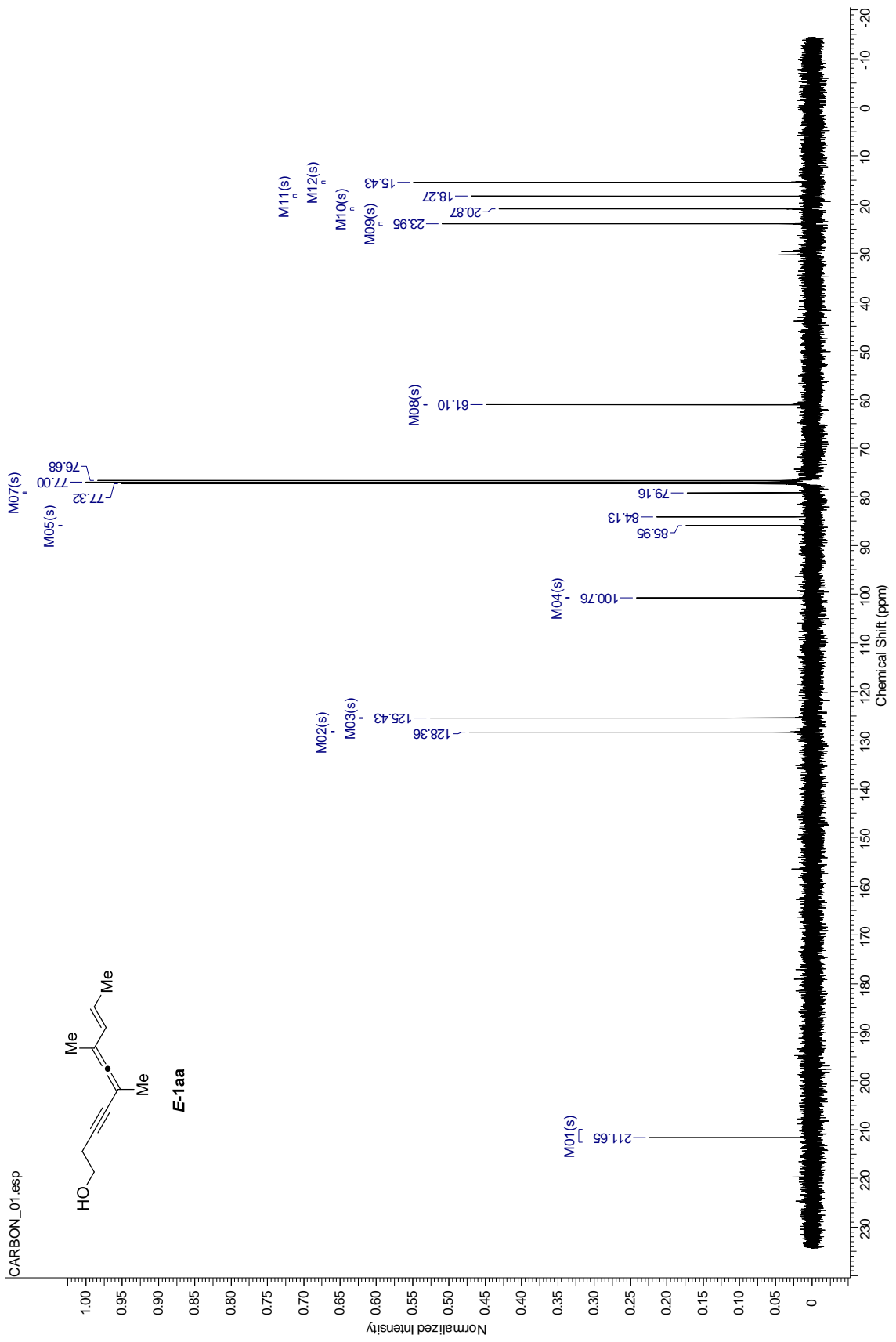
- Rona, P.; Crabbe, P. A Novel Allene Synthesis. *J. Am. Chem. Soc.* **1968**, *90* (17), 4733–4734.
- Rosales, V.; Zambrano, J. L.; Demuth, M. Regioselective Palladium-Catalyzed Alkylation of Allylic Halides with Benzylic Grignard Reagents. Two-Step Synthesis of Abietane Terpenes and Tetracyclic Polyprenoid Compounds. *J. Org. Chem.* **2002**, *67* (4), 1167–1170.
- Ruitenbergh, K.; Kleijn, H.; Elsevier, C. J.; Meijer, J.; Vermeer, P. Palladium(O)-Promoted Synthesis of Functionally Substituted Allenes by Means of Organozinc Compounds. *Tetrahedron Lett.* **1981**, *22* (15), 1451–1452.
- Sherry, B. D.; Fürstner, A. Iron-Catalyzed Addition of Grignard Reagents to Activated Vinyl Cyclopropanes. *Chem. Commun. (Camb)*. **2009**, No. 46, 7116–7118.
- Tamura, M.; Kochi, J. K. Vinylation of Grignard Reagents. Catalysis by Iron. *J. Am. Chem. Soc.* **1971**, *93* (6), 1487–1489.
- Tolstikov, G. A.; Romanova, T. Y.; Kuchin, A. V. A New Method for the Synthesis of Vinyl- and Di-Allenenes Assisted by Organoaluminium Compounds. *J. Organomet. Chem.* **1985**, *285* (1-3), 71–82.
- Trost, B. M.; Fullerton, T. J. New Synthetic Reactions. Allylic Alkylation. *J. Am. Chem. Soc.* **1973**, *95* (1), 292–294.
- Trost, B. M.; Sorum, M. T.; Chan, C.; Rühter, G. Palladium-Catalyzed Additions of Terminal Alkynes to Acceptor Alkynes. *J. Am. Chem. Soc.* **1997**, *119* (4), 698–708.
- Tsuboi, S.; Ishii, N.; Sakai, T.; Tari, I.; Utaka, M. Oxidation of Alcohols with Electrolytic Manganese Dioxide, Its Application for the Synthesis of Insect Pheromones. *Bulletin of the Chemical Society of Japan*. 1990, pp 1888–1893.
- Tsuji, J. *Transition Metal Reagents and Catalysts Transition Metal Reagents and Catalysts*; 2000; Vol. 0.
- Tsuji, J.; Takahashi, H.; Morikawa, M. Organic Syntheses by Means of Noble Metal Compounds XVII. Reaction of π -Allylpalladium Chloride with Nucleophiles. *Tetrahedron Lett.* **1965**, *6* (49), 4387–4388.
- Urabe, H.; Suzuki, K.; Sato, F. *J. Am. Chem. Soc.* **1997**, *119*, 10014-10027.

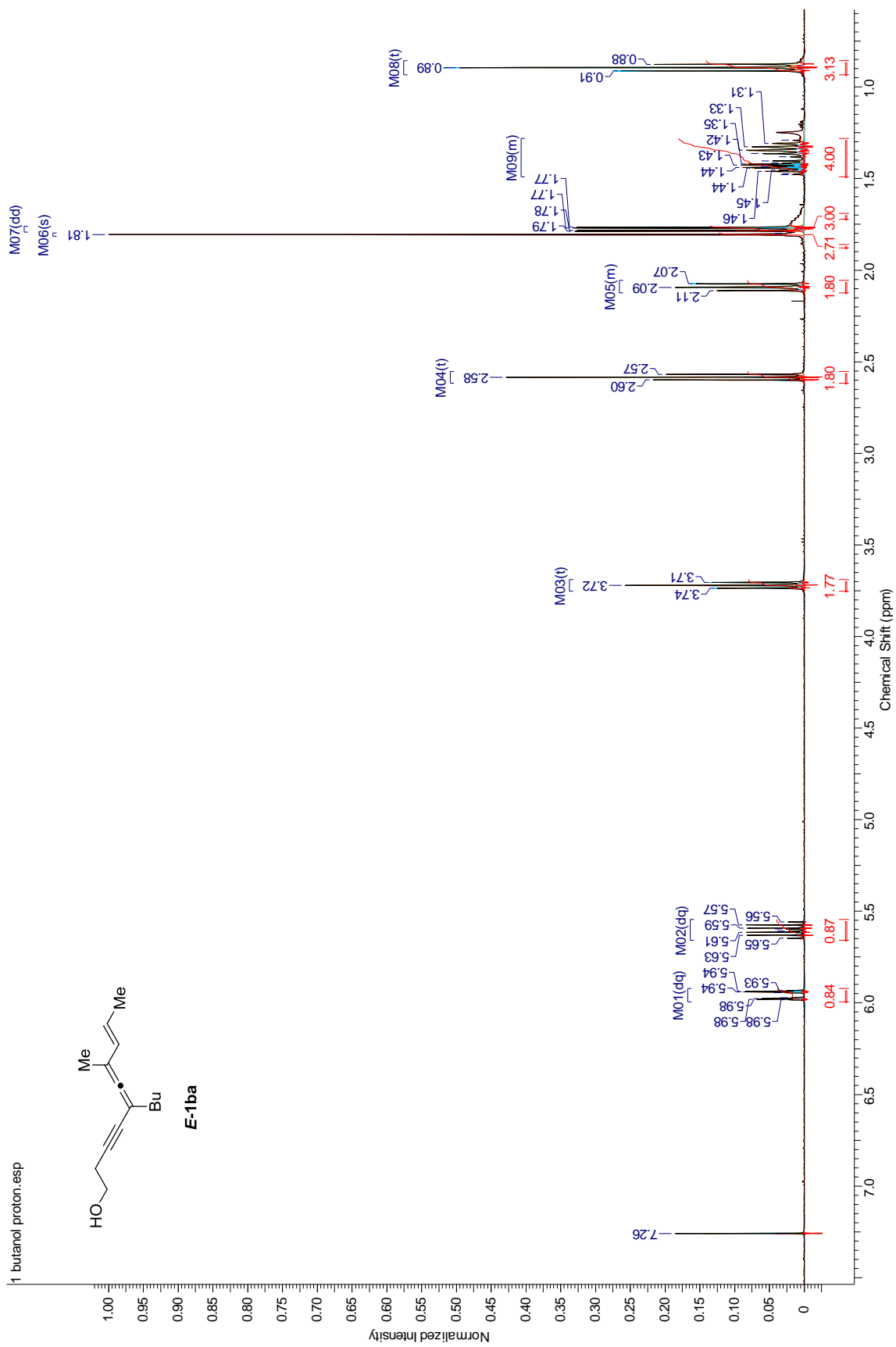
- Üçüncü, M.; Karakuş, E.; Kuş, M.; Akpınar, G. E.; Aksın-Artok, Ö.; Krause, N.; Karaca, S.; Elmacı, N.; Artok, L. Rhodium- and Palladium-Catalyzed 1,5-Substitution Reactions of 2-En-4-Yne Acetates and Carbonates with Organoboronic Acids. *J. Org. Chem.* **2011**, *76* (15), 5959–5971.
- Watson, S. C.; Eastham, J. F. Colored Indicators for Simple Direct Titration of Magnesium and Lithium Reagents. *J. Organomet. Chem.* **1967**, *9* (1), 165–168.
- Wilfred L. F. Armarego and Christina Li Lin Chai. *Purification of Laboratory Chemicals*, 7th ed.; Elsevier, 2014.
- Williams, D. B. G.; Lawton, M. Drying of Organic Solvents: Quantitative Evaluation of the Efficiency of Several Desiccants. *J. Org. Chem.* **2010**, *75* (24), 8351–8354.
- Yanagisawa, A.; Nomura, N.; Yamamoto, H. Iron-Catalyzed Kharasch-Type Reaction Between Grignard Reagents and Allylic Phosphates. Highly S_N2 Selective Cross-Coupling Process. *Synlett* **1991**, *1991* (07), 513–514.
- Yoshida, M.; Hayashi, M.; Shishido, K. Palladium-Catalyzed Diastereoselective Coupling of Propargylic Oxiranes with Terminal Alkynes. *Org. Lett.* **2007**, *9* (7), 1643–1646.
- Yu, S.; Ma, S. Allenes in Catalytic Asymmetric Synthesis and Natural Product Syntheses. *Angew. Chemie Int. Ed.* **2012**, *51* (13), 3074–3112.
- Zaleskiy, S. S.; Ananikov, V. P. Pd₂(dba)₃ as a Precursor of Soluble Metal Complexes and Nanoparticles: Determination of Palladium Active Species for Catalysis and Synthesis. *Organometallics* **2012**, *31* (6), 2302–2309.
- Zhao, S.-C.; Ji, K.-G.; Lu, L.; He, T.; Zhou, A.-X.; Yan, R.-L.; Ali, S.; Liu, X.-Y.; Liang, Y.-M. Palladium-Catalyzed Divergent Reactions of 1,6-Enyne Carbonates: Synthesis of Vinylidenepyridines and Vinylidenepyrrolidines. *J. Org. Chem.* **2012**, *77* (6), 2763–2772.

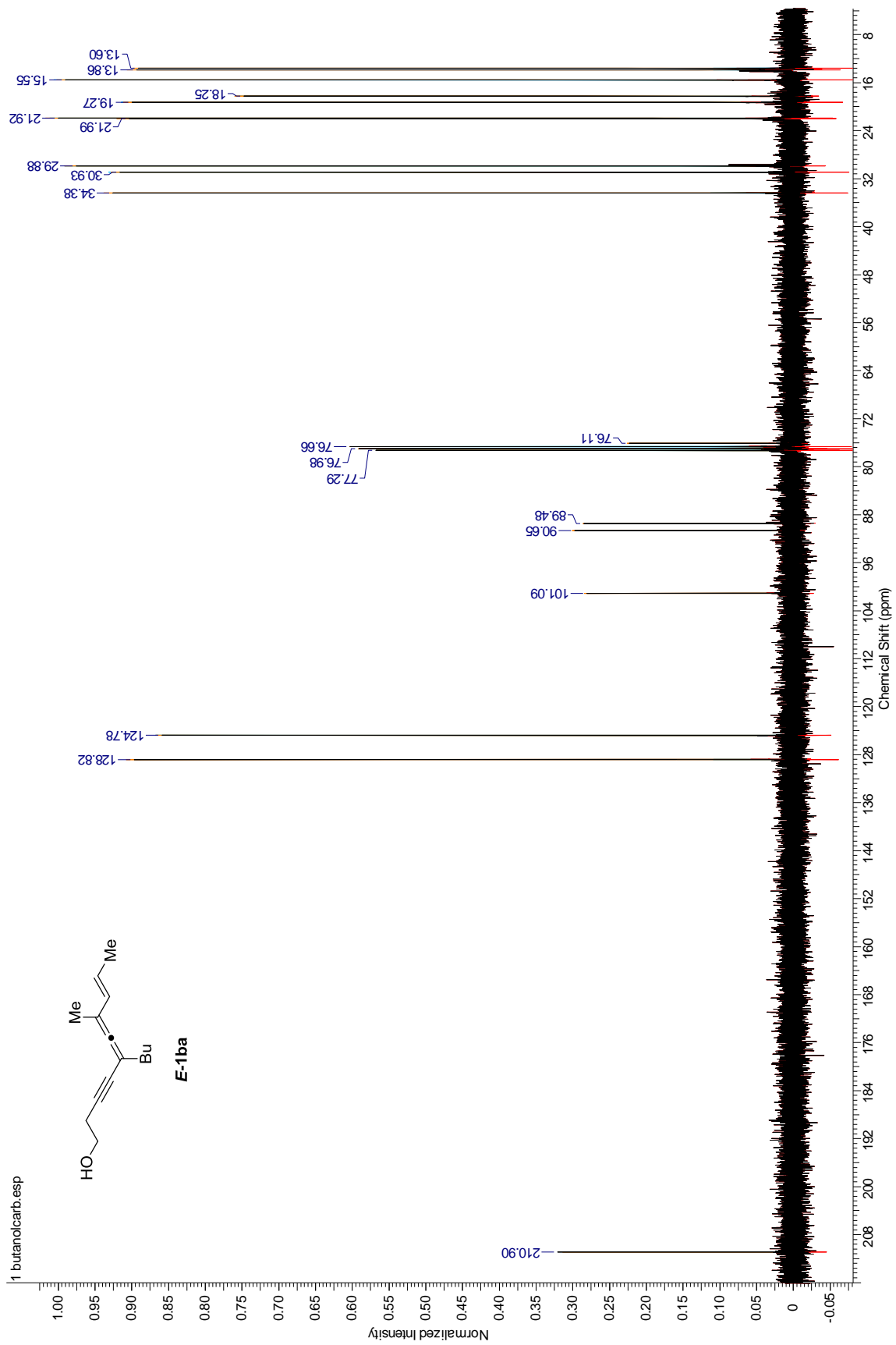
APPENDIX A

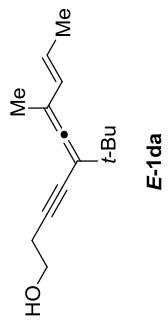
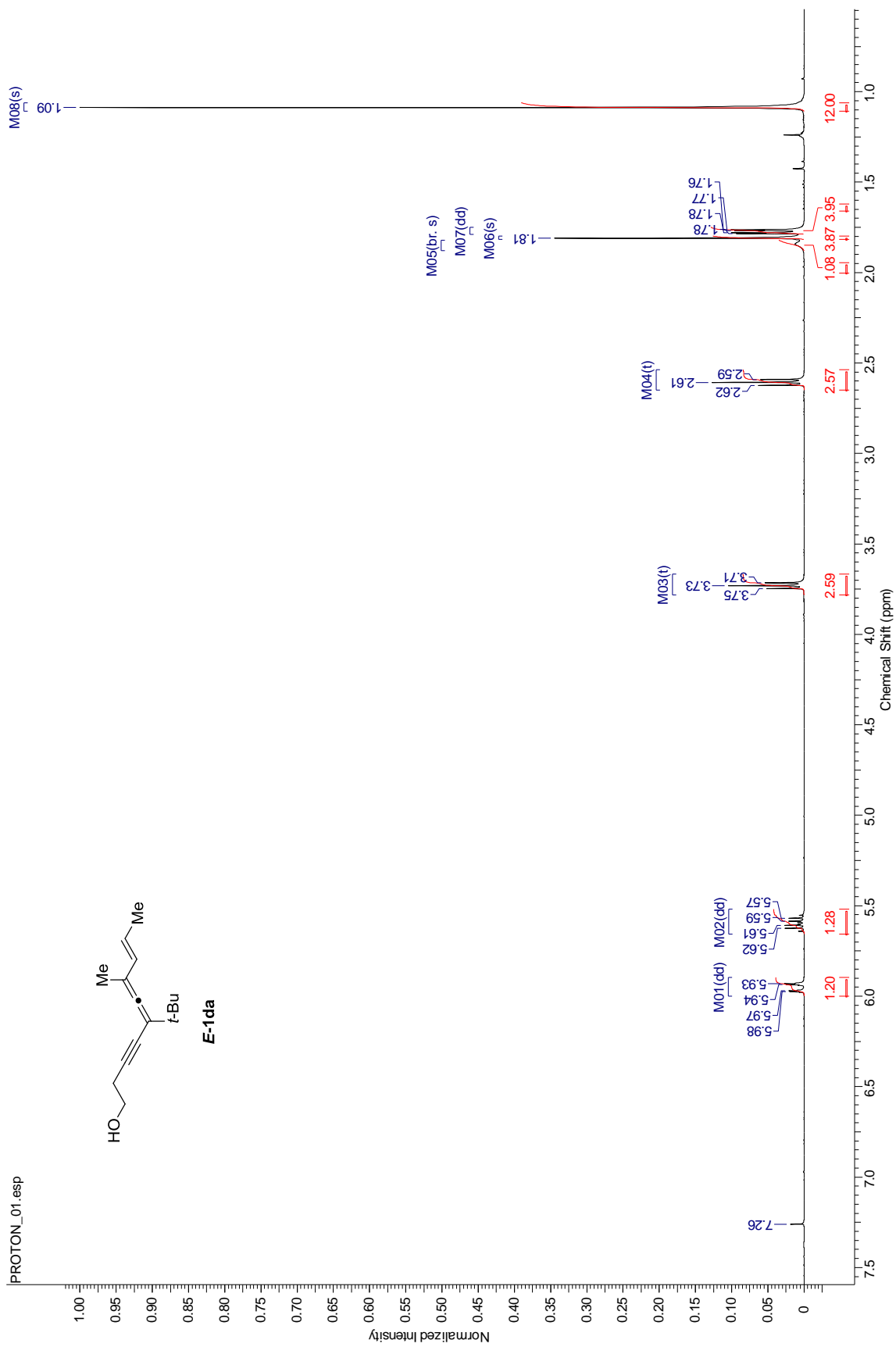
^1H NMR AND ^{13}C NMR SPECTRUM OF PRODUCTS

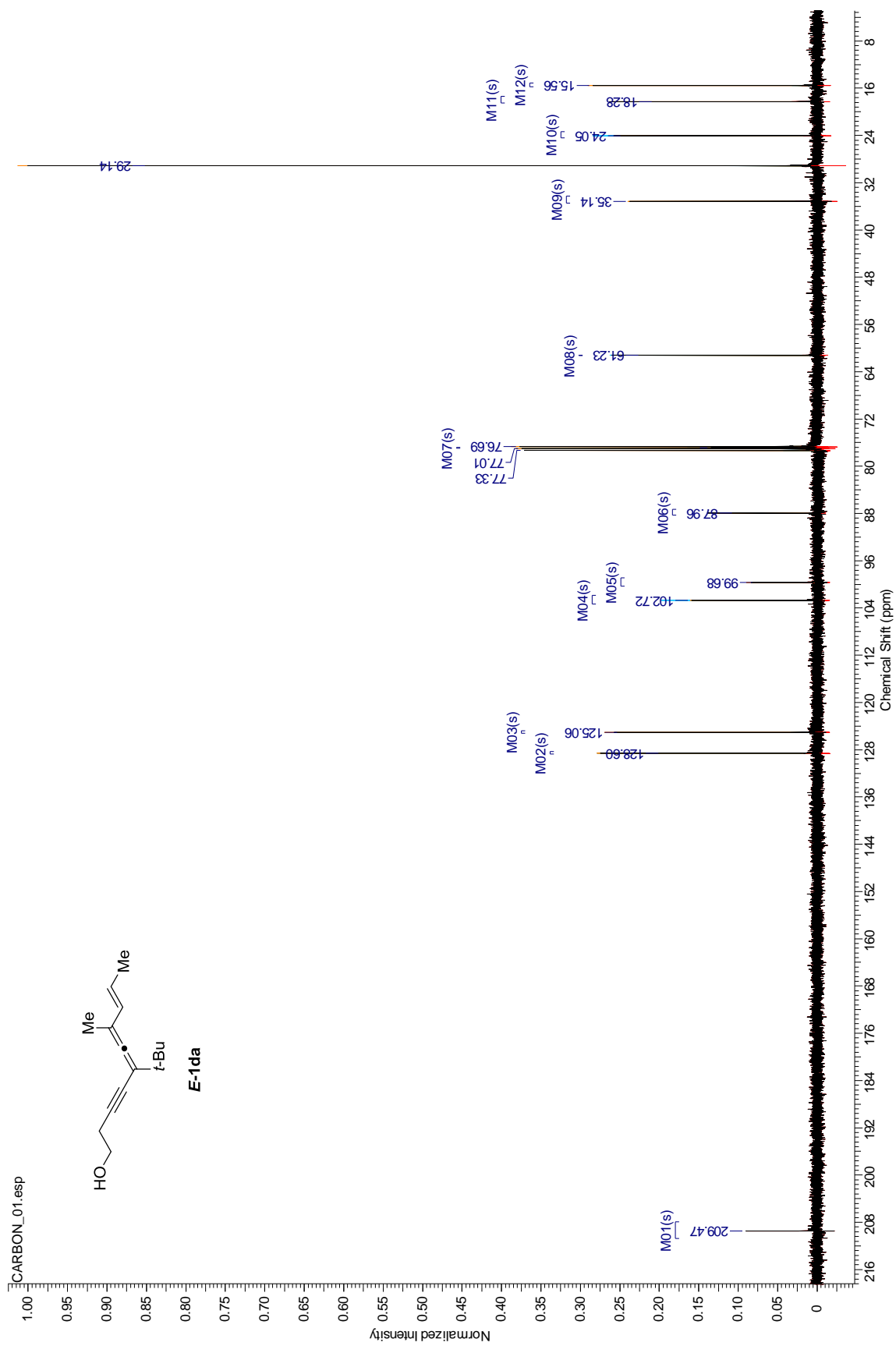


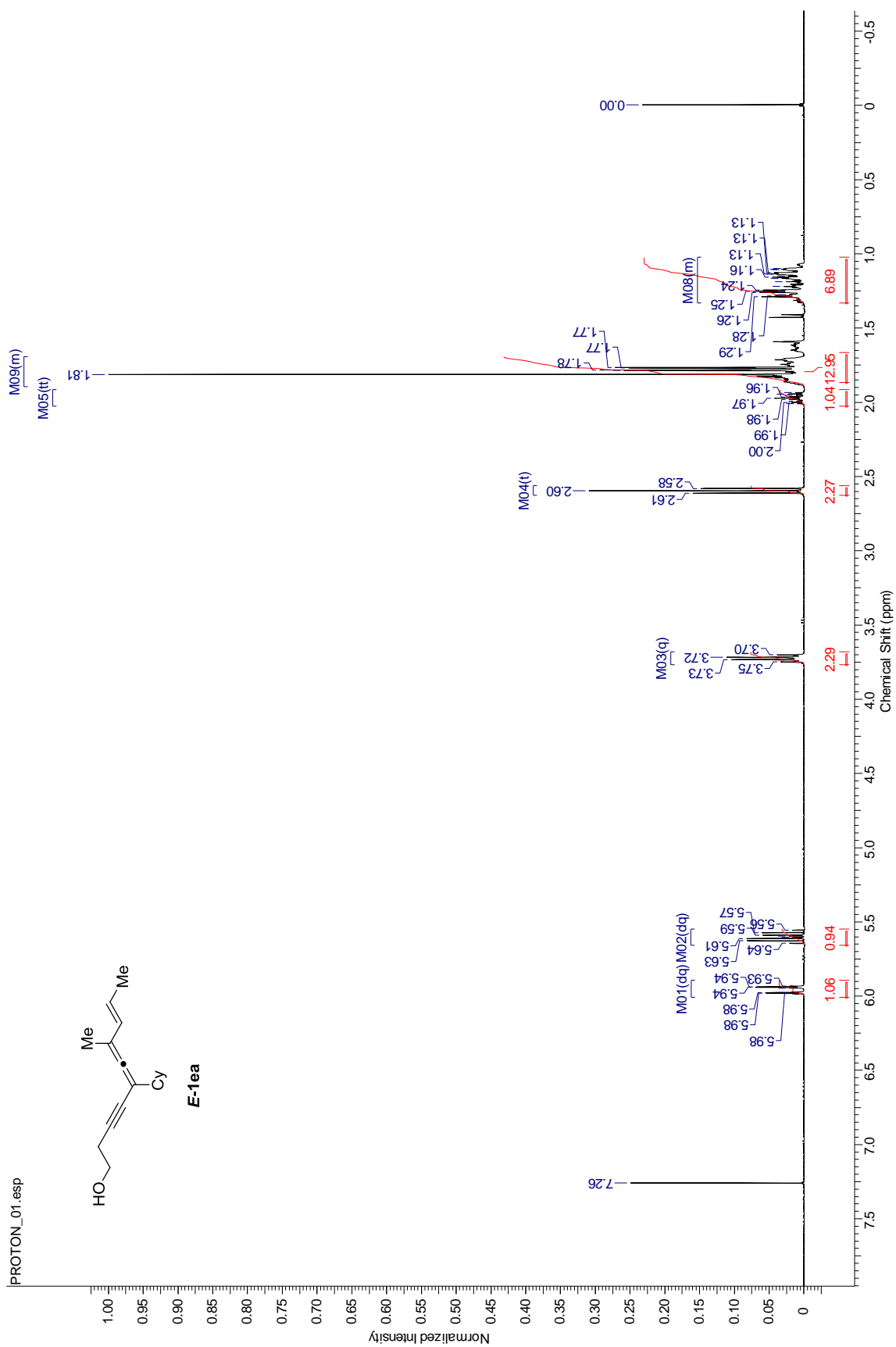


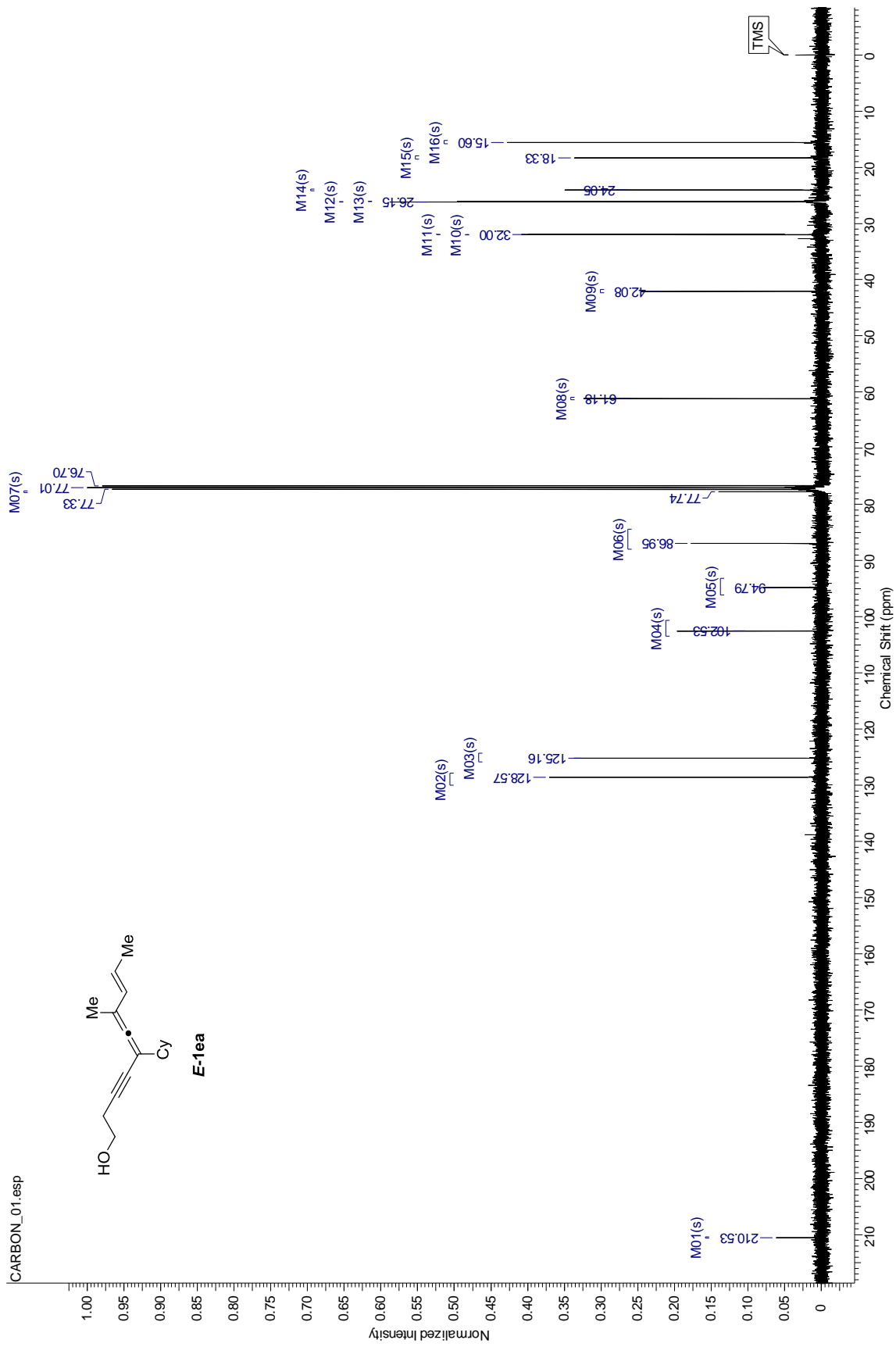


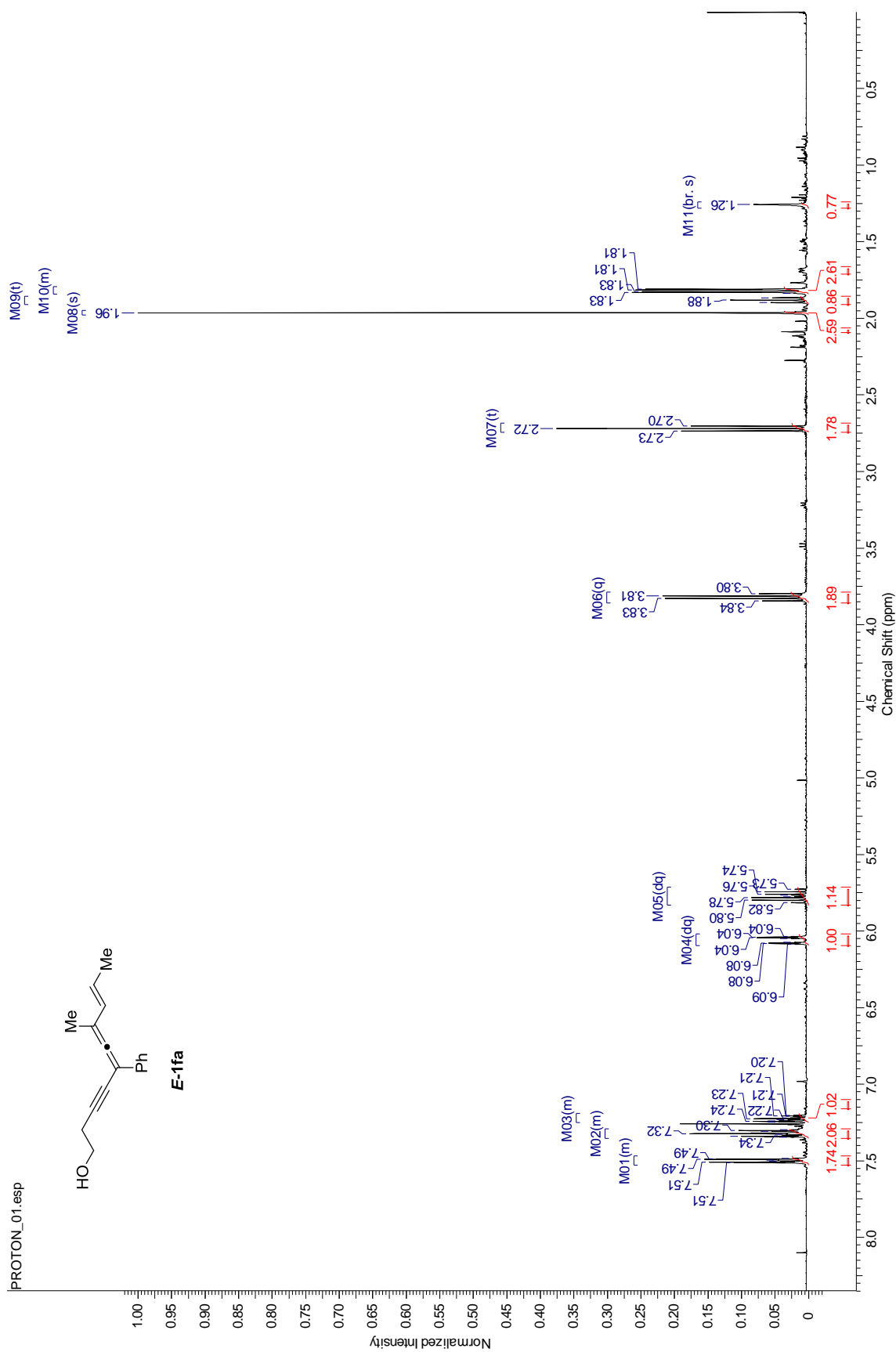


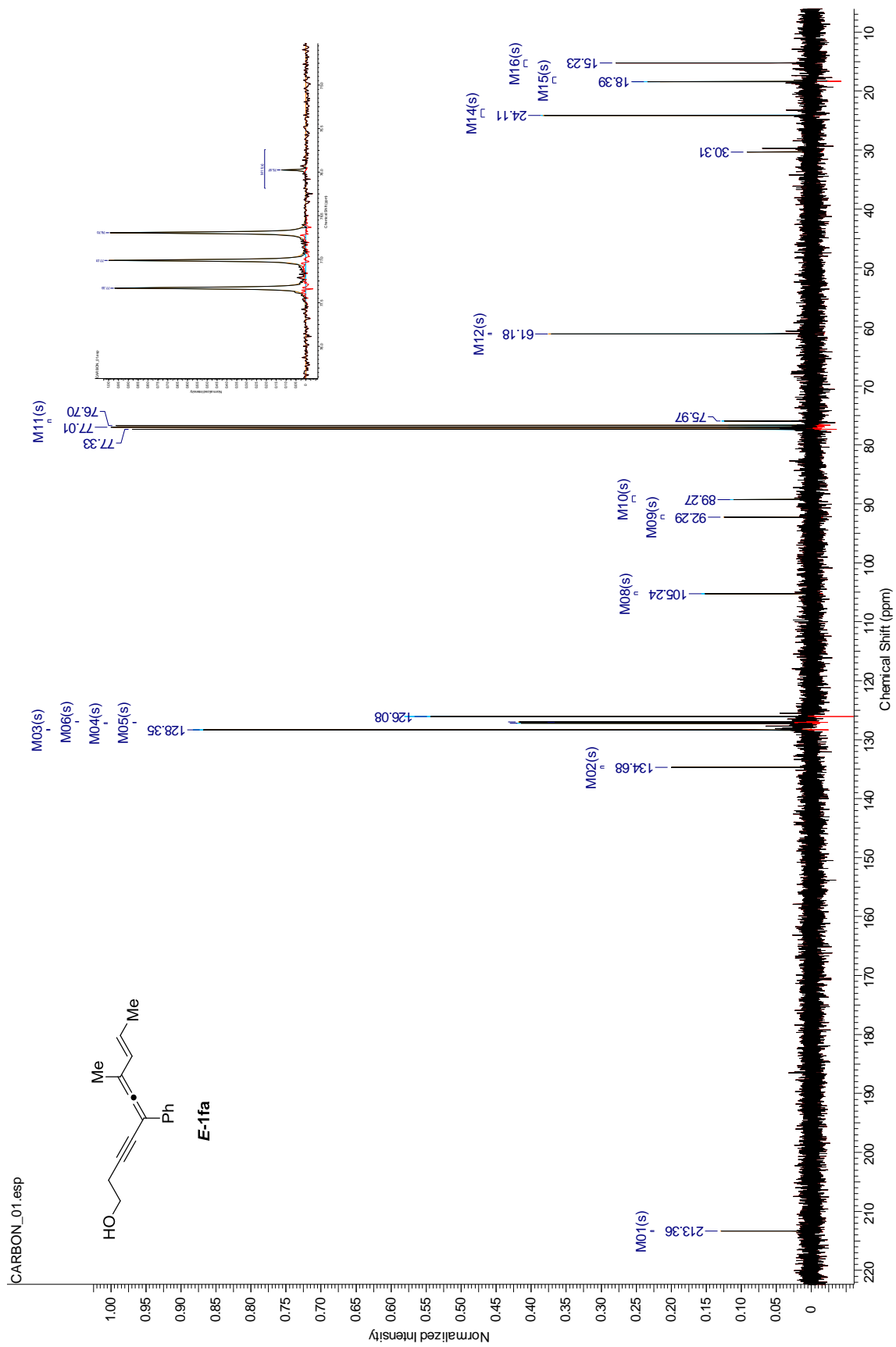


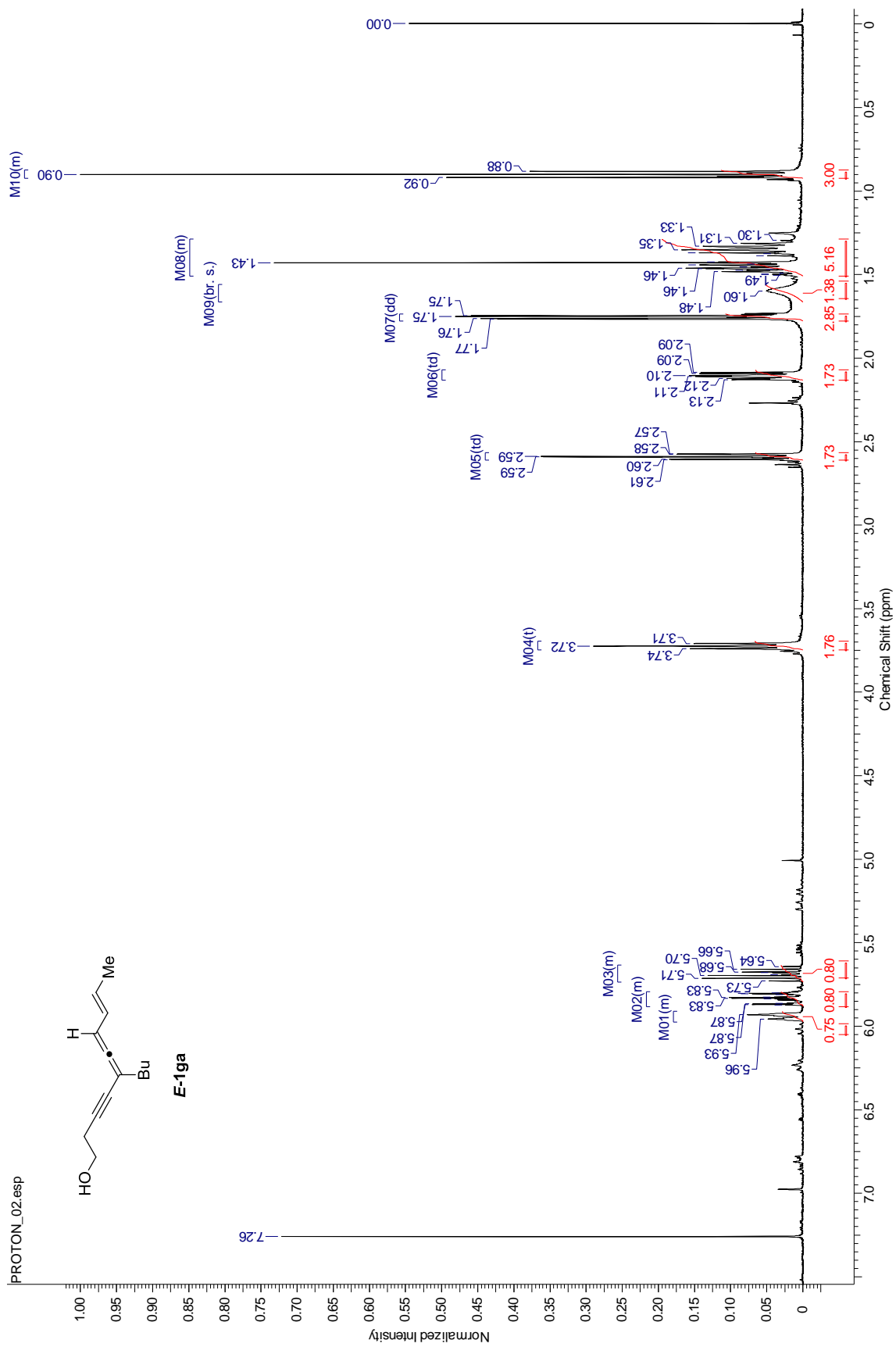


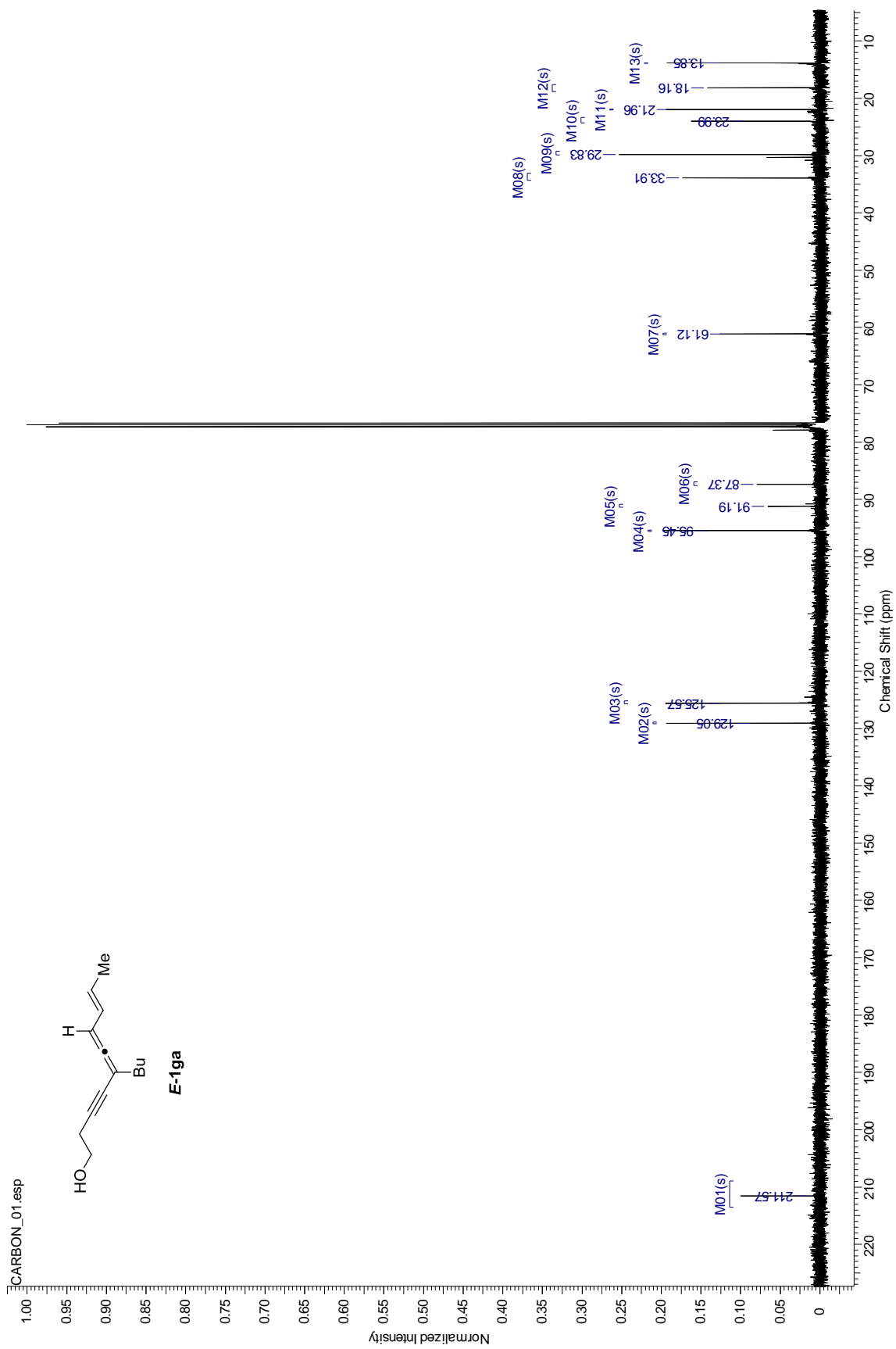


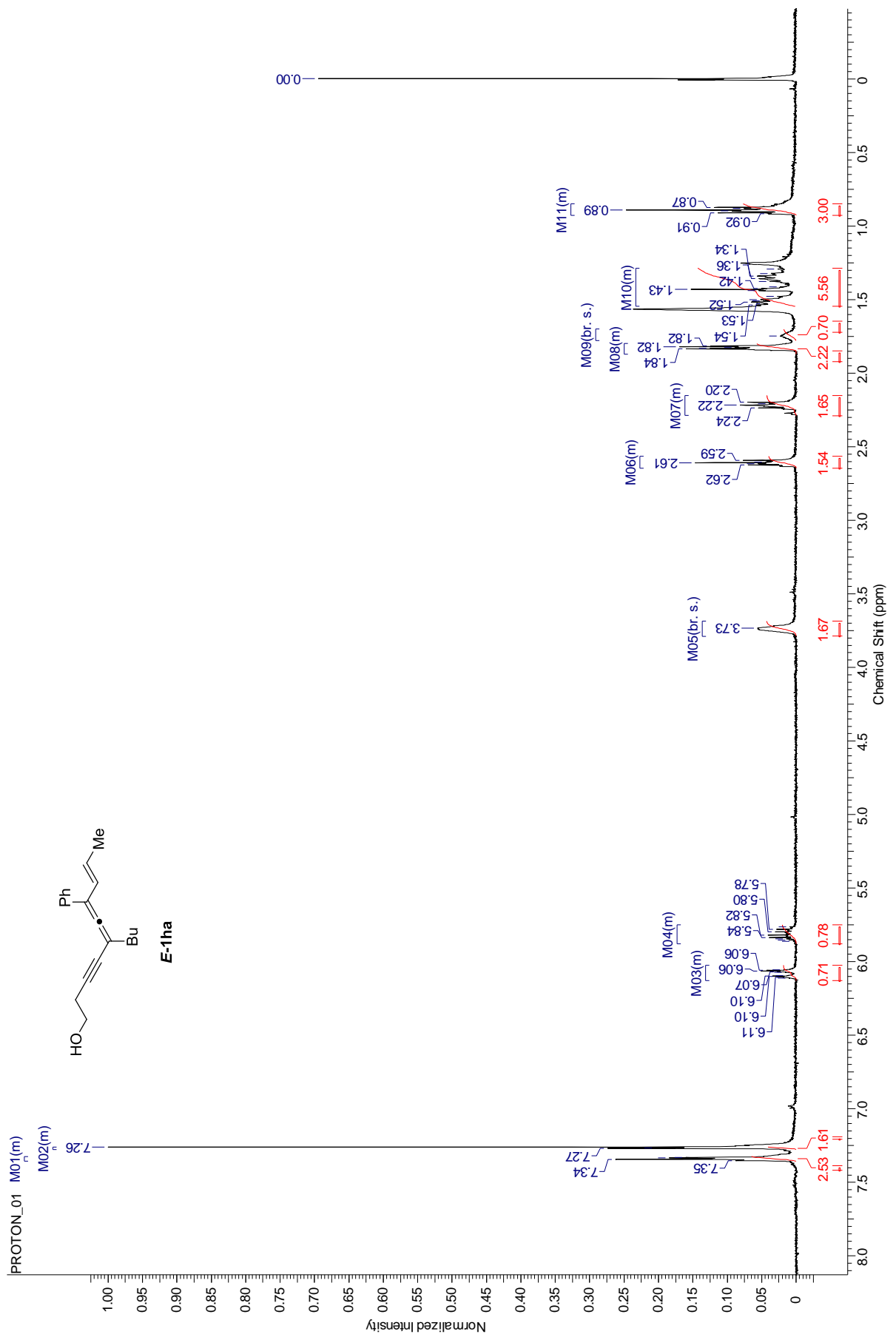


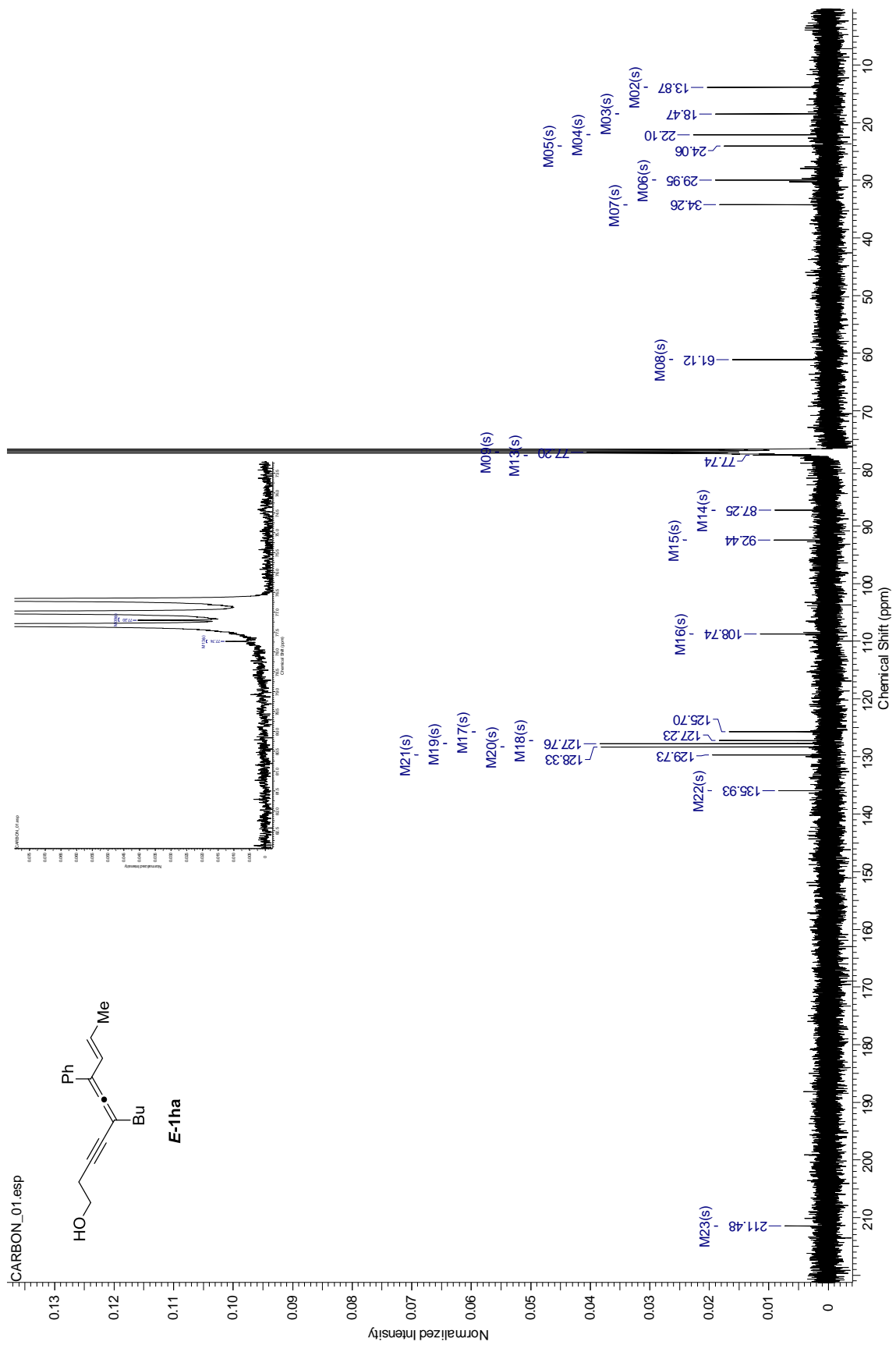


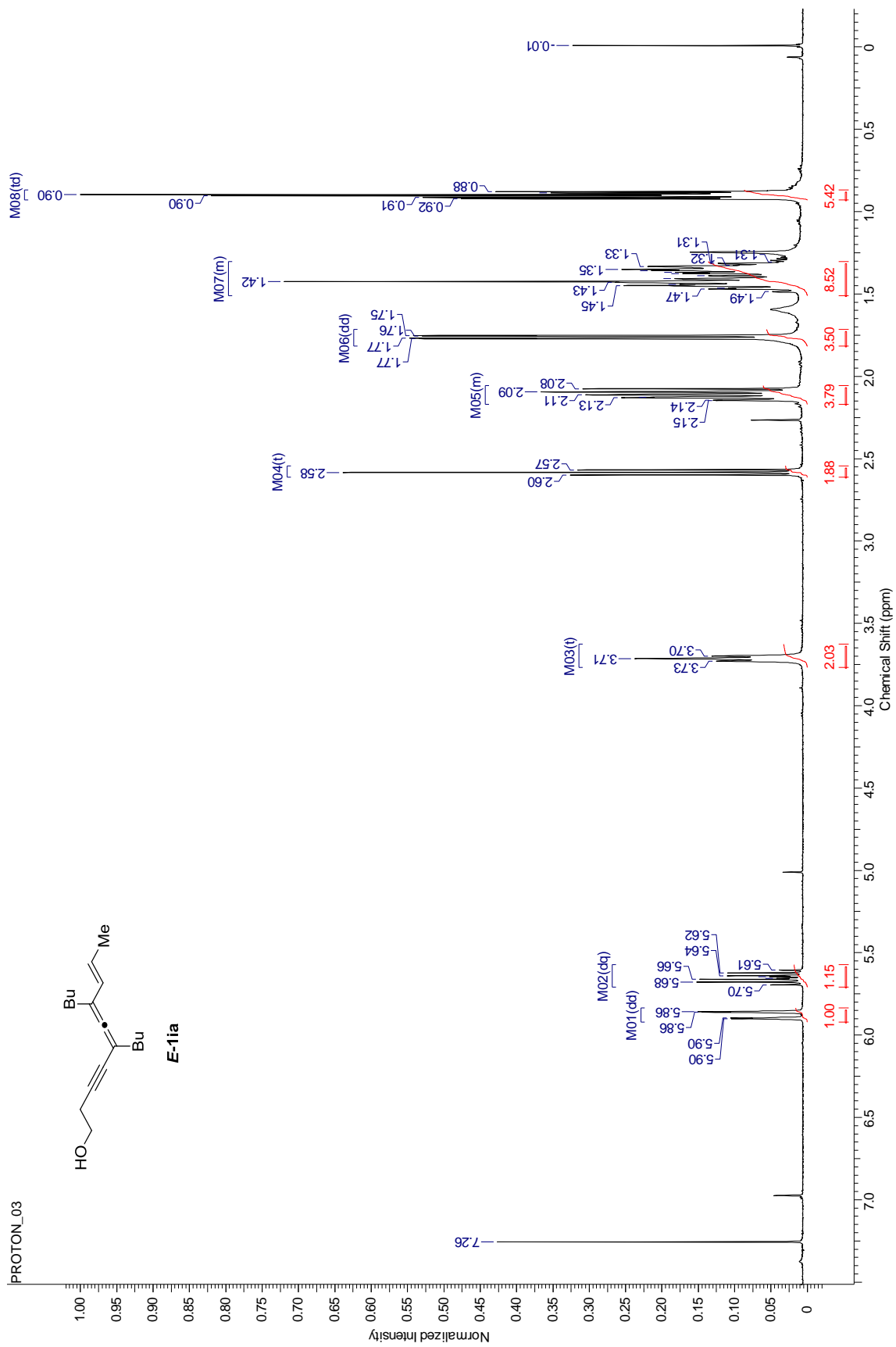


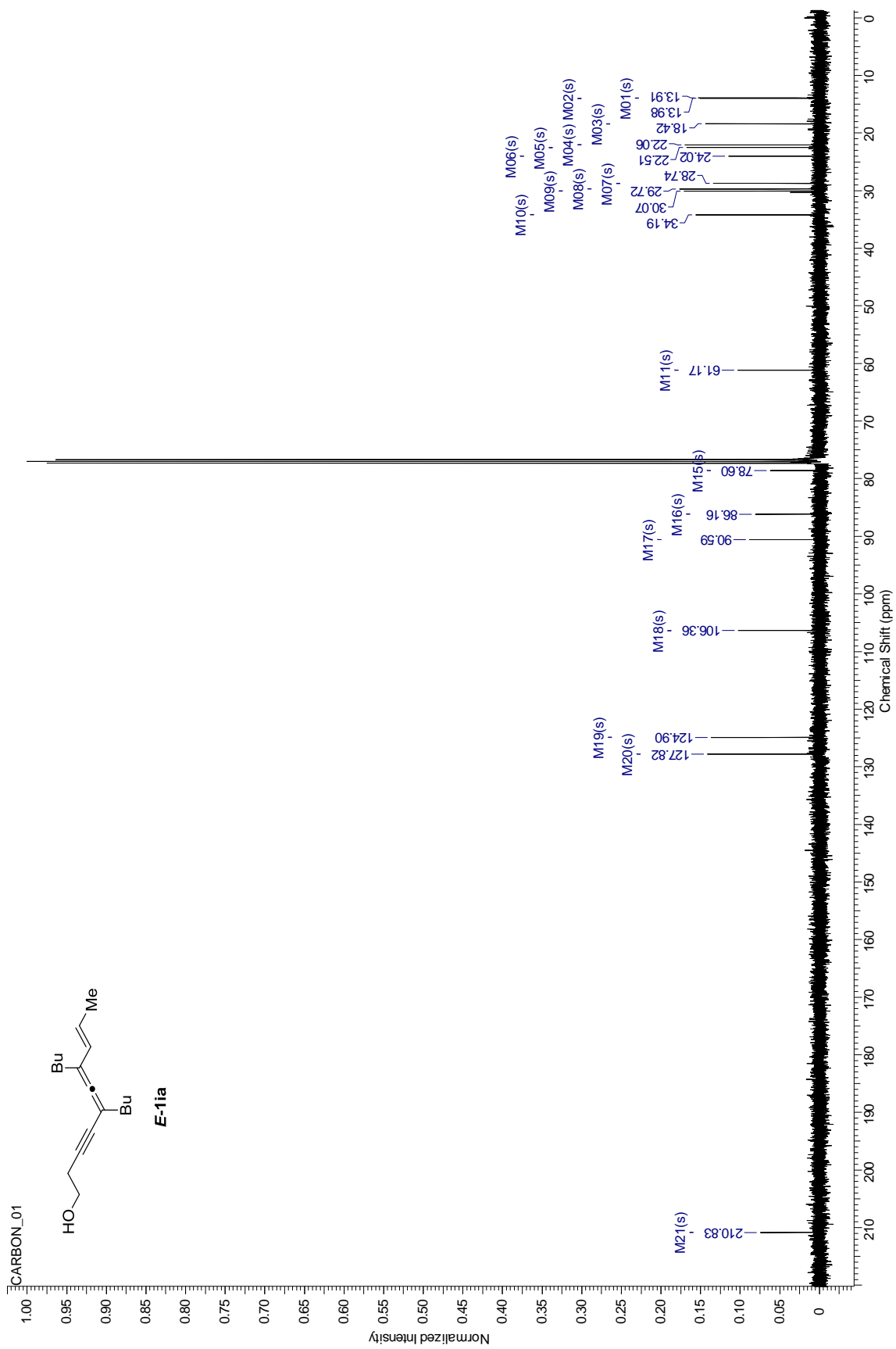


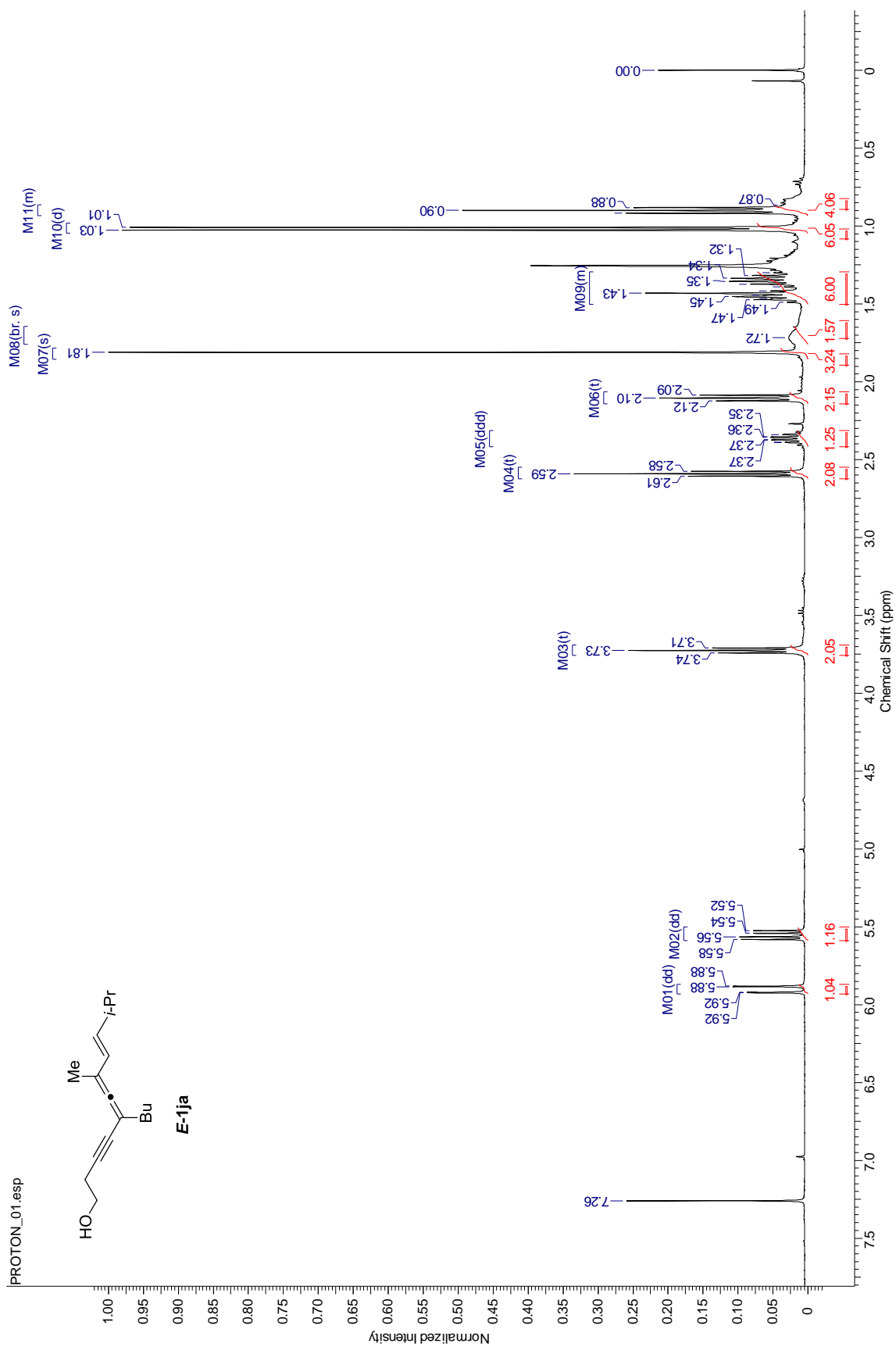


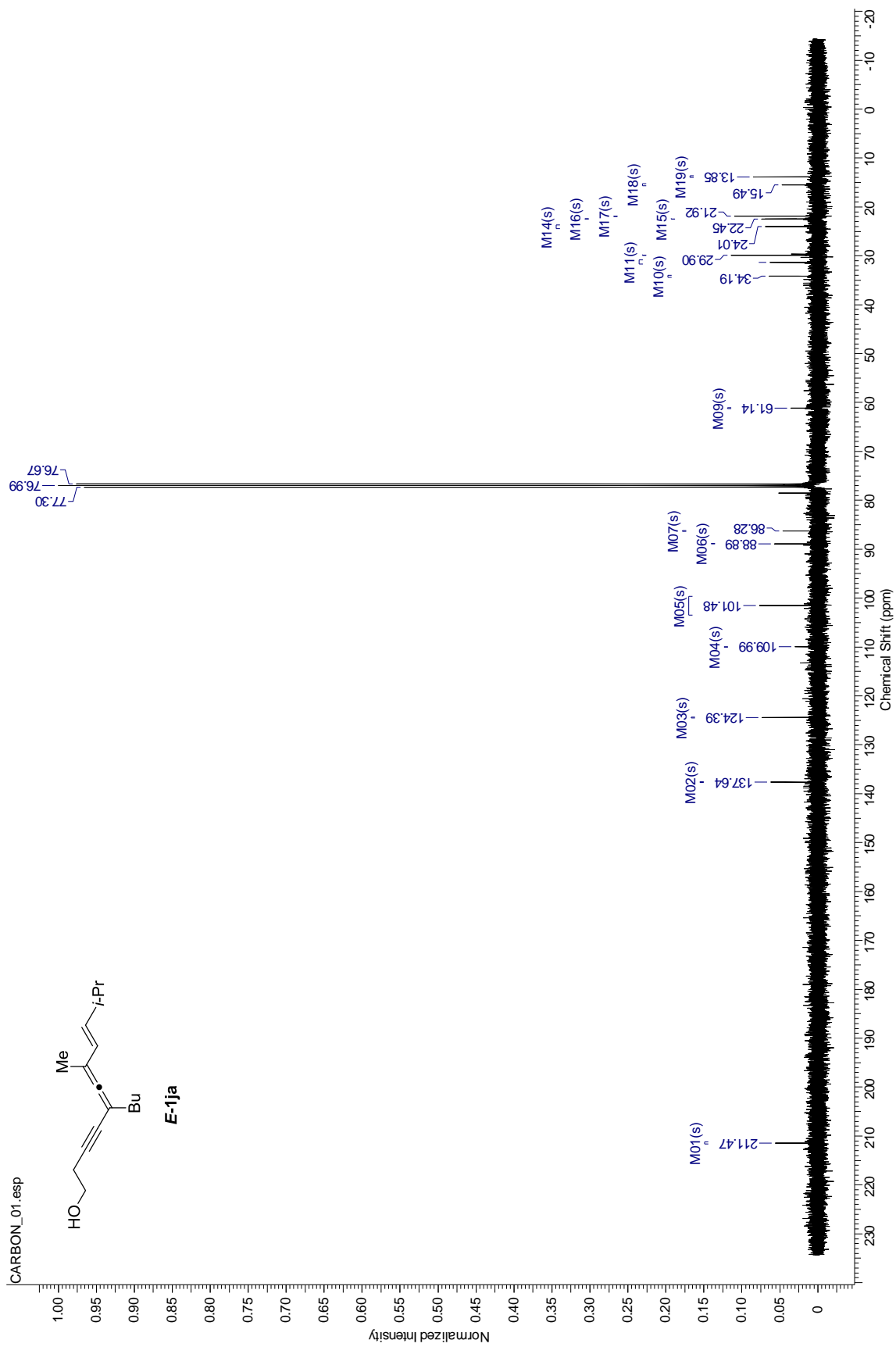


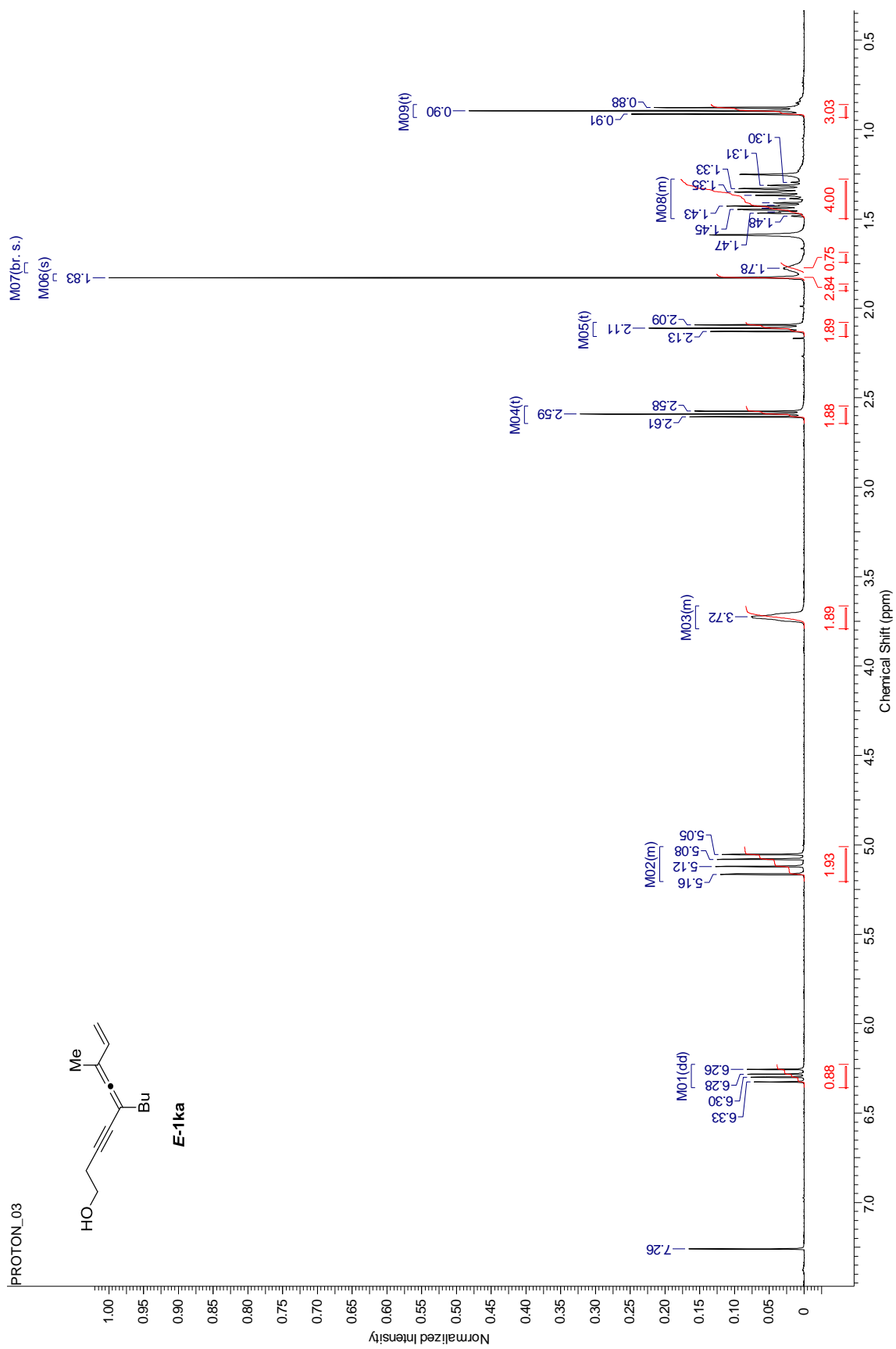


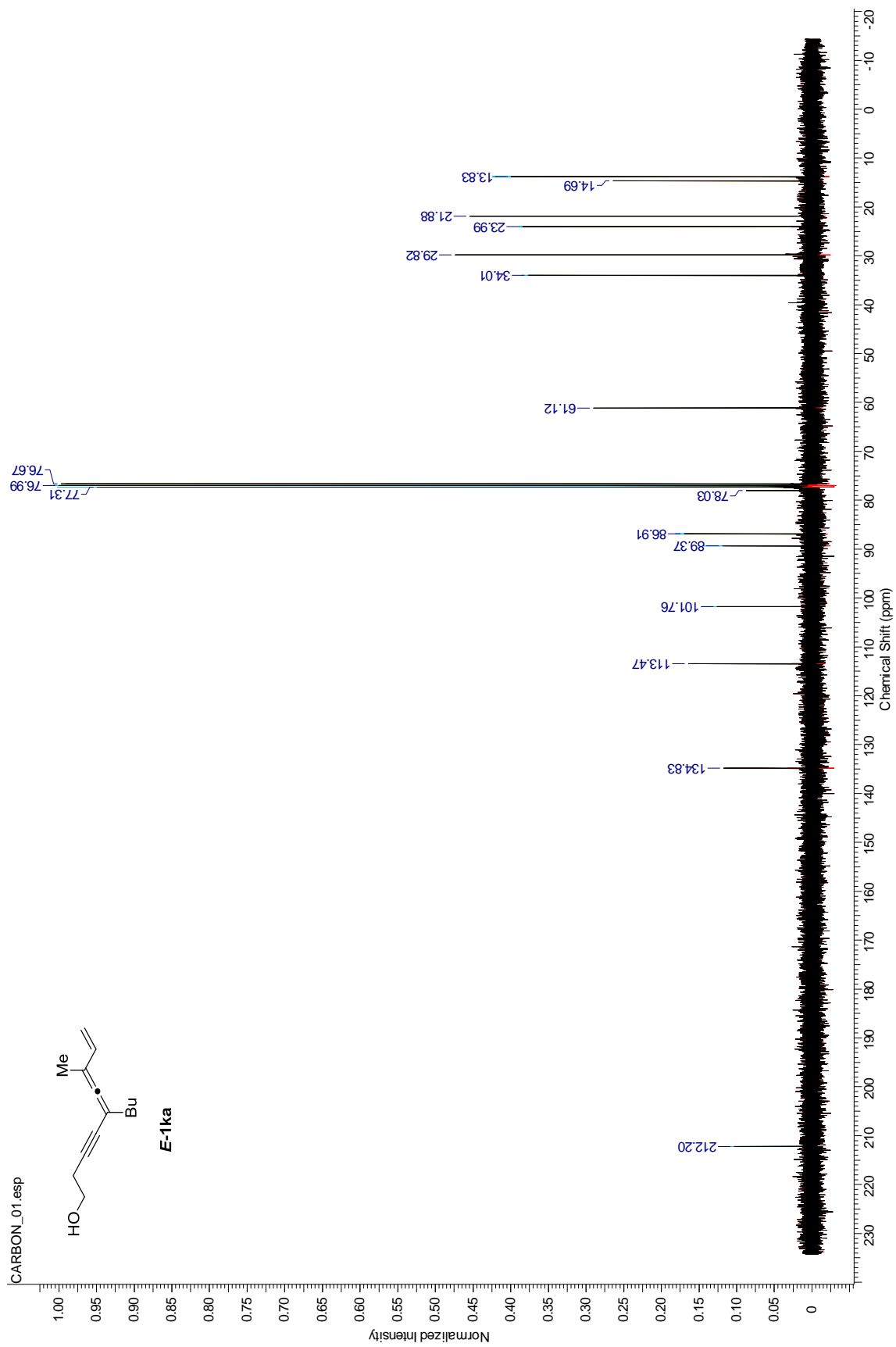


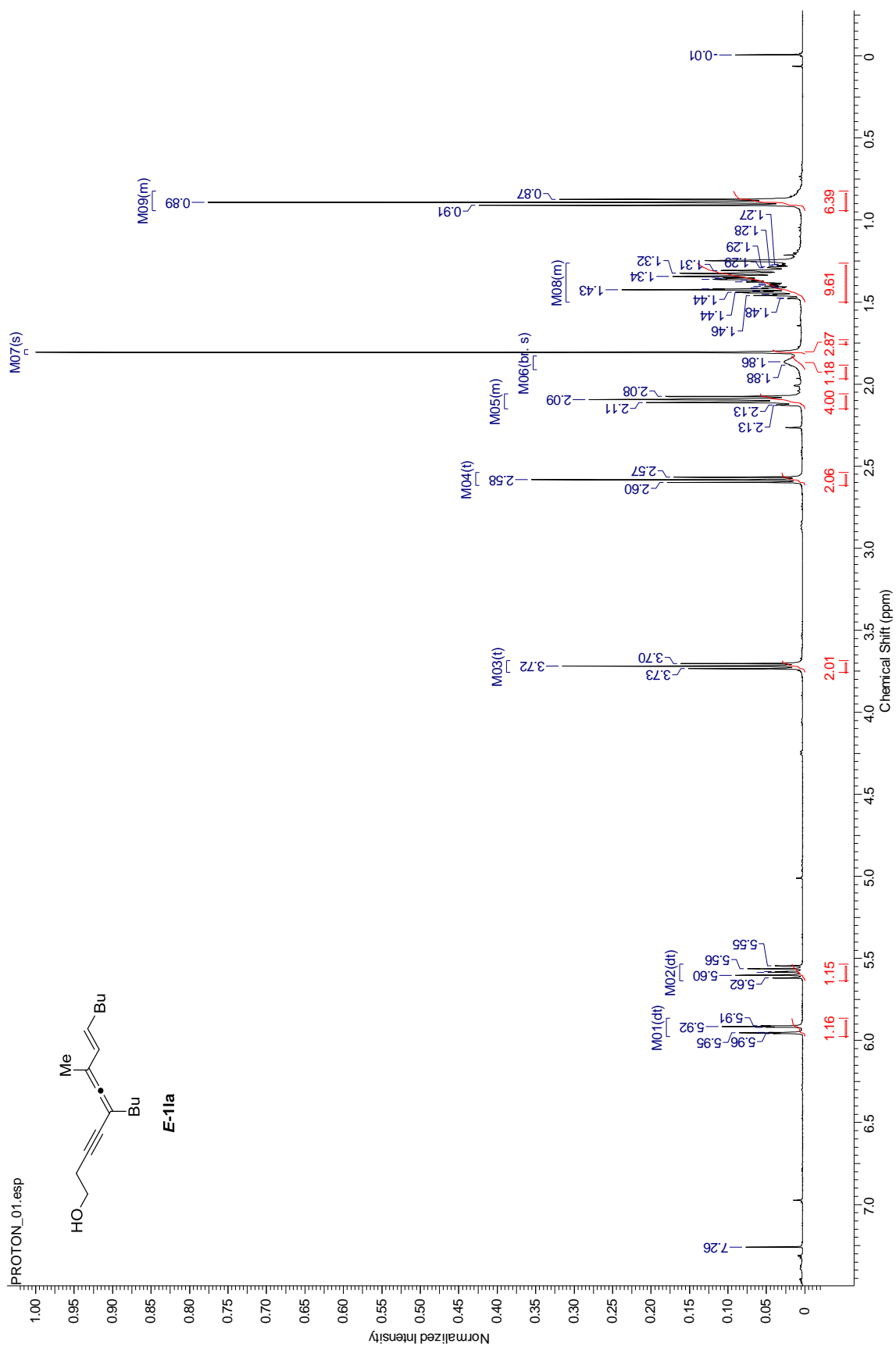


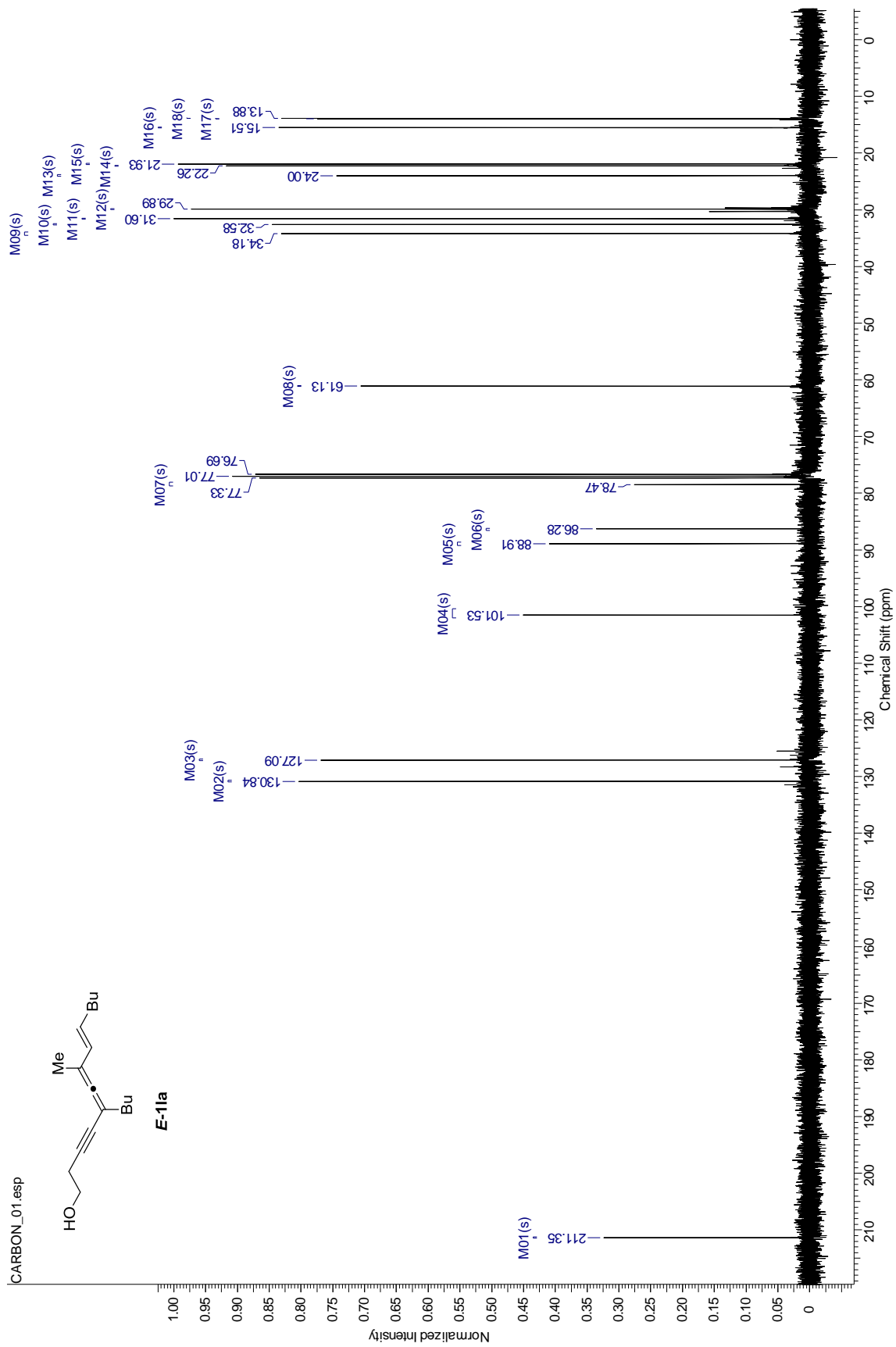


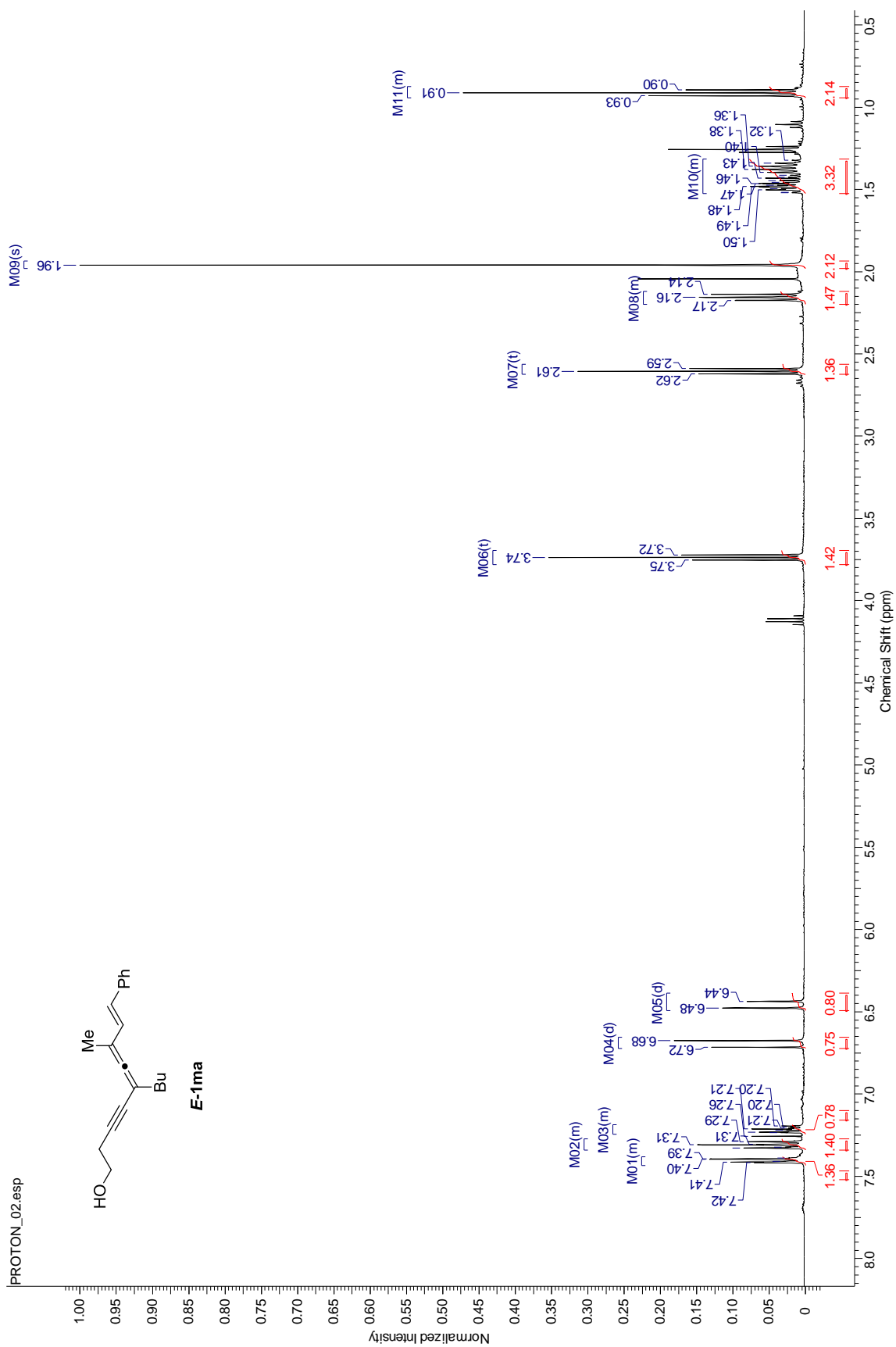


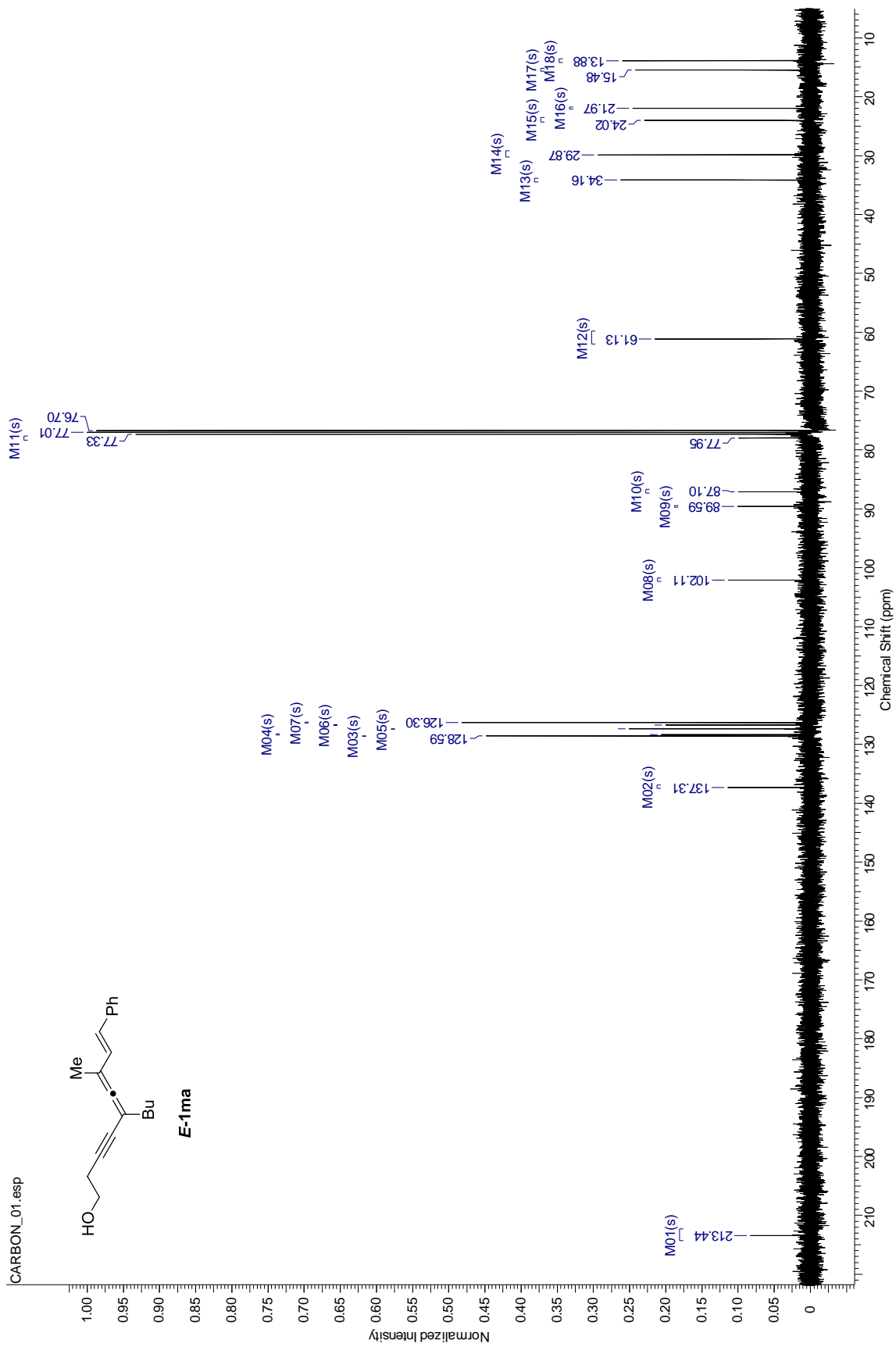


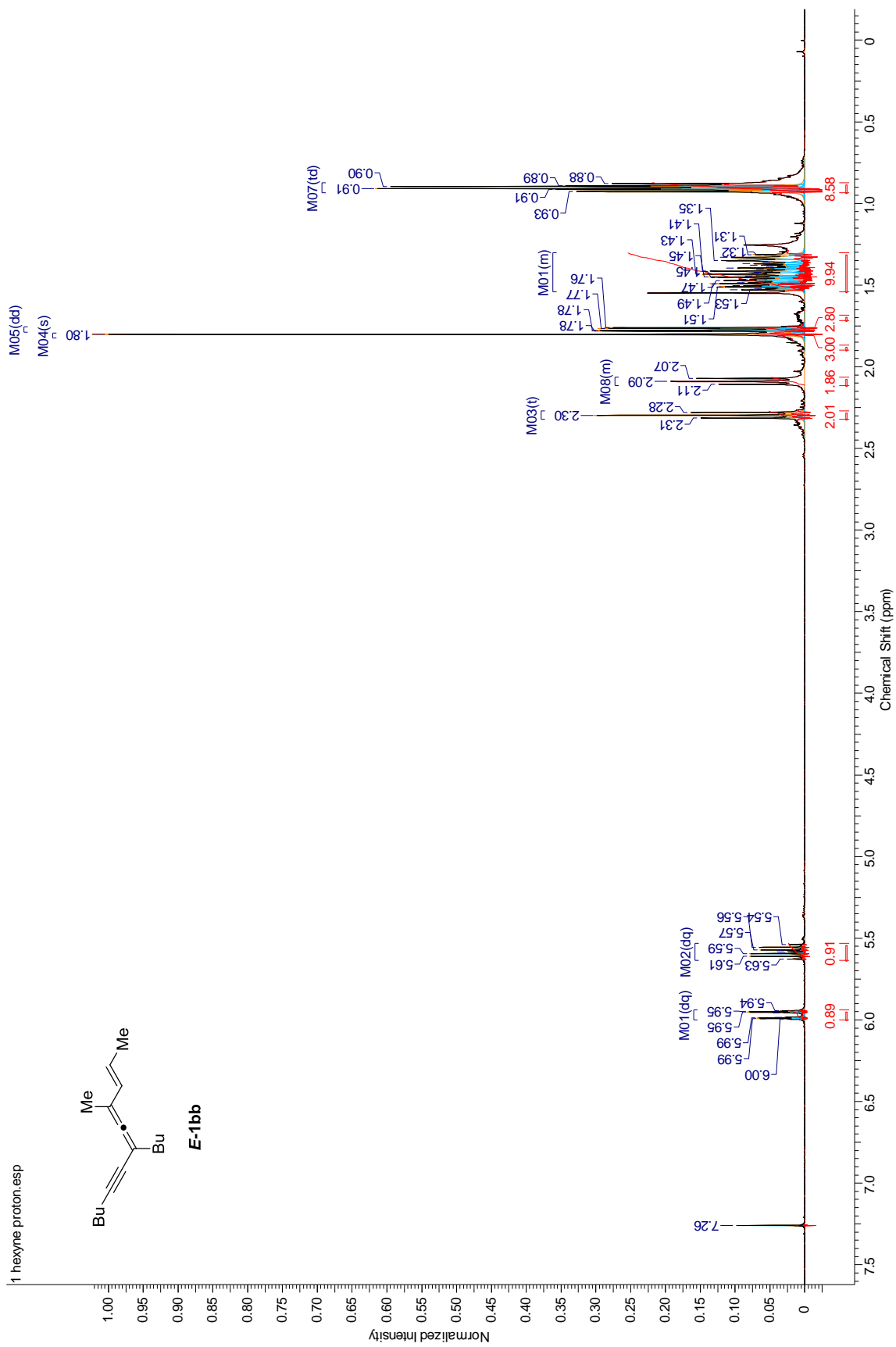


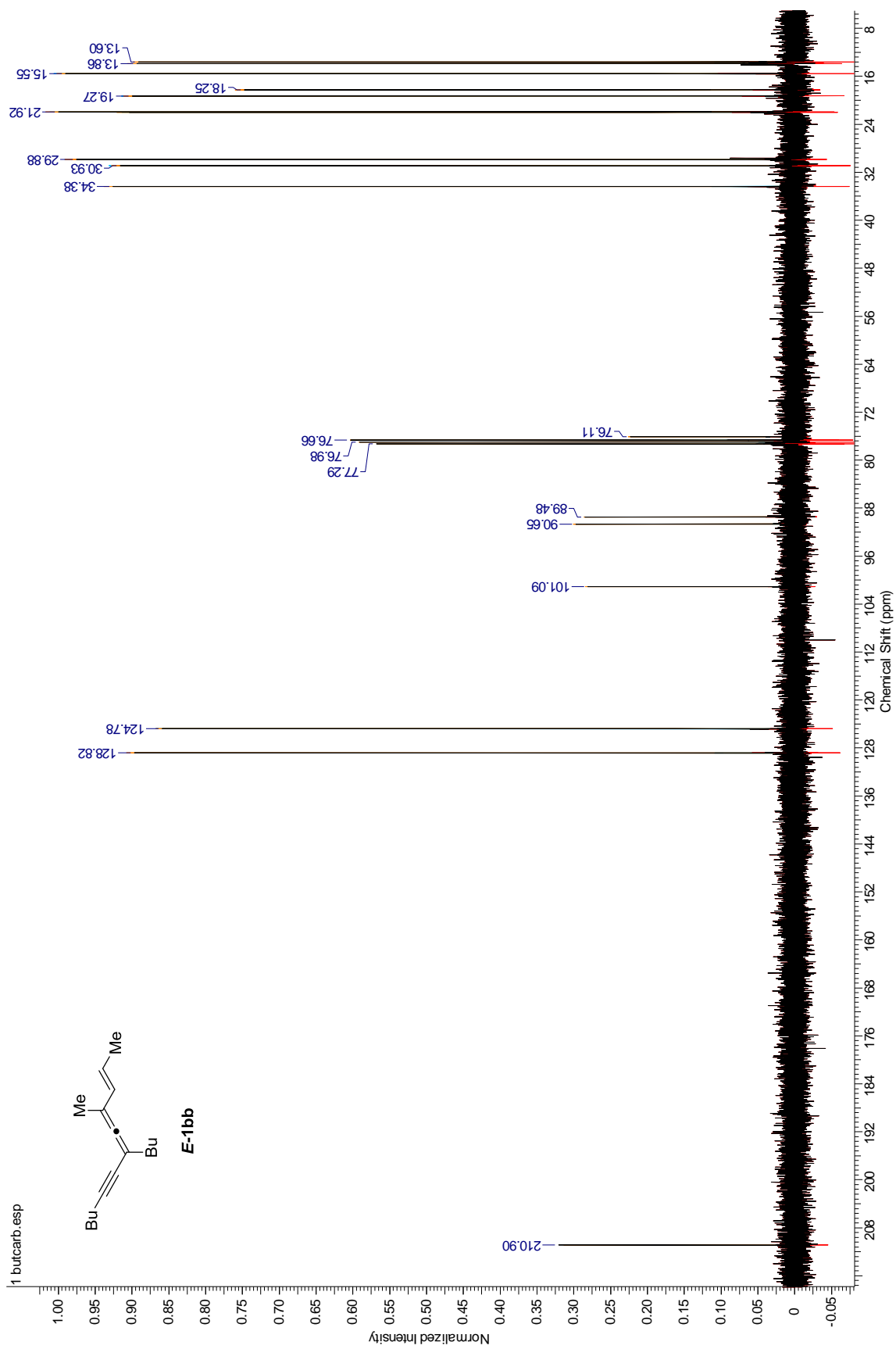


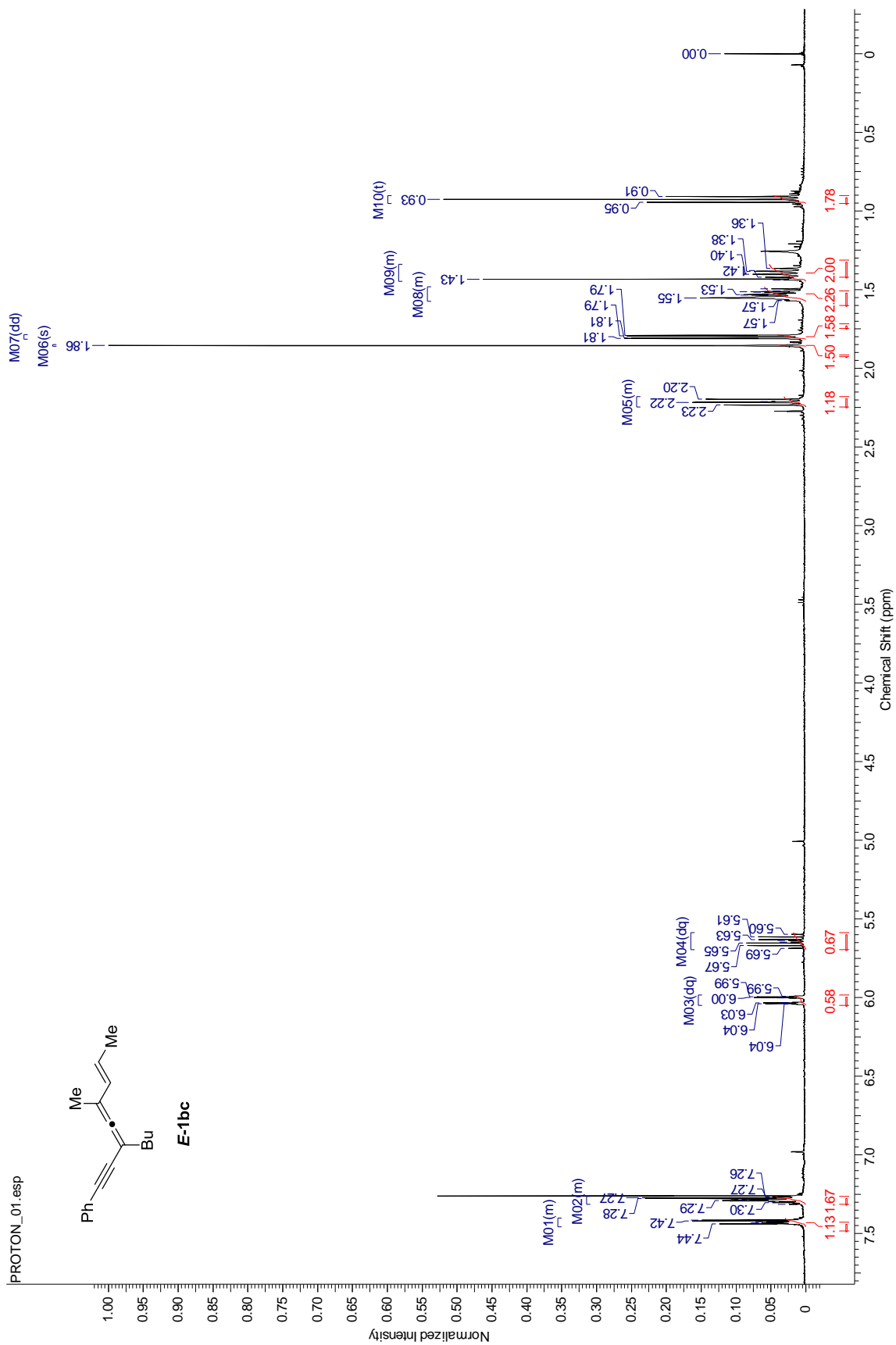


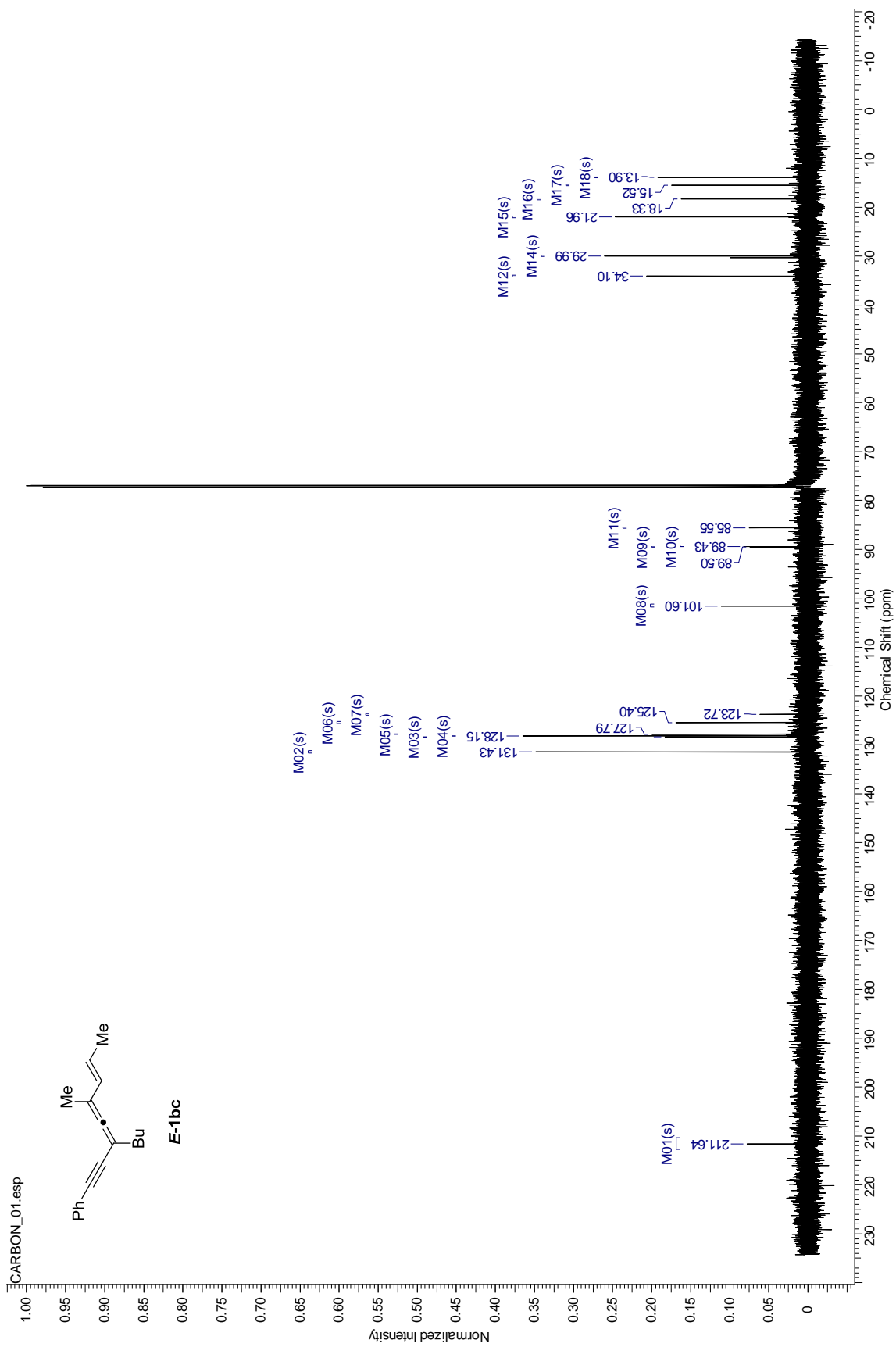


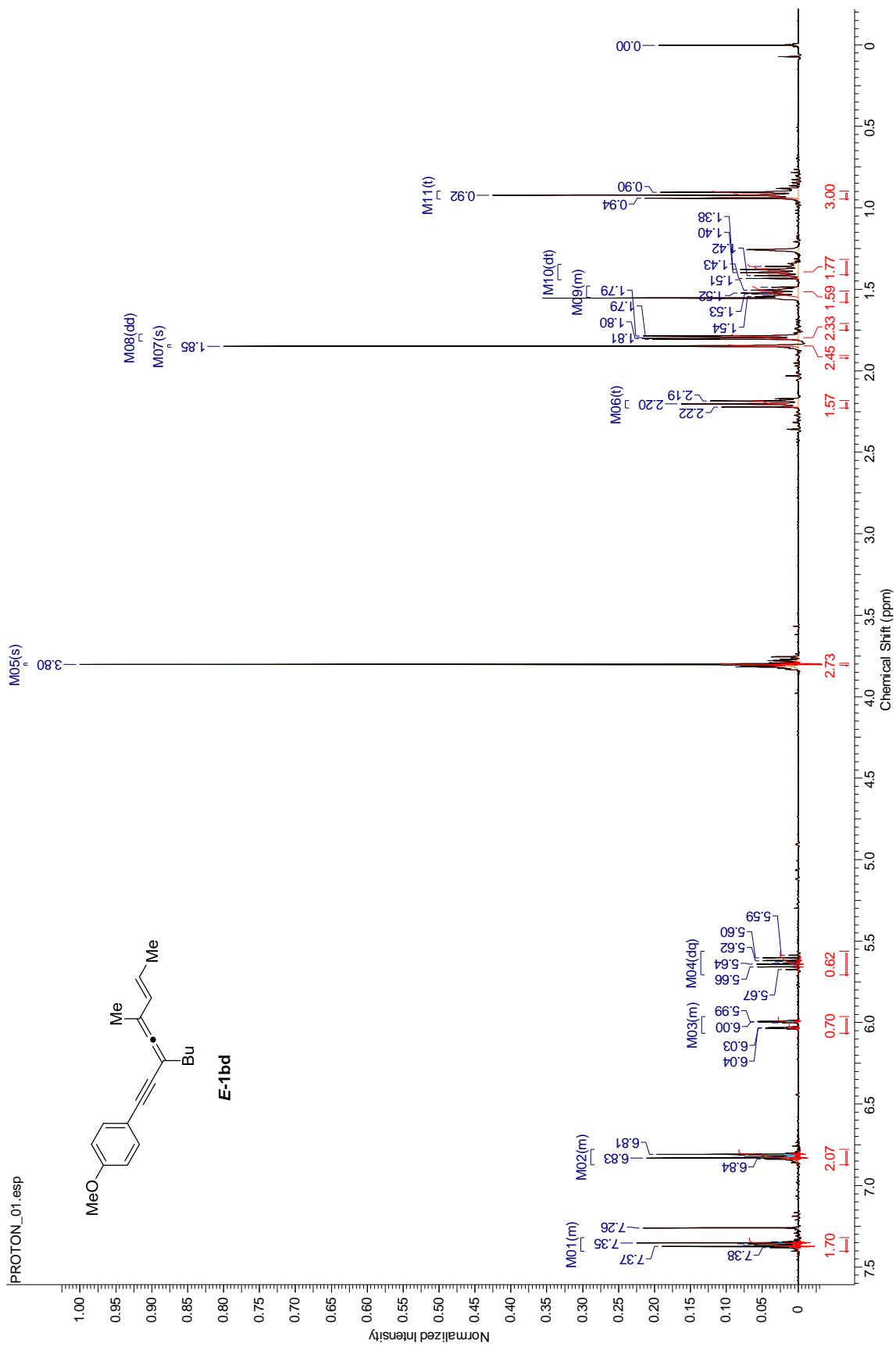


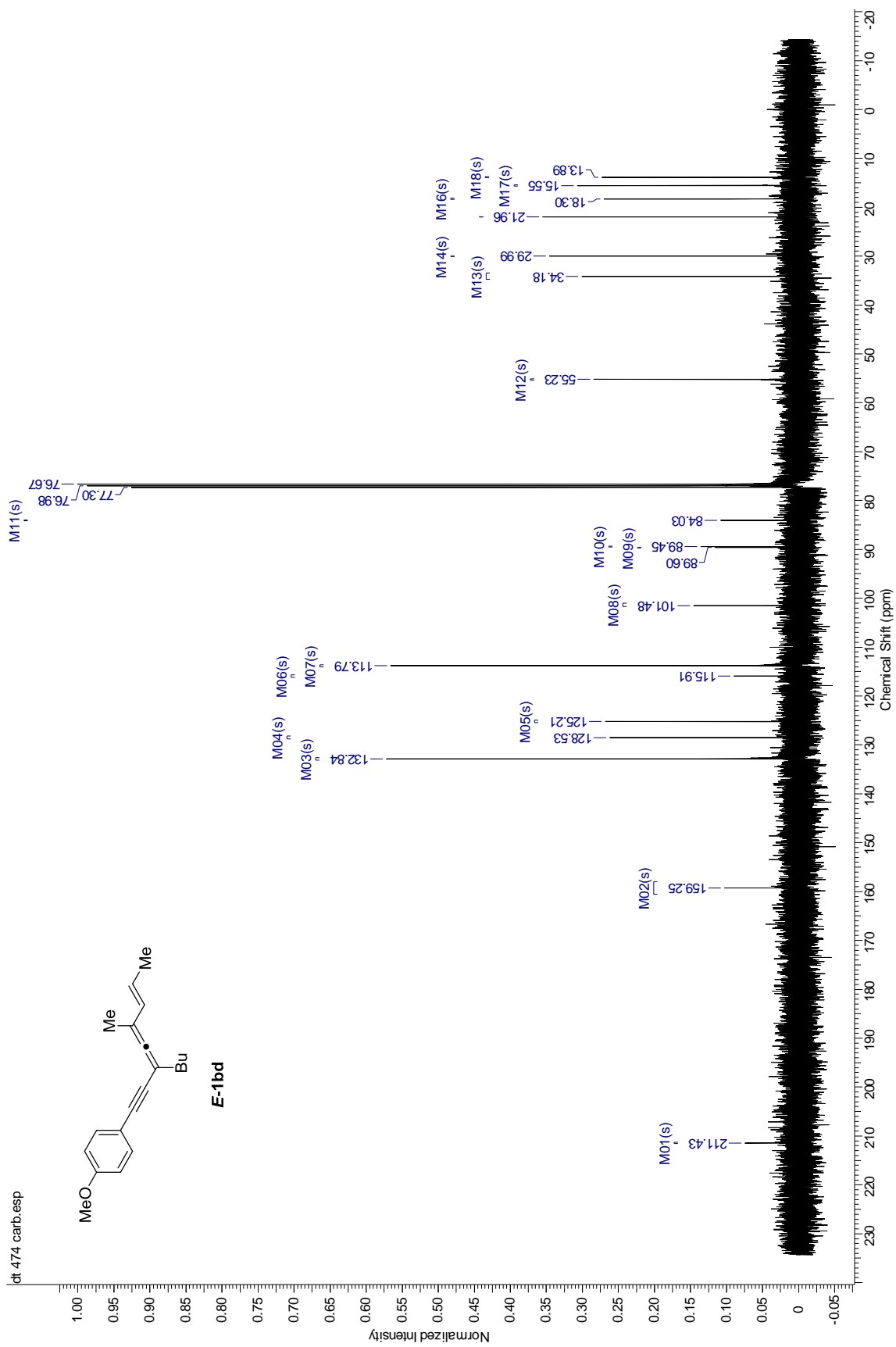


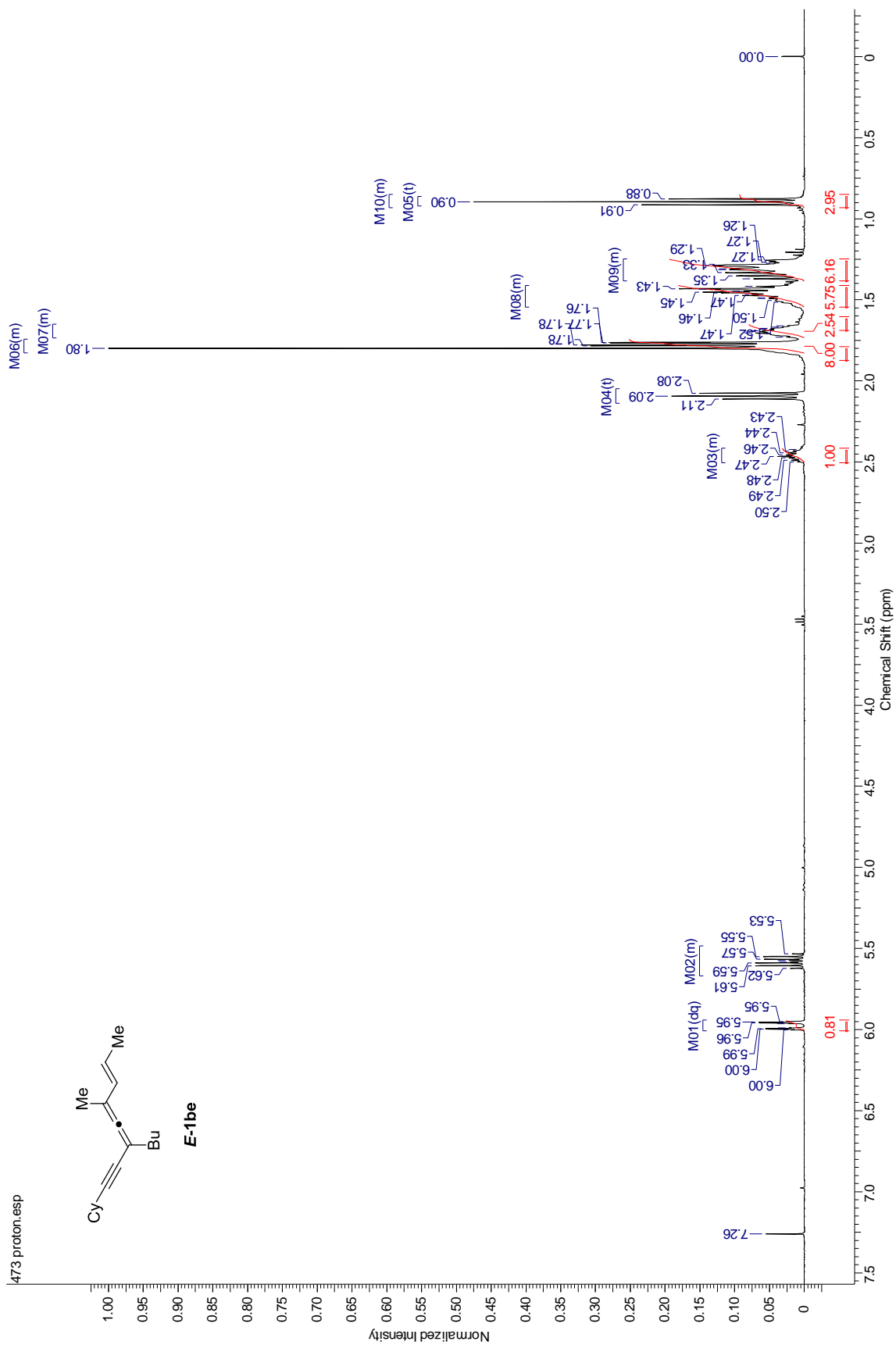


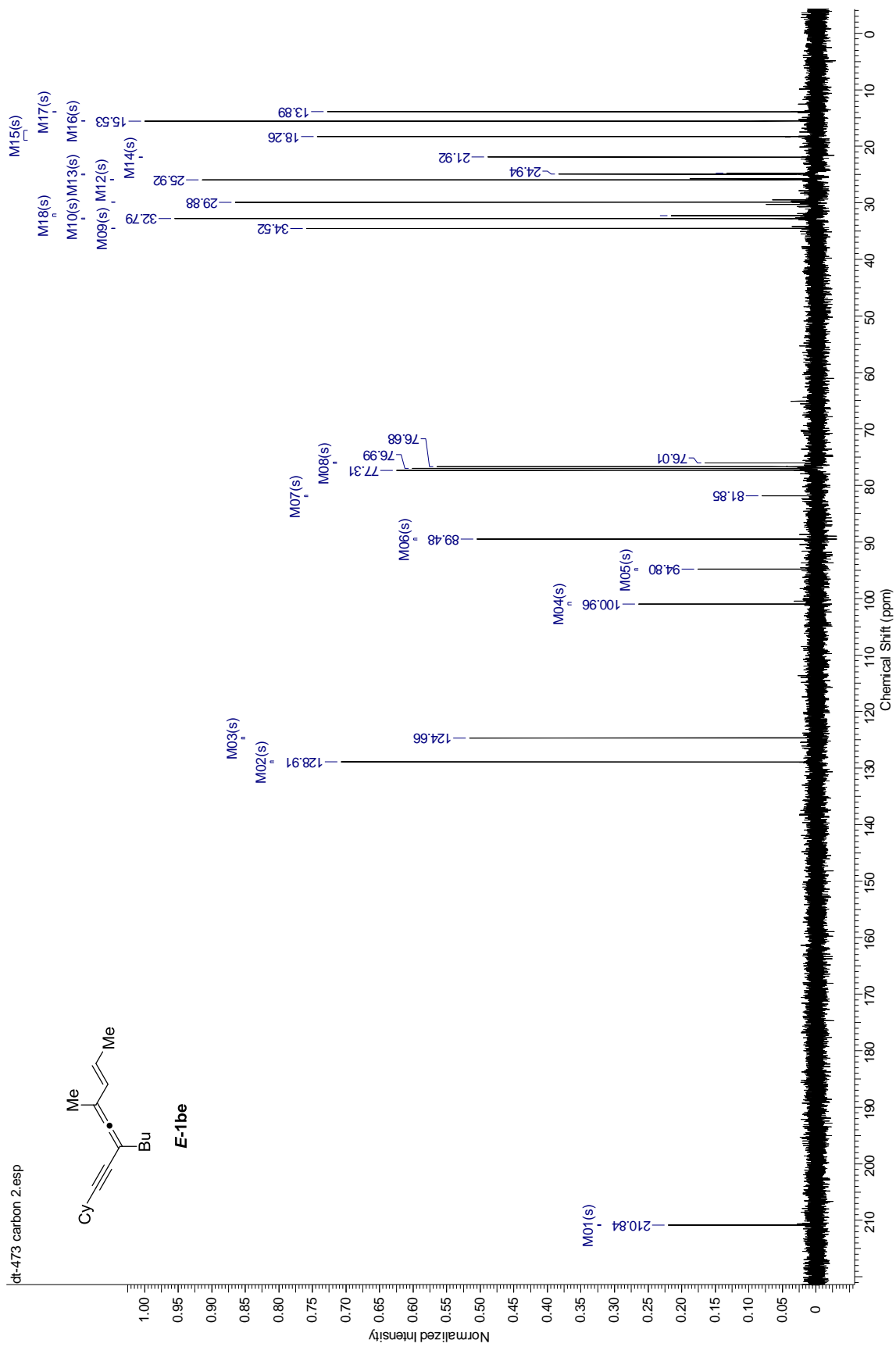


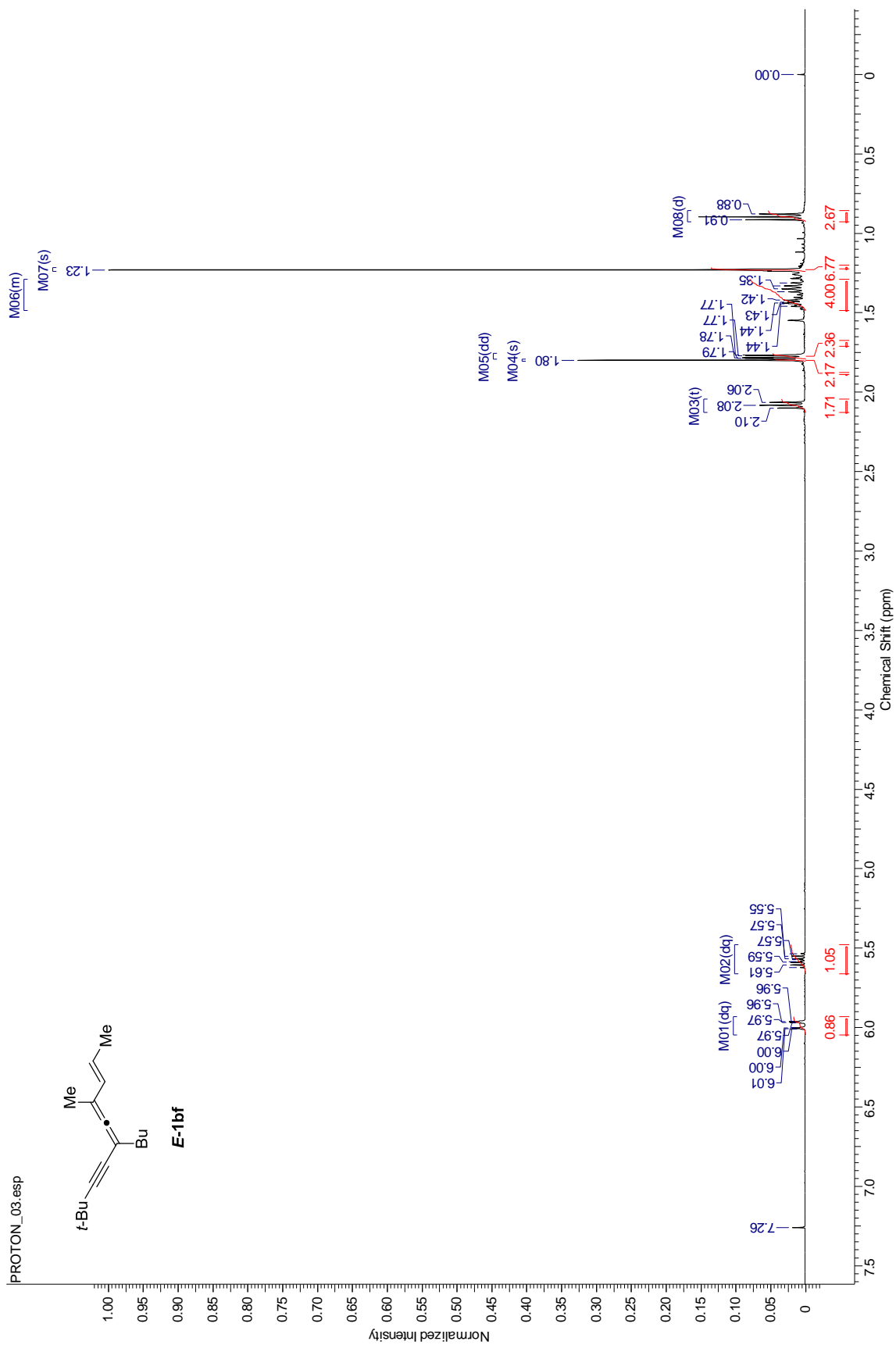


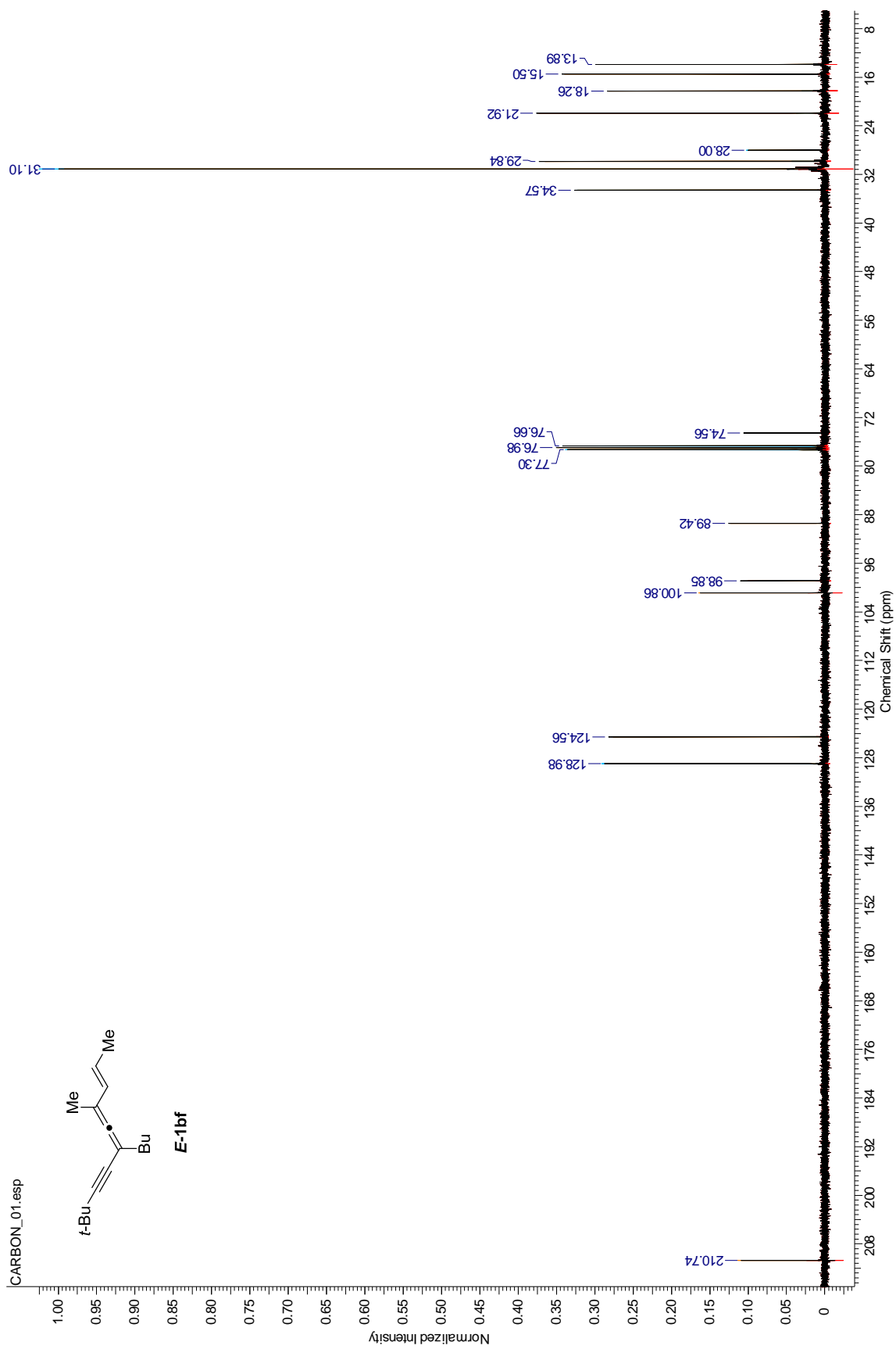


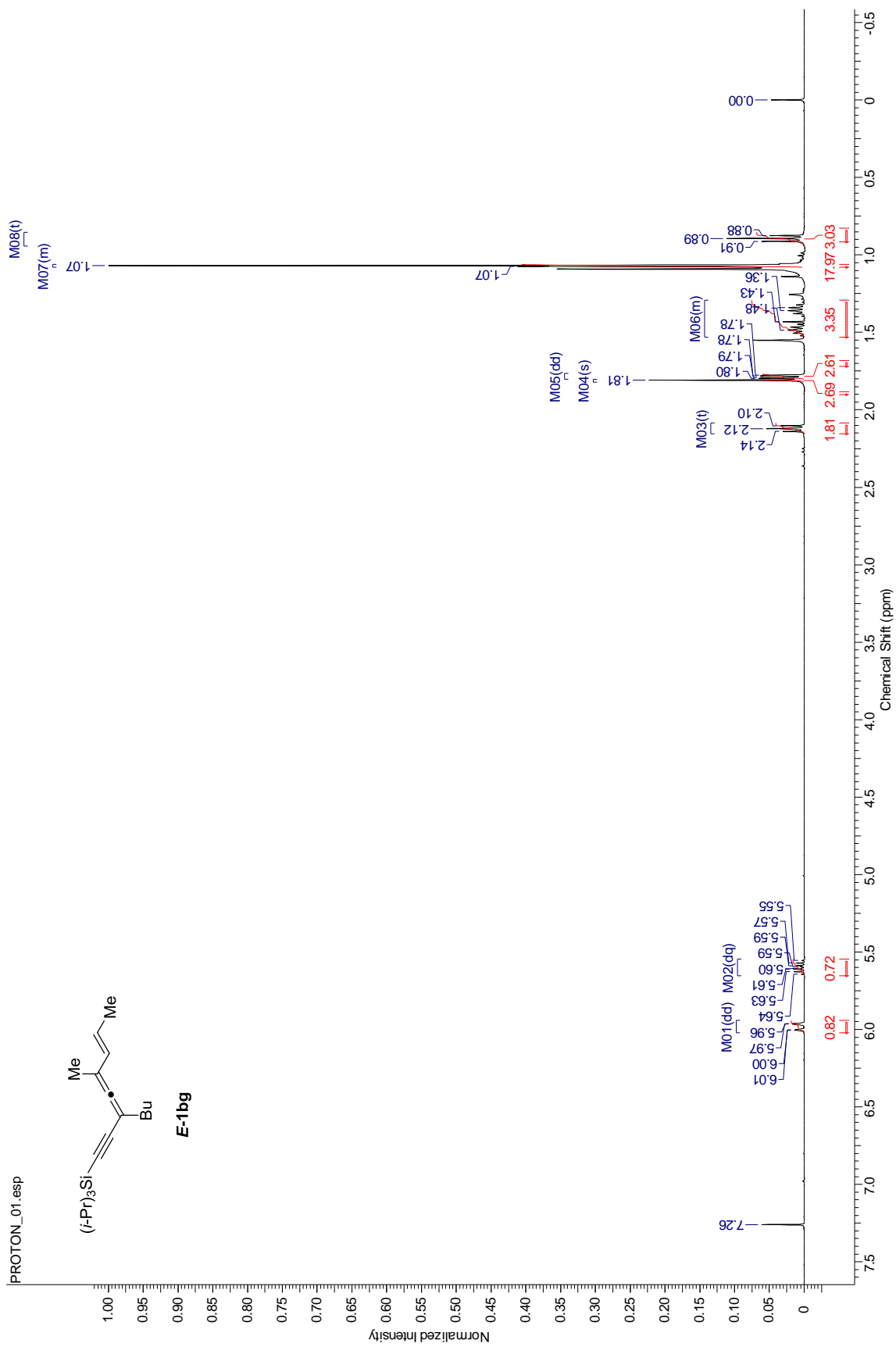


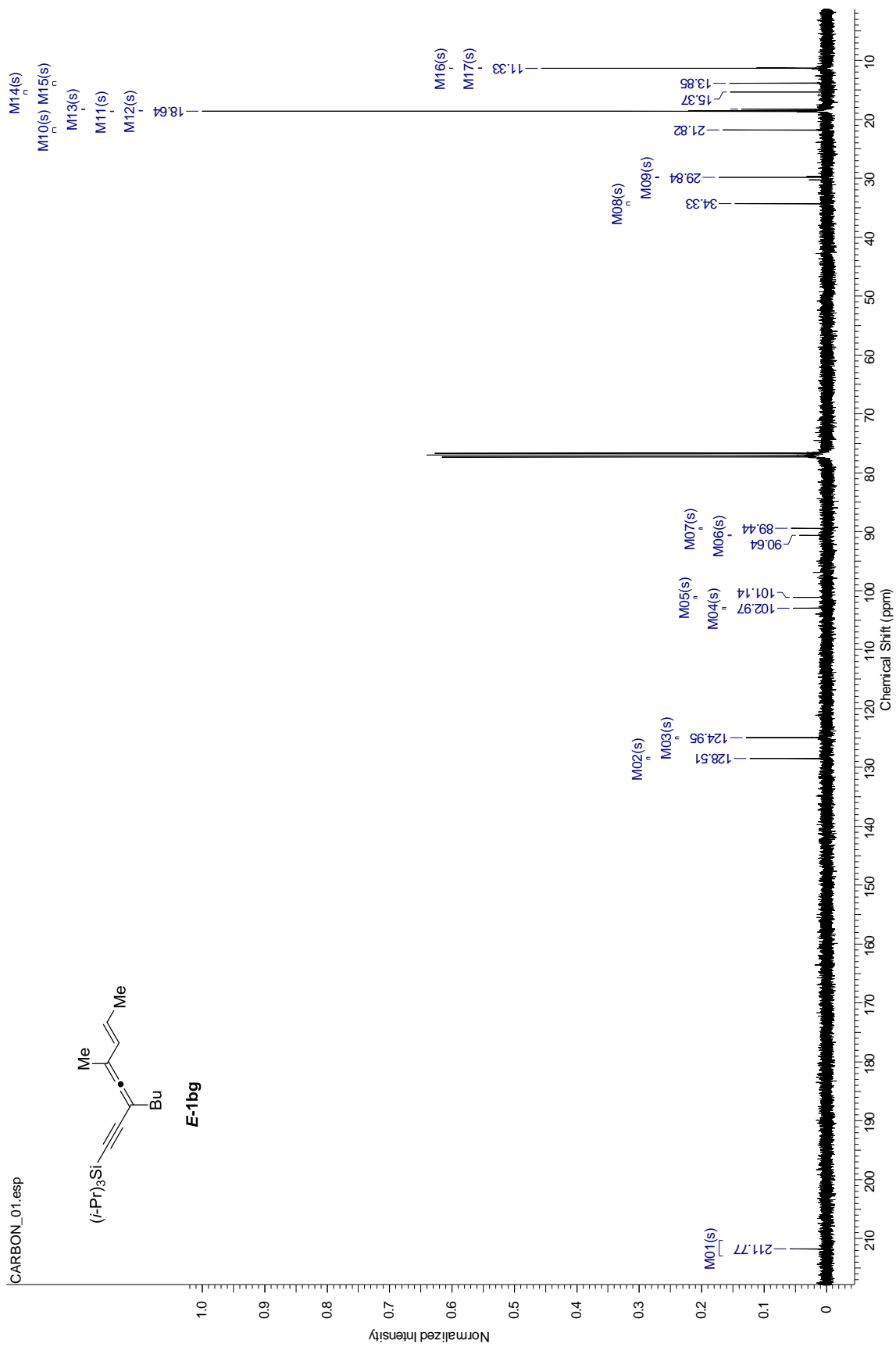


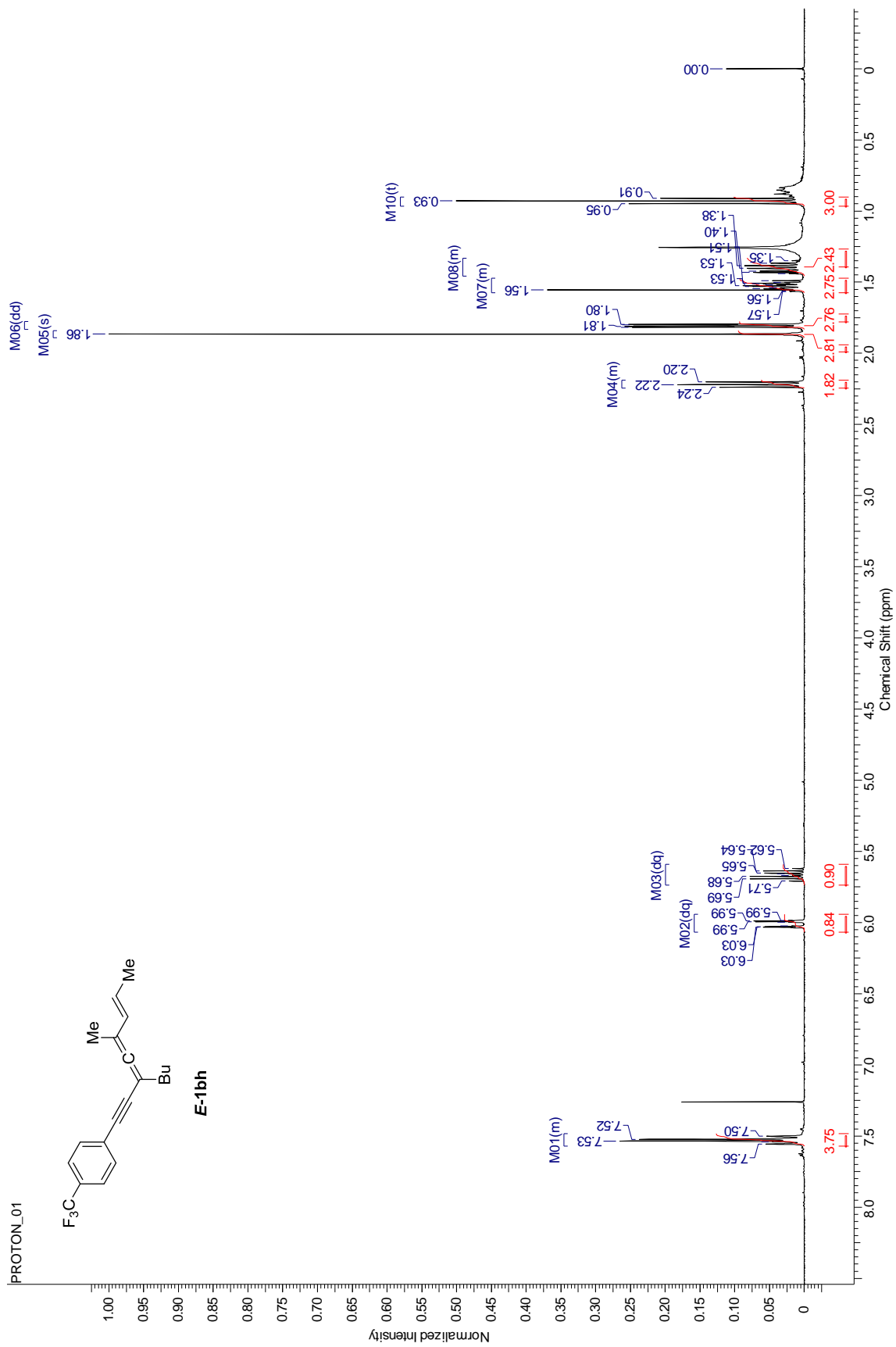


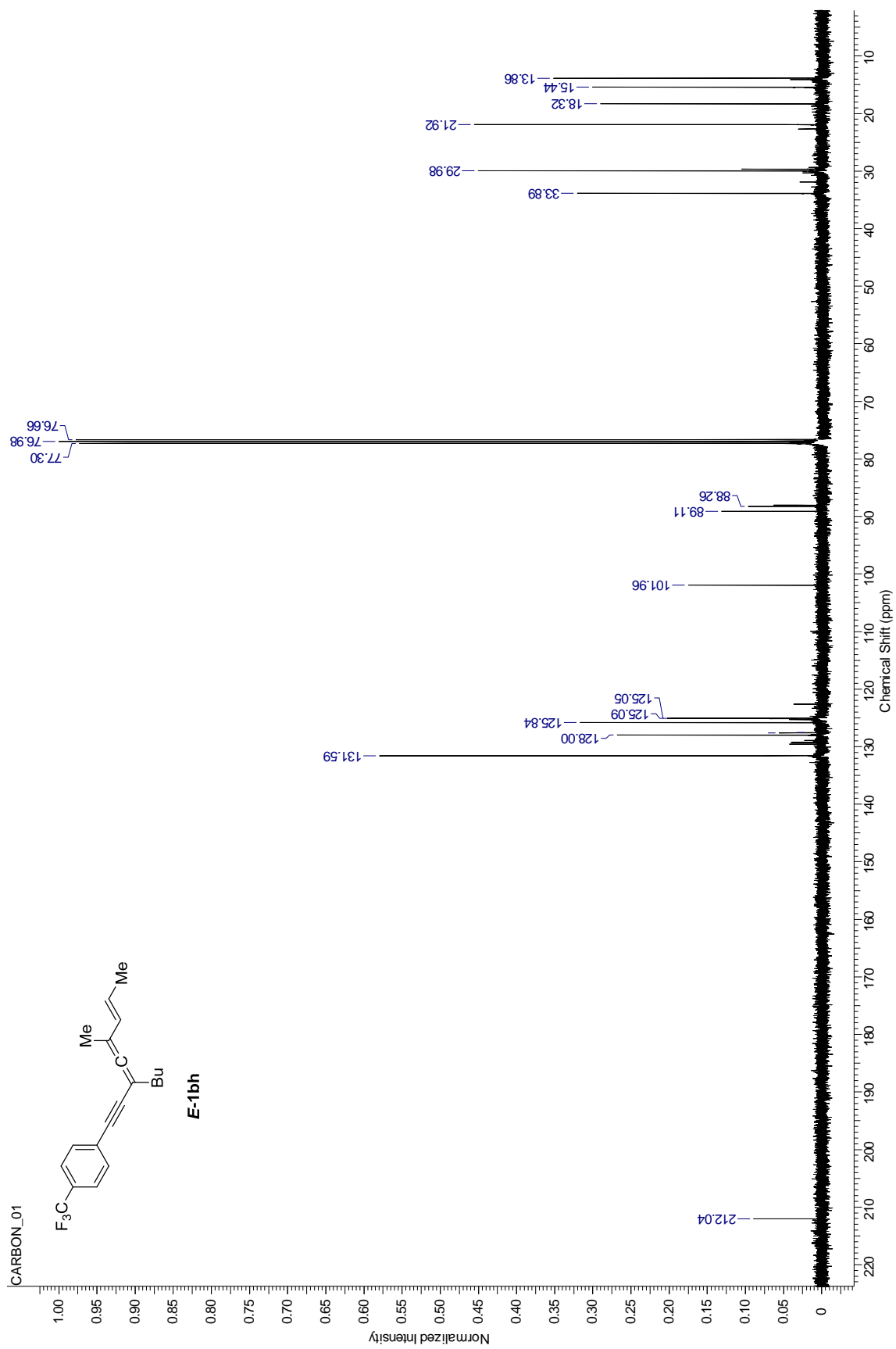


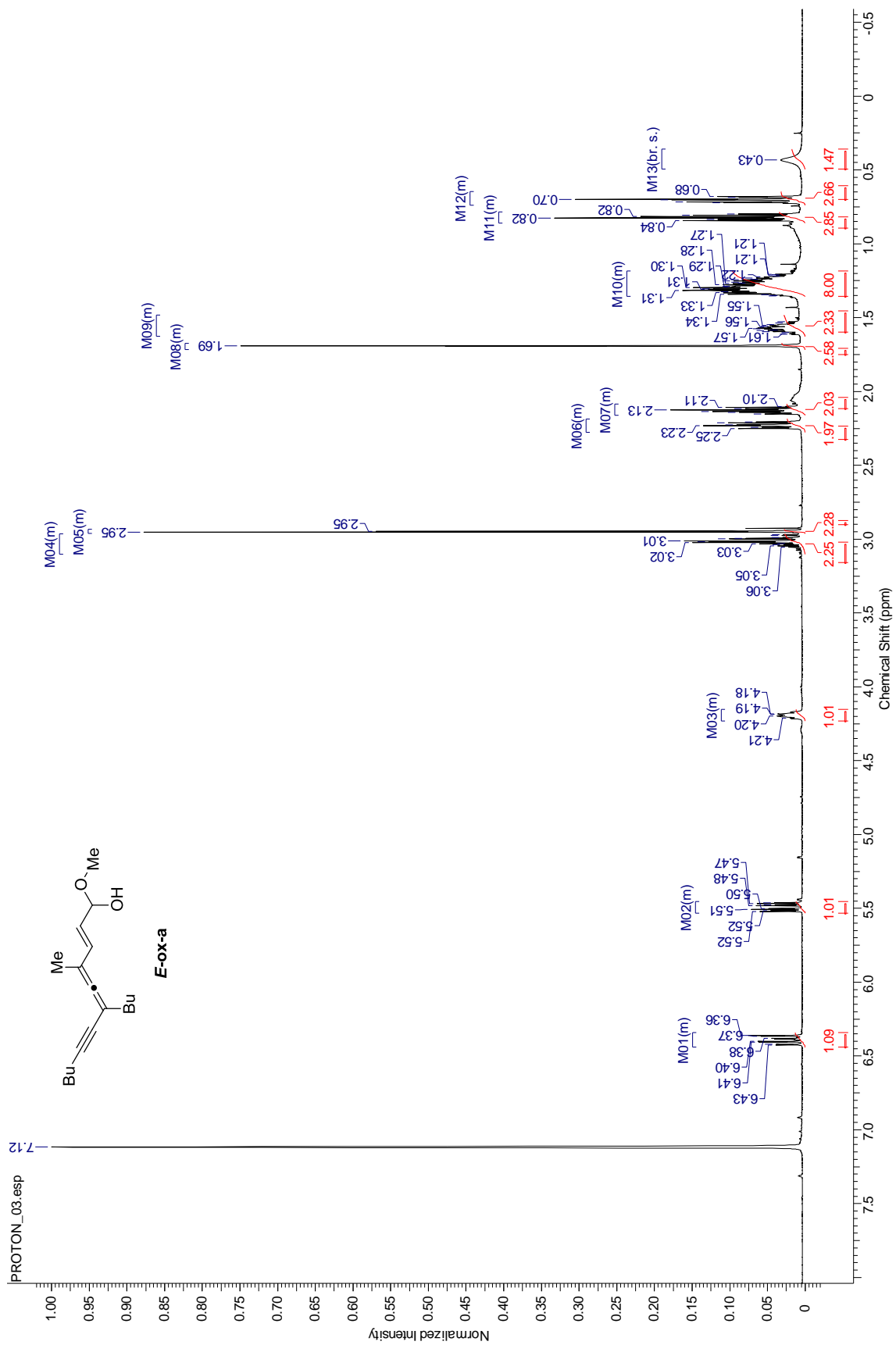


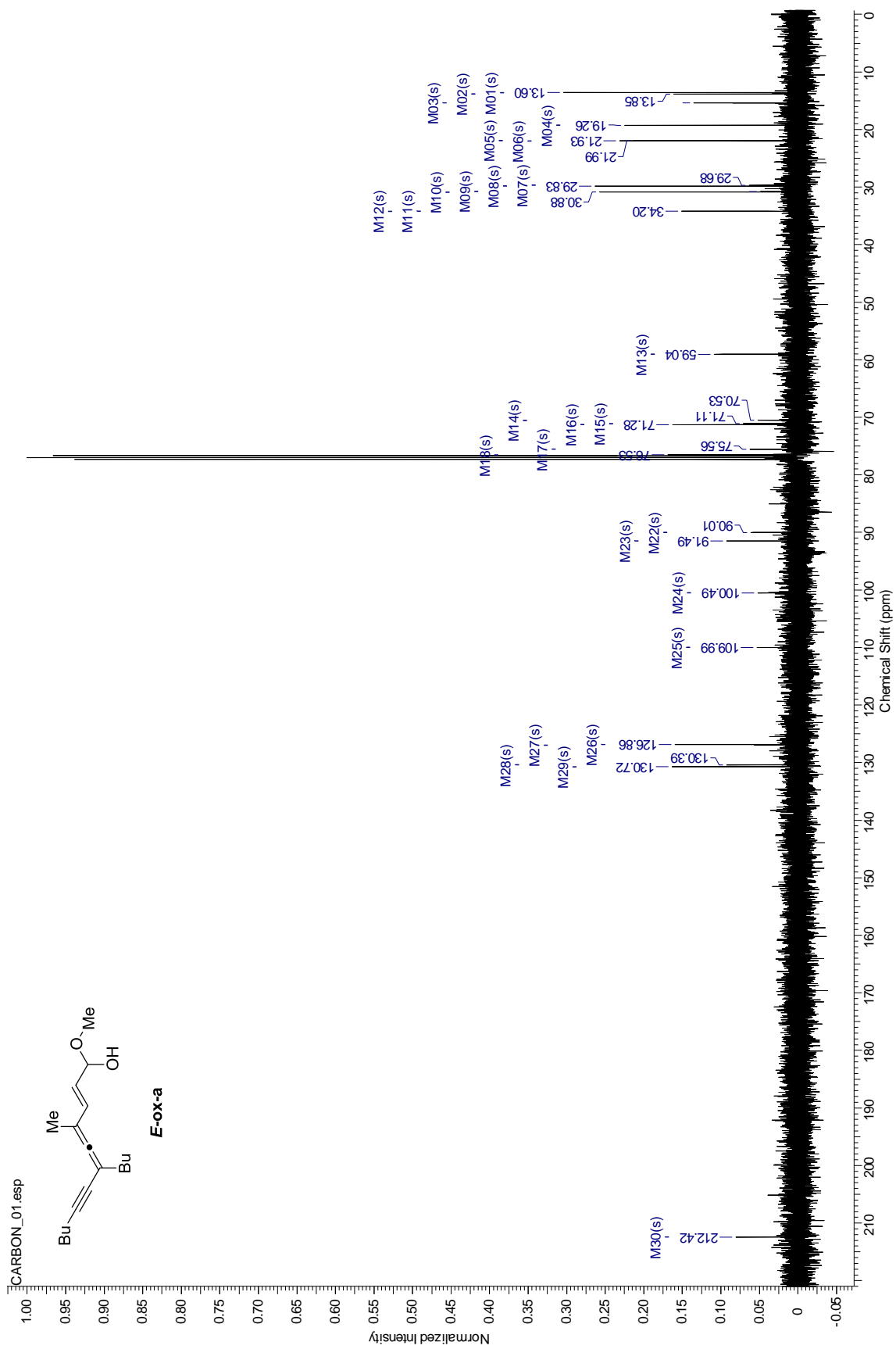


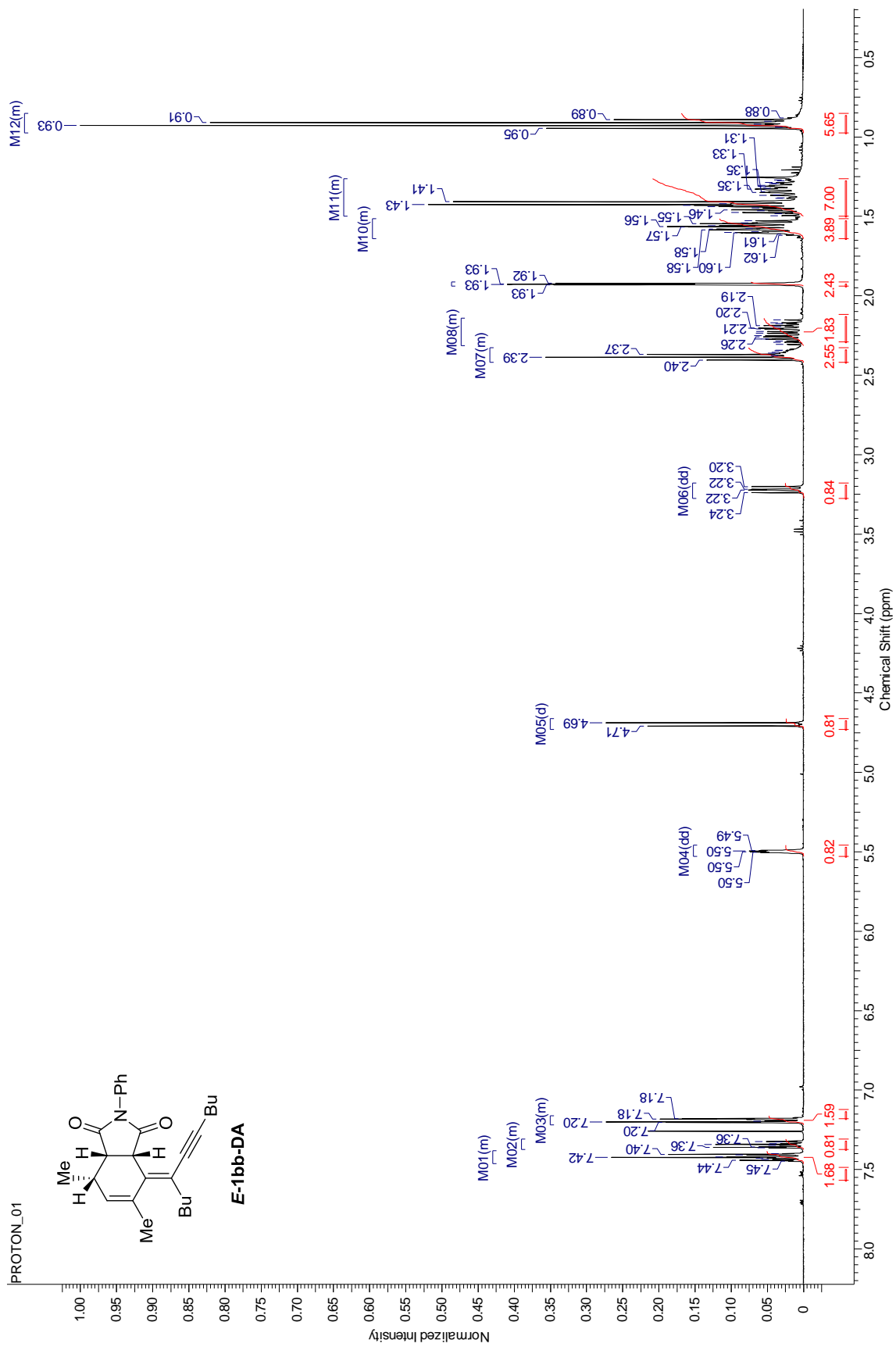


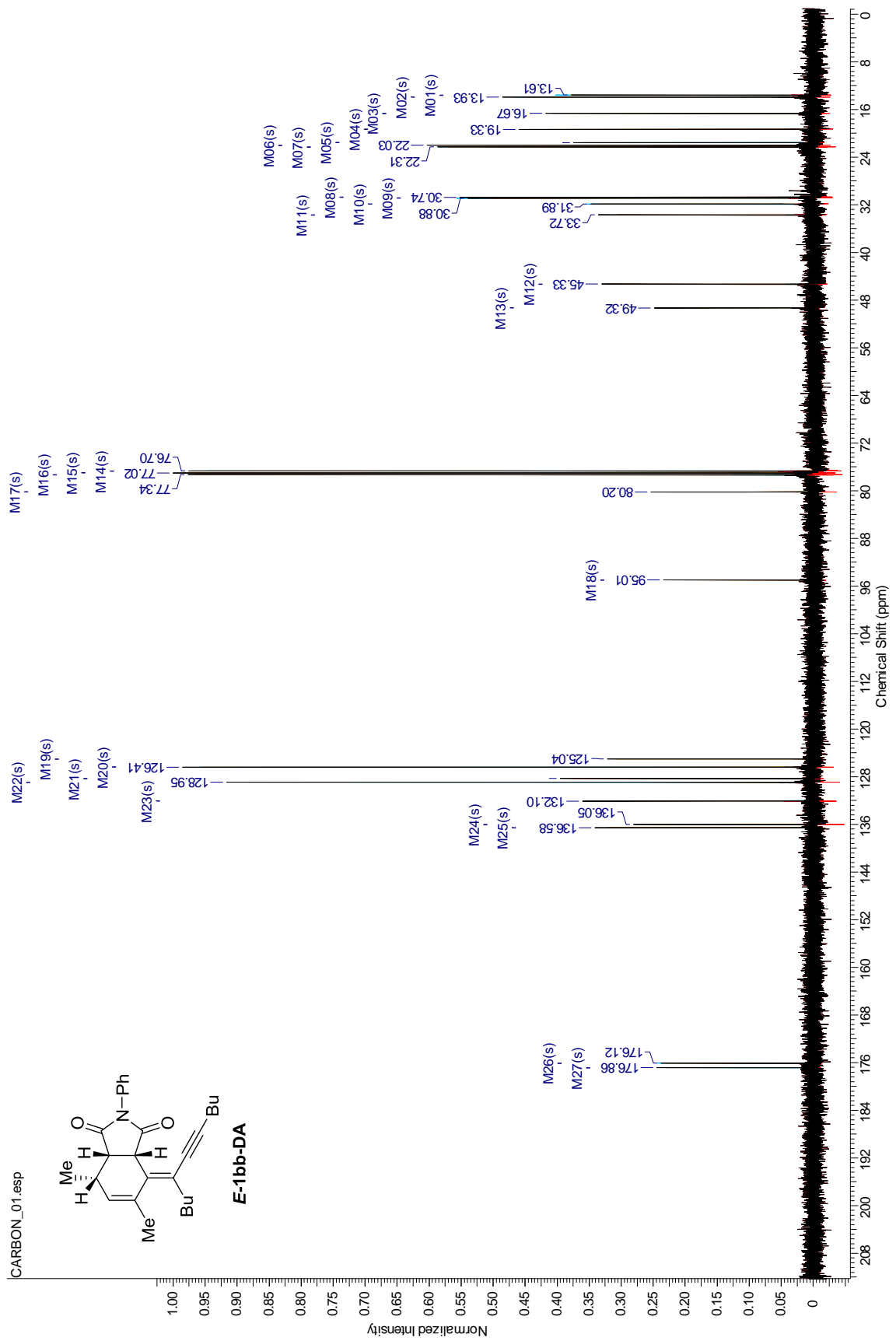


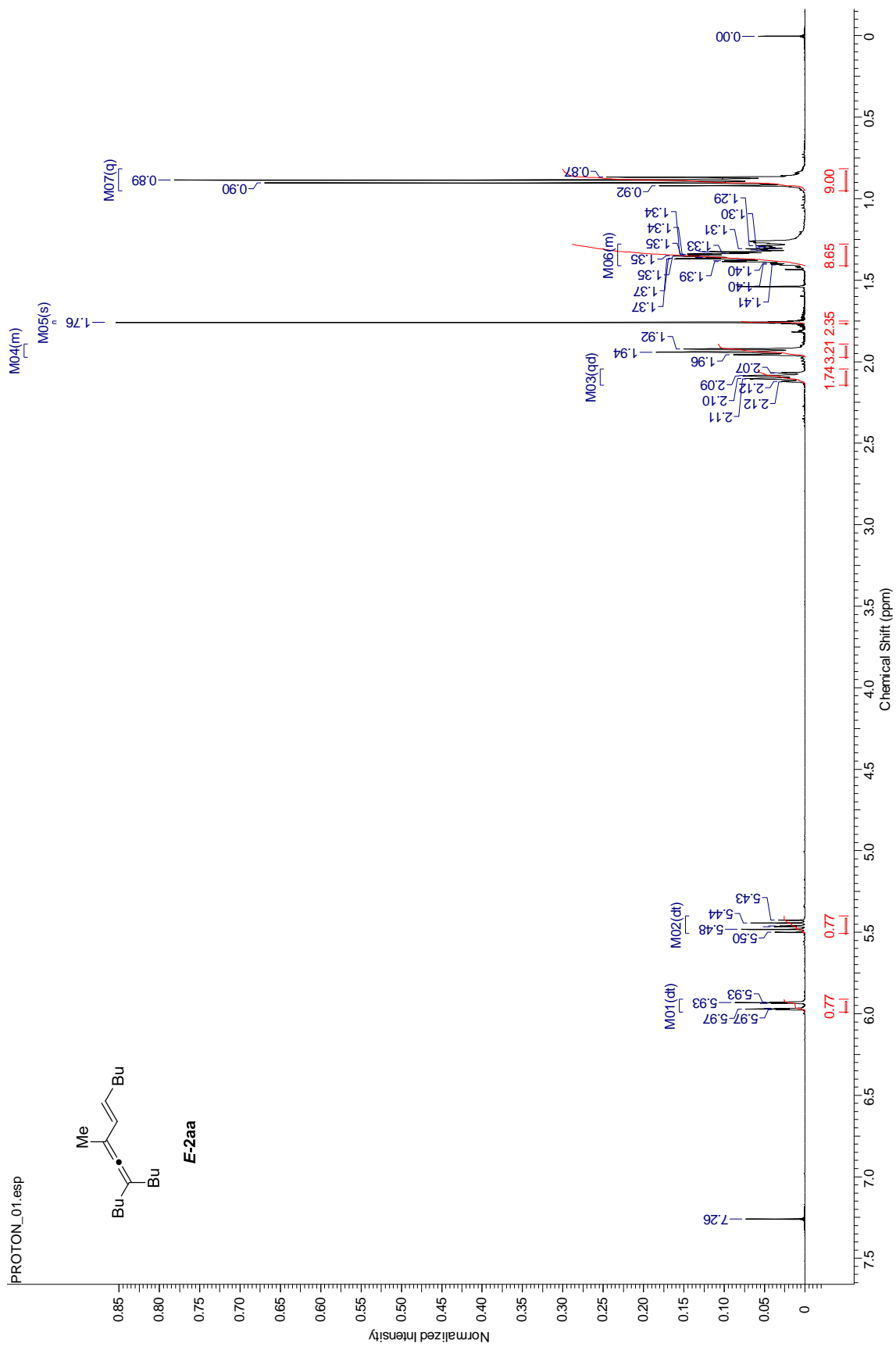


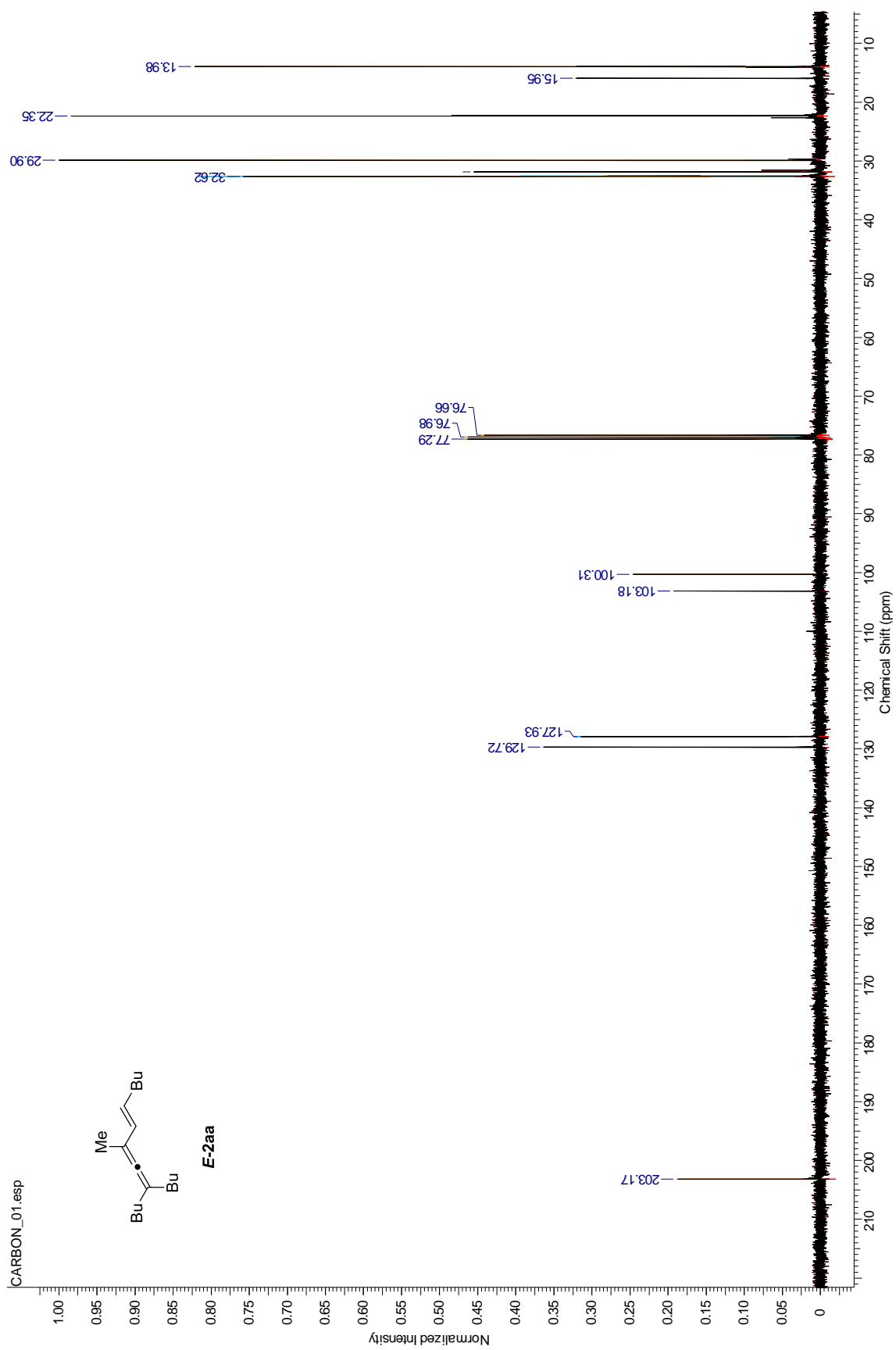


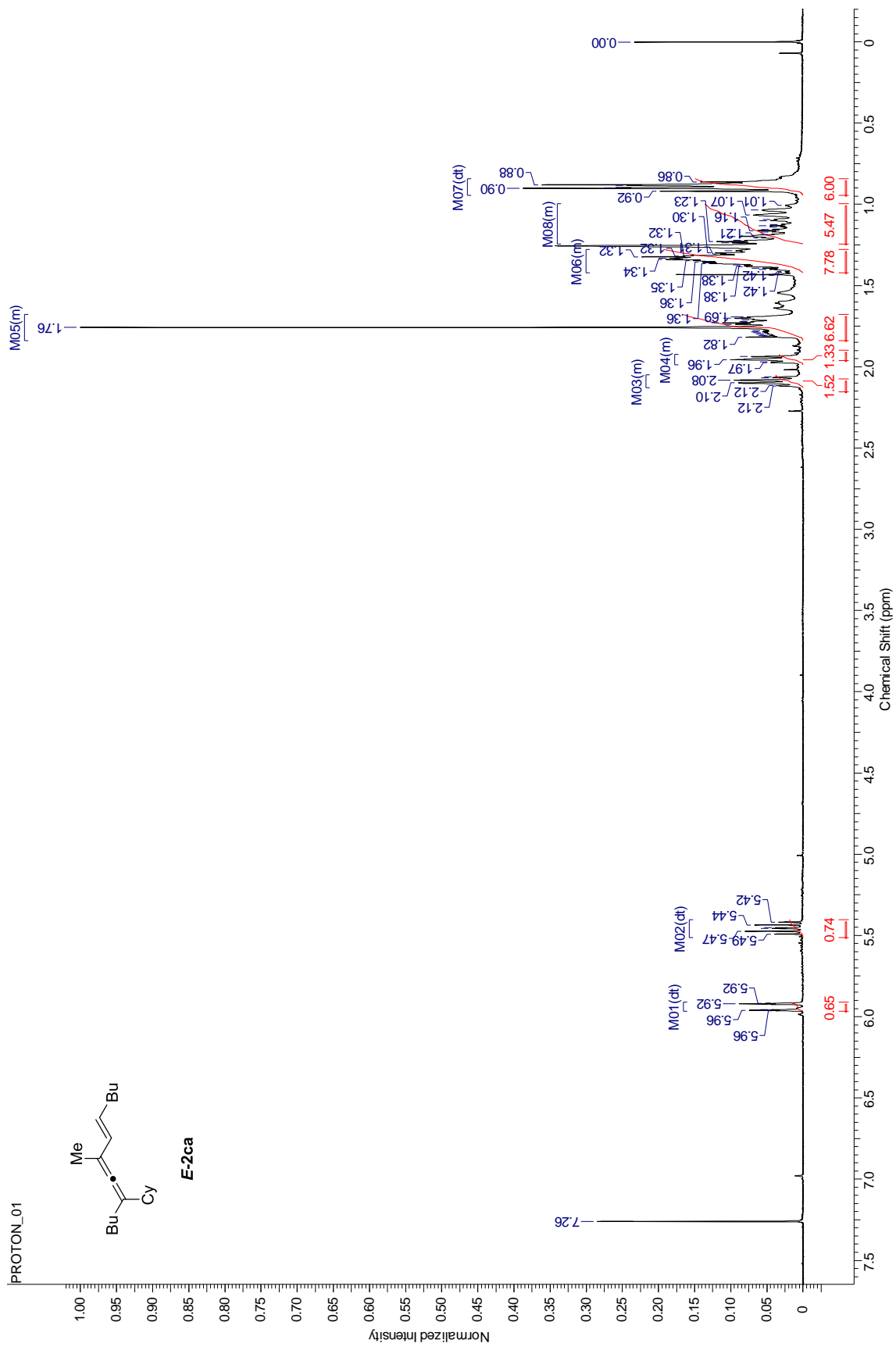


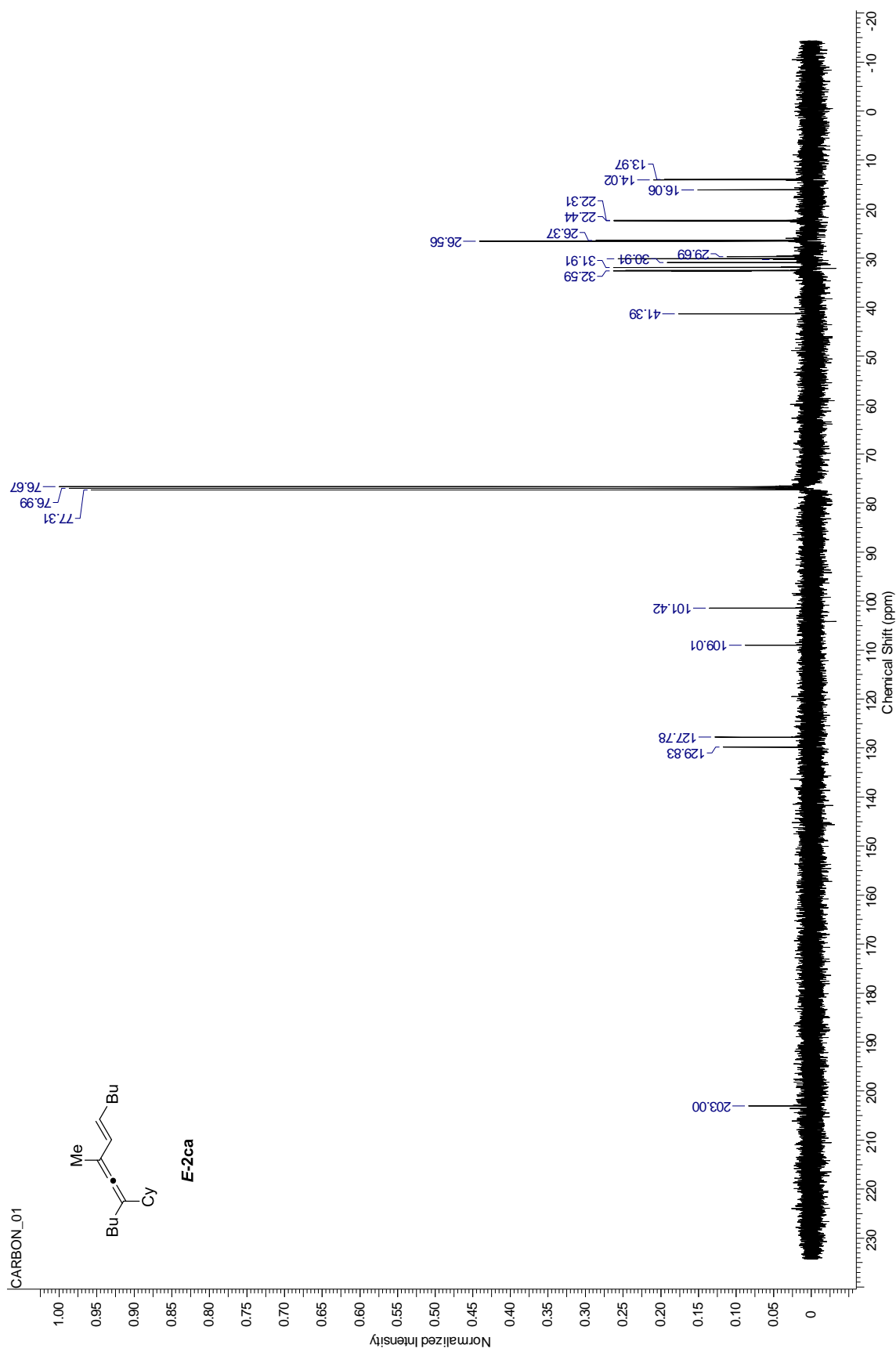


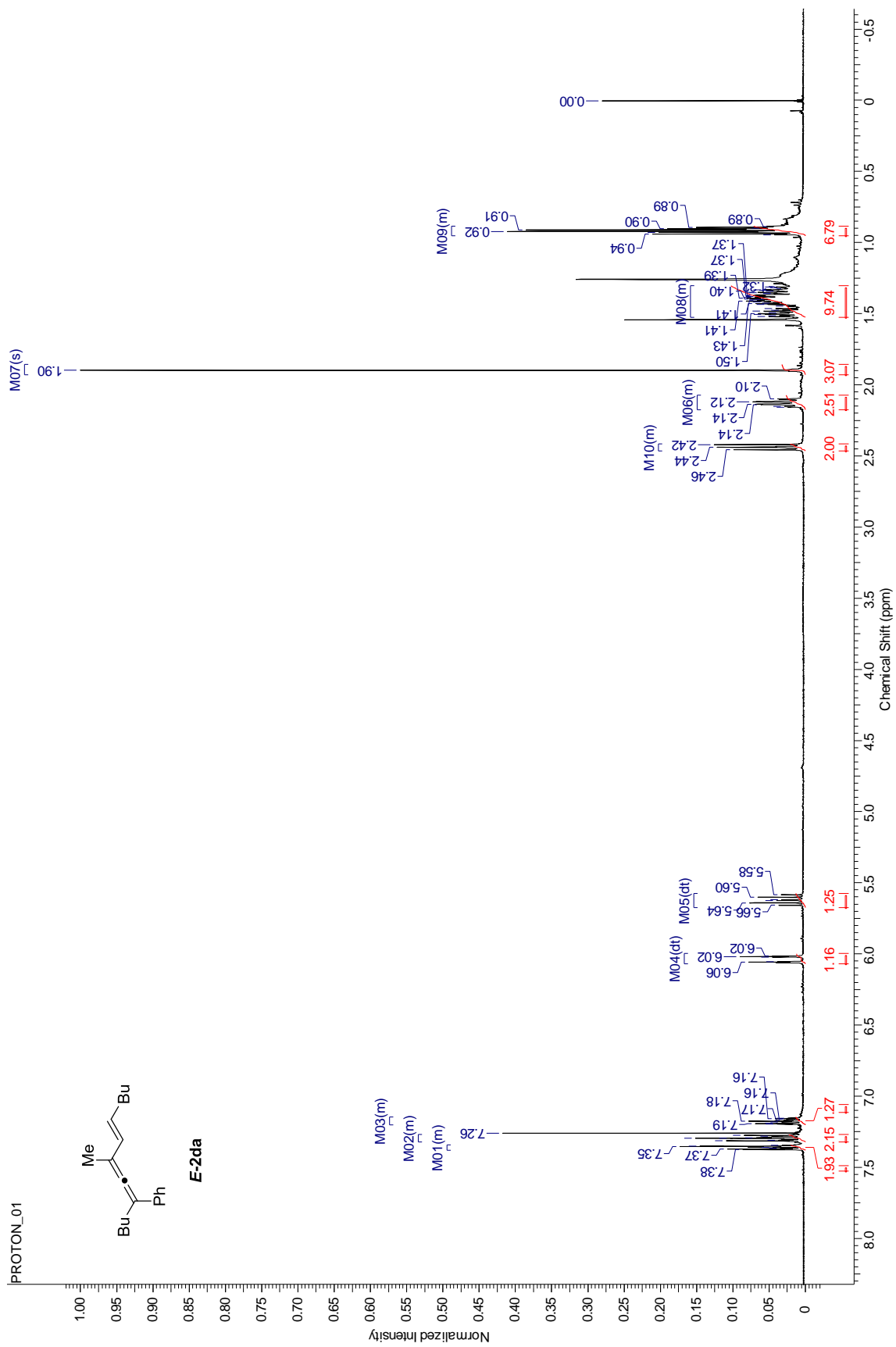


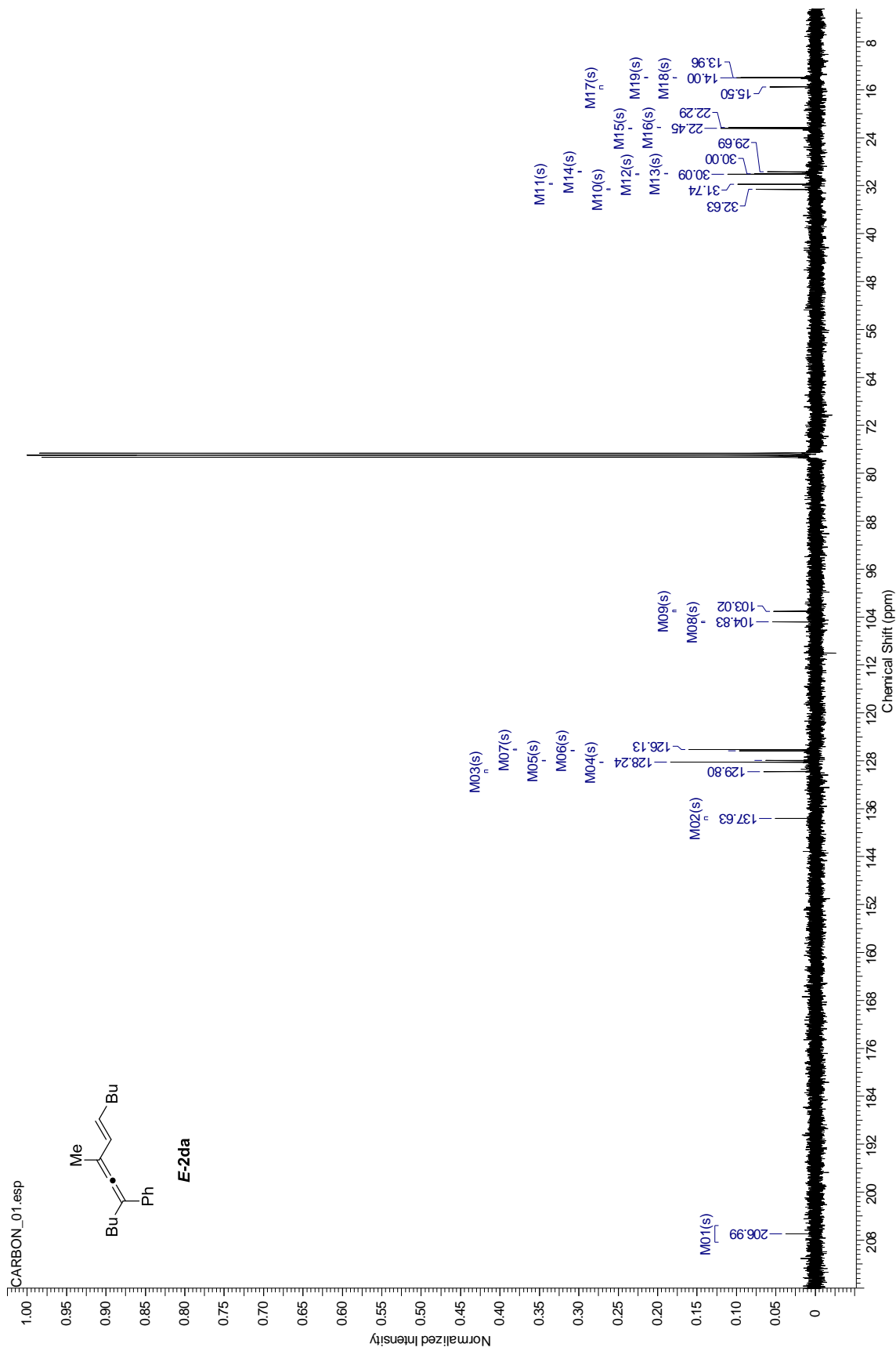


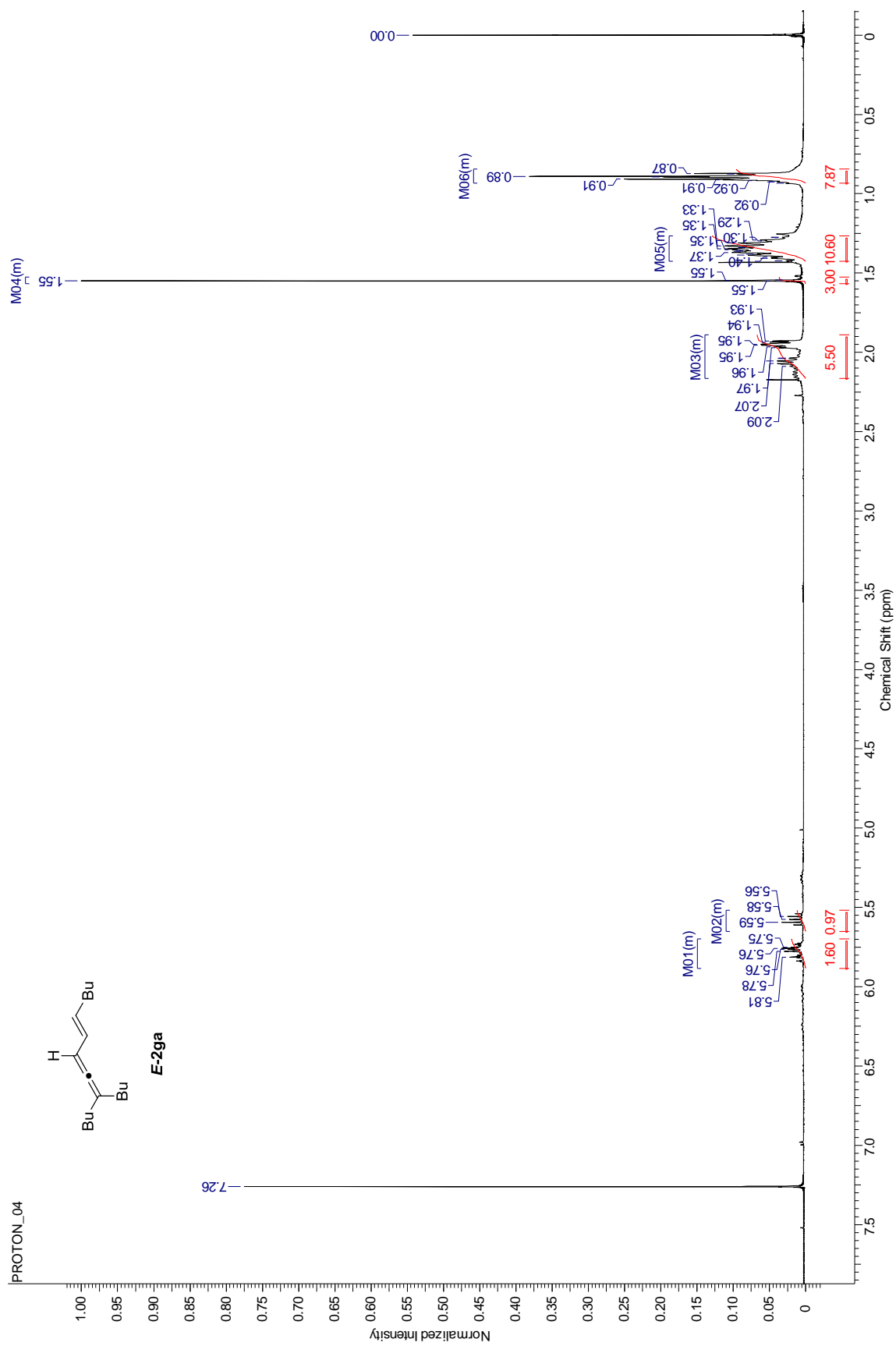


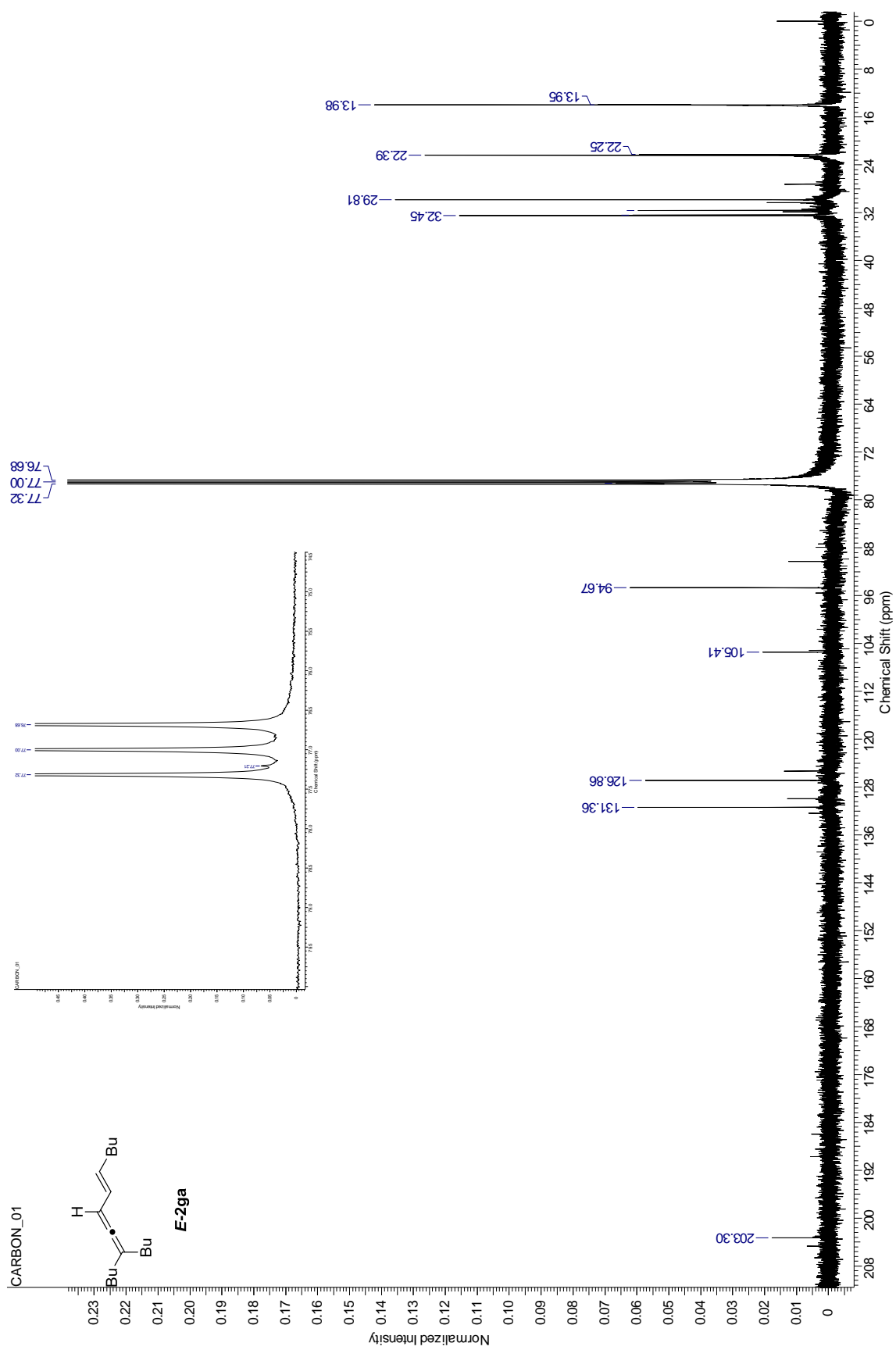


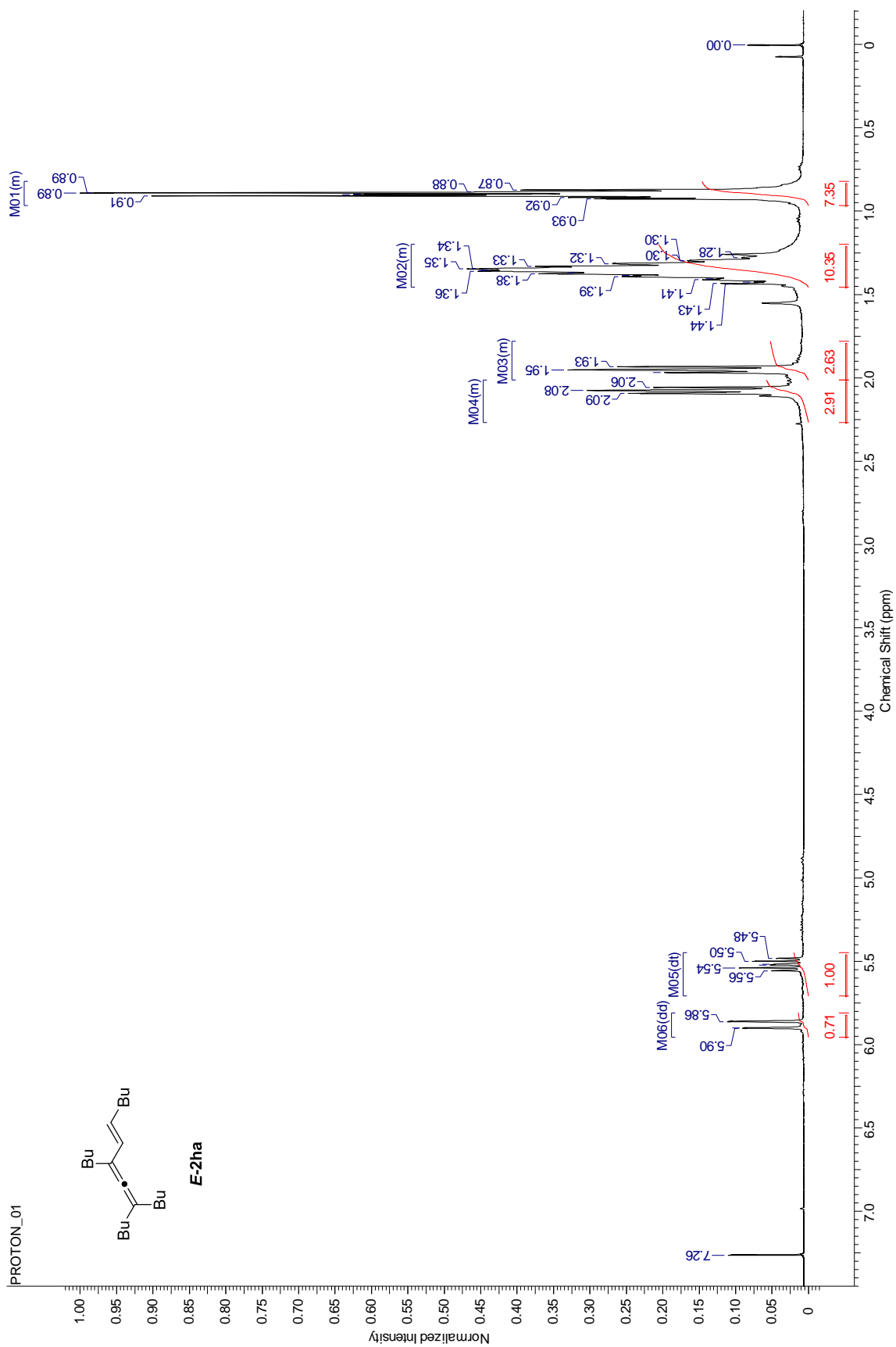


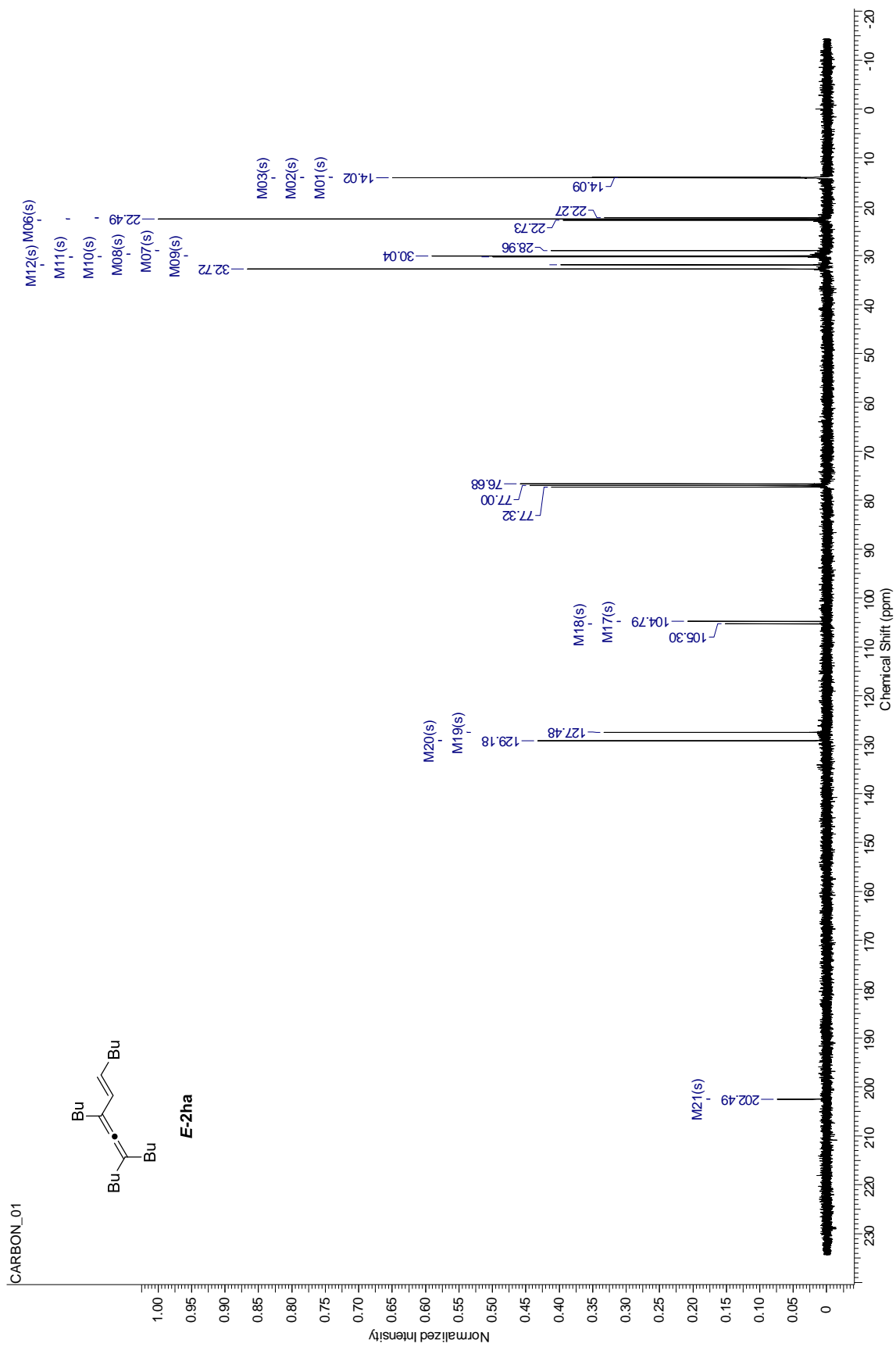


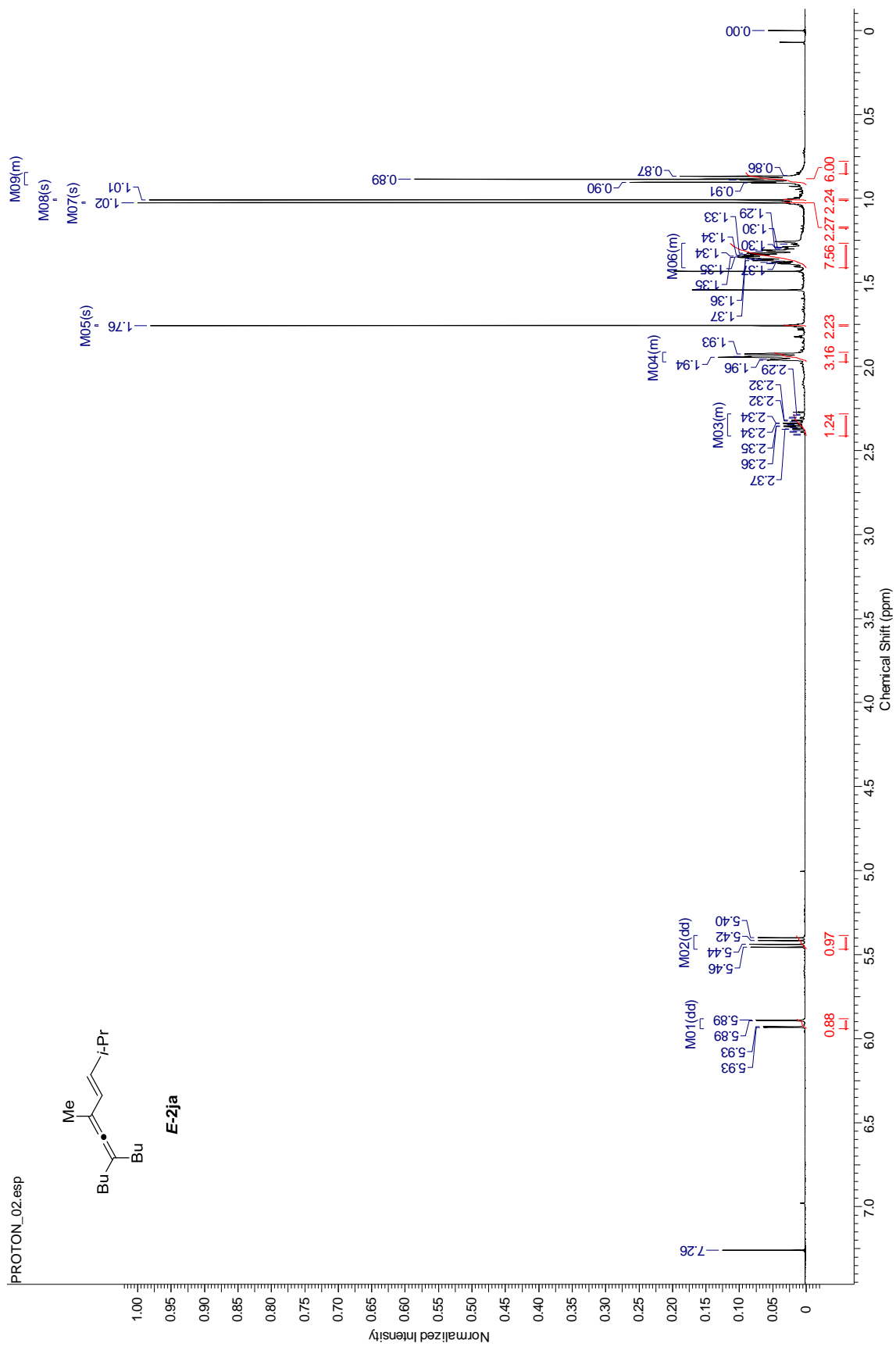


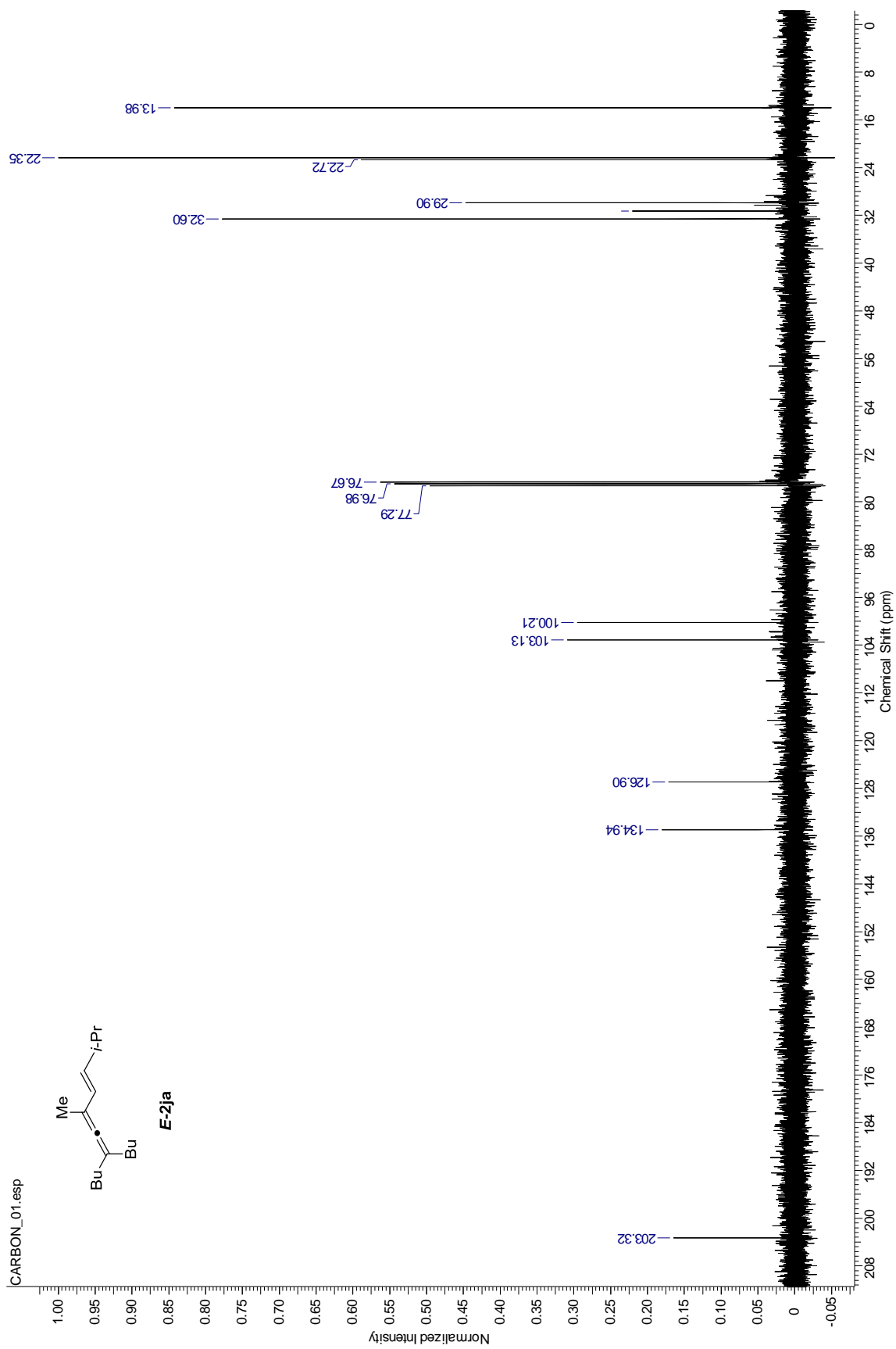


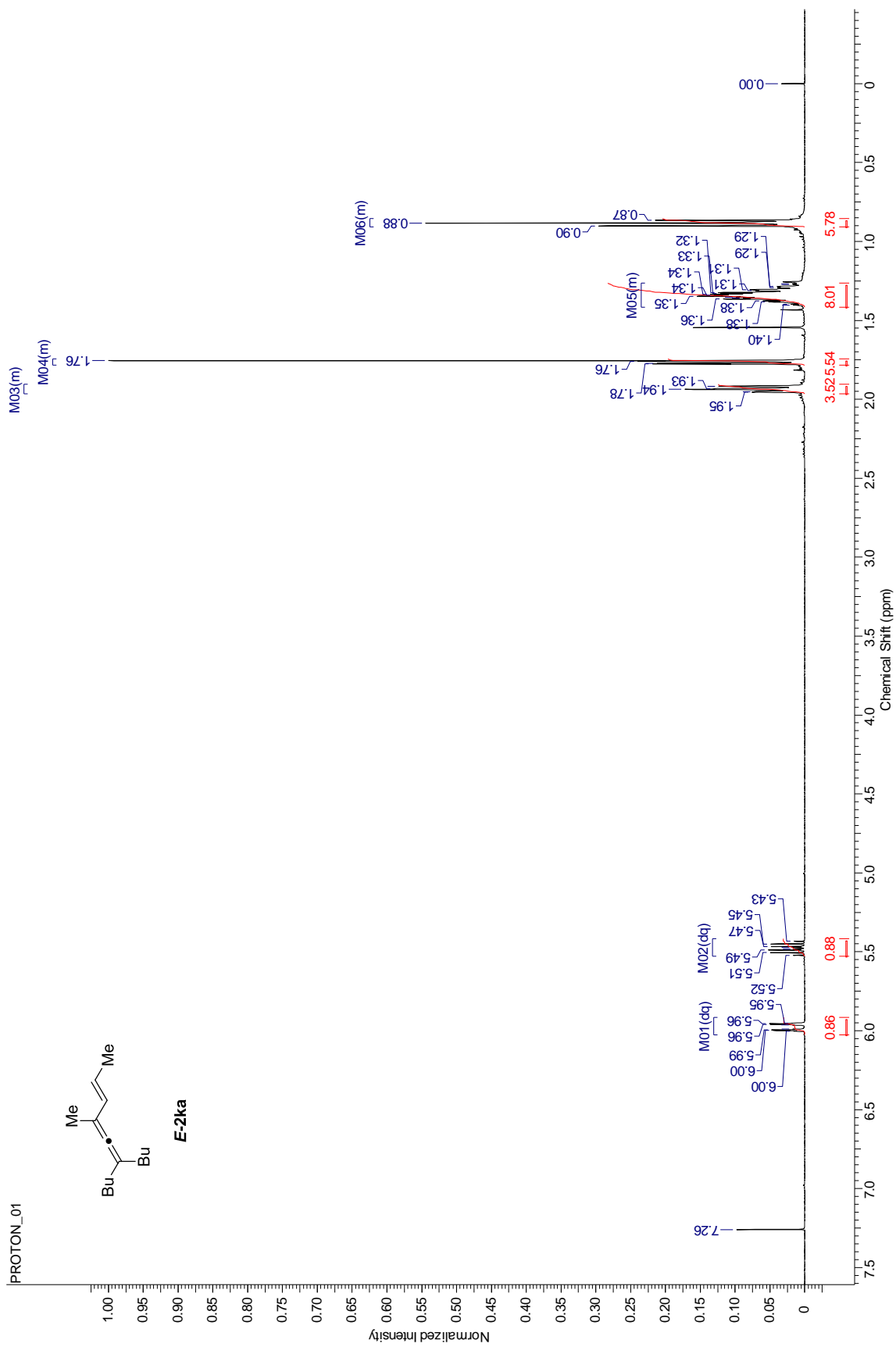


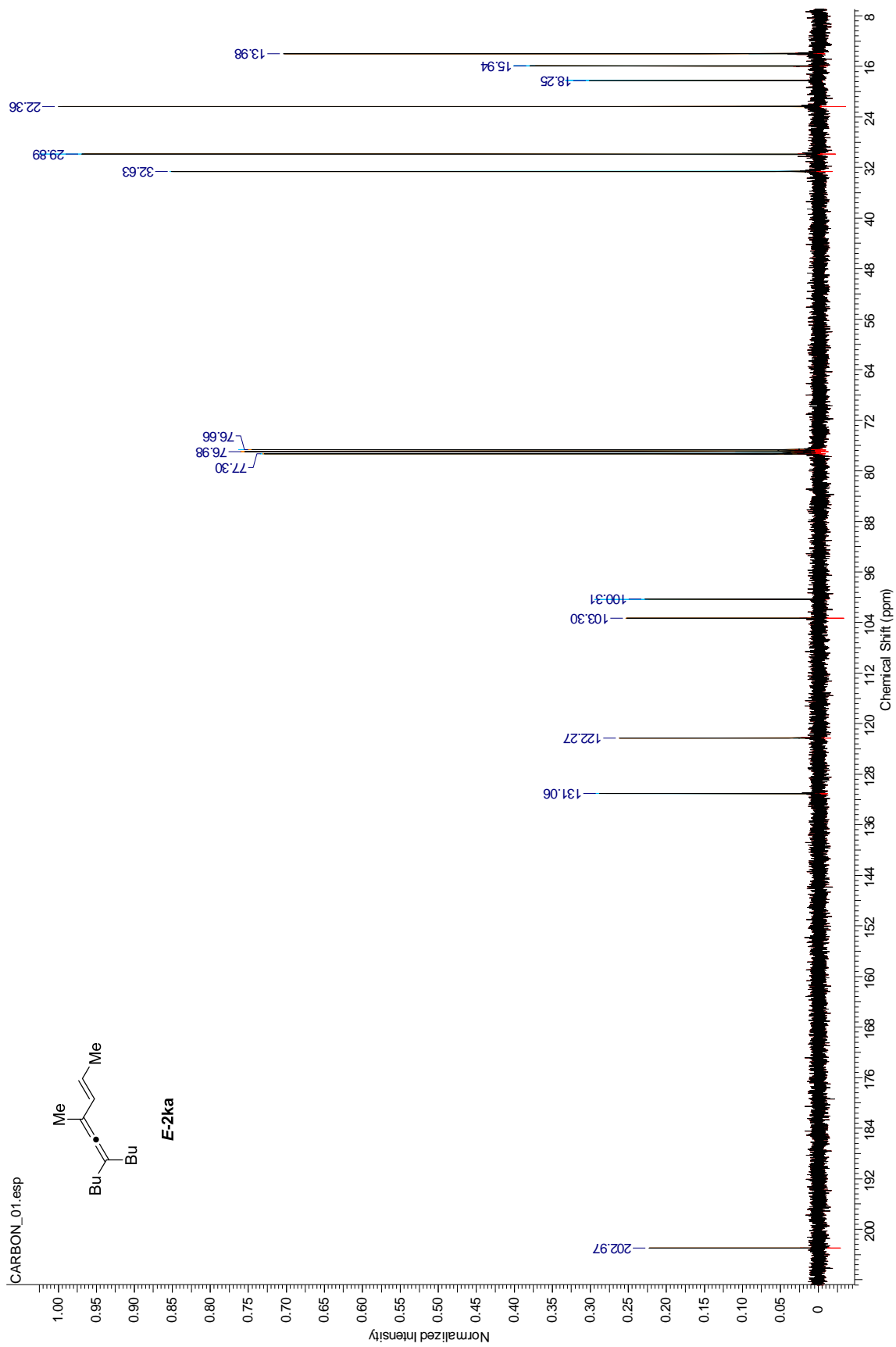


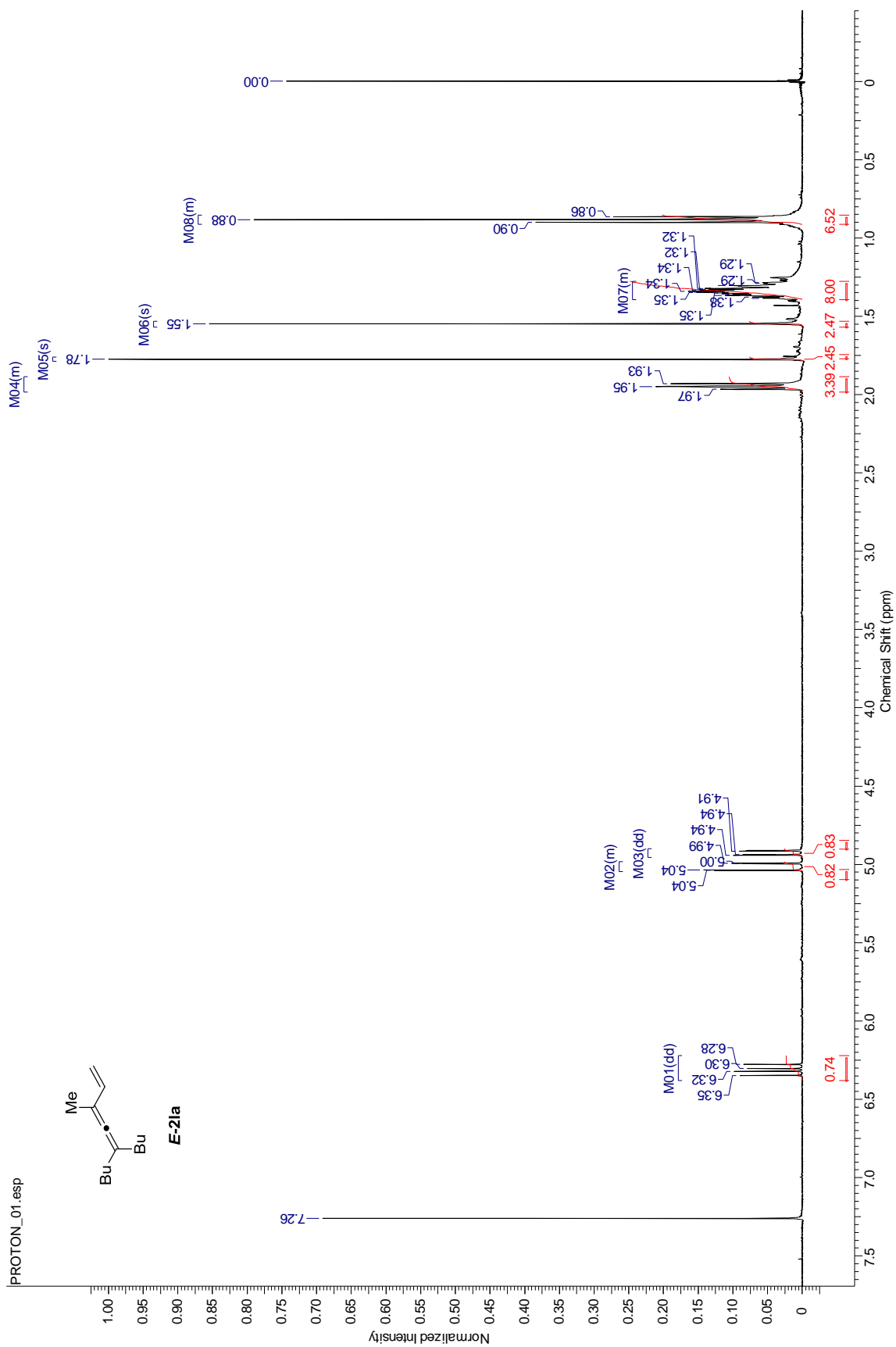


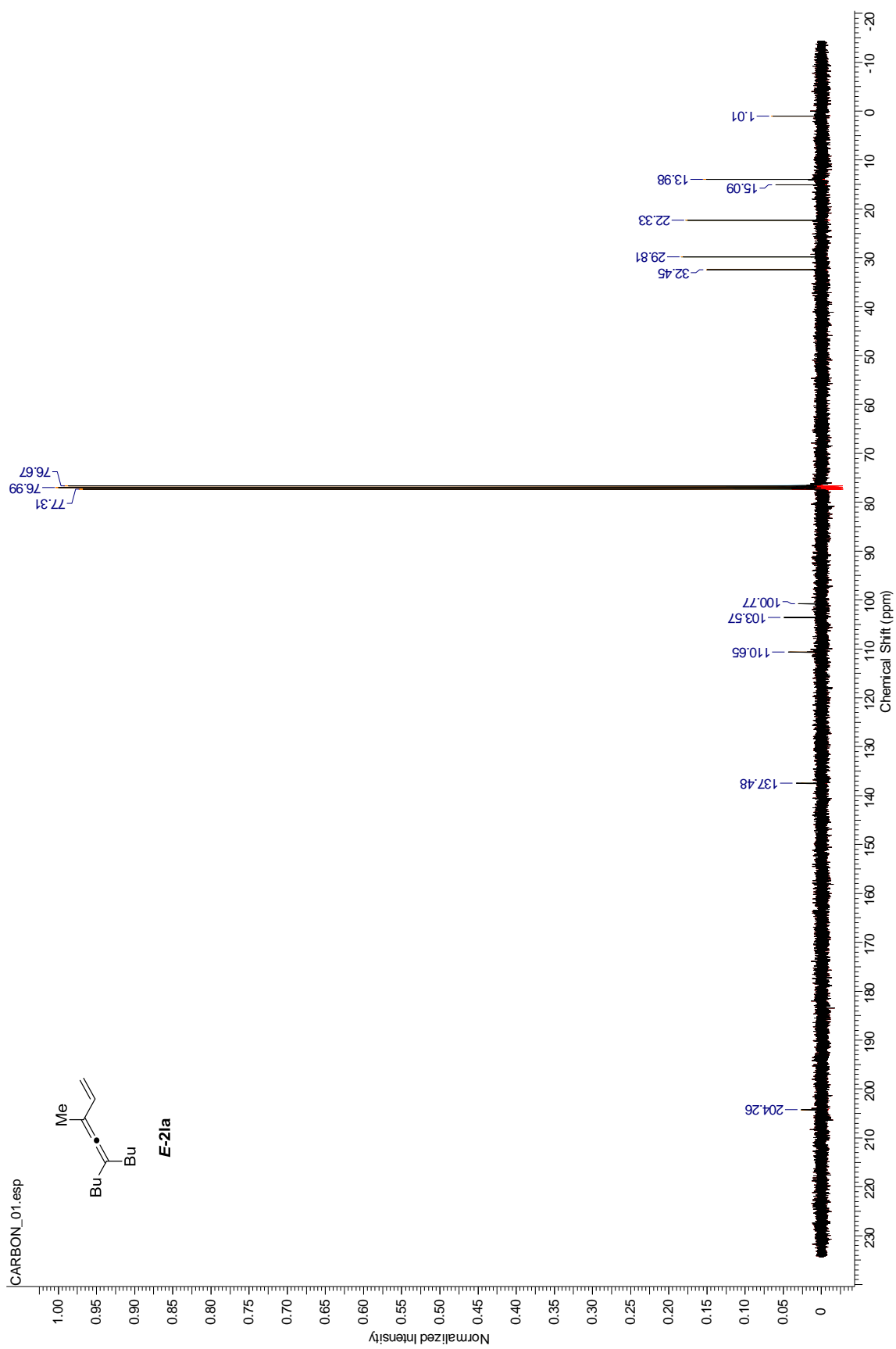


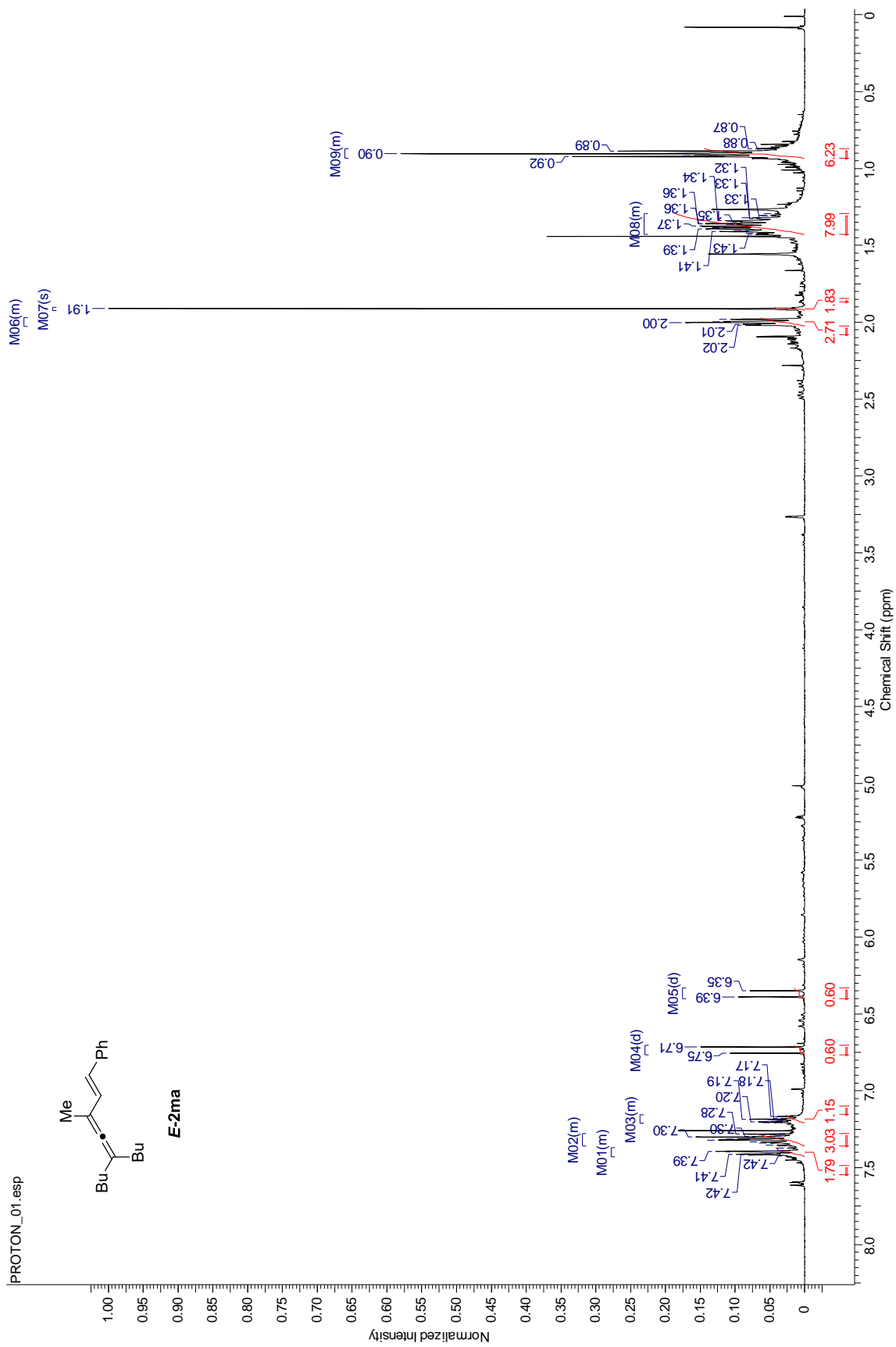


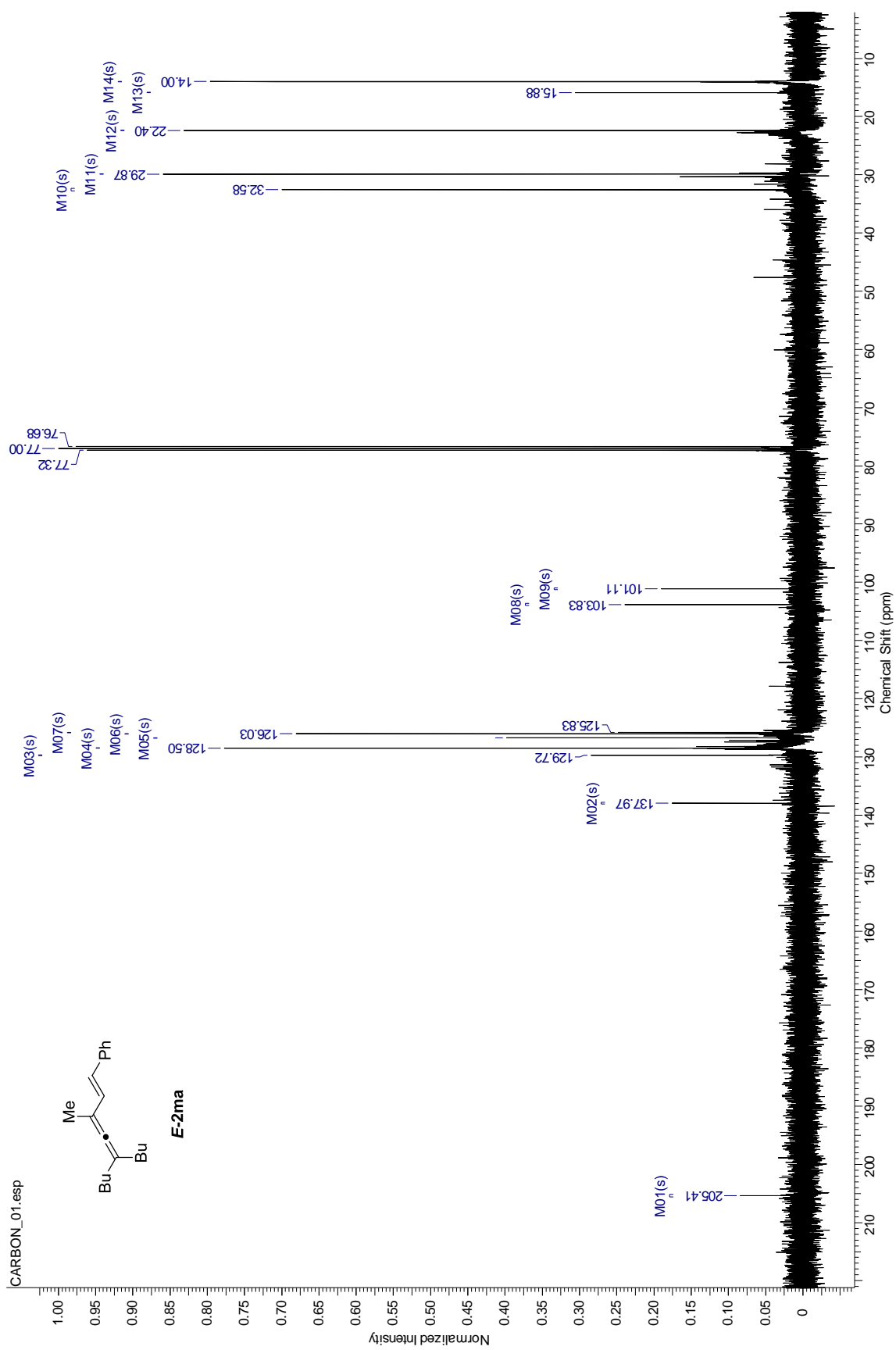


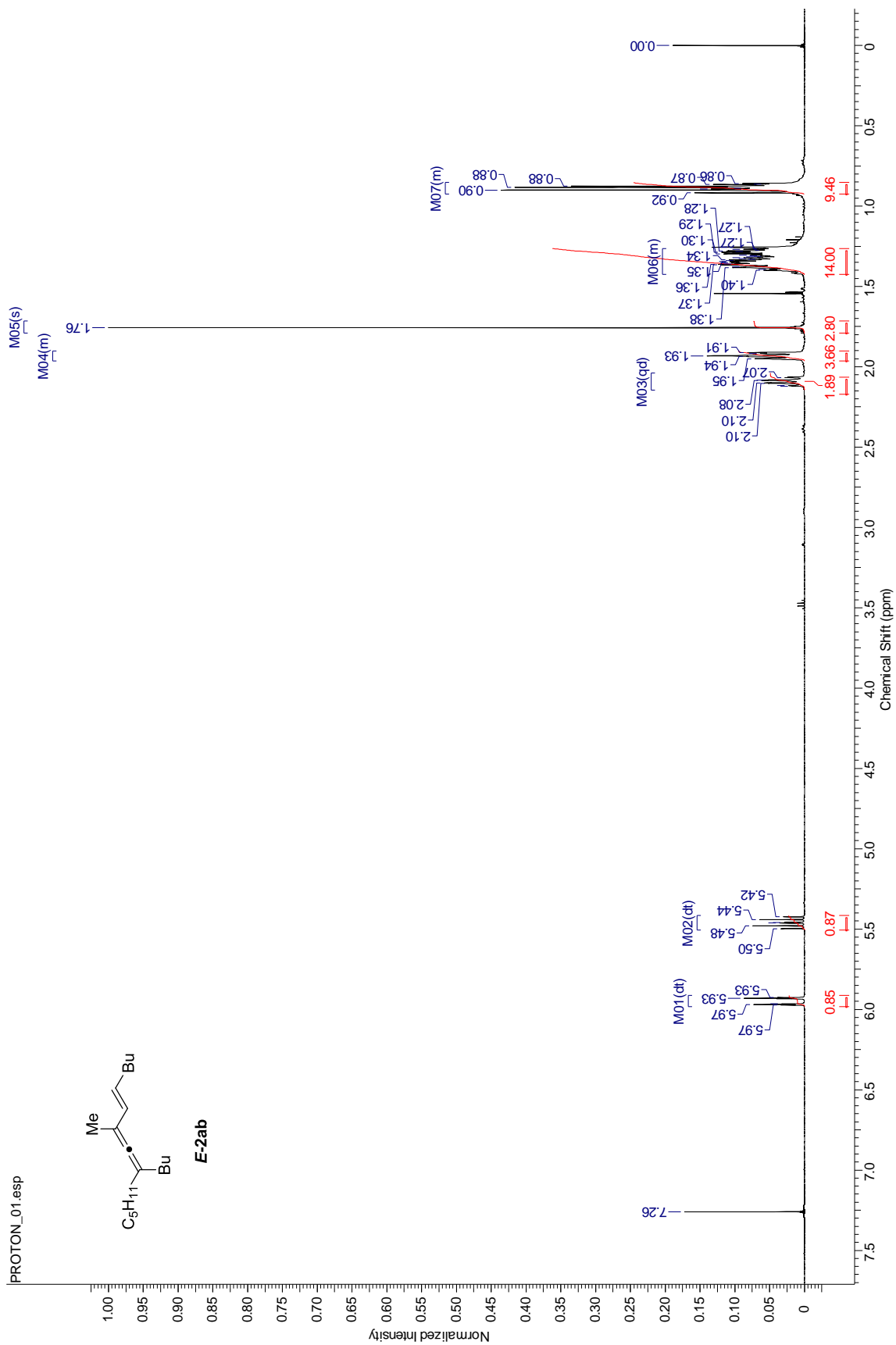


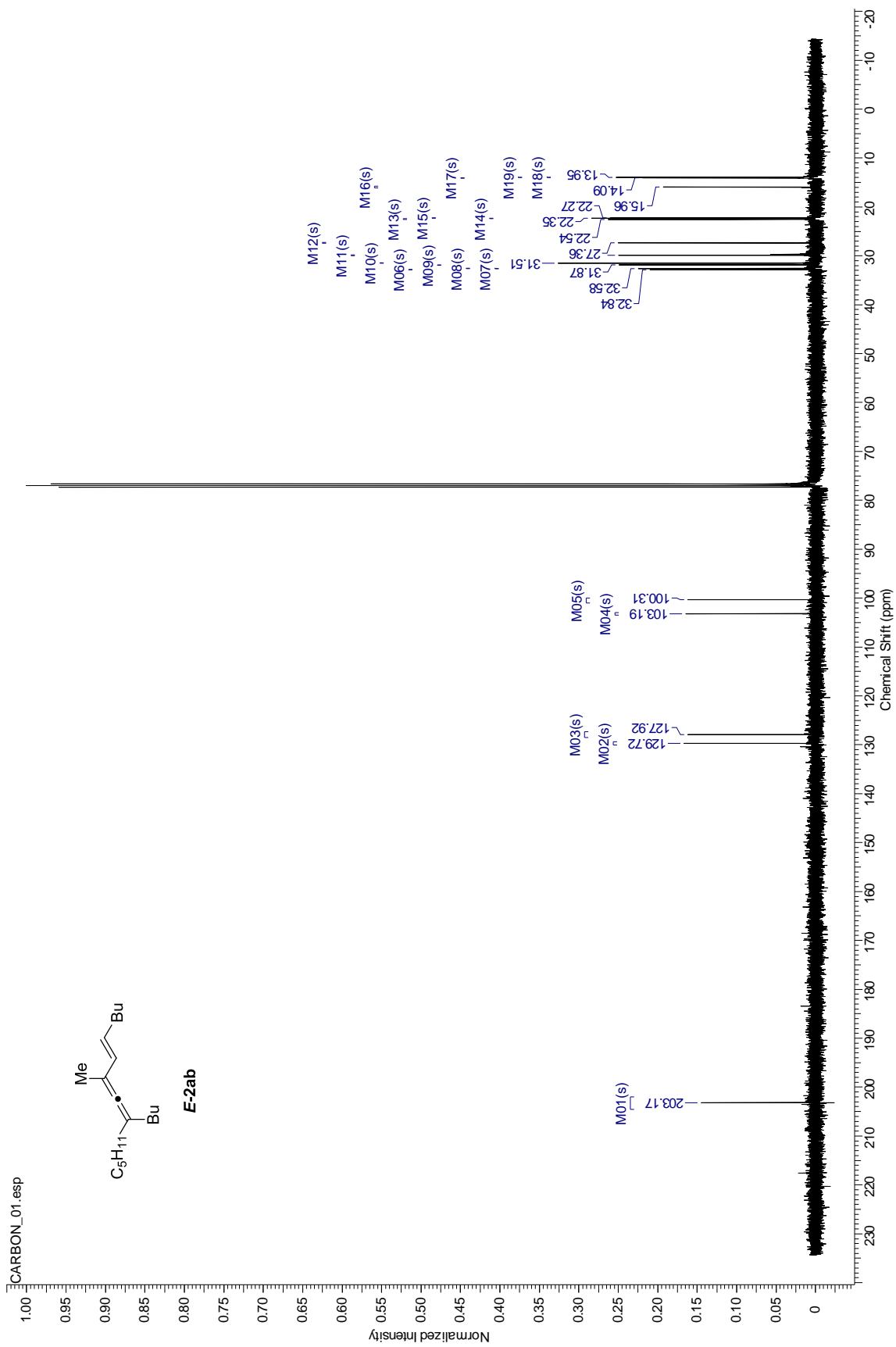


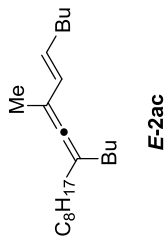
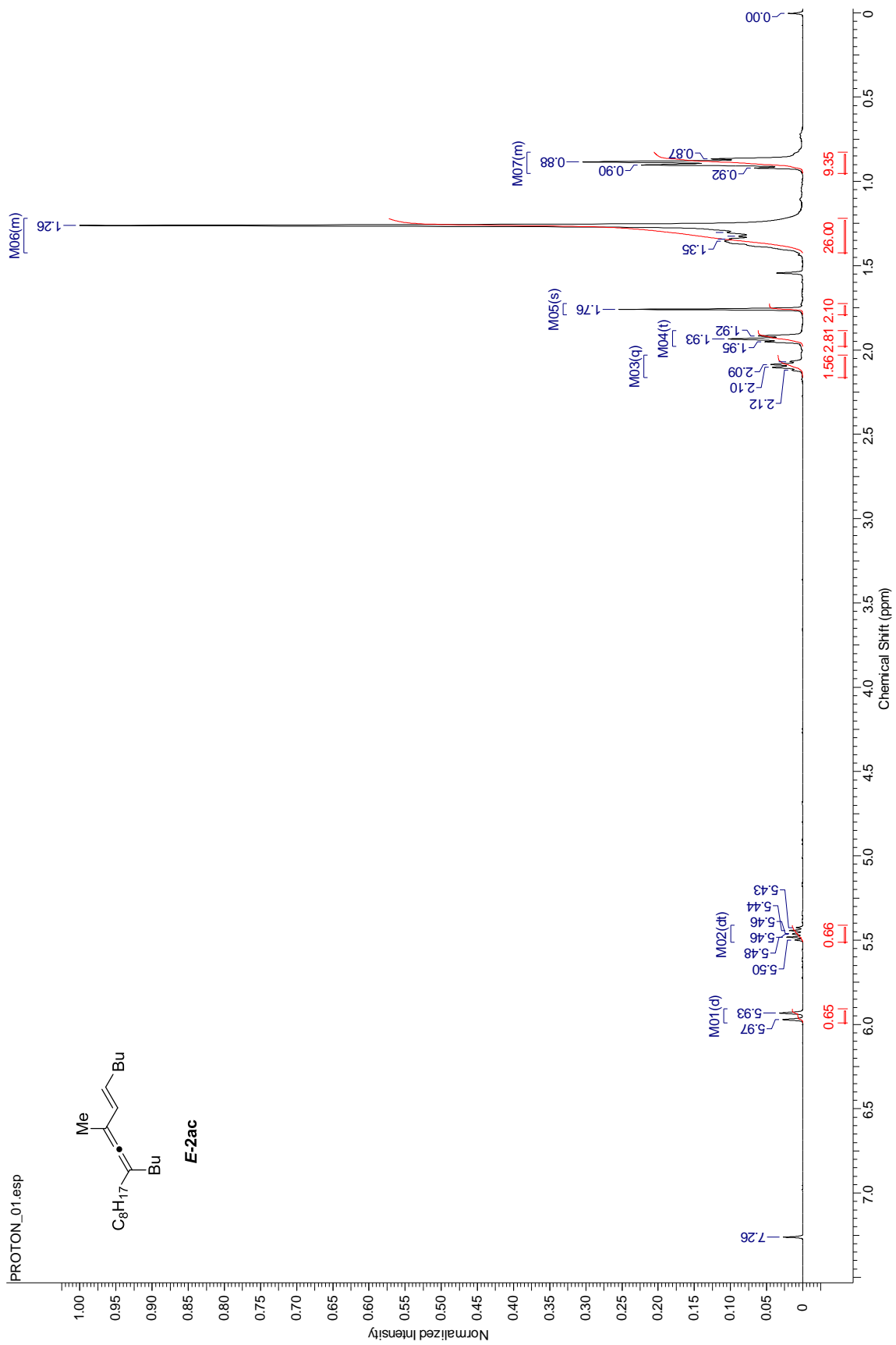


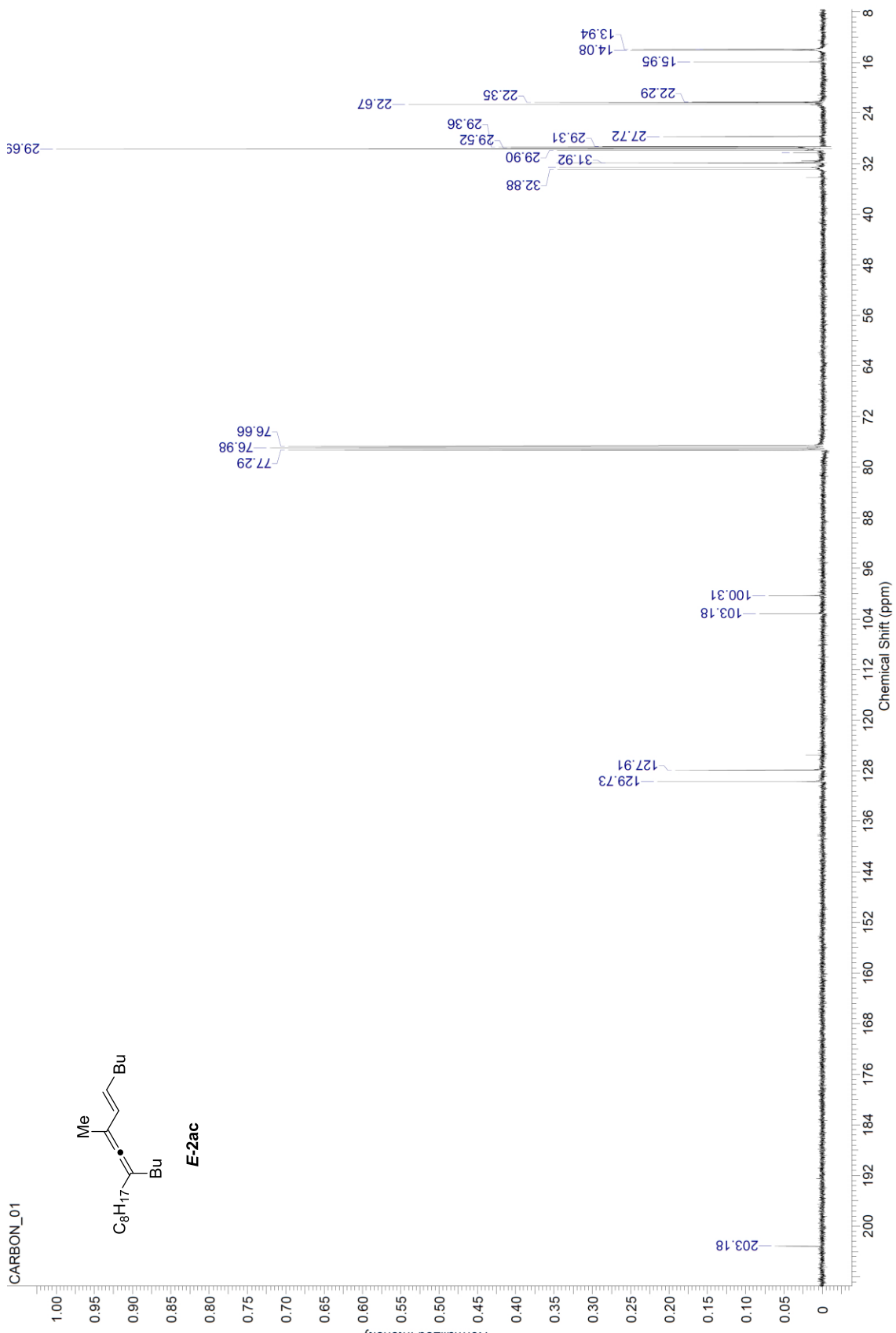


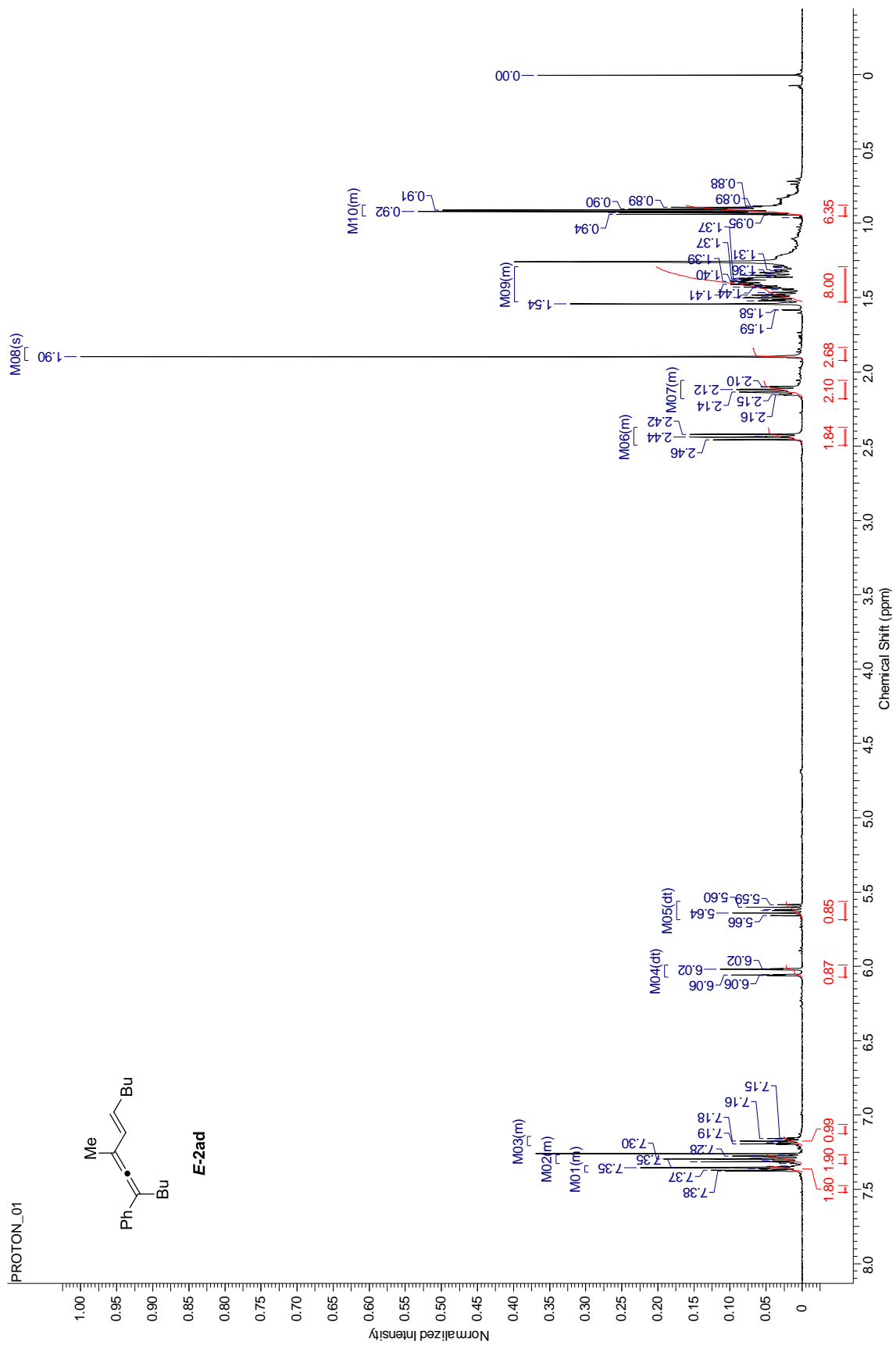


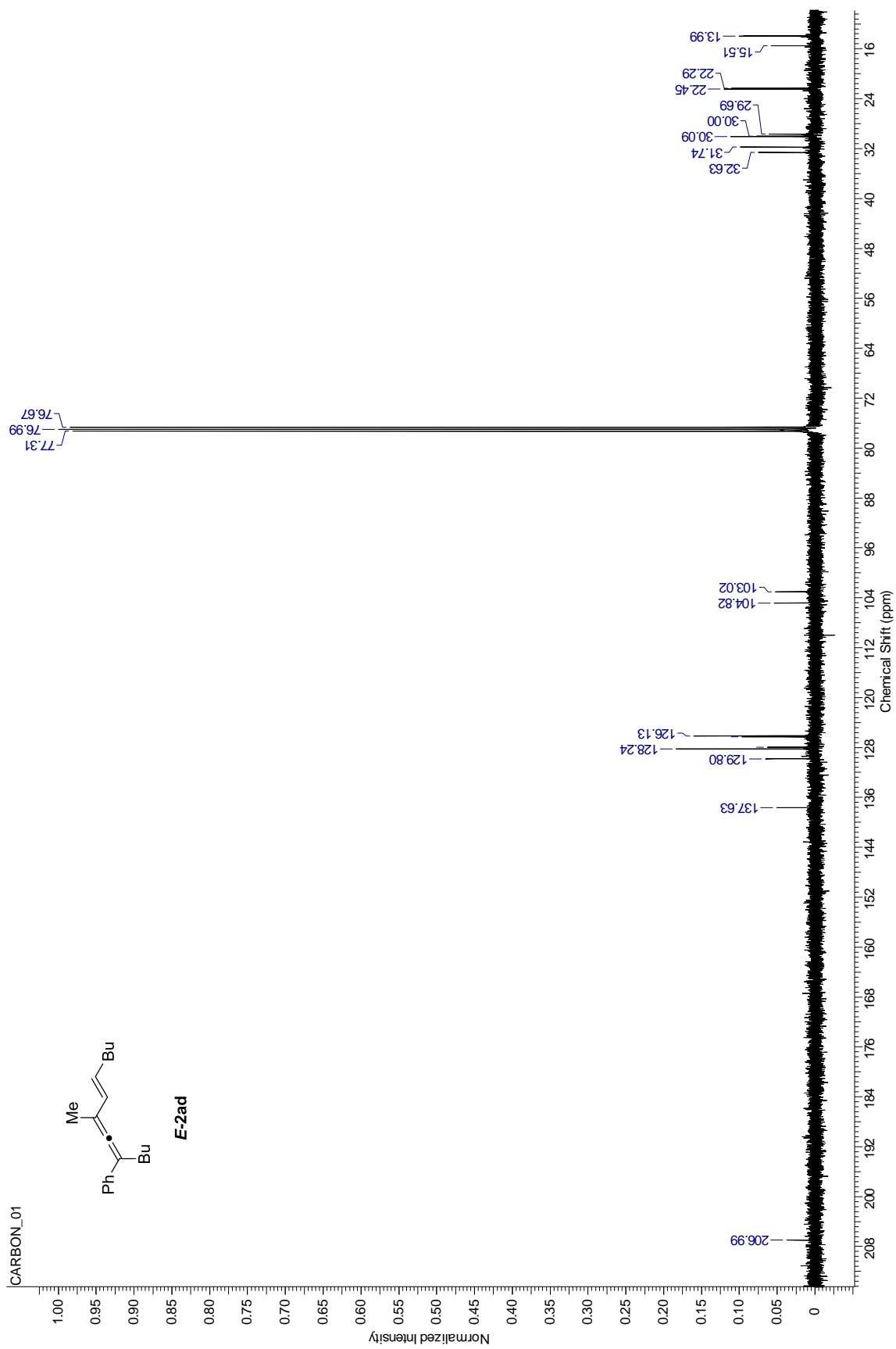


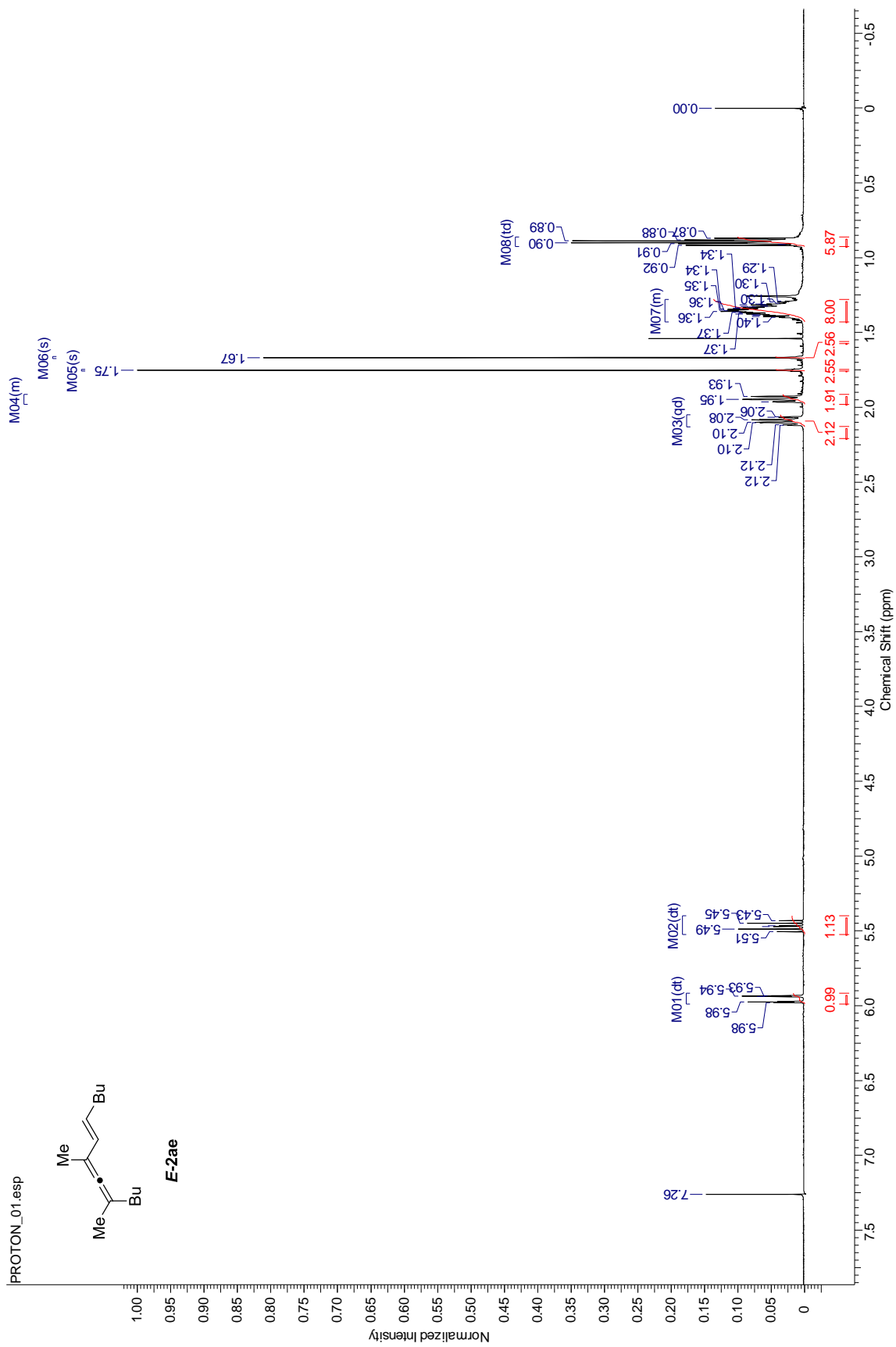


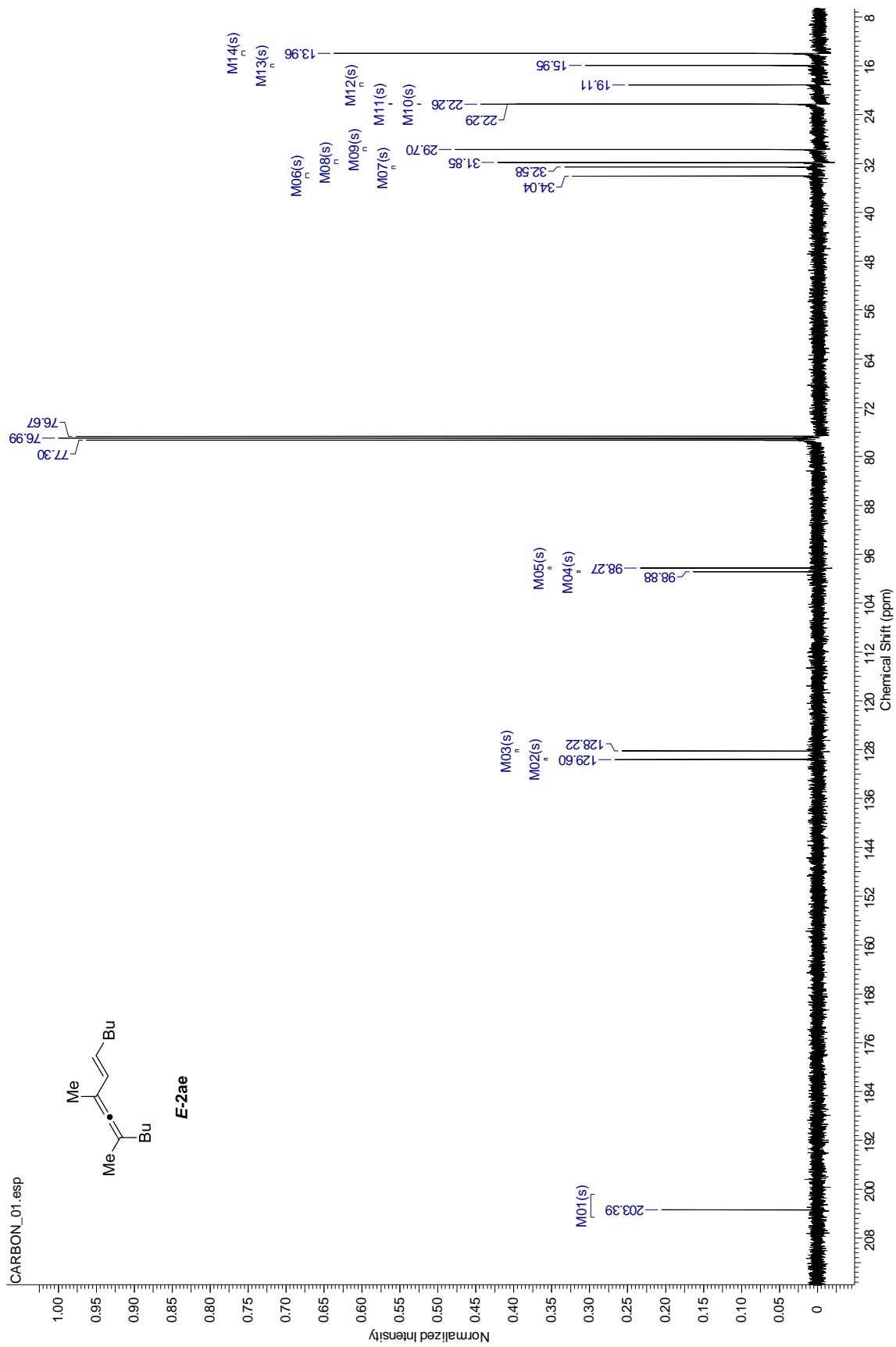


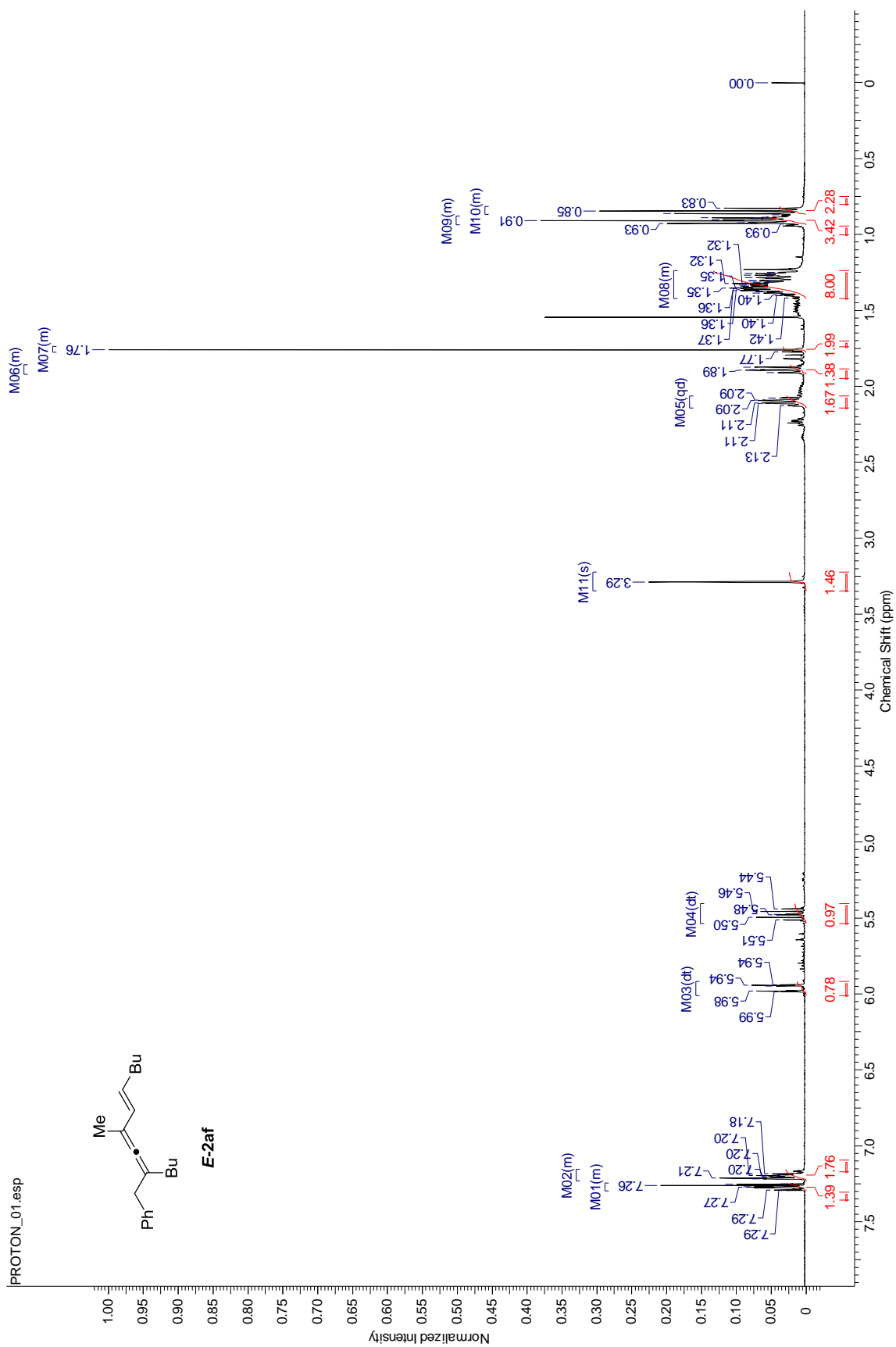


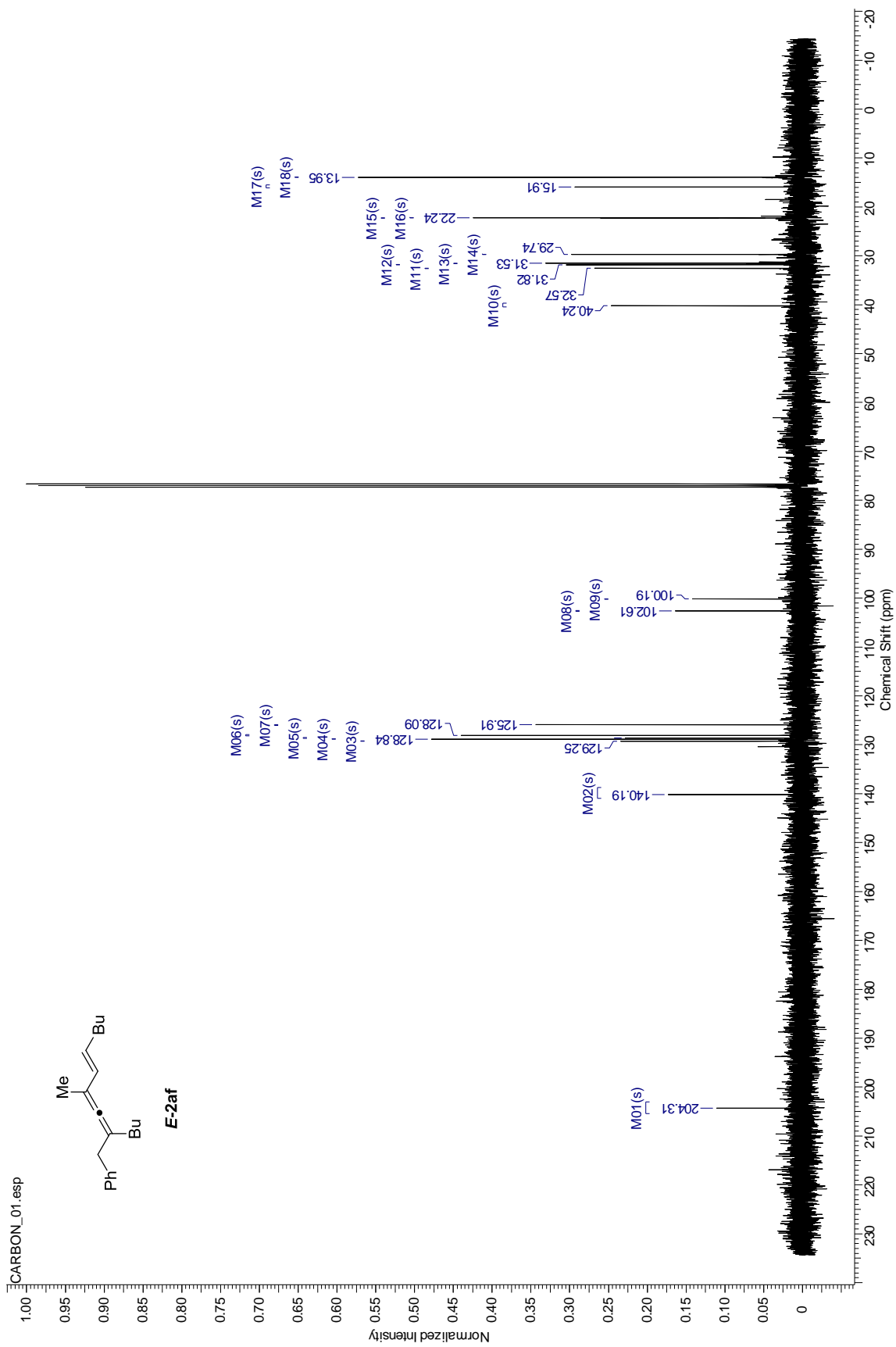






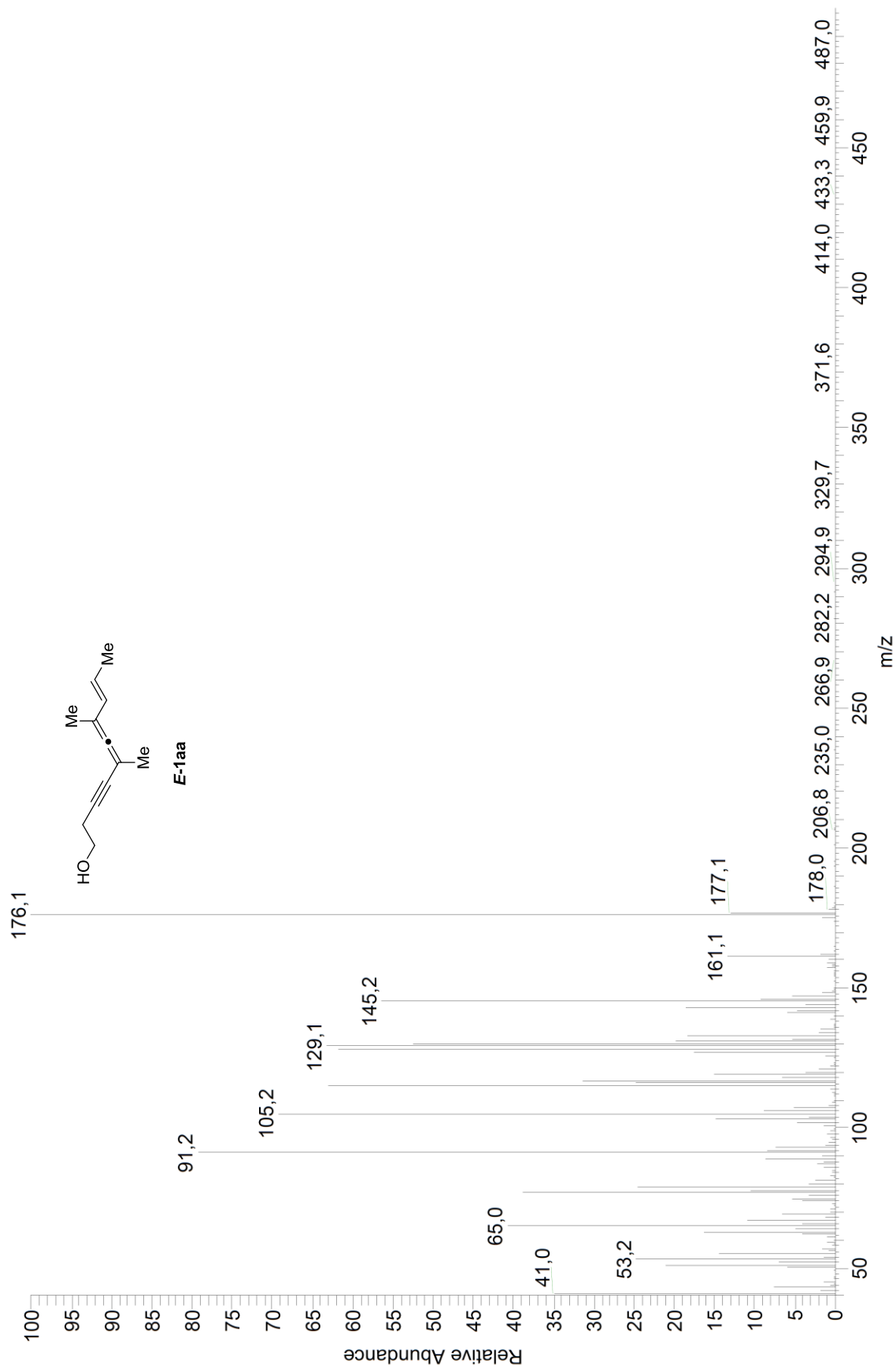


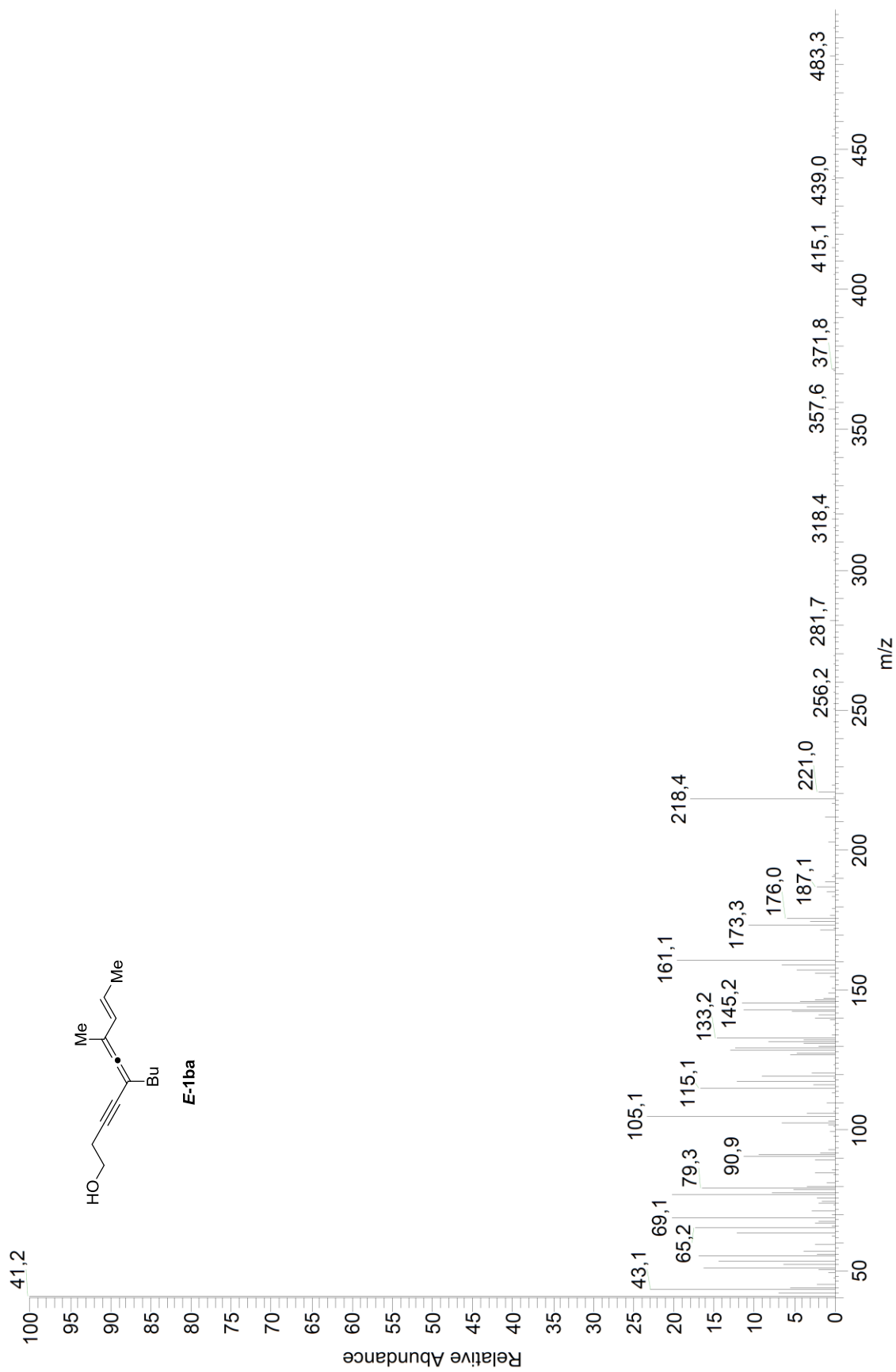


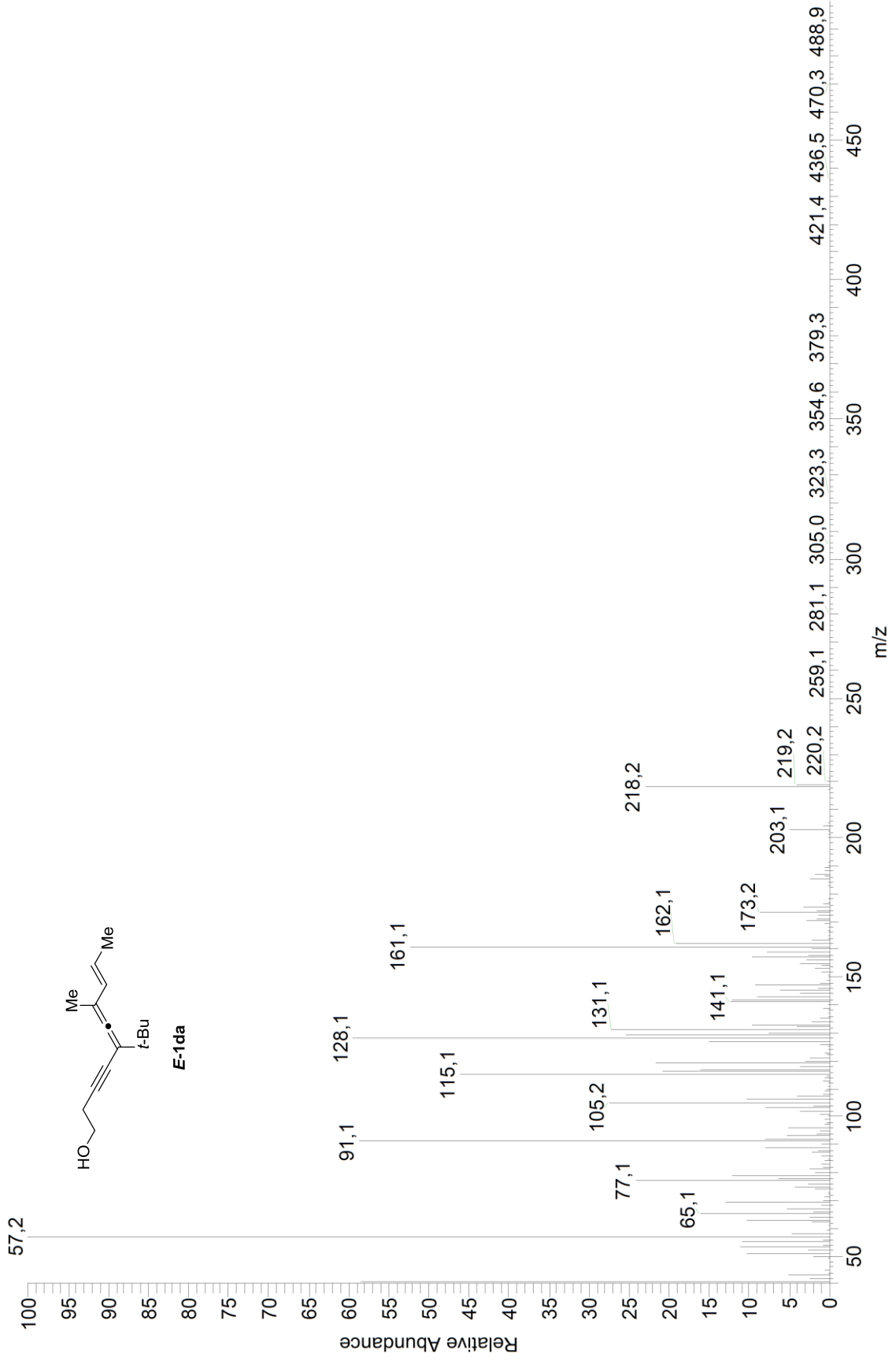


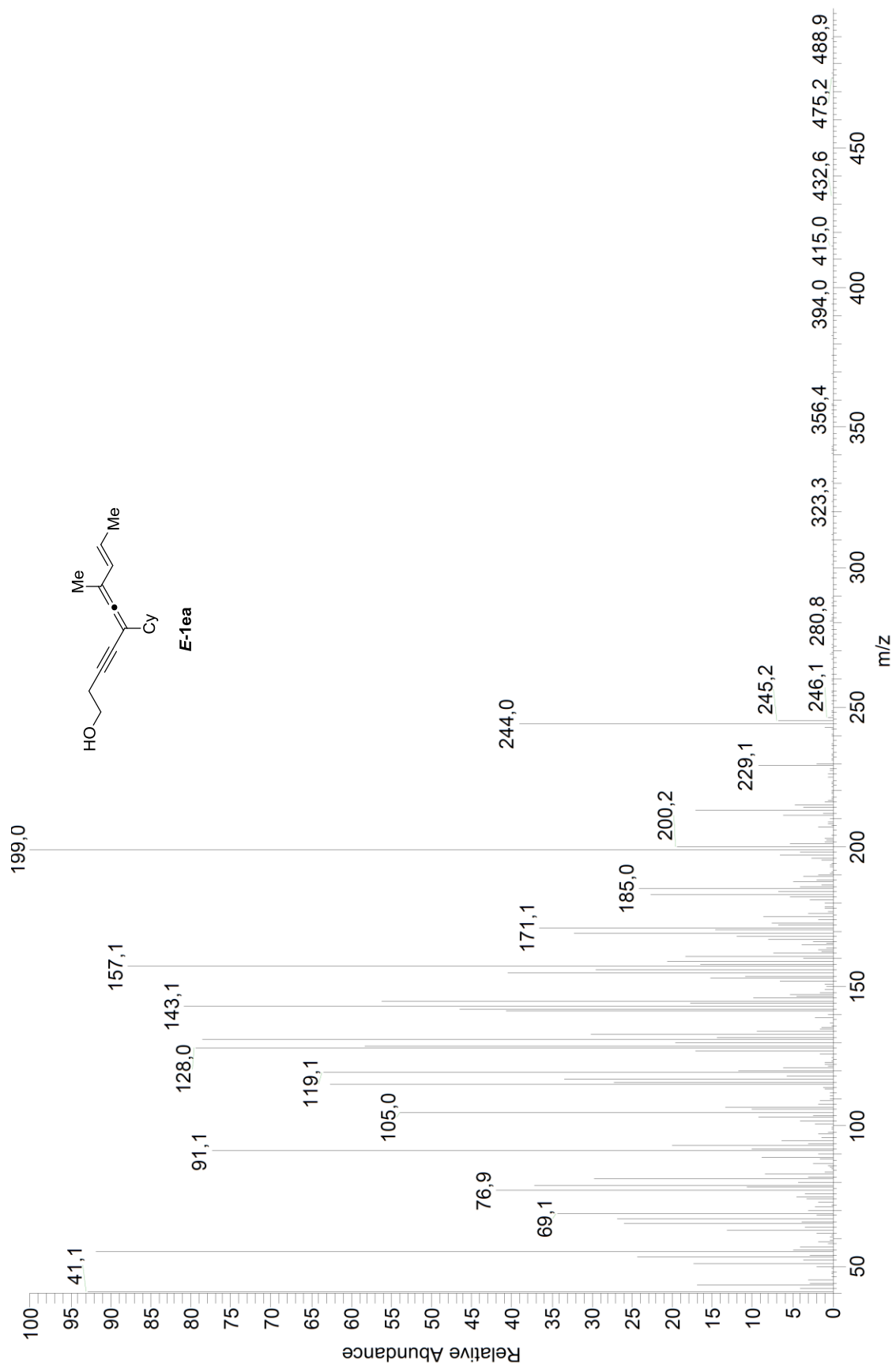
APPENDIX B

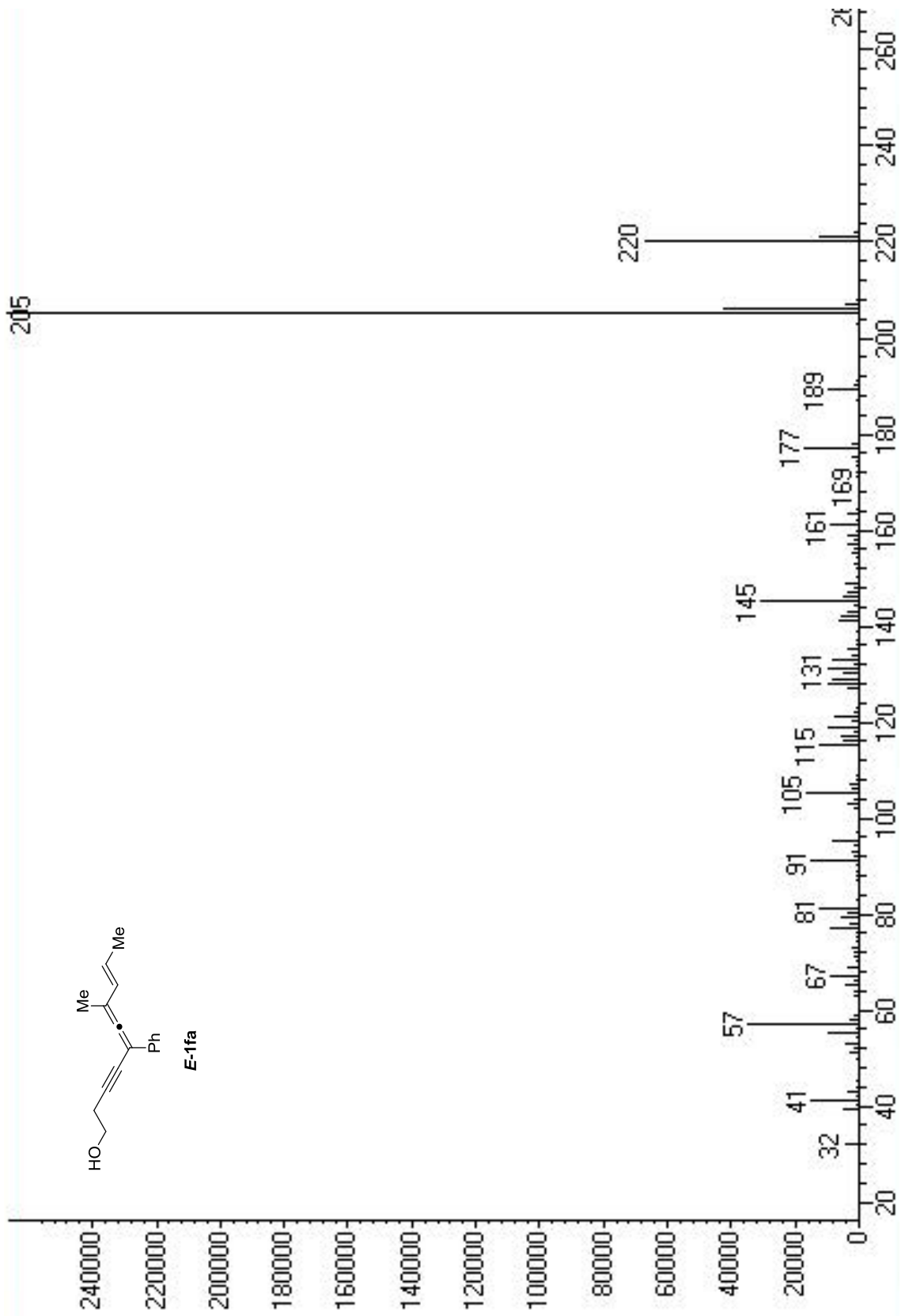
MASS SPECTRA OF PRODUCTS

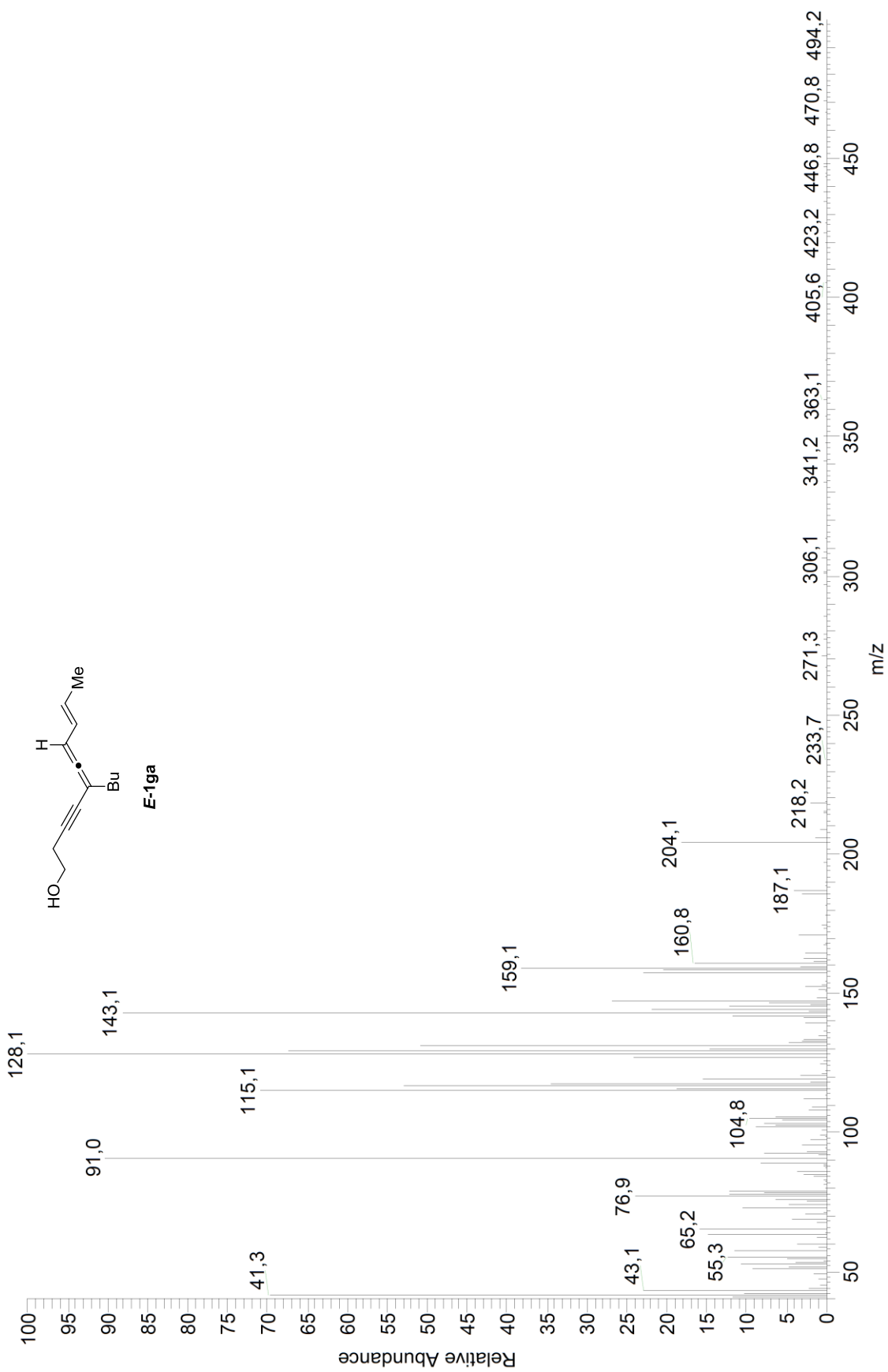


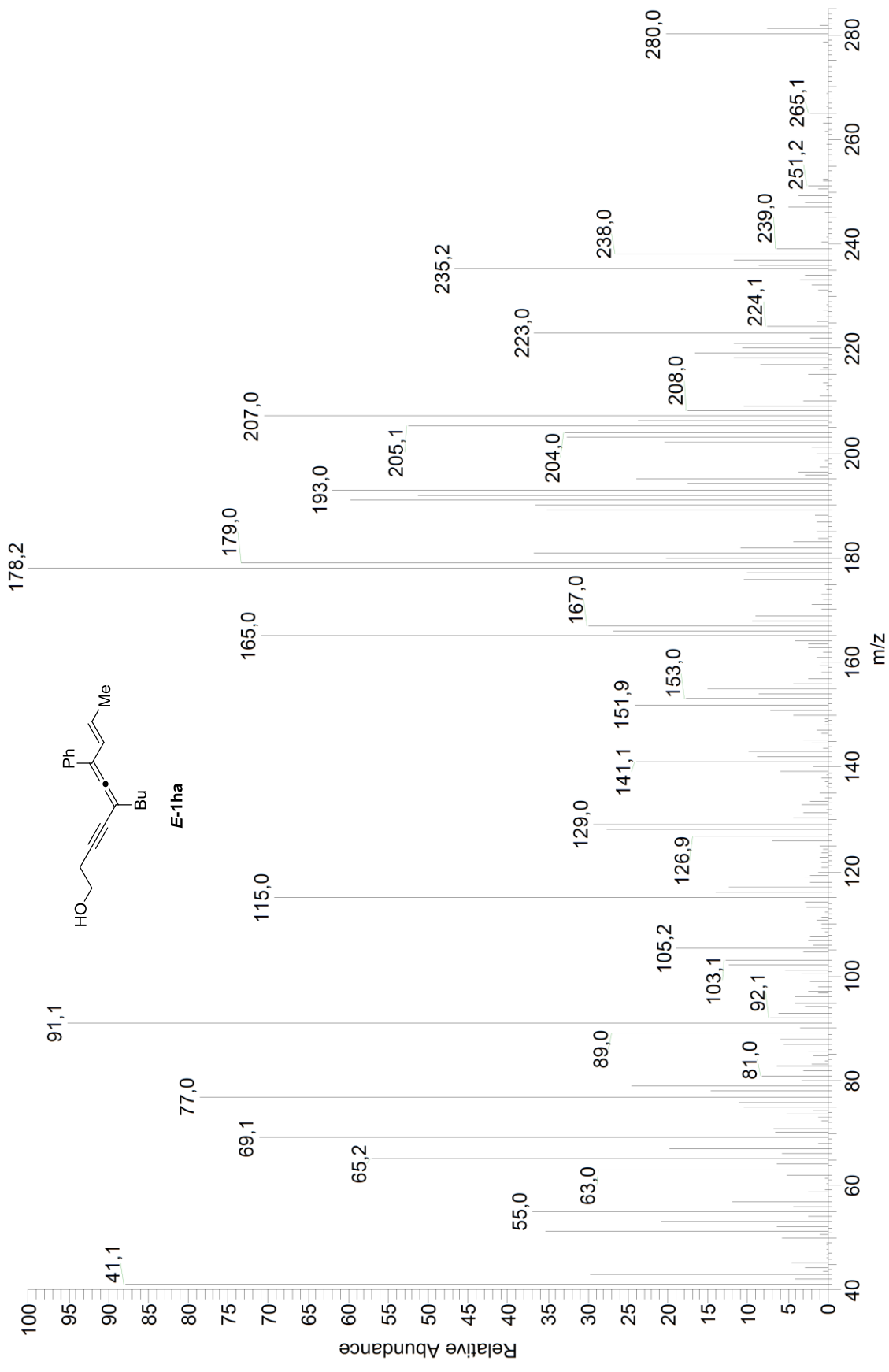


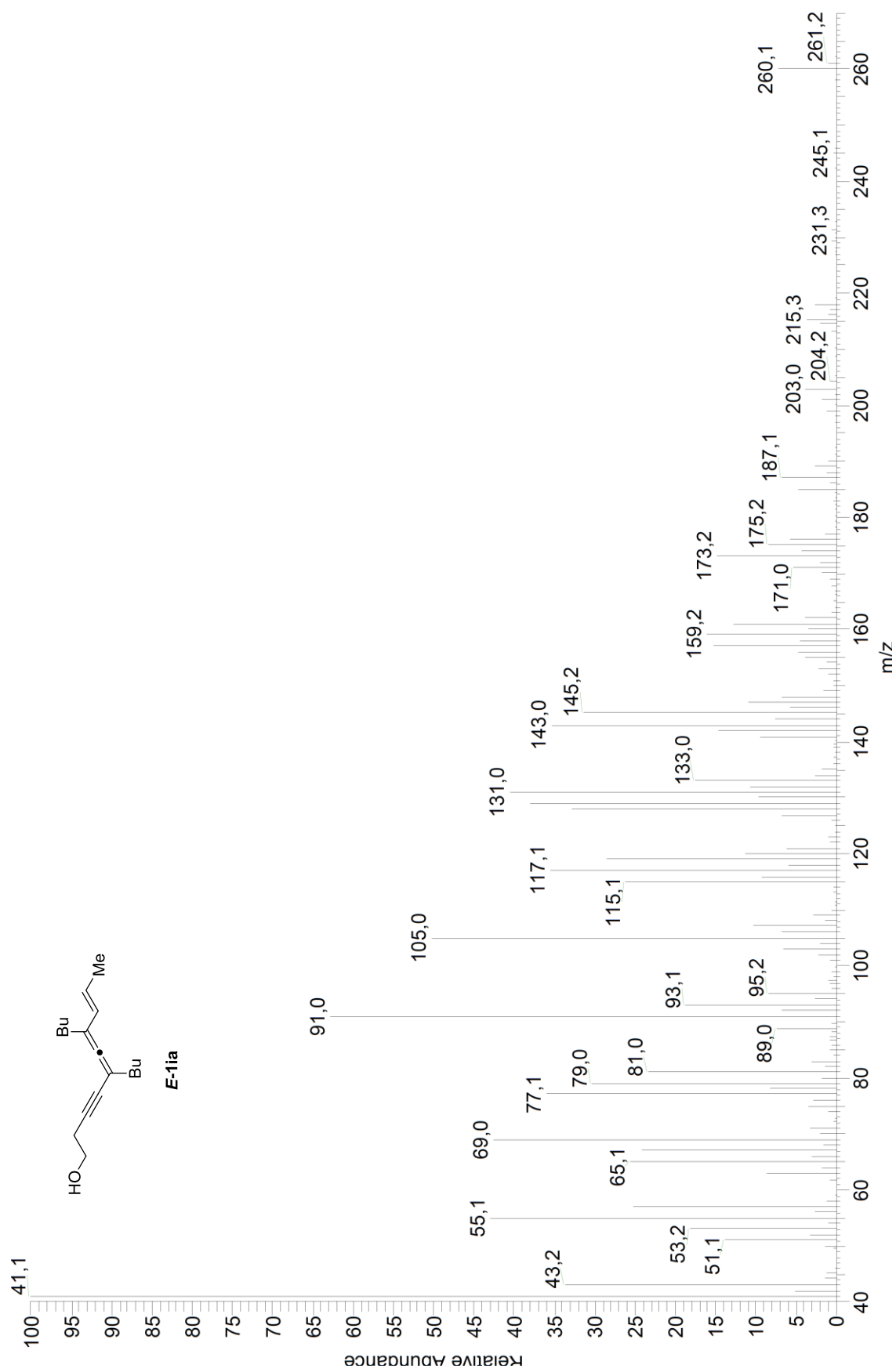


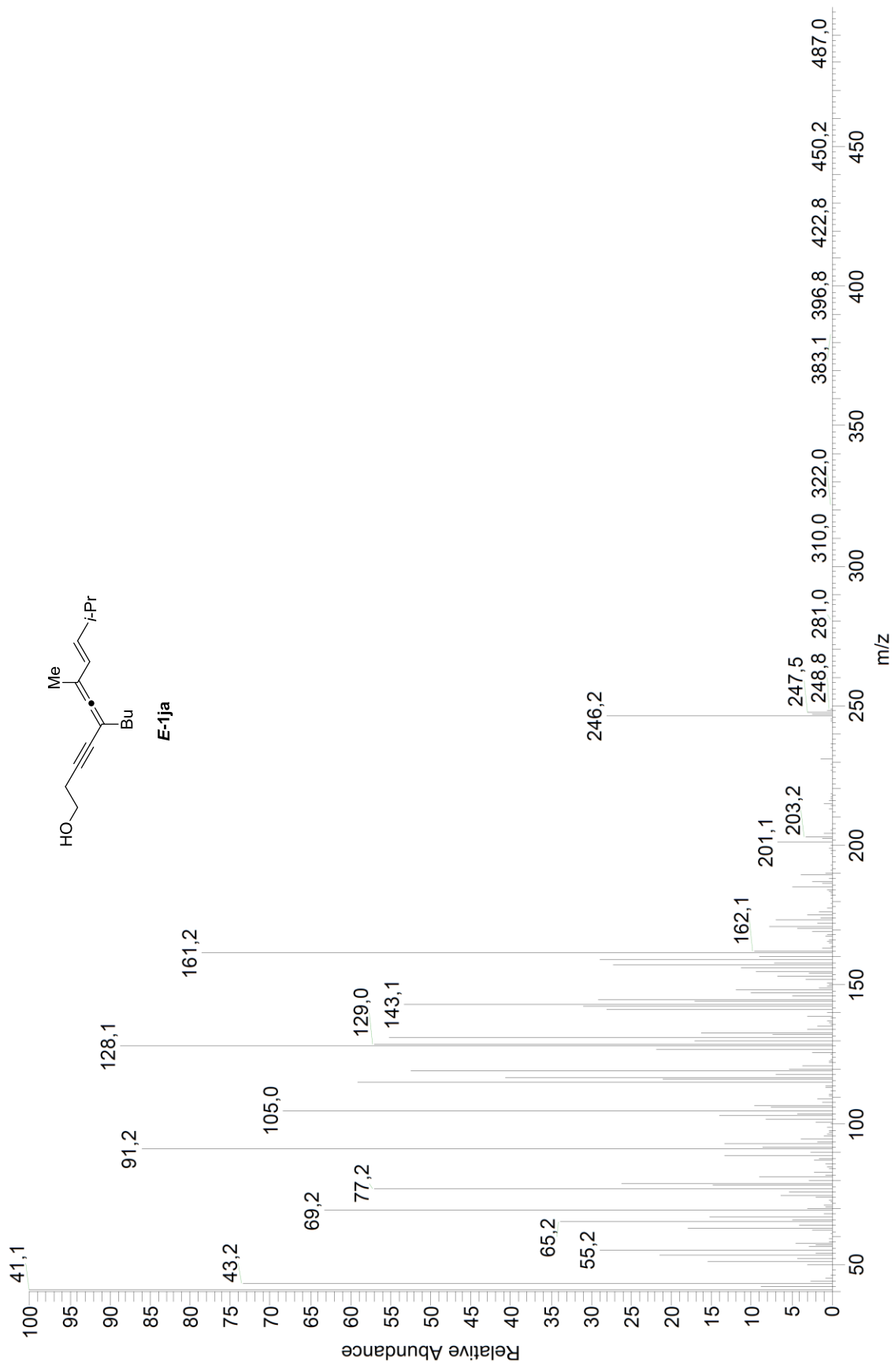


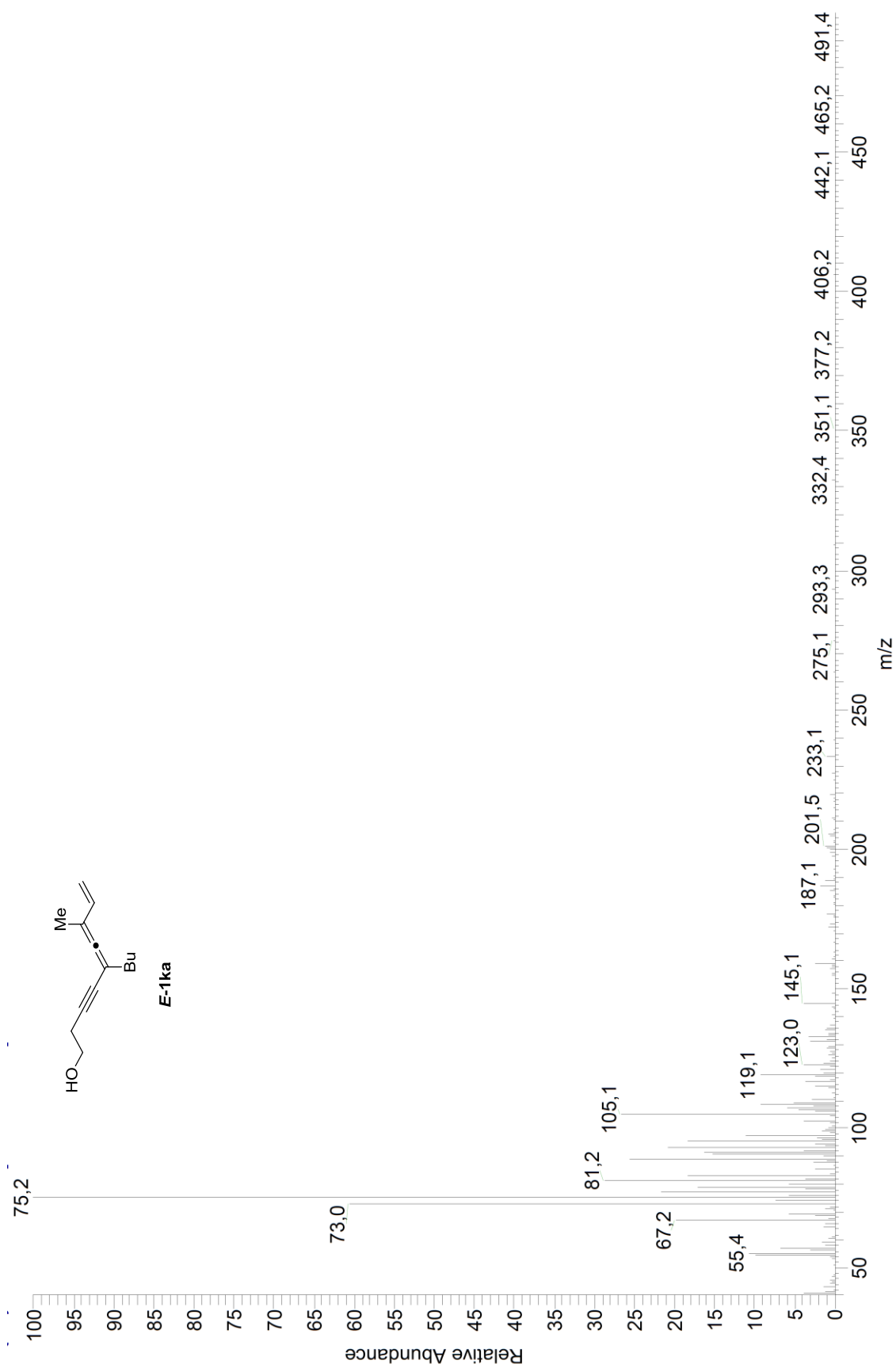


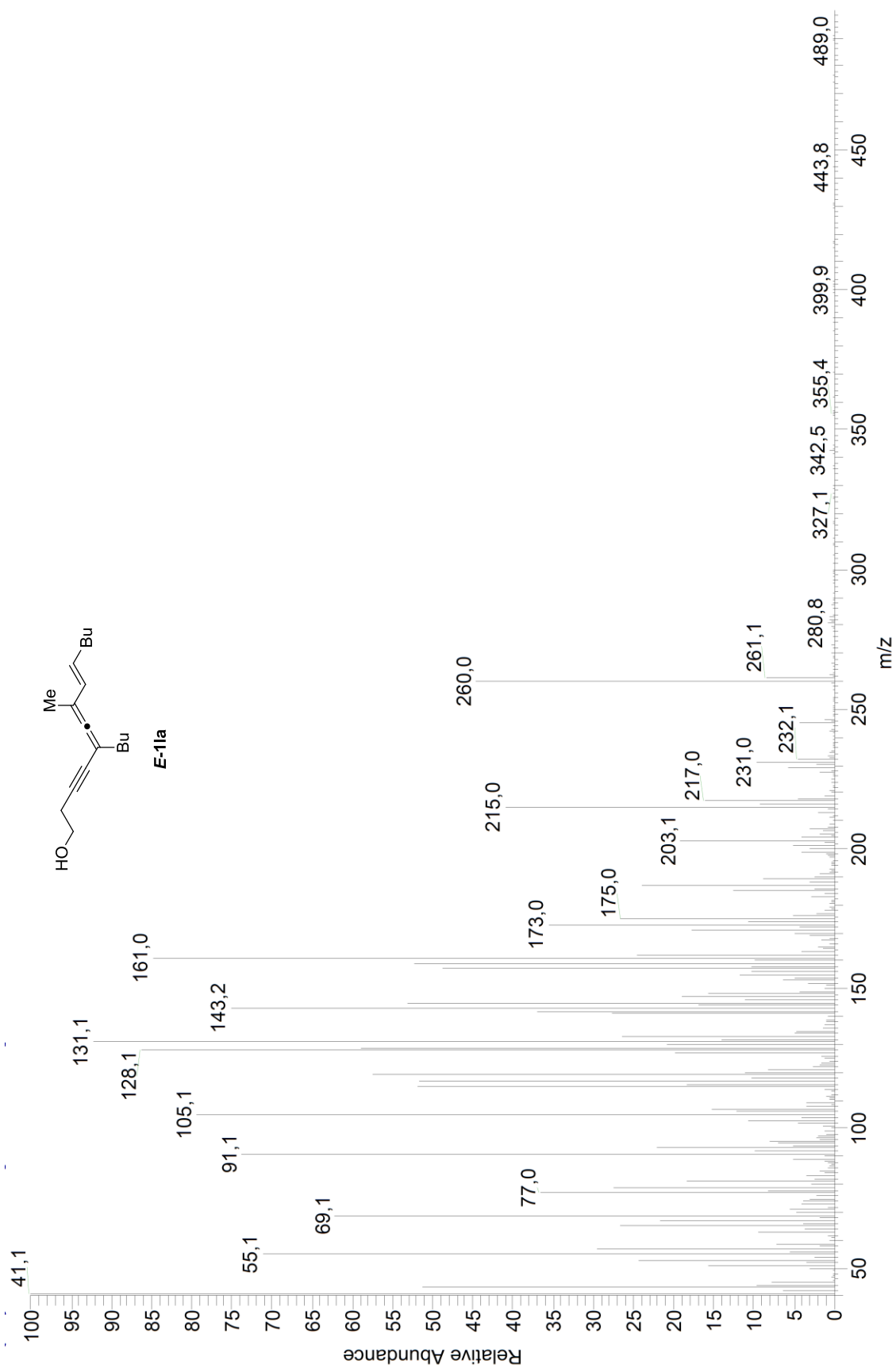


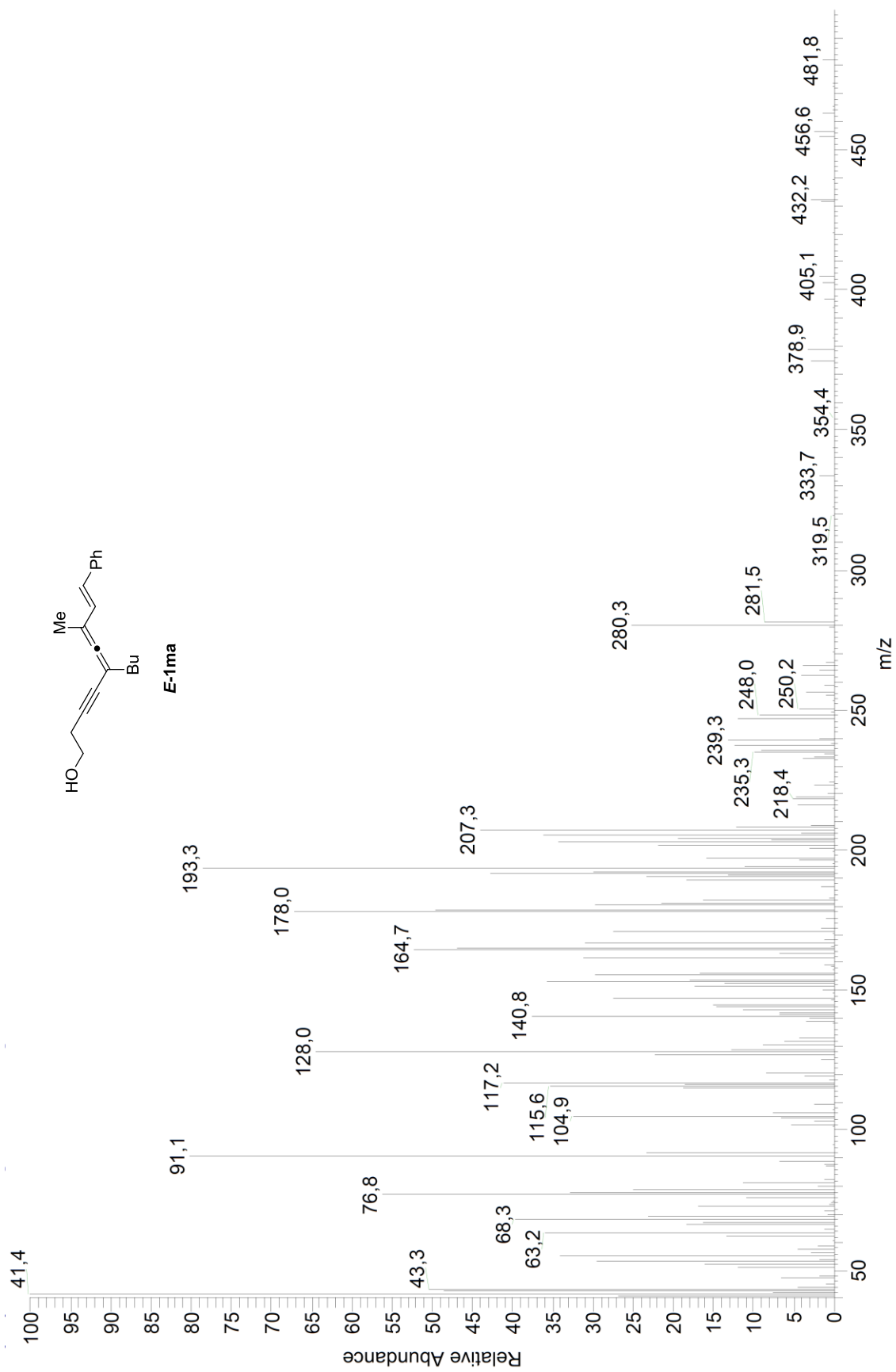


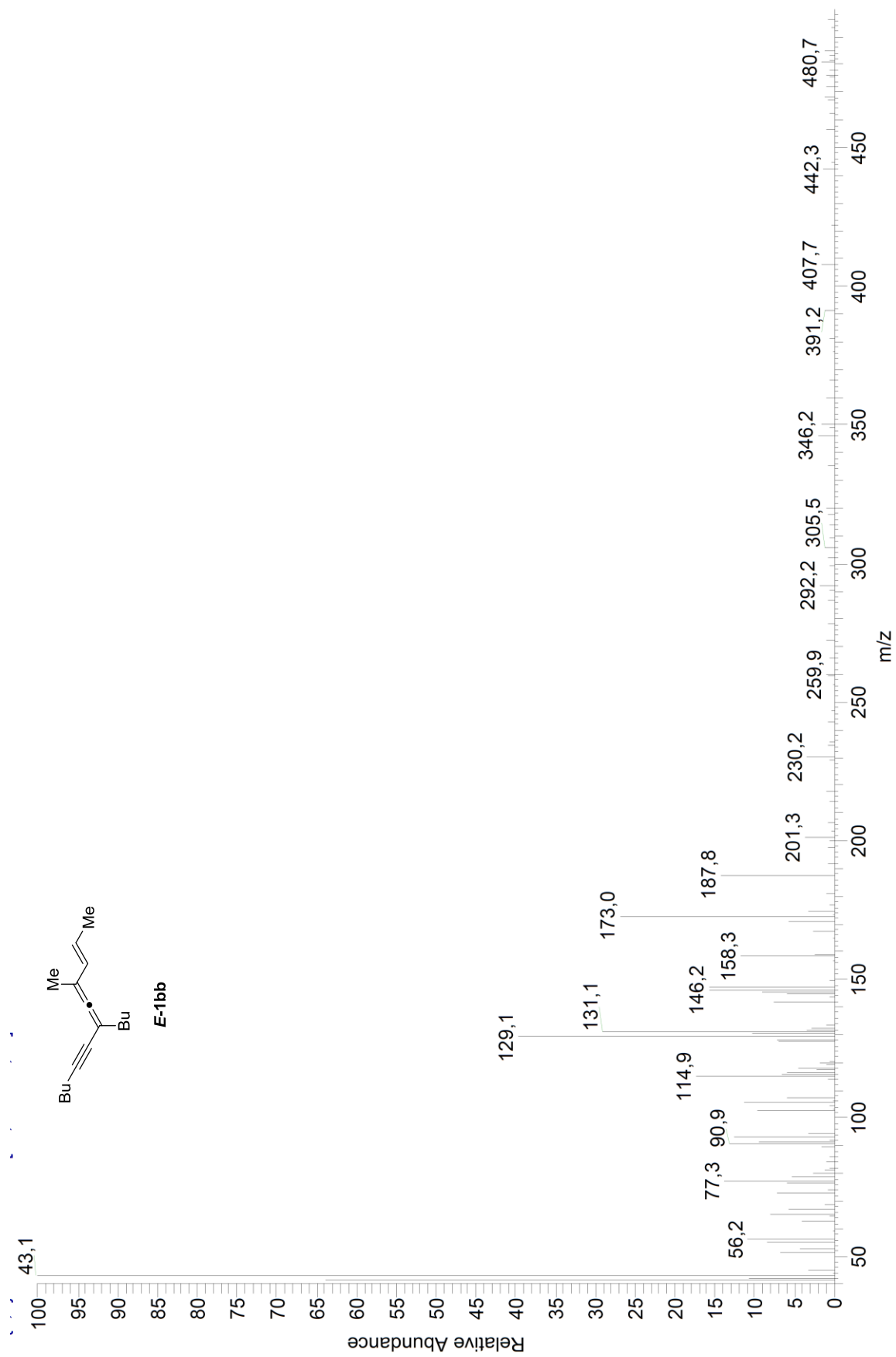


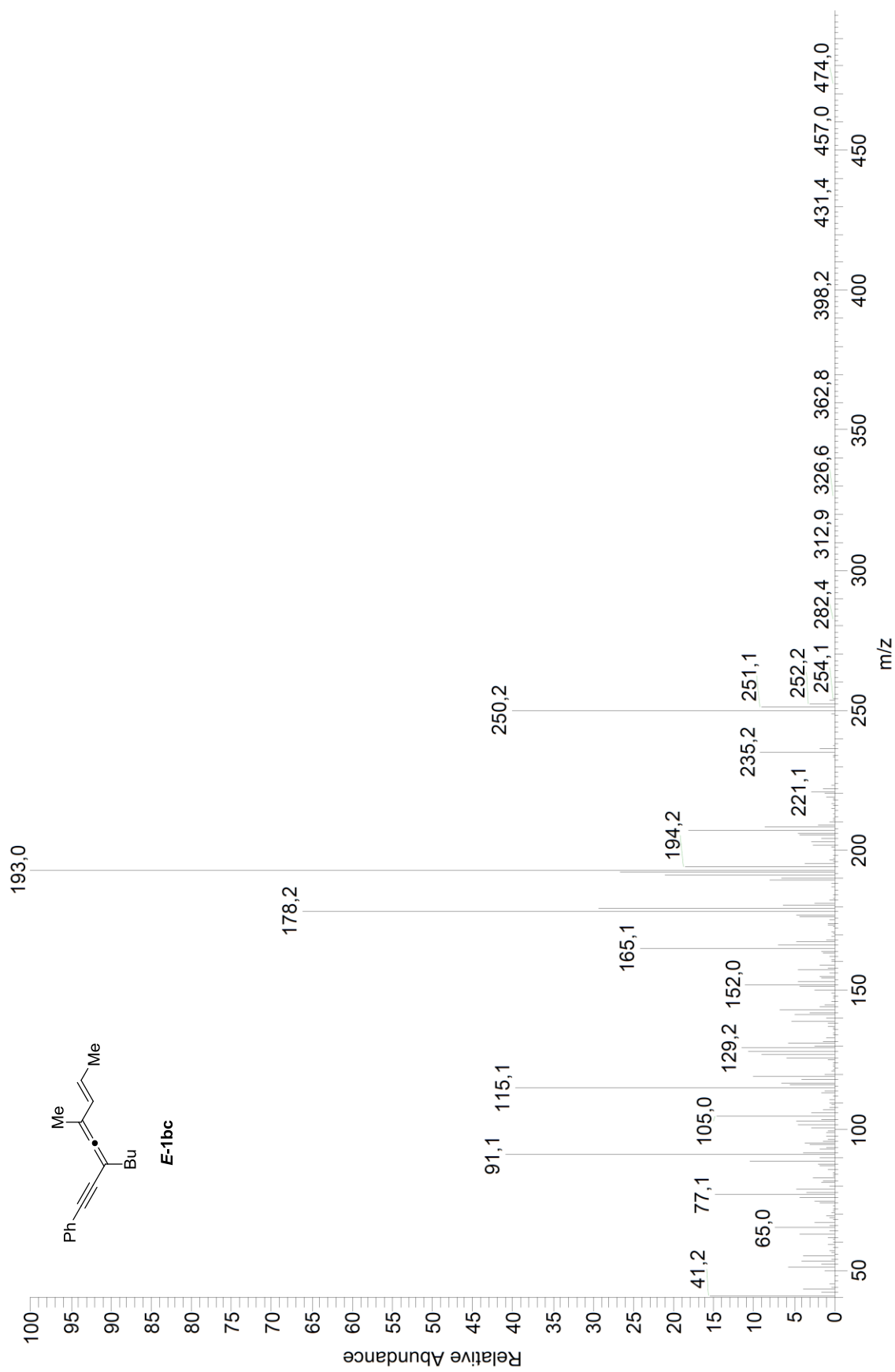


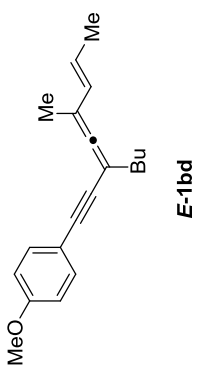
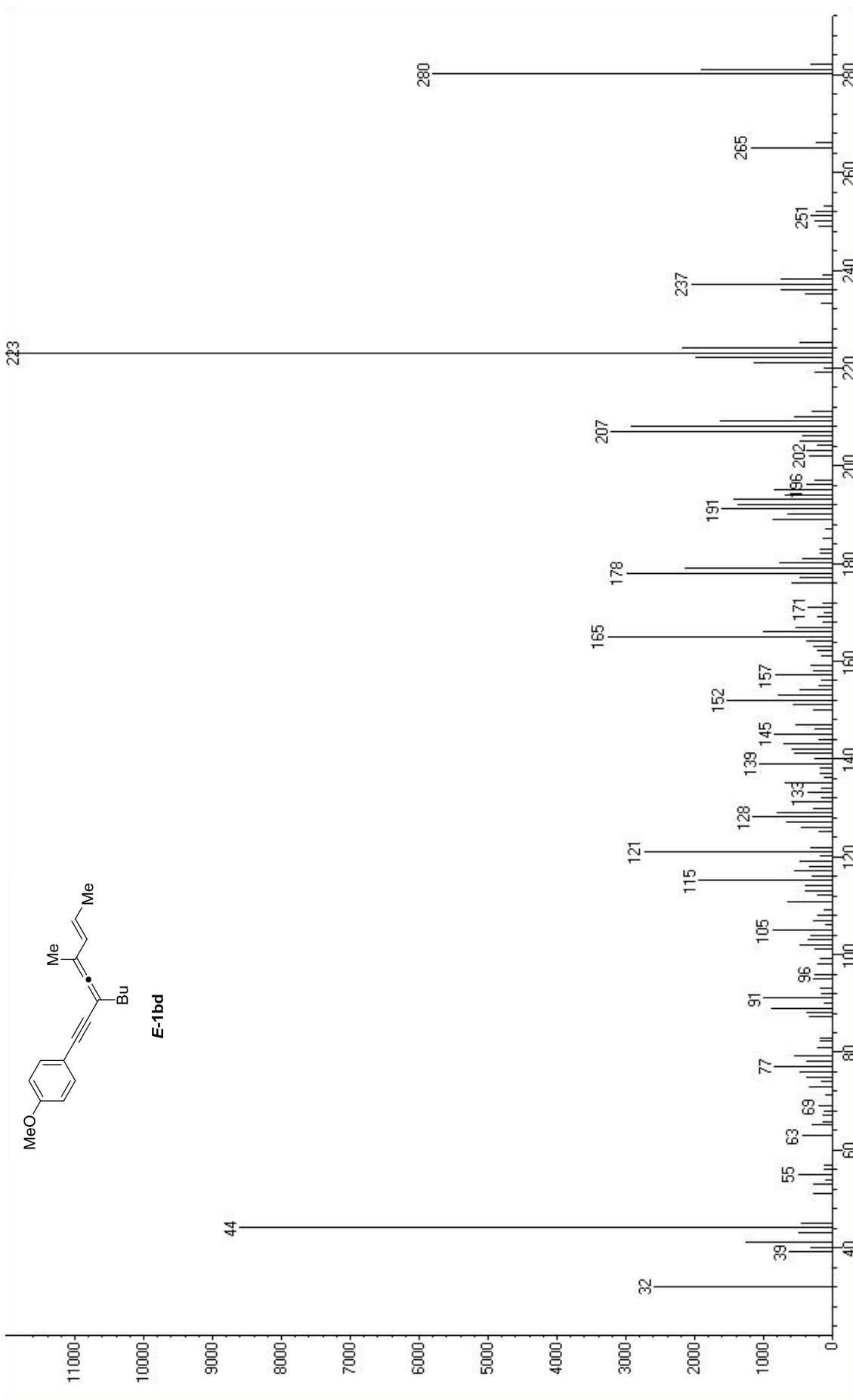


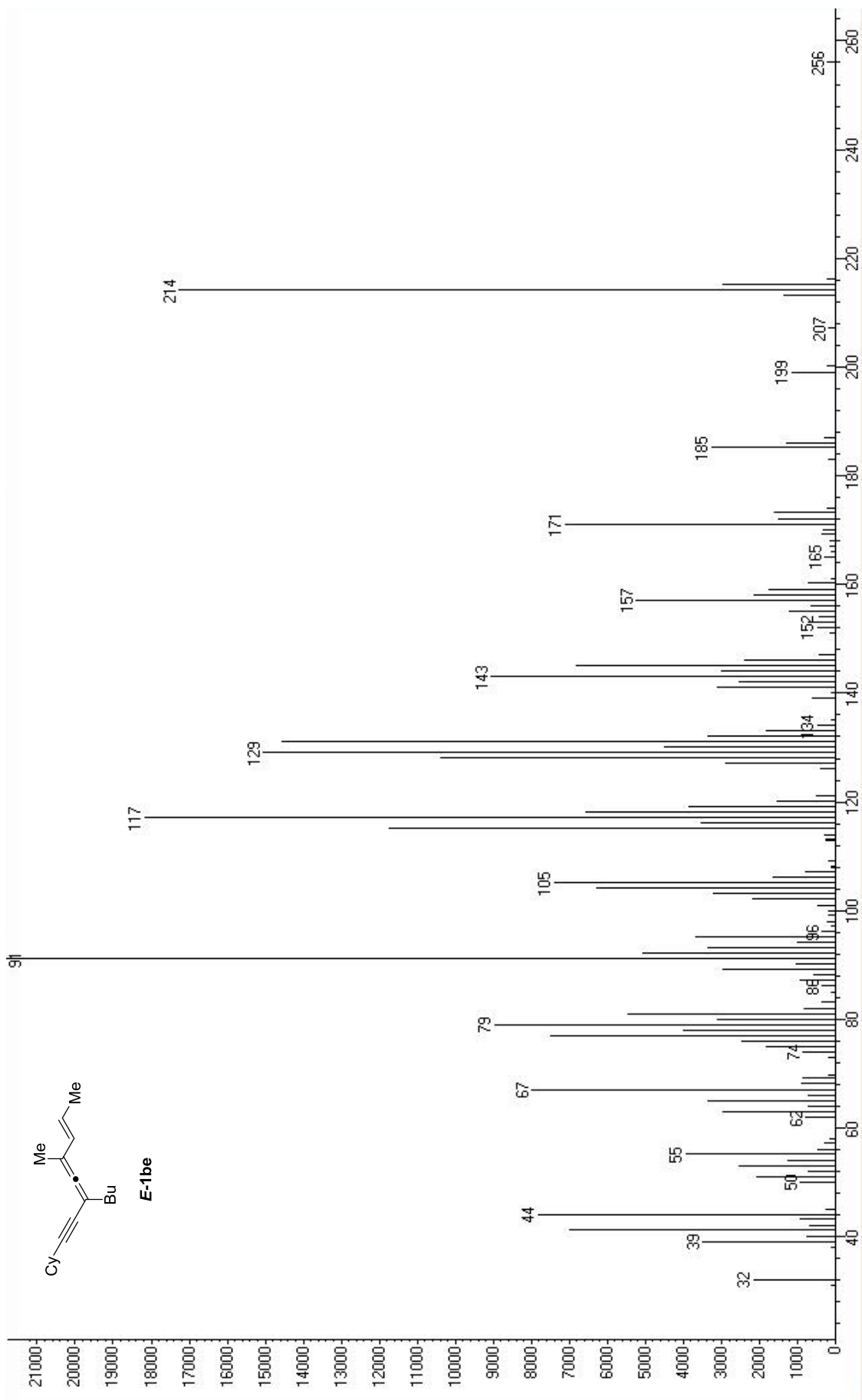


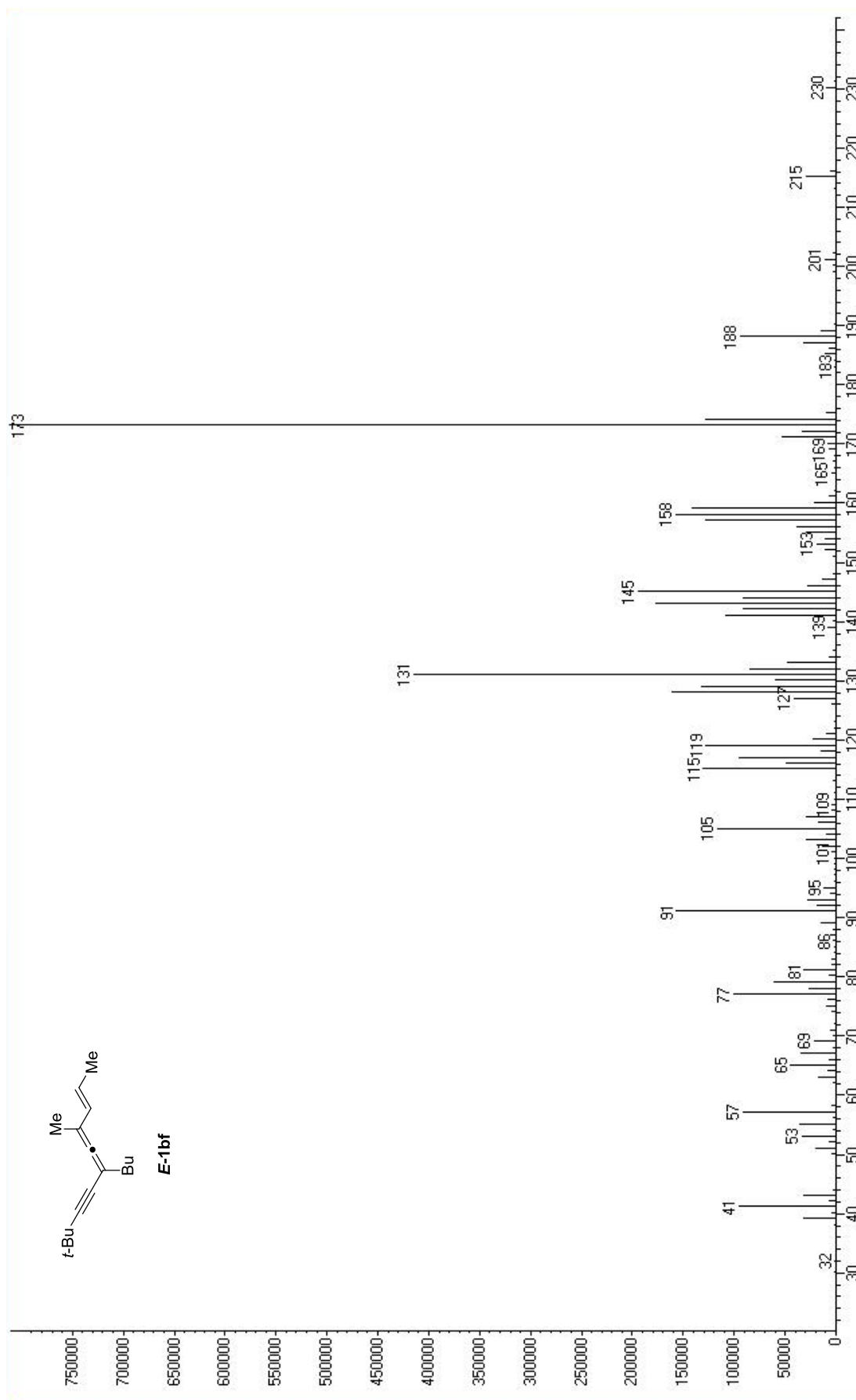


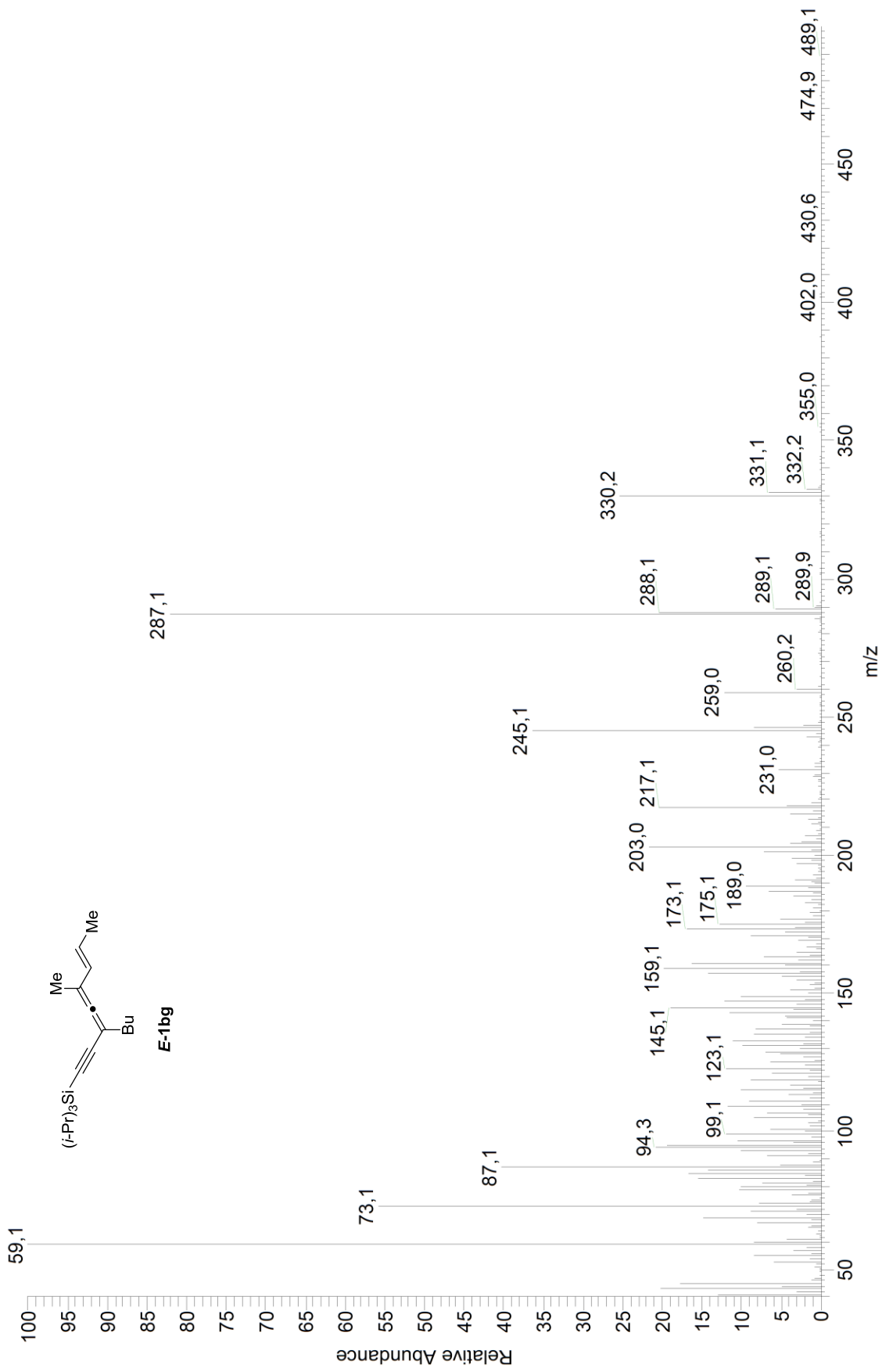


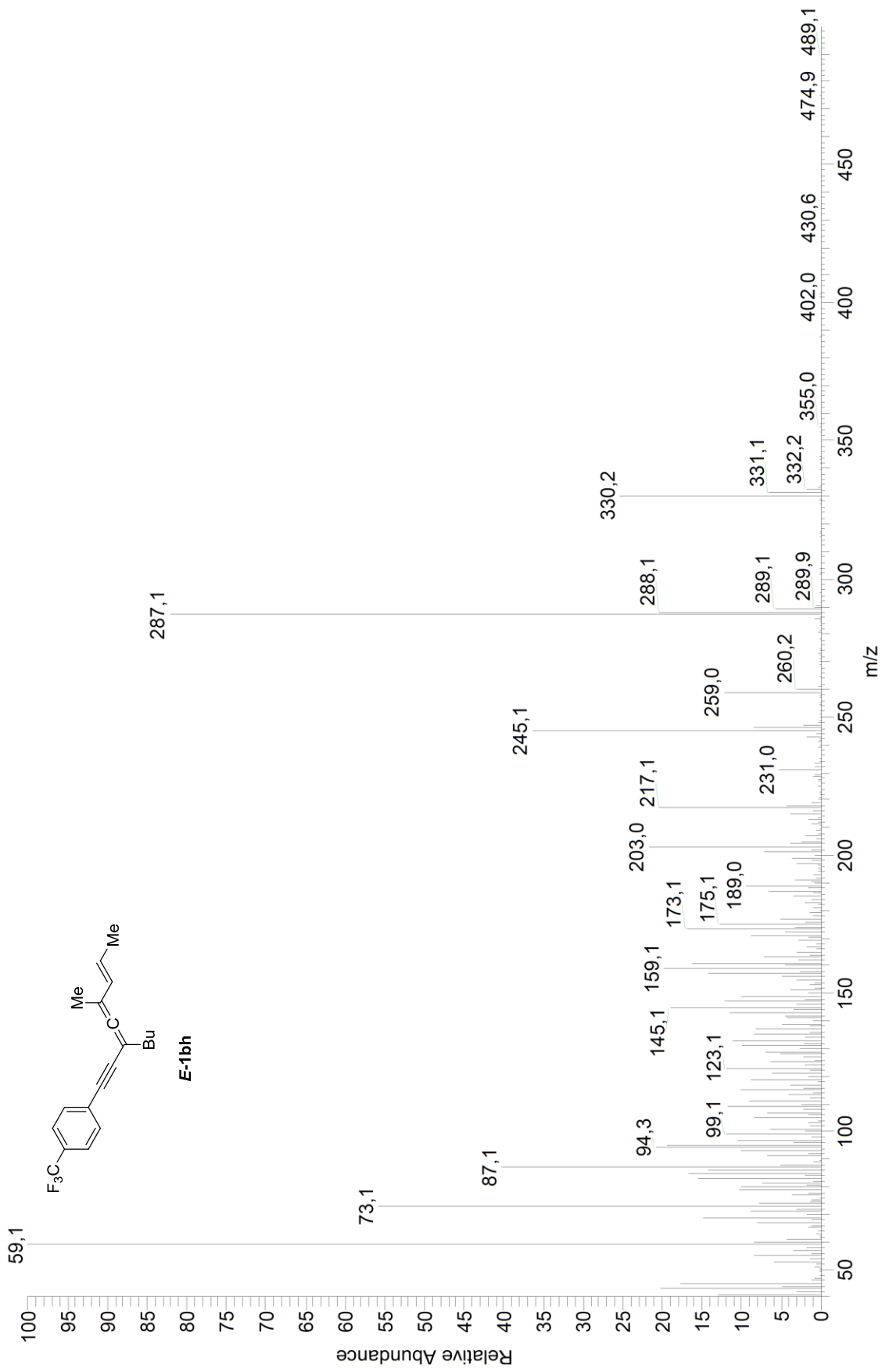


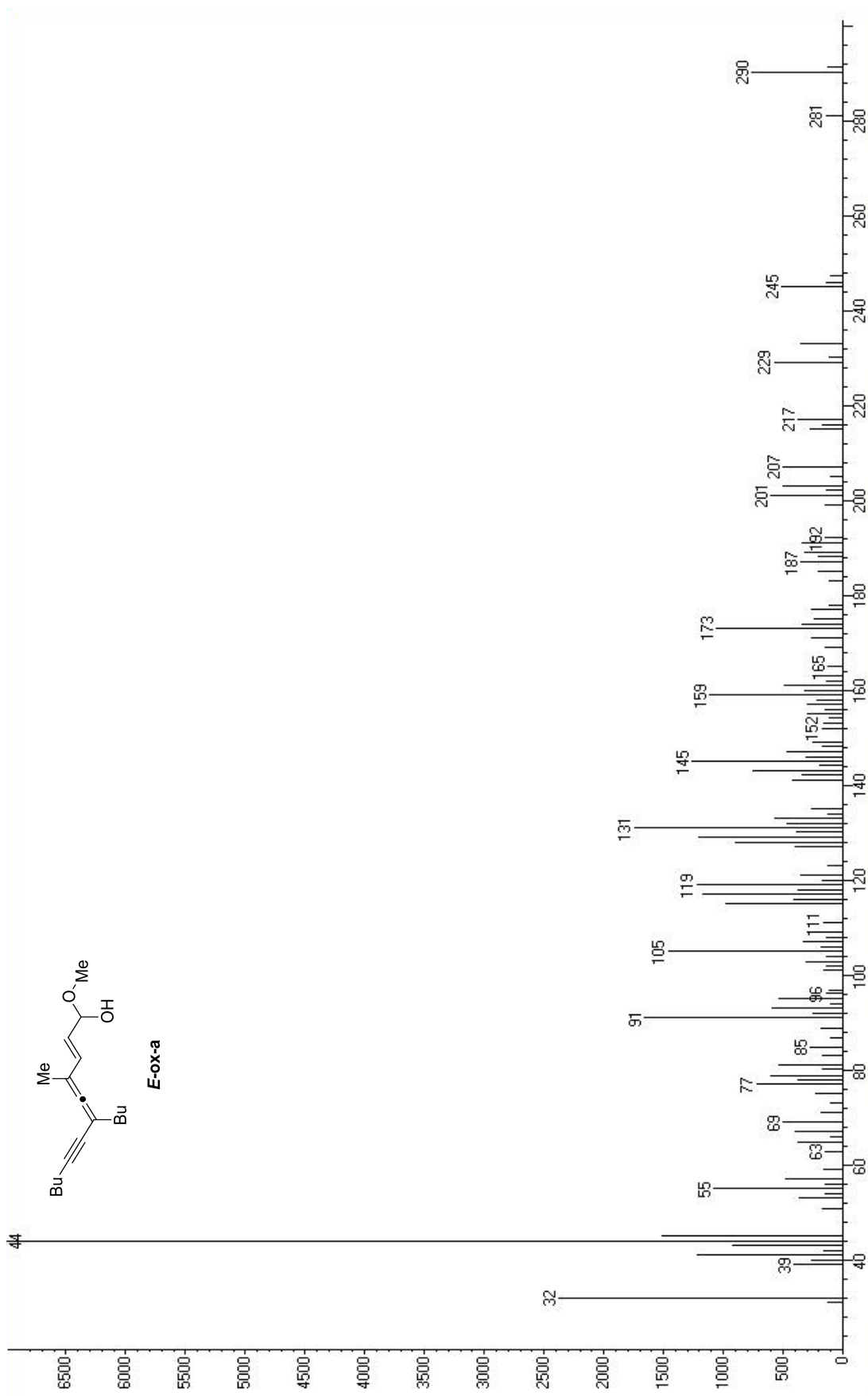




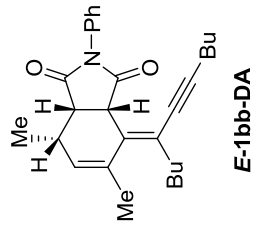
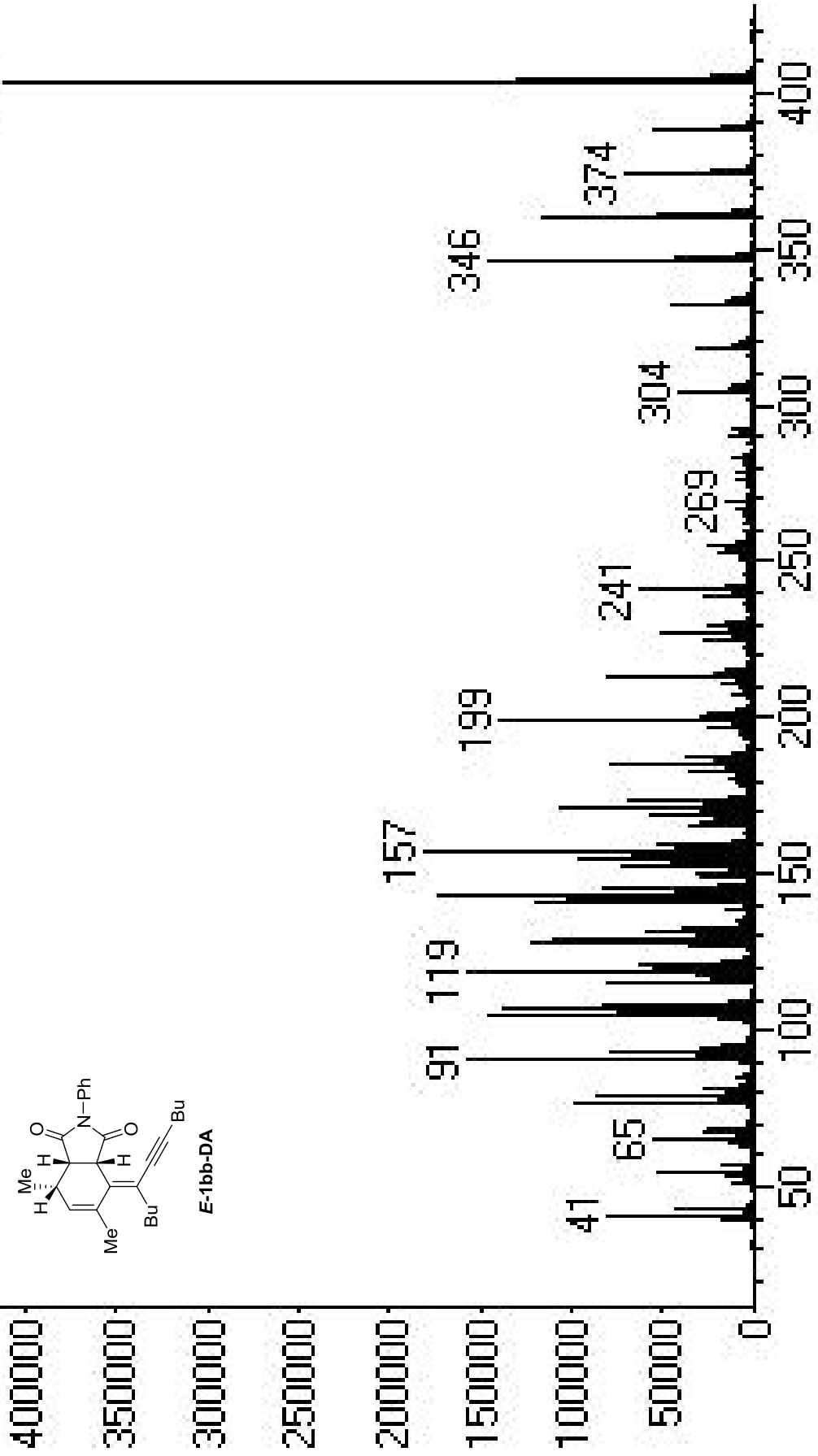


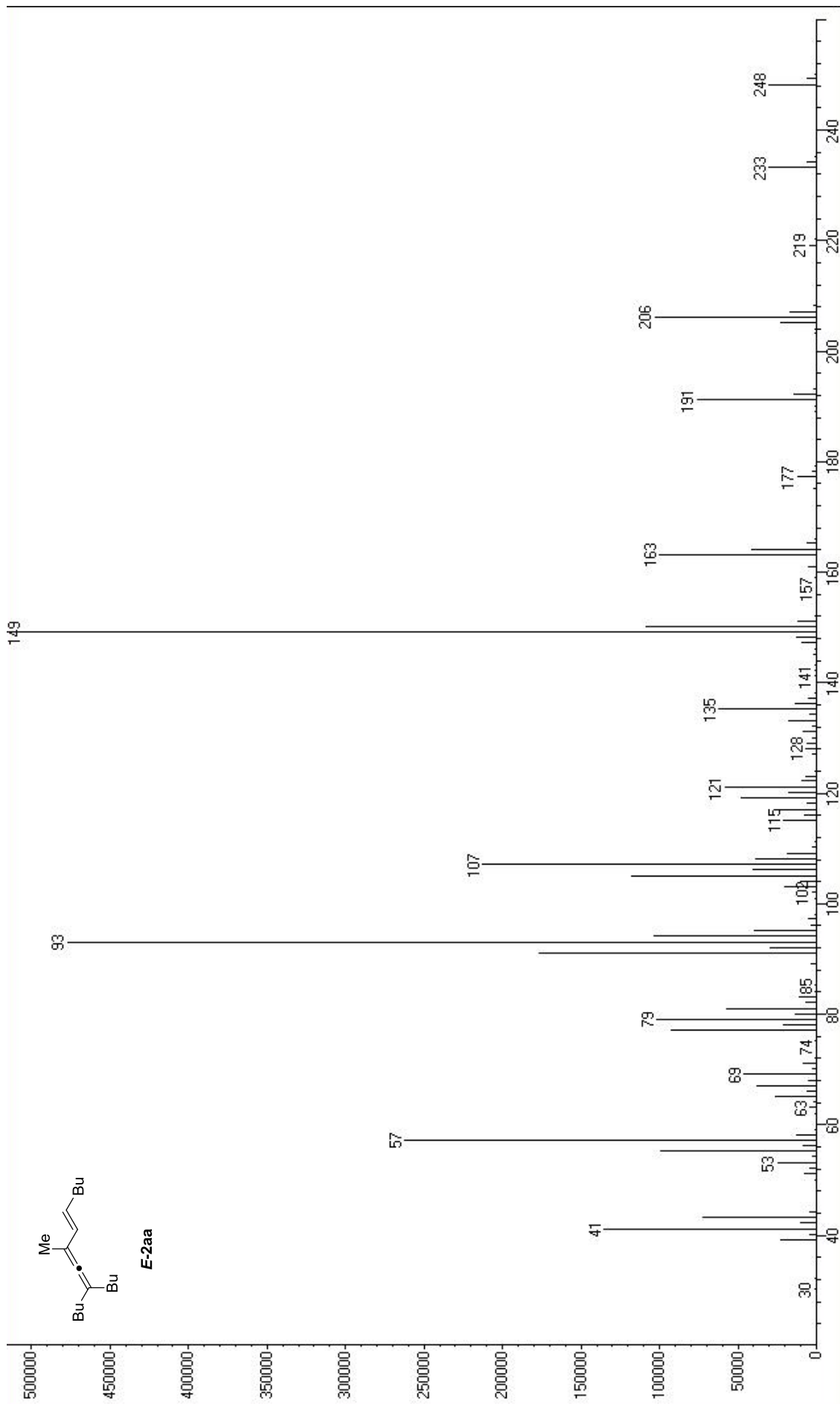


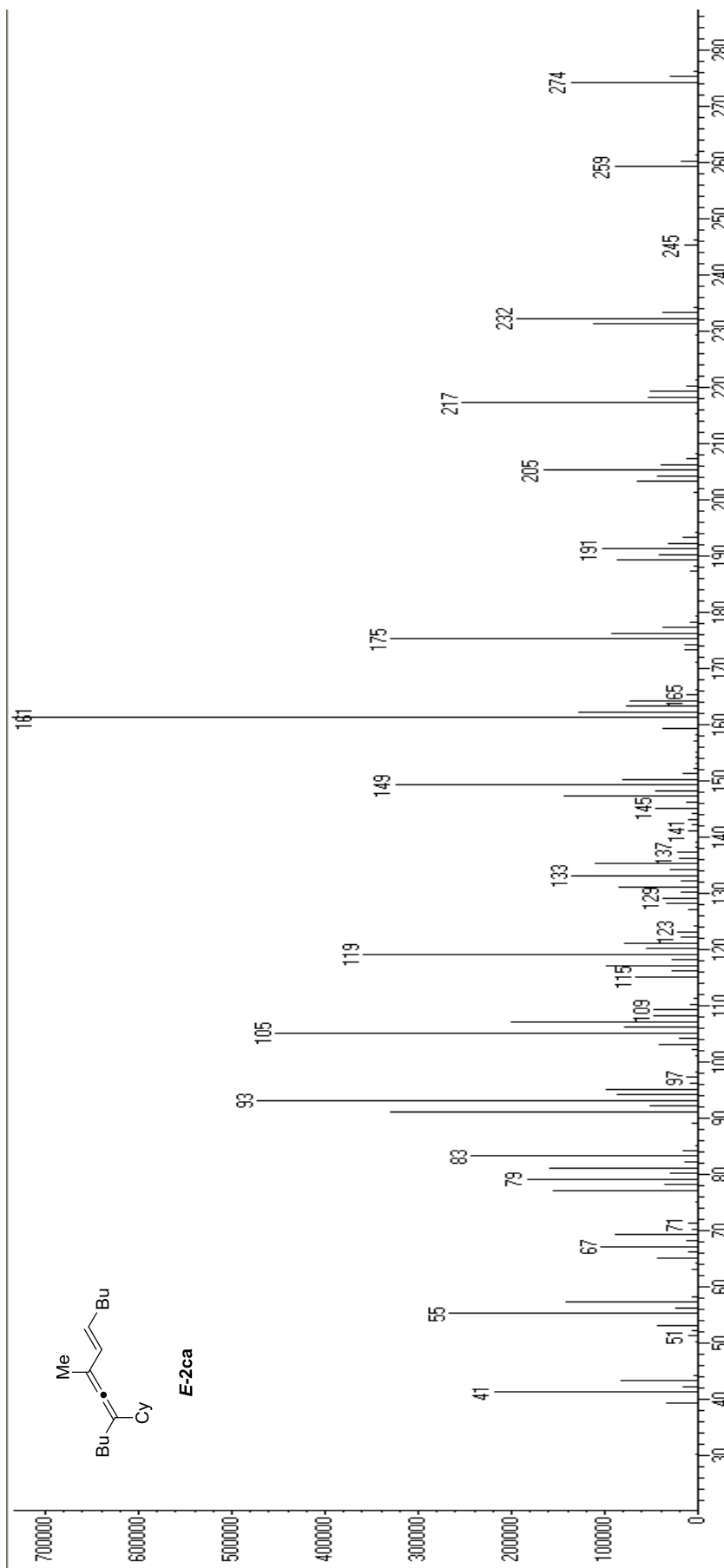


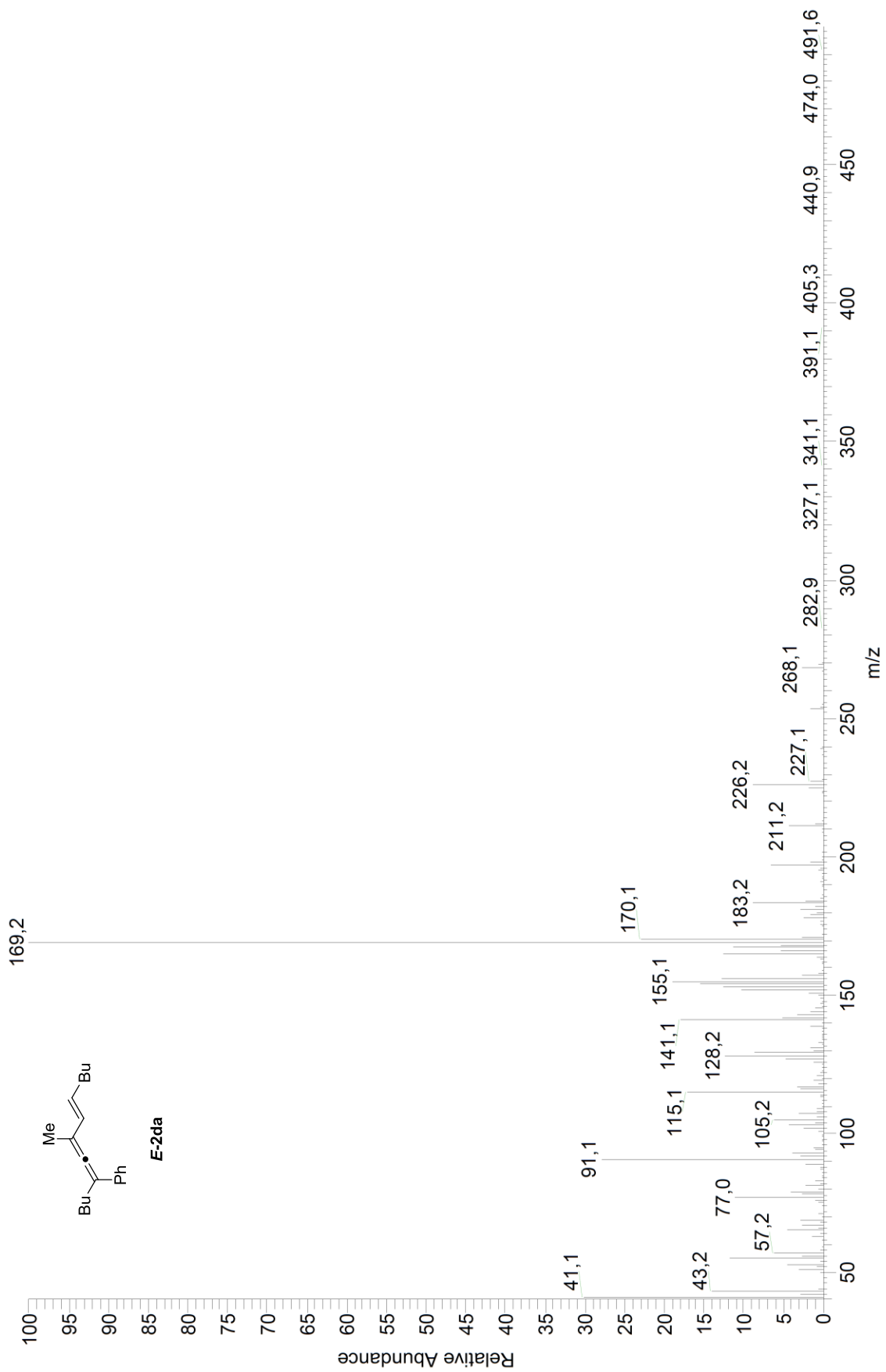


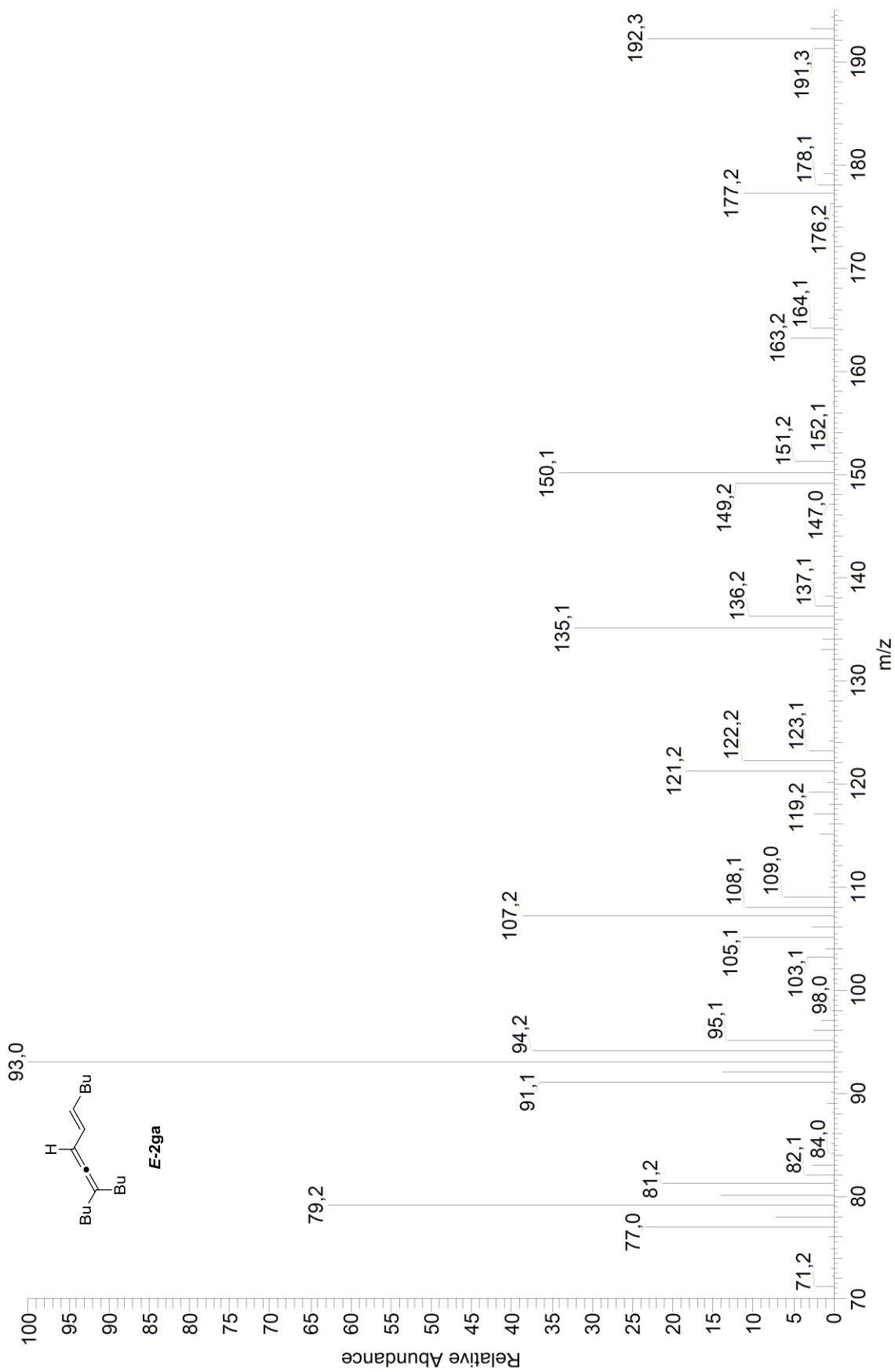
Scan 5311 (41.230 min): DT-S9E.D
403

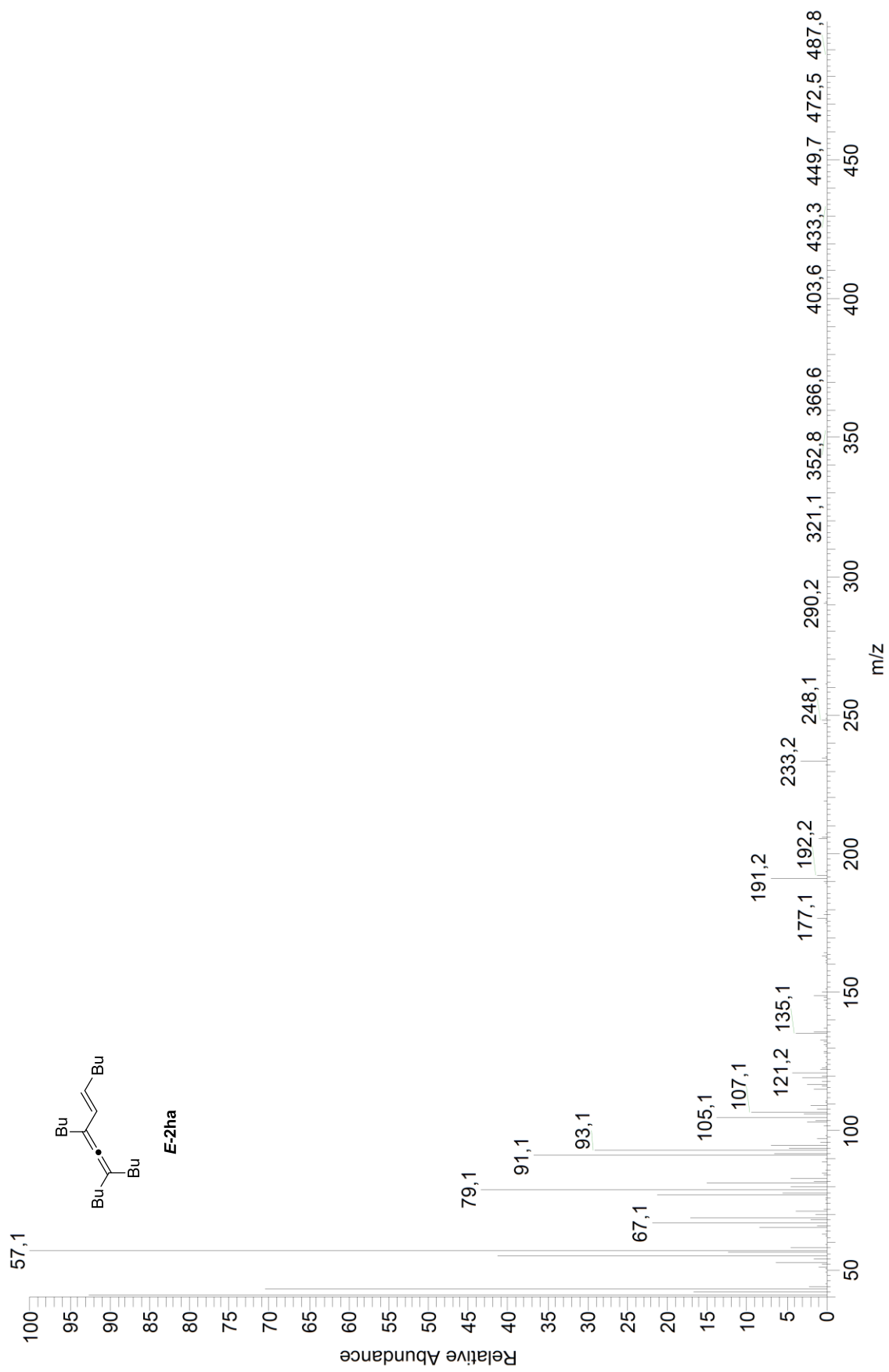


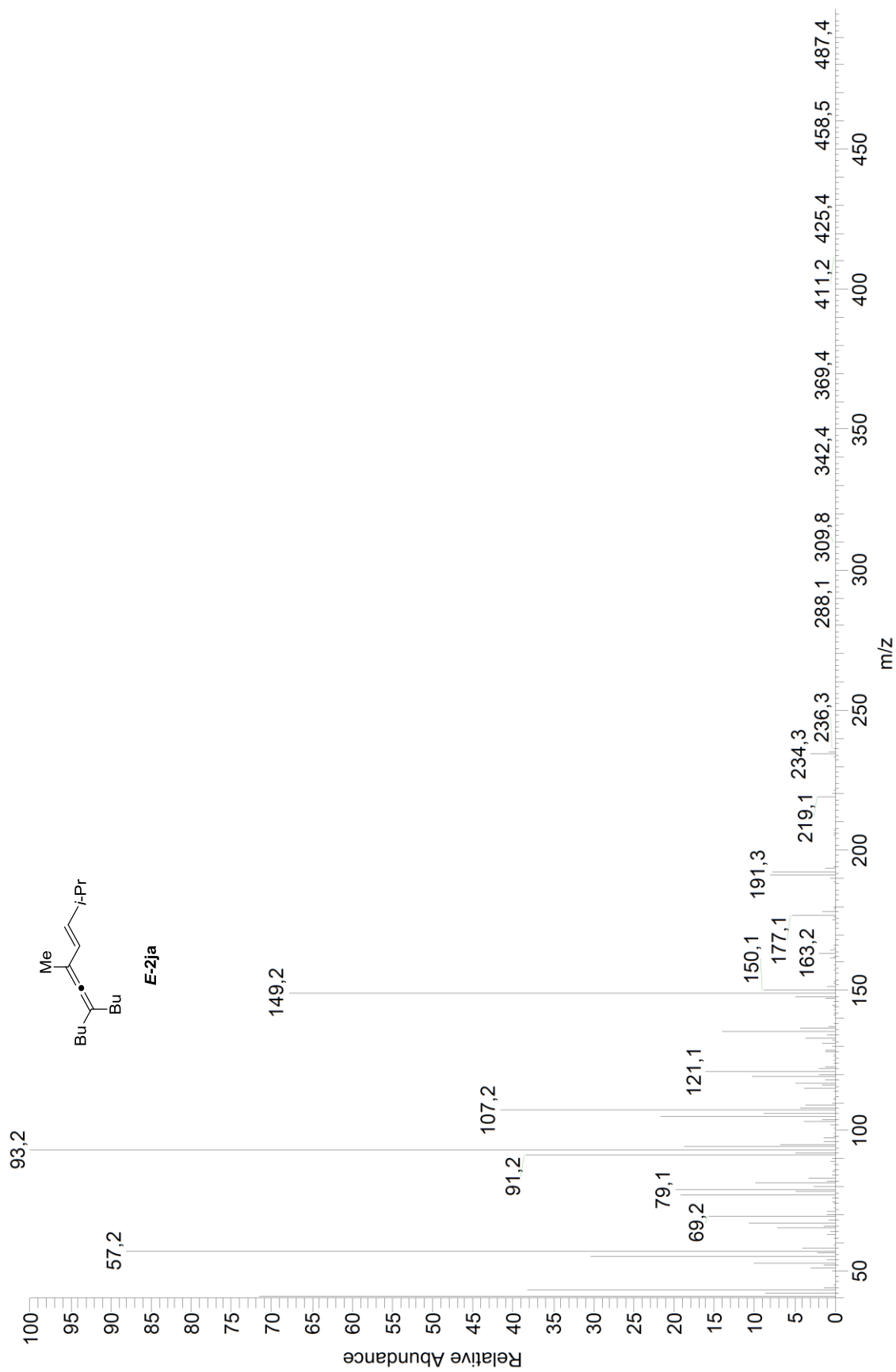


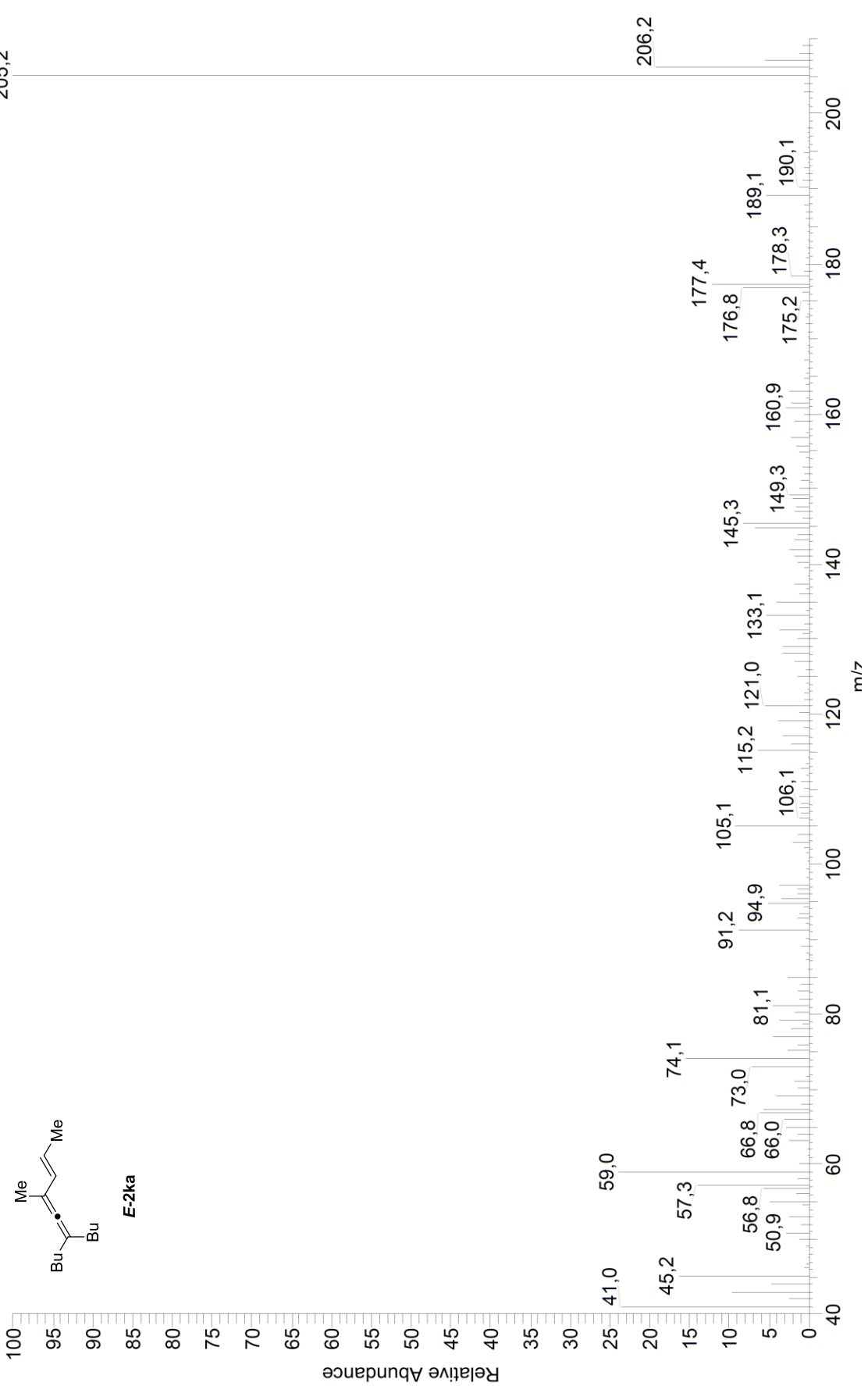


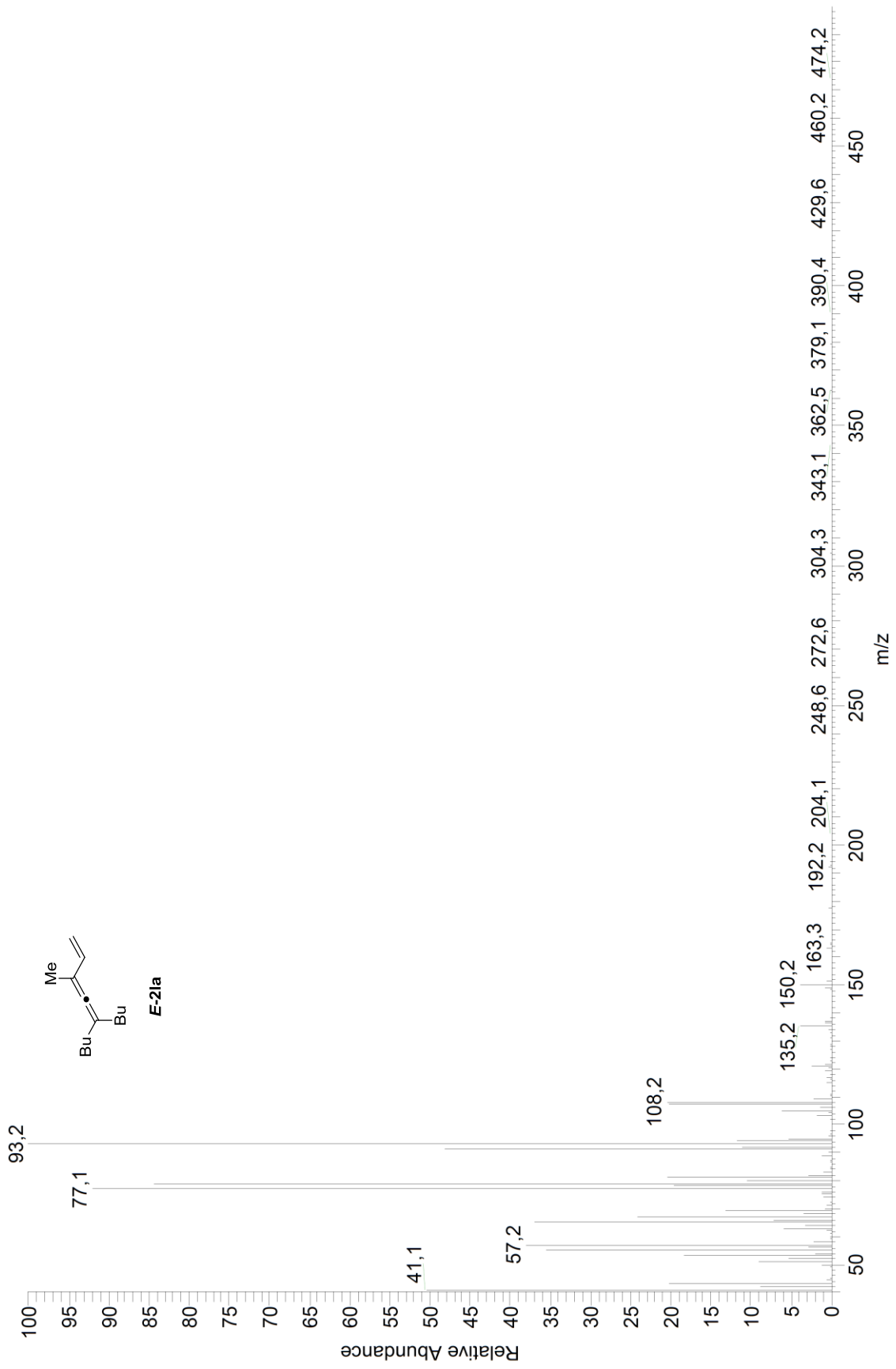


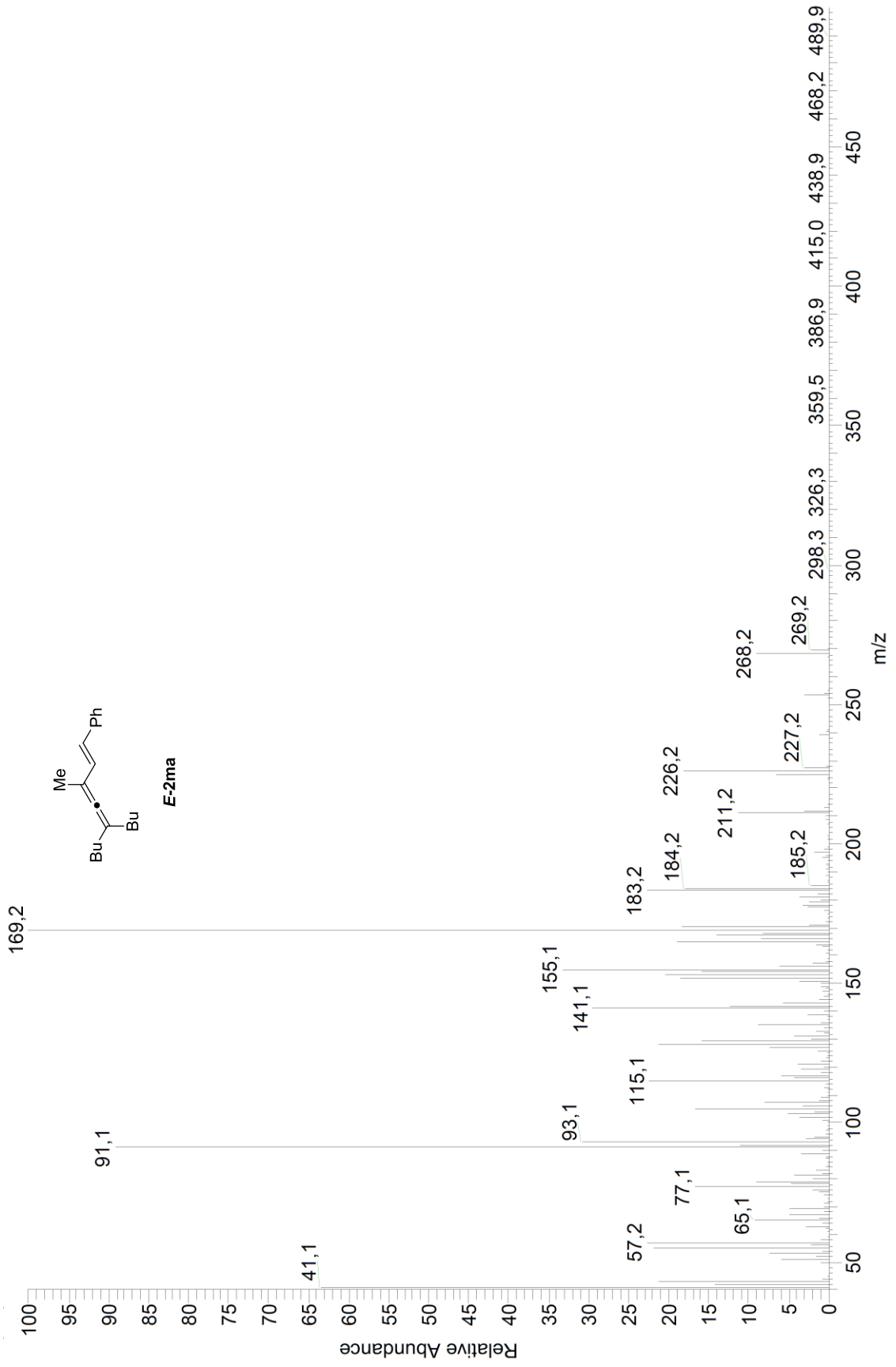


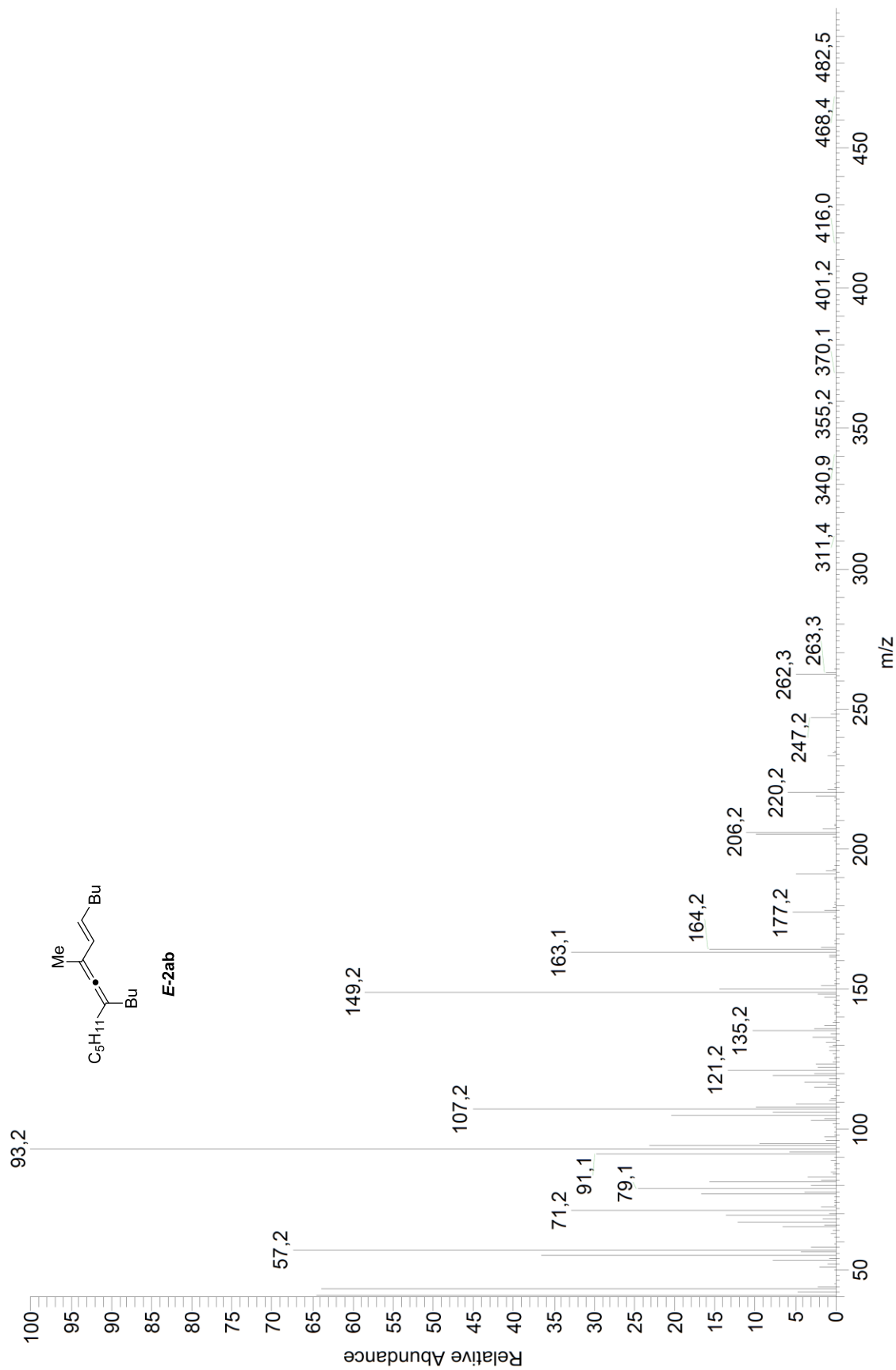


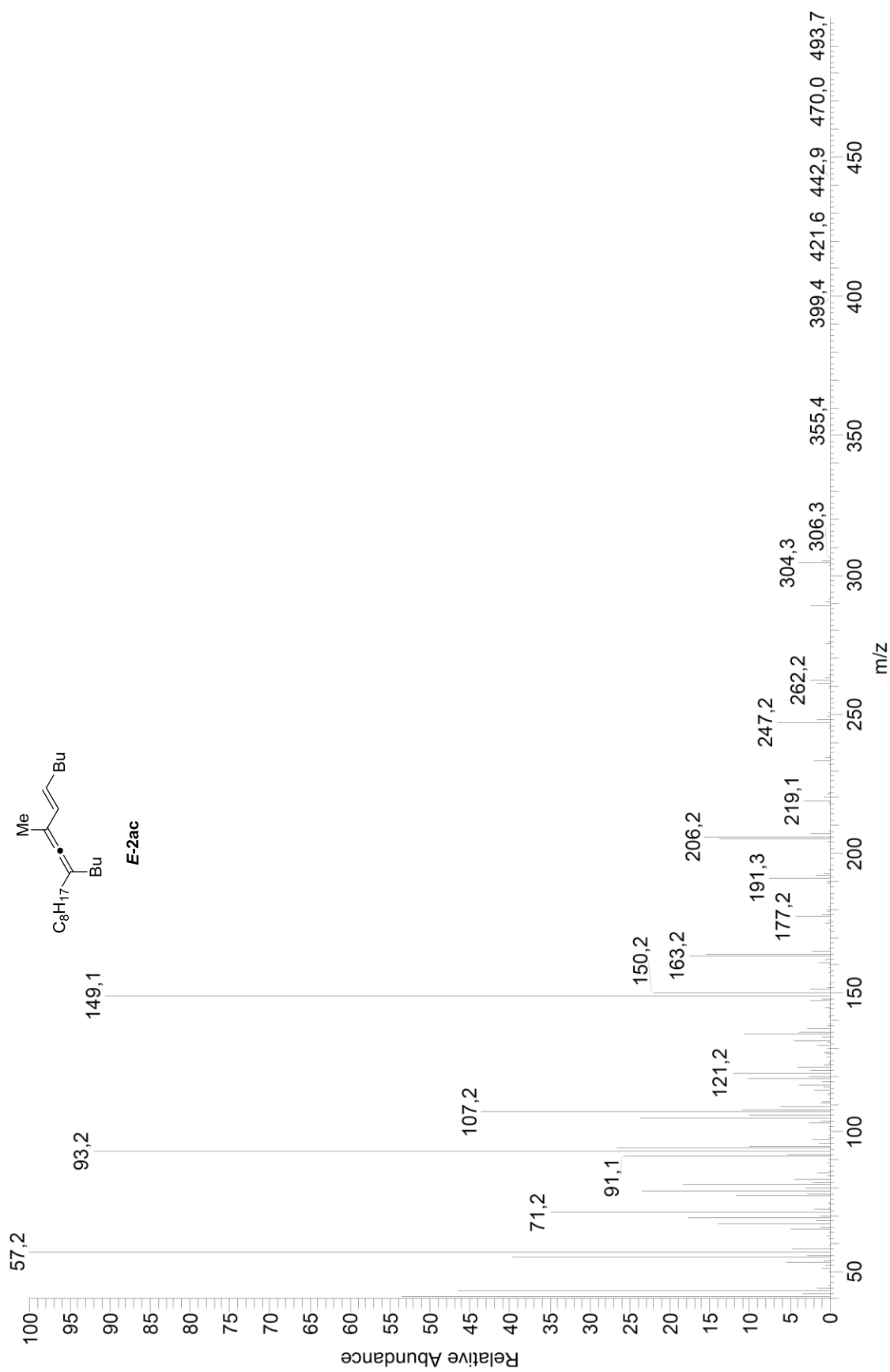


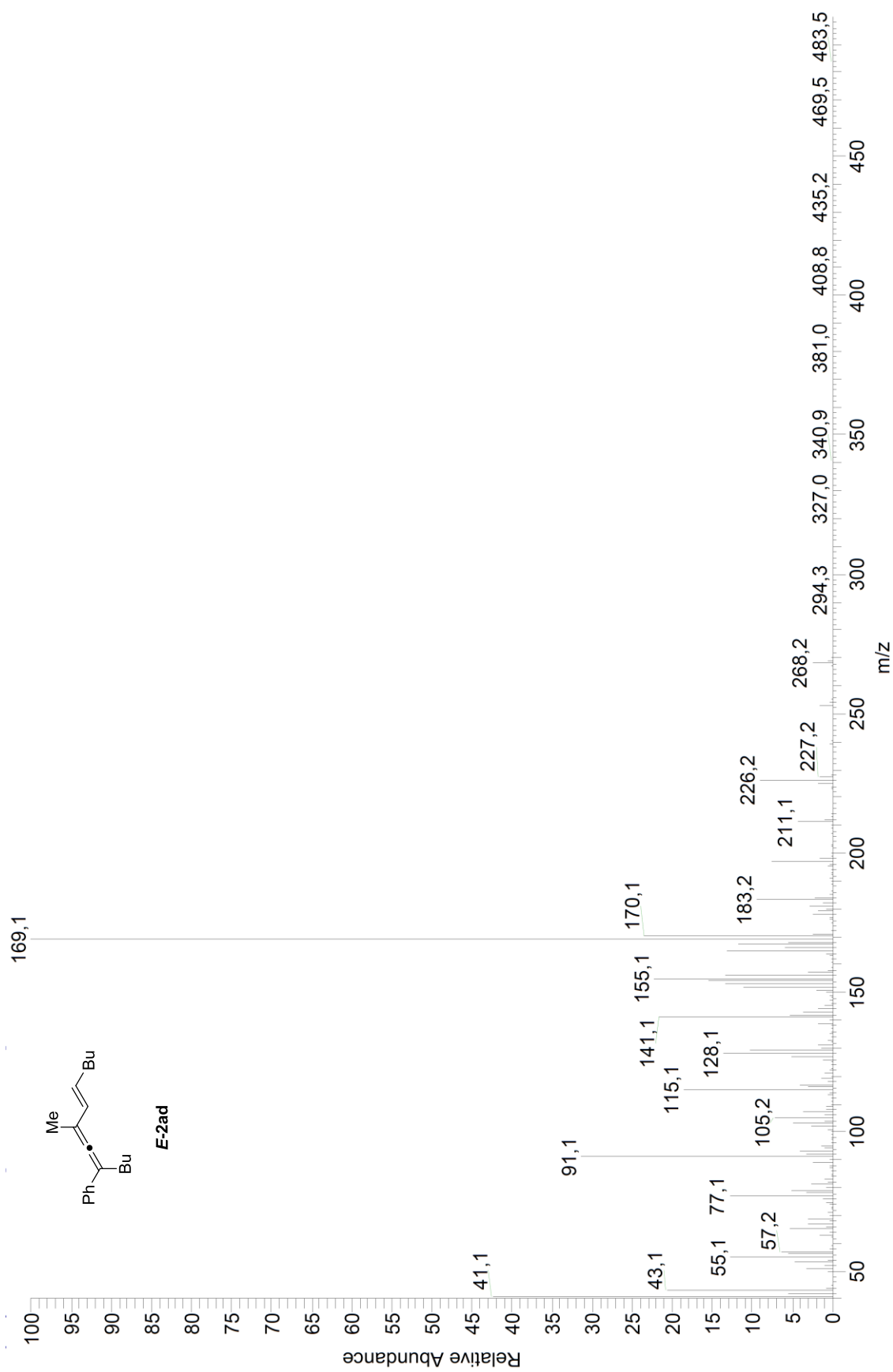


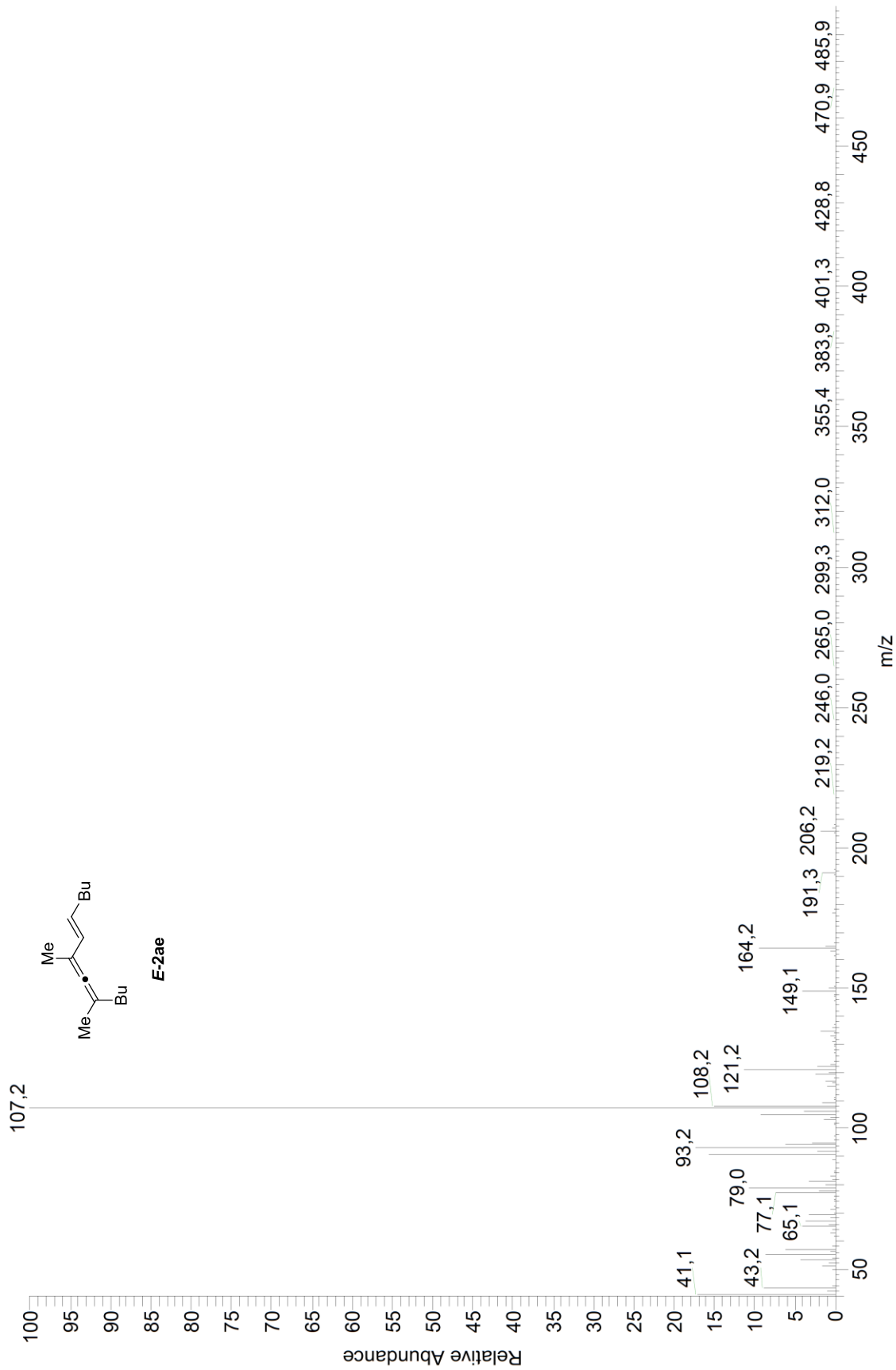


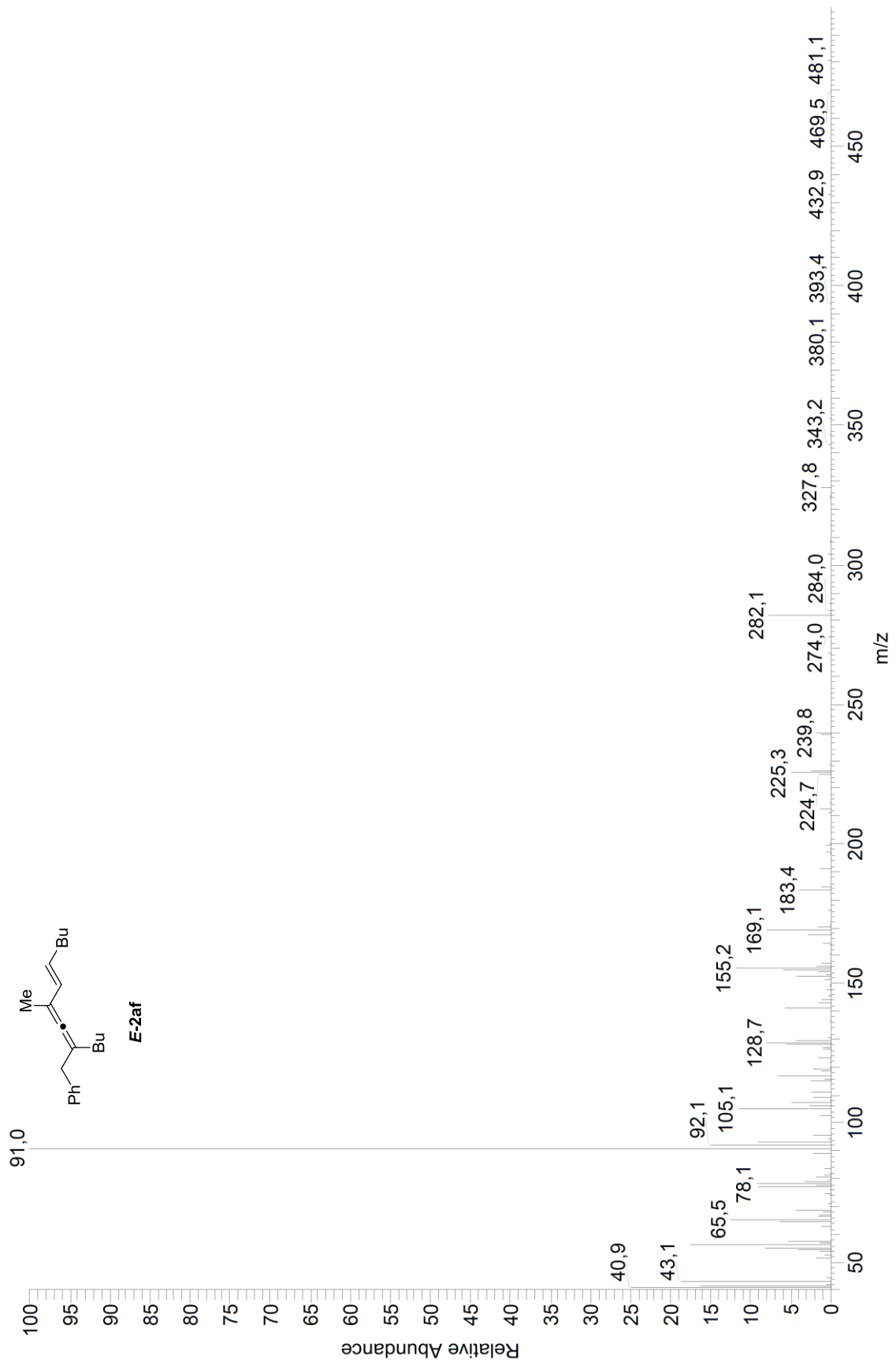












CURRICULUM VITAE

Personal Information

Name: Dođan

Surname: TAÇ

Birth Place: Trabzon

Birth Date: 8th April 1983

Education

2011-2016 **IZMIR INSTITUTE OF TECHNOLOGY**, *Chemistry Department*.

-PhD in Organic Chemistry-

2009-2011 **IZMIR INSTITUTE OF TECHNOLOGY**, *Chemistry Department*.

-MS in Bioorganic Chemistry-

2002-2008 **ESKISEHIR OSMANGAZI UNIVERSITY**, *Chemistry Department*.

-BS in Chemistry-

Experience

2014–2016 **TUBITAK–113Z155**, Project Assistant , IZTECH.

Participated actively in each step of the project (project proposal, experimental work, reporting).

2011–2014 **TUBITAK–210T092**, Project Assistant , IZTECH.

Responsible one of the section of this project, which involves transition metal catalyzed coupling reactions.

Symposium, Presentation and Training

8th AES-MMEOS 2014 - Organizing Committee

TÜBİTAK 2237 Proje Hazırlama , Yazma ve Yürütme Eğitimi, 2014 – Participant

Poster P. Dogan Taç and Levent Artok, Palladium(0)-Catalyzed Alkynylation Reactions of (E)-Enyne Carbonates, 8th AES-MMEOS, 2014, IZMIR/TURKEY.

Poster P. Dogan Taç, I. Arınç Aytaç, Melih Kus, Fırat Zıyanak, A. Osman Karatavuk, Levent Artok, Iron-Catalyzed 1,5-(SN²)-Substitution of Enyne Acetates and Oxiranes, 9th AES-MMEOS, 2016, STOCKHOLM/SWEDEN.